Understanding Climate-Driven Processes for Data-Scarce Mountain Glaciers

Insights from Reanalysis Data and Global Climate Models, as well as In-Situ and Remote Sensing Sources

Dissertation
zur
Erlangung der Naturwissenschaftlichen Doktorwürde
(Dr. sc. nat)

vorgelegt der
Mathematisch-naturwissenschaftlichen Fakultät
der
Universität Zürich

von
Simone Marianna Schauwecker
aus
Schaffhausen SH und Feuerthalen ZH

Promotionskommission

PD. Dr. Christian Huggel (Vorsitz und Leitung der Dissertation)
Dr. Mario Rohrer
Dr. Nadine Salzmann
Dr. Holger Frey
Prof. Dr. Andreas Vieli
Prof. Dr. Jan Seibert

Zürich, 2017

Summary

Most glaciers in the world have been shrinking since the middle of the 19th century. Vanishing glaciers in the tropical Andes and the Himalayas may have severe local and regional impacts on water availability and natural hazards. The observed changes in high mountains, together with the often strong emotional and spiritual connection of local cultures to glaciers, have given rise to worries about adaptation to climate change and related glacier shrinkage.

Despite the increasing concern about the future of glaciers in countries like India and Peru, there are still important knowledge gaps in understanding the complex interplay between glaciers and climate. It is still not completely unraveled how glaciers react to changes in climate variables like humidity, cloud cover, air temperature and precipitation. One important reason for this incomplete understanding is the data scarcity at high elevations in many parts of the world. Although national weather services, as well as numerous research institutions and groups have made large efforts to monitor the climate at high altitudes, long time series are still sparse and the station density is often low at elevations where glaciers exist. Since remote sensing and reanalysis data have the potential to fill these gaps, it is important to know their potential and limitations. The general aim of this work was to study changes in key climate variables and impacts on glacier mass and energy balance based on simple but robust approaches and multiple data sources, such as in-situ, remote sensing and reanalysis data and global climate models.

A first focus of this thesis lies on the energy balance of debris-covered glaciers. Supraglacial debris cover is an important surface characteristic altering glacier surface energy and mass fluxes. Thick debris has an insulating effect and leads to reduced ablation compared to a debris-free surface, while thin debris increases ablation due to the low albedo. Since debris-covered glaciers are widespread in the Indian Himalaya, it is crucial to know the debris extent and thickness. Here, an approach to estimate debris thickness was developed based on several assumptions on the meteorological conditions and debris properties. Several approaches to estimate wind velocity as well as shortwave and longwave radiation were developed and presented and the applicability of reanalysis data was tested. The resulting debris thickness map is related to large uncertainties – especially for thick debris. However, there is great potential to identify parts of the glacier with thin debris, which is important information for hydrological models and future glacier scenarios.

To understand glacier shrinkage in the Cordillera Blanca in Peru, past trends of the key climate variables air temperature, freezing level and precipitation were studied using in-situ and reanalysis data. A method to homogenize meteorological station data was developed in order to identify

significant trends. Reanalysis data of the upper troposphere indicate that the increase in precipitation recorded in the beginning of the 90s was related to stronger winds from the east, bringing more humidity from the Atlantic and Amazon basin to the mountains. The findings from meteorological data showed that the temperature increase not linear, but characterized by years of strong increases or jumps, followed by periods of slower warming or even stagnant temperatures. It was found that glaciers are retreating in this region, despite of a slowdown in warming and an increase in precipitation in the last 30 years. Based on a simple approach, it was shown that the observed precipitation increase was likely not large enough to balance the increased ablation due to rising temperatures. The estimated glacier reaction times indicate that large glaciers may still be reacting to a strong warming that happened some decades ago. Glaciers are in an imbalance with the present-day climate and especially small and low-elevated glaciers will disappear in a few years or decades.

These findings also highlight that the snowfall level is a crucial parameter in glacier energy and mass balance of tropical glaciers. The altitude of the snow/rain transition is decisive since it determines not only accumulation, but also ablation via the snowline, albedo and net shortwave radiation - the primary energy source for ablation. Based on several data sources (including novel data sets from a Micro Rain Radar, TRMM Precipitation Radar bright band and meteorological in-situ stations) and a simple approach bringing together knowledge from studies on different tropical glaciers, this study shows that the wet season snowfall level is approximately at the terminus elevation of the largest glaciers and that a close relation between glacier extents and freezing level exists. The wet season freezing level was used as indicator to estimate future glacier extents by the end of this century. The results impressively show that glaciers may shrink strongly even under optimistic emission scenarios. Under the most pessimistic scenario, only few patches of snow, ice and firn may remain at the summit of the largest mountains in Peru.

The approaches presented here provide new insights into climate-driven processes on high-mountain glaciers and their interplay with key climate variables. This thesis summarizes the main result and gives an overview of different applications of in-situ as well as reanalysis and remote sensing data, showing possibilities and limitations when such data are used to study climate-driven glacier surface processes in data-poor regions.

Zusammenfassung

Seit der Mitte des 19. Jahrhunderts schwinden die meisten Gletscher dieser Welt. Ein Rückgang der Gletscher hat Auswirkungen auf die Wasserverfügbarkeit und neu gebildete Seen können unerwartet ausbrechen und verheerende Überflutungen verursachen. In Zukunft braucht man Strategien, um sich den klimatisch bedingten Veränderungen in den Bergregionen anzupassen.

Trotz zunehmender Besorgnis über die Veränderungen der Umwelt, versteht man noch immer nicht alle Zusammenhänge zwischen dem Klima und Gletschern. Es ist noch nicht vollständig erforscht, wie Gletscher auf Veränderungen einzelner Klimagrössen wie Feuchtigkeit, Lufttemperatur oder Niederschlag reagieren. Vor allem fehlende Daten in Gebirgsregionen verhindern ein ganzheitliches Verständnis dieser Zusammenhänge. Nationale Wetterdienste, aber auch unzählige Forschungsinstitutionen und –gruppen messen seit Jahren und Jahrzehnten wichtige Klimavariablen in grossen Höhen. Dennoch gibt es relativ wenige lange und komplette Zeitreihen. Reanalysedaten und Fernerkundung haben ein grosses Potential um diese Datenlücken zu füllen, doch man muss Vor- und Nachteile dieser Daten kennen. Das Hauptziel dieser Arbeit war es, die Veränderungen von entscheidenden Klimavariablen und deren Einfluss auf die Massen- und Energiebilanz der Gletscher besser zu verstehen. Dazu wurden einfache aber robuste Ansätze und Experimente entwickelt und mehrere Datentypen eingesetzt, z.B. lokale Wetter-, sowie Fernerkundungs- und Reanalysedaten und globale Klimamodelle.

In einem ersten Schritt ging es darum, die Energiebilanz von schuttbedeckten Gletschern besser zu verstehen. Wo Gletscher mit Schutt bedeckt sind, wird die Eisschmelze stark beeinflusst. Mächtiger Schutt wirkt isolierend, hingegen führt eine dünne Sediment- oder Schuttbedeckung aufgrund der niedrigen Albedo zu verstärkter Schmelze. Da es im Himalaya unzählige stark schuttbedeckte Gletscher gibt, muss man nicht nur die Ausdehnung, sondern auch die Dicke des Schuttes kennen. In dieser Arbeit wurde ein neuer Ansatz vorgestellt, um die Schuttmächtigkeit für Gletscher ohne detaillierten lokale Messungen abzuschätzen. Dazu wurden Windgeschwindigkeit und kurz- und langwellige Strahlung anhand verschiedener Methoden und Reanalysedaten abgeschätzt. Die modellierte Schuttdicke ist mit grossen Unsicherheiten verbunden, besonders für mächtigen Schutt. Trotzdem erzielt die Methode relativ gute Resultate für dünne Schutt- und Sedimentbedeckungen. Diese Information ist besonders wichtig für hydrologische Modelle und zukünftige Gletscherszenarien.

Um den heutigen Gletscherrückgang in der Cordillera Blanca in Peru zu verstehen, wurden Veränderungen der Lufttemperatur und des Niederschlags der letzten Jahrzehnte untersucht. Als

Datengrundlage dienten Reanalyse- und lokale Wetterdaten. Bevor Klimaveränderungen berechnet werden können, müssen die Wetterdaten kontrolliert und homogenisiert werden. Reanalysedaten der oberen Troposphäre zeigen, dass der Niederschlagsanstieg anfangs der 1990er Jahre mit verstärkten Ostwinden zusammenhängen könnte. Wenn Ostwinde zunehmen, wird mehr Feuchtigkeit vom Atlantik und dem Amazonas her Richtung Anden transportiert. Obwohl in den letzten 30 Jahren die Erwärmung eher nachgelassen und der Niederschlag sogar zugenommen hat, sind die Gletscher in der Cordillera Blanca stark zurückgegangen. Dank eines einfachen Ansatzes wurde gezeigt, dass der beobachtete Niederschlagsanstieg sehr wahrscheinlich die erhöhte Ablation auf Grund wärmerer Temperaturen nicht ausgleichen konnte. Auch die Reaktionszeiten der Gletscher deuten darauf hin, dass besonders grosse Gletscher noch immer auf den starken Temperaturanstieg vor einigen Jahren bis Jahrzehnten reagieren und kleine Gletscher in den nächsten Jahrzehnten verschwinden werden. Die Resultate zeigen, dass der Temperaturanstieg kein lineares Phänomen ist, sondern dass es einige Jahre mit starker Erwärmung oder sprunghaften Veränderungen geben kann. Ebenso gut kann es vorkommen, dass die Temperatur während einiger Jahre weniger stark ansteigt oder sogar konstant bleibt.

Die Resultate weisen darauf hin, dass die Schneefallgrenze ein wichtiger Parameter ist, um die Massenbilanz tropischer Gletscher zu verstehen. Diese Grösse ist besonders wichtig, da sie sowohl Akkumulation, als auch Ablation steuert. Die Schneefallgrenze beeinflusst die Schneelinie, wodurch die Albedo und kurzwellige Strahlungsbilanz bestimmt werden. Da in Bergregionen in Peru noch immer wenige Daten gemessen werden, weiss man wenig über die Null- und Schneefallgrenze und deren regionale und zeitliche Variabilität. Anhand verschiedener Daten wurde gezeigt, dass sich die Schneefallgrenze in den meisten Fällen ungefähr auf der Höhe der Gletscherzungen befindet und dass es einen engen Zusammenhang zwischen Gletscherausdehnung und Null- sowie Schneefallgrenze gibt. Die Nullgradgrenze der Regenzeit wurde daher als Indikator für die Gletscherausdehnung definiert, um damit die Gletscherstände Ende dieses Jahrhunderts abzuschätzen. Die Resultate zeigten eindrücklich, dass Gletscher sogar unter dem optimistischsten Emissionsszenario weiterhin stark zurückgehen werden. Falls das pessimistischste Szenario zutrifft, werden in Zukunft möglicherweise nur die höchsten Gipfel mit kleinen Schnee-, Firn- und Gletscherfelder bedeckt sein.

Die hier vorgestellten Ansätze erlaubten es, einzelne entscheidende Klimavariablen und deren Veränderungen, sowie Oberflächenprozesse von Gletscher und deren Zusammenhang mit dem Klima in Regionen mit fehlenden Daten besser zu verstehen. In dieser Arbeit werden verschiedene Datentypen, Methoden und Resultate präsentiert und diskutiert.

Contents

Abbreviations

AAR	Accumulation Area Ratio
ANA	Autoridad Nacional del Agua
ASTER	Advanced Spaceborne Thermal Emission and Reflection Radiometer
BB	Bright band
CB	Cordillera Blanca
CIIADERS	Centro de Información e Investigación Ambiental de Desarrollo Regional Sostenible
CMIP	Coupled Model Intercomparison Project
CV	Cordillera Vilcanota
DEM	Digital Elevation Model
DTR	Daily Temperature Range
ECMWF	European Centre for Medium-Range Weather Forecasts
ECV	Essential Climate Variable
ELA	Equilibrium Line Altitude
ENSO	El Niño-Southern Oscillation
ERA	Reanalysis at ECMWF
FL	Freezing level
FLH	Freezing level height
GANAL	Global Analysis data
GDEM	Global Digital Elevation Map
GLIMS	Global Land and Ice Measurements from Space
GLOF	Glacier Lake Outburst Flood
GPCC	Global Programme Climate Change
GPM	Global Precipitation Measurement
IHCAP	Indian Himalayas Climate Adaptation Programme
IMD	India Meteorological Department
JAXA	Japan Aerospace Exploration Agency
LPDAAC	Land Processes Distributed Active Archive Center
MERRA	Modern-Era Retrospective Analysis for Research and Applications
METAR	Meteorological Aerodrome Report
MRR	Micro Rain Radar
NASA	National Aeronautics and Space Administration
NCAR	National Center for Atmospheric Research
NCEP	National Centers for Environmental Prediction
NOAA	National Oceanic and Atmospheric Administration
PACC	Programa de Adaptación al Cambio Climático en el Perú
PDO	Pacific Decadal Oscillation

PR	Precipitation Radar
RCP	Representative Concentration Pathways
RGI	Randolph Glacier Inventory
SDC	Swiss Agency for Development and Cooperation
SENAMHI	Servicio Nacional de Meteorología e Hidrología de Perú
SEPA	Southeastern Pacific Anticyclone
SL	Snowfall level
SLH	Snowfall level height
SPOT	Satellite Pour l'Observation de la Terre
TRMM	Tropical Rainfall Measuring Mission
UGRH	Unidad de Glaciología y Recursos Hídricos
UNASAM	Universidad Nacional Santiago Antúnez de Mayolo, Huaraz
VPR	Vertical Profile of Reflectivity
WGMS	World Glacier Monitoring Service

Part I Synopsis

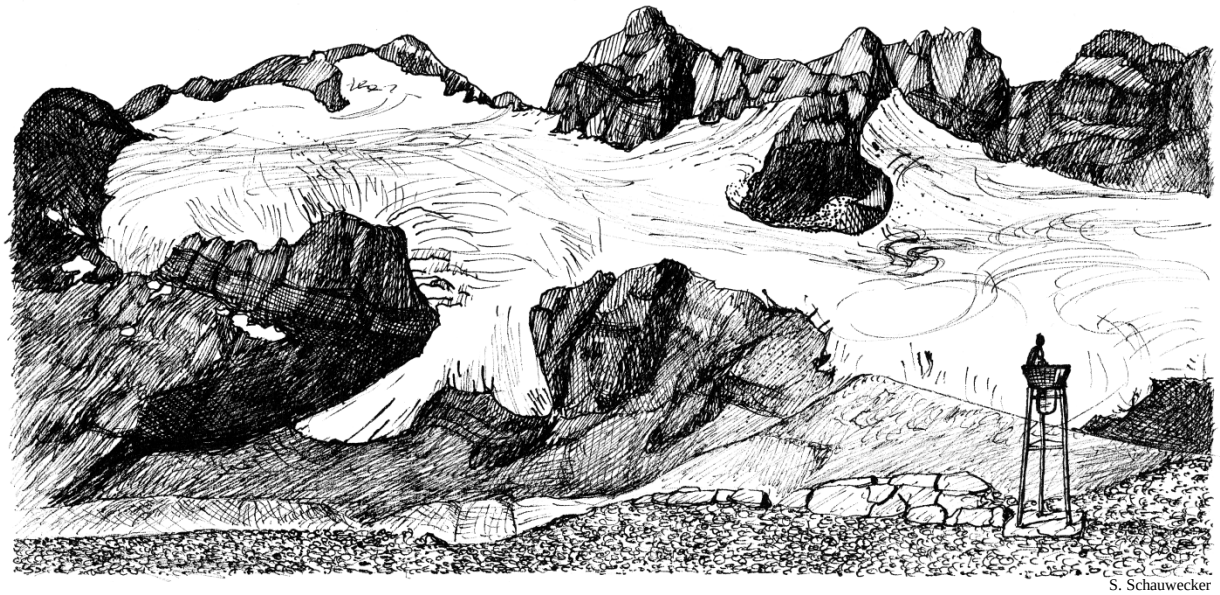

S. Schauwecker

1 Introduction

This thesis was developed within the framework of two projects on climate change adaptation, both funded by the Swiss Agency of Development and Cooperation (SDC): The Indian Himalayas Climate Adaptation Programme (*IHCAP*) and the project *Glaciares 513*, followed by *Glaciares+* since 2015. A focus of both projects lies on improving the knowledge of a changing climate and shrinking glaciers and strengthening capacities of local institutions and specialists in finding adaptation measures. To achieve these goals, existing knowledge is shared and exchanged between Swiss and Indian and Peruvian institutions, respectively. Important knowledge gaps are identified and addressed in a number of studies on glacier and climate related topics. In this context, this thesis was focusing on relevant research questions in both regions, the Indian Himalaya and the Peruvian Andes.

1.1 Motivation

The warming of the climate system is unequivocal and there is no doubt that many of the observed changes during the last century are unprecedented over decades to millennia (*IPCC*, 2013). Changes in glacier extents are noticeable for everybody and it is recognized by a broad public that rising temperatures lead to increased ice melt. The relation between climatic warming and melting glaciers, together with the sensitive response of glaciers to changes in precipitation and air temperature, make glaciers very reliable and unequivocal indicators (e.g. *Hastenrath and Ames*, 1995; *IPCC*, 2001). They have been selected for this reason as a terrestrial Essential Climate Variable (ECV) by the Global Climate Observing System (*GCOS*, 2003).

Glaciers play a crucial role in the hydrological system of our Planet and have an important impact on the landscape, which is perceived and interpreted by people observing them (e.g. *Haeberli*, 2005; *Carey*, 2007; *Gagné et al.*, 2014). The rivers that originate in the high mountains of the Andes and Himalayas are among the largest river systems on Earth and large human populations depend on their water downstream (e.g. *Kaser et al.*, 2010; *Schaner et al.*, 2012). On a regional or local scale, glaciers and glacier changes in Peru and the Indian Himalaya are important since shrinking glaciers alter seasonal or annual water availability (e.g. *Baraer et al.*, 2012; *Kaser et al.*, 2010); societies downstream rely on fresh water from glacier melt for drinking water, hydropower or irrigation (e.g. *Xu et al.*, 2009; *Drenkhan et al.*, 2015; *Immerzeel et al.*, 2010); glacier shrinkage is related to changing hazards (e.g. *Reynolds*, 1992; *Carey*, 2005; *Vilímek et al.*, 2015); and glacier retreat

affects cultural, social and economic components for people in their vicinity (e.g. *Vergara et al.*, 2007; *Chevallier et al.*, 2011; *Allison*, 2015).

Due to the important role of glaciers around the world, the ongoing and projected changes in glacier volumes have led to concerns about water availability and glacier hazards in the future. An increasing number of climate change adaptation programs with a clear focus on water resources show that the challenge of adaptation to changes in the cryosphere has been recognized by high political levels (*Salzmann et al.*, 2014; *Rasul and Sharma*, 2015). The increasing need of adaptation measures requires high-mountain studies addressing climate change and glacier shrinkage – especially in data poor regions (*Viviroli et al.*, 2011).

Despite the increasing concern about impacts of shrinking glaciers, there is still limited knowledge of climate change and process understanding on climate-glacier interactions in high-mountain regions like the Tropical Andes or the Himalayas (*Bolch et al.*, 2012; *Rabatel et al.*, 2013; *Salzmann et al.*, 2014; *Fernández and Mark*, 2015). Climate change is not only global warming; also other components besides air temperature are changing, such as precipitation, humidity and wind. To study the glacier reaction to changes in these climate variables, the processes at the glacier surface have to be understood. Since the glacier mass and energy fluxes at the glacier-atmosphere interface are strongly influenced by surface characteristics, such as the snowline (e.g. *Rabatel et al.*, 2012), debris cover (e.g. *Scherler et al.*, 2011) or ice cliffs (e.g. *Winkler et al.*, 2010), their impacts have to be studied carefully. To address this knowledge gap, we have to define relevant key climate variables and understand how variations in these variables impact glacier volumes via the mass and energy balance.

One reason for missing studies on glaciers and interactions with climate in many regions is the sparse and sometimes controversial observational data (e.g. *Bradley et al.*, 2006; *Salzmann et al.*, 2009; *Diaz et al.*, 2014). In addition to political, financial and economic obstacles (e.g. *Beniston et al.*, 2012), measurements on remote glaciers around the world are logistically difficult. The term "remote" is relative and depends not only on the distance of the glaciers to a community, city or research institute, but also on the accessibility of the glacier that depends on infrastructure, political and social situation of the region and the hazard situation. However, spatially and temporally coherent and homogenous climate data are a prerequisite for studies on glacier and climate. Where high-resolution in-situ data are missing or sparse, other data sets have the potential to provide complementary information. For example, global climate model (e.g. *López-Moreno et al.*, 2014) and reanalysis data (e.g. *Hofer et al.*, 2010), as well as remote sensing data (e.g. *Scheel et al.*, 2011) are an essential basis for various applications in climate and glacier research where in-situ measurements are sparse. The main advantage of these products is their global or regional coverage and temporal and spatial resolution, which is expected to further increase in the future. For climatological and glaciological studies in mountainous regions it is therefore crucial to assess the potential and limitations of these data sets.

1.2 Objectives and research questions

There are still important knowledge gaps in understanding climate-driven glacier surface processes and the response of glaciers to changes in key climate variables in data scarce high-mountain regions. Figure 1 illustrates the main objective and the individual research questions of this thesis, as well as data used in the four studies.

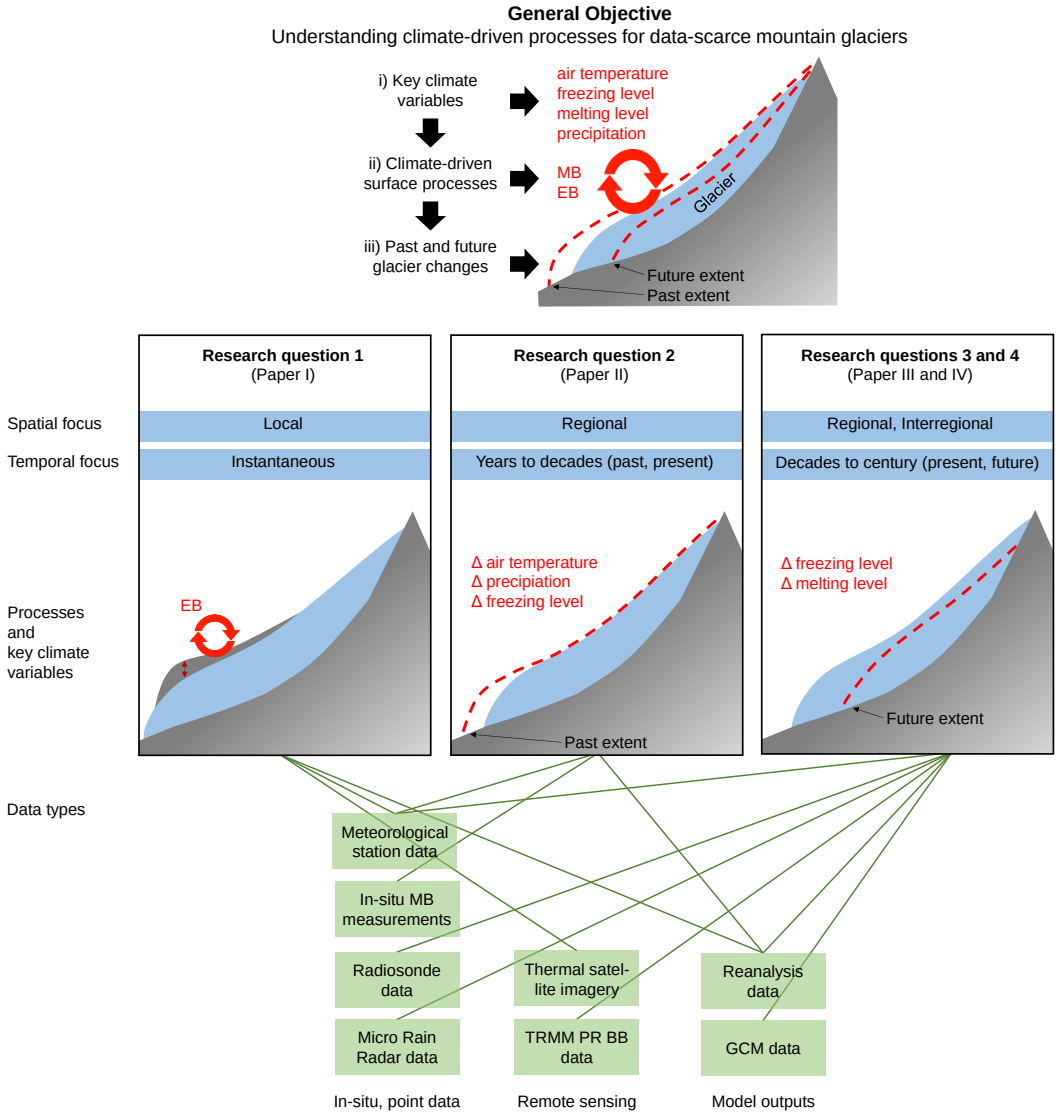

Figure 1 A schematic overview of the general objective (top) and specific topics at different temporal and spatial scales, the key climate variables and climate-driven processes (middle) and the data used in the different studies (green). EB: Energy balance; MB: Mass balance; GCM: Global Climate Model; TRMM PR BB: Tropical Rainfall Measuring Mission Precipitation Radar bright band).

The main scope of this thesis is to contribute to an improved understanding of climate-driven surface processes for data-poor high-mountain glaciers (Figure 1, top). It involves three main steps: i) defining key climate variables and assessing their changes, ii) studying climate-driven surface processes (mass and energy balance) and iii) developing approaches to understand and discuss past and future glacier extents. The four main research questions were developed for different temporal and spatial foci (Figure 1, middle). A further goal was to apply and evaluate data of different "remoteness": in-situ (meteorological station data, radiosondes, Micro Rain Radar) and reanalysis, global climate model and remote sensing data sets (Figure 1, bottom).

The four research questions are:

Research question 1: How can supraglacial debris thickness be estimated using an energy balance model?

The first research question focuses on the local processes at the debris-atmosphere interface. A recently developed method has the potential to derive debris thickness based on the energy balance at the debris-atmosphere interface and thermal images. The main scope was to further develop this approach and evaluate the performance and uncertainty that arises when applying it to a debris-covered Himalayan glacier where detailed field measurements are sparse. The final goal was to derive a map of debris thickness.

Research question 2: What are recent trends in precipitation and air temperature in the Cordillera Blanca and what is the relation of these trends to observed glacier changes in the last decades?

Several studies have focused on changes in air temperature at regional scales, but no detailed study was available addressing the changes in climate in the Cordillera Blanca. Therefore, it is unclear how the key climate variables (air temperature and precipitation) have changed since the 1960s and how these trends have evolved in these 50 years. A further goal was to discuss glacier shrinkage in view of the observed changes in climate using different approaches.

Research question 3: Are remotely sensed data suitable for estimating the snow/rain transition in mountainous regions?

The snowfall level is another key climate variable influencing glacier mass balance of high-mountain glaciers. The third research question focuses on a data product from TRMM Precipitation Radar, the bright band, which has the potential to serve for snow/rain transition estimations. The applicability of TRMM Precipitation Radar bright band data in a high mountain region in Kashmir, India, is analyzed and the limitations and uncertainties of extrapolation techniques based on constant temperature lapse rates to estimate the snow/rain transition are assessed.

Research question 4: What is the present-day and future freezing level and how could a future rise in the freezing level affect glacier extents?

Tropical glaciers in Peru react strongly to changes in the freezing level, mainly via the snowfall level, surface albedo and net shortwave radiation. The focus of the last paper was to assess the freezing level and snow/rain transition over the two most glacierized mountain ranges in Peru, the Cordillera Blanca and the Cordillera Vilcanota, based on multiple data sources. The rise in the freezing level until the end of this century is evaluated based on climate model projections for different greenhouse gas emissions scenarios and, glacier extents by the end of this century are estimated and discussed.

1.3 Organization of the thesis

This thesis is structured in three parts: *Part I* provides a synopsis of the thesis. After a general introduction and the presentation of the research questions (*Chapter 1*), the thematic and scientific background related to the research questions is reviewed (*Chapter 2*). Then, the methods and results of the research papers are summarized (*Chapter 3*) and the main findings are discussed and evaluated in a broader context (*Chapter 4*). Finally, the synopsis is concluded and an outlook into future possible research in this field is presented (*Chapter 5*). *Part II* contains the four journal publications. *Part III* consists of the personal bibliography, the curriculum vitae and acknowledgements. The following four publications form the core of this thesis.

Paper I (Research question 1)

Schauwecker, S., M. Rohrer, C. Huggel, A. Kulkarni, AL. Ramanathan, N. Salzmann, M. Stoffel, and B. Brock (2015). Remotely sensed debris thickness mapping of Bara Shigri Glacier, Indian Himalaya. Journal of Glaciology, 61(228), 675-688.

Contributions of the PhD candidate: Conception and design of the work, further developing the method presented by *Foster et al.* (2012), developing methods to estimate wind speed and energy fluxes as well as vertical temperature profiles, analysis and interpretation of meteorological data, model implementation in MATLAB, designing and conducting sensitivity and uncertainty analyses, drafting and writing the article

Paper II (Research question 2)

Schauwecker, S., M. Rohrer, D. Acuña, A. Cochachin, L. Dávila, H. Frey, C. Giráldez, J. Gómez, C. Huggel, M. Jacques-Coper, E. Loarte, N. Salzmann, and M. Vuille (2014). Climate trends and glacier retreat in the Cordillera Blanca, Peru, revisited. Global and Planetary Change, 119, 85-97.

Contributions of the PhD candidate: Conception and design of the work, developing the homogenization method, data analysis and interpretation, developing approaches to discuss the glacier imbalance and shrinkage, drafting and writing the article

Paper III (Research question 3)

Schauwecker, S., M. Rohrer, M. Schwarb, C. Huggel, A. P. Dimri, and N. Salzmann (2016), Estimation of snowfall limit for the Kashmir Valley, Indian Himalayas, with TRMM PR Bright Band information, Meteorologische Zeitschrift, 25, 501-509.

Contributions of the PhD candidate: Conception and design of the work, analysis and interpretation of TRMM Precipitation Radar and meteorological station data, drafting and writing the article

Paper IV (Research question 4)

Schauwecker, S., M. Rohrer, C. Huggel, J. Endries, N. Montoya, R. Neukom, B. Perry, N. Salzmann, M. Schwarb, and W. Suarez. (2016). The freezing level in the tropical Andes, Peru: an indicator for present and future glacier extents. Journal of Geophysical Research – Atmospheres, in review.

Contributions of the PhD candidate: Conception and design of the work, analysis and interpretation of multiple data sets, developing an experiment to relate freezing level height to glacier extents, drafting and writing the article

2 Thematic and scientific background

In the following chapter, the study sites and the role of glaciers in the natural and social environment are described. Furthermore, main climate-driven surface processes of tropical and debris-covered Himalayan glaciers and key climate variables are reviewed and finally, the different data sets are presented. Both study regions are highly glacierized and provide substantial water resources to downstream communities. In both regions, water availability is expected to decrease in the future calling for adaptation measures, but data are scarce at the elevations of glaciers and process understanding is still limited.

2.1 Study sites

2.1.1 Climate and glaciers in the Western Himalaya, India

The two study sites lie in the Western Himalaya (Figure 2). The Kashmir Valley is located in the state Jammu and Kashmir, Bara Shigri glacier is located in Himachal Pradesh.

The highly debris-covered Bara Shigri Glacier is the largest glacier of Himachal Pradesh (*Dutt*, 1961; *Tiwari et al.*, 2012). The smaller Chhota Shigri glacier in the west (not studied here) is a benchmark glacier for process-understanding in this part of the Himalayan range (*Kumar et al.*, 1987; *Wagnon et al.*, 2007; *Azam et al.*, 2014). Both glaciers are located in the Chenab basin, a main tributary of the Indus river. The median elevation of the glacier-covered area is 5060 m asl. and about 16% of the glacier area is debris covered (*Frey et al.*, 2012).

The average elevation of the Kashmir valley is 1600 m asl. and the surrounding mountains rise higher than 4000 m asl. The climate of Kashmir Valley is temperate and characterized by wet and cold winters and relatively dry and moderately hot monsoon seasons (*Kumar and Jain*, 2010). On average, the total annual precipitation sum is ~700 mm. Similar to the climate of the Chenab basin, the Kashmir valley is characterized by a relatively high amount of rain and snowfall in winter due to the western disturbances and summer precipitation events caused by the southwestern monsoon. Radiosonde observations show that the 0°C isotherm ranges from 2300 to 5100 m asl. during the monsoon season and from 250 to 1600 m asl. during winter (*Mondal and Sarkar*, 2003).

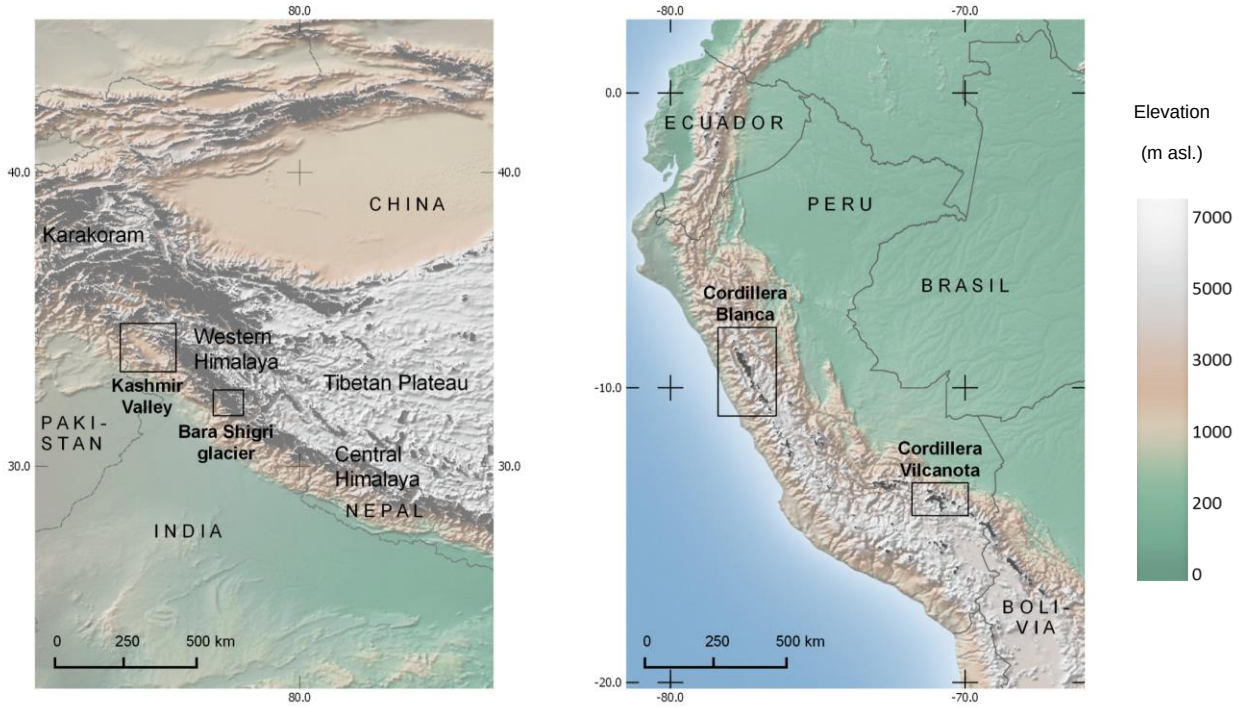

Figure 2 Overview map of the study areas (left) Bara Shigri glacier and Kashmir Valley and (right) Cordillera Blanca and Cordillera Vilcanota. Country boundaries and the DEM are from *Natural Earth* (2016), glacier outlines (grey) from the Randolph Glacier Inventory (RGI, *Pfeffer et al.*, 2014).

2.1.2 Climate and glaciers in the Central Andes, Peru

Peru hosts about 70% of the total glacier area within the tropics (*Kaser et al.*, 1999). Most of the Peruvian glaciers are located in the Cordillera Blanca, Ancash region, followed by the Cordillera Vilcanota, Cusco region (Figure 2). Few large glacier tongues in the Cordillera Blanca reach down to less than 4500 m asl. (*Racoviteanu et al.*, 2008), whereas in the Cordillera Vilcanota, there are no glaciers below this elevation (*Salzmann et al.*, 2013). The highest peaks reach up to almost 6400 in both mountain ranges. The debris-covered area in the Cordillera Blanca is ~2.5-3% (*Silverio and Jaquet*, 2005; *Racoviteanu et al.*, 2008). In the Cordillera Vilcanota, debris cover is of little regional importance (*Salzmann, et al.*, 2013), however on a point scale, debris cover may have large effects on melt. The rock glaciers and debris-covered glaciers are currently not studied in much detail, with some exceptions such as studies on the Jatunraju glacier (formerly spelled Hatunraju; *Lliboutry*, 1977, 1986; *Emmer et al.*, 2015).

The Rio Santa drains the western part of the Cordillera Blanca and flows to the northwest into the Pacific, while the eastern part drains into the Amazon. The drainage system of the Cordillera Vilcanota is relatively complex, but all streams finally flow into the Atlantic. Similar to other glaciers in the world, glaciers of Peru are strongly retreating (e.g. *Kaser et al.*, 1990; *Hastenrath and Ames*, 1995; *Georges*, 2004, *ANA*, 2010; *Rabatel et al.*, 2013). For the Cordillera Vilcanota,

Salzmann et al. (2013) found a massive areal ice loss between 1962 and 2006 of 32%. This loss is comparable to the Cordillera Blanca, where approximately 22.4% of the glacier area has vanished between the 1970s and the 2003 (*Racoviteanu*, 2008, confirmed also by *ANA*, 2003).

The climate of the study regions is characterized by a pronounced seasonality mainly in precipitation, cloud cover and specific humidity (*Kaser*, 2001). The pronounced dry season spans from May to September, while the wet season is dominant in austral summer (*Kaser and Georges*, 1997). The seasonal distribution of precipitation is caused by the onset and demise of the South American monsoon system (*Garreaud et al.*, 2009). During the wet season, precipitation mainly results from easterly winds transporting moisture from the Amazon Basin and the Atlantic (*Garreaud et al.*, 2003). In contrast to the strong seasonality in precipitation, the region is characterized by a low variability in air temperature throughout the year.

Similar to other regions around the world, air temperature has been rising in the last decades. For the area of the Cordillera Blanca, *Mark and Seltzer* (2005) reported a temperature increase of 0.39°C per decade between 1951 and 1999 and less warming of 0.26°C per decade between 1962 and 1999. In the Cordillera Vilcanota, for the period 1965-2009, air temperature trends are about 0.2° per decade (based on NCEP/NCAR reanalysis data), while station data show lower trends (*Salzmann, et al.*, 2013). Precipitation changes are more difficult to document than temperature trends because of missing station records (*Rabatel et al.*, 2013). Since precipitation is characterized by a large spatial variability, no clear pattern of increasing or decreasing precipitation can be found on a regional scale for the tropical Andes (*Vuille et al.*, 2003).

Due to the strong seasonality in precipitation, mass accumulation mostly occurs during the wet season (*Kaser et al.*, 1990; *Kaser*, 2001). During the dry season, there is only little or no accumulation and also ablation is reduced (*Kaser*, 2001). A typical characteristic of tropical glaciers in Peru is the almost constant vertical mass balance gradient above the 0°C level. Gradients below this elevation are markedly higher compared to glaciers in the Alps (*Kaser*, 1995; *Kaser*, 2001; *Sicart et al.*, 2011). This causes that the Accumulation Area Ratio (AAR) is typically higher (e.g. assumed to be 75% by *Kaser and Georges*, 1997) and the reaction of the glacier terminus to a shift in the Equilibrium Line Altitude (ELA) is stronger (*Kaser*, 1999).

2.1.3 The role of glaciers in the environment

Studies on glaciers in the tropical Andes and Western Himalaya are often motivated by the crucial role of glaciers in runoff production or natural hazards. In this section, the role of glaciers for the environment and societies in the study regions is unraveled. The importance of glaciers in the study regions is described by reviewing 1) the role of glaciers in the hydrological cycle; 2) impact of changing glaciers on sea level rise; 3) natural hazards linked to glaciers and 4) economic, social and cultural aspects.

Glaciers in the hydrological cycle

Most studies on glaciers in Peru mention the crucial role of meltwater production especially during the dry season. Several studies have shown that the contribution of meltwater from glaciers for catchments in the Cordillera Blanca is remarkable, in the order of 10 to 40% (*Mark and Seltzer*, 2003; *Mark et al.*, 2005; *Schaner et al.*, 2012). For the upper Indus basin (5% glacierized area), *Lutz et al.* (2014) found a similar number of approximately 40% glacier melt of total runoff, whereas *Kaser at el.* (2010) suggest a smaller contribution. The contribution is difficult to quantify and depends on several factors such as proportion of glacier area to catchment size, geology and seasonal climatic conditions (*Salzmann et al.*, 2014). The discharge downstream is modified by various processes that are difficult to quantify (e.g. by precipitation, evaporation, irrigation, damming or exchanges with subsurface flow regimes and groundwater).

Glacier changes affect the hydrological cycle depending on the annual mass balance: compared to a glacier in equilibrium, a positive annual mass balance budget causes a runoff deficit, whereas a negative annual mass budged yields a surplus of runoff from glacier ice. Once glaciers have vanished or reached a new equilibrium, this surplus of runoff is missing downstream and can lead to severe water shortages. The point where the annual runoff is highest due to a high recession rate of glacier ice is often called "peak water" (e.g. *Baraer et al.*, 2012; *Carey et al.*, 2014; *Huss et al.*, 2014; *Salzmann et al.*, 2014). If glaciers vanish in the future, the annual hydrographs of these catchments evolve towards that of a similar glacier free catchment. *Lutz et al.* (2014) projected an increase in runoff until 2050 for the Indus basin, caused primarily by accelerated glacier melt. In most catchments in the Cordillera Blanca, the peak discharge might be already over (e.g. *Baraer et al.*, 2012; *Bury et al.*, 2013; *Carey et al.*, 2014), however these estimations are subject to large uncertainties (discussed also in *Section 4.3*).

One further important aspect of the presence of glaciers in a catchment is the seasonal delay of runoff. Glaciers can act as temporal buffers of discharge, releasing melt water with a certain delay (e.g. *Kaser et al.*, 2003). The runoff contribution of glacier ice is decreasing downstream the catchment, and thus, also the buffering effect and the total glacier contribution get less important. This buffer function is especially important where the local climate is characterized by distinct wet and dry seasons and where rivers enter seasonally arid regions, as e.g. in the Peruvian Andes (*Kaser et al.*, 2010). At the outlet of the Rio Santa, at the dry Pacific coast, the glacier contribution during the dry season is probably more than 30% (*Kaser et al.*, 2010). In contrast, the seasonal delay is negligible, where the lowlands are governed by monsoon climates. In the Indus catchment, the timing of maximum discharge coincides with the precipitation intensive monsoon months (*Lutz et al.*, 2014) and the glacier contribution is probably less than 10% at high elevations. Nevertheless, glacier melt can still be crucial for high-mountain communities (*Kaser et al.*, 2010). In the future, it is likely that the hydrological cycle will change, due to the lack of the glacial buffer during the dry season (*Barry and Seimon*, 2000; *Barnett et al.*, 2005; *Francou and Coudrain*, 2005; *Bradley et al.*, 2006; *Vuille*, 2006).

Sea level rise

The total volume of tropical and Himalayan glaciers is considerably smaller compared to glaciers in high latitudes (Antarctica, Arctic Canada or Alaska), as well to the Greenland and Antarctic ice sheets. *Radić and Hock* (2011) estimated that the contribution of glaciers in South America (0°-30°) is negligible, while the sea level equivalent of the Western Himalaya is estimated 1.2-1.8 mm (*Frey et al.*, 2014).

Glacier hazards

Where glaciers shrink, the number and volume of potentially hazardous lakes may increase. Unstable ice-cored moraines of moraine-dammed lakes can collapse and thus have the potential to burst and produce glacier lake outburst floods (GLOFs, e.g. *Richardson and Reynolds*, 2000; *Schwanghart et al.*, 2016). Additionally, ice-rock avalanches falling into rock-dammed lakes can produce catastrophic events, as recorded e.g. in the Cordillera Blanca (*Carey et al.*, 2012; *Schneider et al.*, 2014; *Schaub et al.*, 2015). It is therefore indispensable to anticipate the formation of new lakes due to shrinking glaciers (*Francou and Coudrain*, 2005, *Hegglin and Huggel*, 2008).

Economic, social and cultural aspects

Many studies mention the important role of glaciers in watershed hydrology, since water from glaciers is used downstream for various human activities like agriculture, industry, hydropower and drinking water (e.g. *Lynch*, 2012). Currently, in the Ancash and Cusco regions, about 55% and 24% of the total area for agriculture is irrigated, respectively, and in the last two decades, the total irrigated area has increased (*Drenkhan et al.*, 2015). Runoff from glaciers in the Peruvian Andes is also used for hydropower generation (e.g. hydroelectric plant in Cañón del Pato in the catchment of the Cordillera Blanca and Machupicchu downstream the Cordillera Vilcanota). Similarly, in the Himalayas, the number of hydropower projects is increasing (*Schwanghart et al.*, 2016) and glacier shrinkage will affect irrigation and hydropower (*Bolch et al.*, 2012).

Beyond economic costs, glacier retreat will also have significant social and cultural costs for people living in the vicinity (*Vergara et al.*, 2007; *Gagné et al.*, 2014). *Williams and Nash* (2006) state that prominent mountains in the Andes are revered as earthly spirits that do not only protect, but also punish local populations. These local deities are called *apu* and were often linked to distant ancestors. For people living close to glaciers, glacier shrinkage is therefore not only a physical process, but also has important implications for the ways that they understand themselves and make meaning in relation to their surroundings (*Allison*, 2015). E.g. locals in the vicinity of the Cordillera Vilcanota have observed the decline of the mountaintop glaciers and a change in runoff and wonder what they have done to cause the fury of the deity and why they are limiting the runoff (*Bolin*, 2009). Similarly, people in the Himalayas from Buddhist societies believe that deities reside on mountaintops to distance themselves from the squalor and pollution of human life (*Allison*, 2015).

To summarize, glaciers are especially important in the study regions, since several of the following criteria are fulfilled:

- glacier meltwater plays a crucial role in runoff (e.g. total annual volume, seasonal contribution, surplus due to vanishing ice)
- runoff is altering under climate change, causing – at least for some seasons – a significant decrease in runoff
- glacier shrinkage contributes substantially to sea level rise
- glacier retreat is related to increasing hazard potential and people are affected by these hazards
- local communities depend on glacier fed rivers for activities such as irrigation, hydropower and tourism
- glaciers have a spiritual significance to people living in the vicinity
- the possibilities to adapt to changes are limited

The importance, however, depends strongly on the site and may be highly variable in space.

2.2 Climate-driven glacier surface processes

Given the present shifts and trends in climate variables, it is crucial to understand glacier surface processes and their relation to climate. Glacier surface processes are here defined as processes that either reduce or add mass or energy to the glacier. Besides surface accumulation and ablation, also other processes contribute to the glacier-wide mass balance such as internal and basal accumulation or calving (*Cogley et al.,* 2011), but the focus of this thesis lies only on the processes that happen at the glacier surface.

The expression "climate-driven glacier surface processes" is used and not "glacier-climate interactions", since the influence of glaciers on climate was not studied. An interaction is defined by an effect that has one to another, the effects being of a reciprocal nature. Even if e.g. *Kuhn* (1981) stated that glaciers of the mid latitudes and tropics have comparatively little effect on the atmosphere compared to large glaciers and ice sheets, and their interaction with climatic elements is restricted to their immediate surroundings, local impacts of glaciers on the local climate are not negligible.

2.2.1 Glacier mass balance

Mass balance is defined as the change in the mass of a glacier (or part of it) over a stated span of time (*Cogley et al.*, 2011). Ablation is defined as all processes that reduce the mass of a glacier and the mass lost by the operation of these processes (*Cogley et al.*, 2011). Here, ablation is defined as surface ablation, although internal ablation, basal ablation or frontal ablation (e.g. calving) can be significant in other contexts. Ablation is mainly dominated by melt, but also sublimation plays an important role in the tropical Andes, especially during the dry season (e.g. *Wagnon et al., 1999*;

Francou et al., 2003; *Favier et al.*, 2004a, 2004b; *Winkler et al.*, 2009; *Gurgiser et al.*, 2013a). Accumulation is defined as all processes that add to the mass of the glacier and the mass gained by the operation of any of these processes (*Cogley et al.*, 2011). Here, it is referred to accumulation as any solid precipitation adding mass at the glacier surface. For the topical Andes of Peru, the main types of solid precipitation are snow and graupel (*Poremba et al.*, 2015). Precipitation was defined in this work as key climate variable, since it has the potential to counter or balance increased ablation due to e.g. increased air temperatures.

2.2.2 Energy balance of a dry debris-covered glacier surface

In this section, the importance of supraglacial debris in glacier-atmosphere mass and energy fluxes is explained and the energy balance of a dry debris surface under clear-sky conditions is presented, since it was used to estimate debris thickness in *Paper I*.

Supraglacial debris alters the glacier energy and mass fluxes at the atmosphere–glacier interface (e.g. *Brock et al.*, 2007; *Collier et al.*, 2015). Several studies have shown relations between debris thickness and ablation rates of the ice beneath (e.g. *Östrem*, 1959; *Nakawo and Young*, 1981; *Mattson et al.*, 1993; *Kayastha et al.*, 2000; *Han et al.*, 2006; *Mihalcea et al.*, 2006; *Takeuchi et al.*, 2000; *Nicholson and Benn*, 2006; *Kellerer-Pirklbauer et al.*, 2008; *Mihalcea et al.*, 2008b; *Brock et al.*, 2010; *Reid and Brock*, 2010; *Lambrecht et al.*, 2011). Where ice is covered with very thin debris, melt is enhanced compared to clean ice as a result of increased absorption of solar radiation due to lower albedo and the related rapid heat transfer. On the other hand, melt rates are reduced where debris is thicker than a few centimeters, as less surface heat will be conducted through the debris layer and transferred to the ice as compared to ice without debris cover. Hence, from a hydrological perspective, it is crucial to know where debris is thin enough to enhance melt or above a critical thickness to reduce melt compared to a bare-ice surface. Improved knowledge of the response of glaciers to climate change and climate-debris feedbacks are essential for the quantification of glacier runoff as well as for present and future water availability (*Wagnon et al.*, 2007; *Brock et al.*, 2010; *Zhang et al.*, 2011; *Reid et al.*, 2012; *Lejeune et al.*, 2013; *Juen et al.*, 2014). This is why both, the debris-covered area and debris thickness are critical variables for melt. Glaciers with extensive mantles of supraglacial debris on their ablation areas are widely present in many high mountain ranges including the Himalayas (e.g. *Nakawo et al.*, 1986; *Scherler et al.*, 2011; *Bolch et al.*, 2012; *Frey et al.*, 2012). Debris-cover is less common in the Peruvian Andes, but some glaciers have debris-covered tongues (e.g. *Silverio and Jaquet*, 2005). In the Himalayas, an expansion of sediment and rock covered areas has been observed in recent decades. This is mostly due to glacier surface lowering and unstable adjacent slopes, two processes which are likely associated with climate change (*Bolch et al.*, 2008; *Schmidt and Nüsser*, 2009; *Shukla et al.*, 2009; *Bhambri et al.*, 2011).

The energy balance equation describes that the change in heat stored within a defined volume of debris is equal to the sum of all fluxes towards the debris volume, for a dry debris-covered dry surface given by:

$$\Delta D = S_{net} + L_{net} + H + G$$

where (ΔD) is the rate of change in heat stored within debris, S_{net} is net shortwave radiation, L_{net} is net longwave radiation, H is the sensible turbulent heat flux and G the conductive heat flux. Energy contribution provided by rain and latent heat are neglected for a dry debris surface. The debris layer can be broken down into several layers (e.g. *Reid and Brock*, 2010; *Rounce et al.*, 2015), or treated as a single volume (e.g. *Foster et al.*, 2012). For solving the energy balance, the single energy fluxes have to be estimated. A detailed description of the method used in *Paper I*, the estimation of the fluxes, debris properties and meteorological conditions can be found in *Part II Section 1.4*.

2.2.3 Energy balance of tropical glaciers

In the following, a brief summary of the energy balance of tropical glaciers is given, highlighting the most important components and key climate variables. The most important climate-driven energy fluxes are net shortwave and longwave radiation, as well as turbulent fluxes. Other fluxes like conductive heat or ground penetrating flux of solar radiation are not discussed here.

Net shortwave radiation

Net shortwave radiation is the main source of energy for melting snow and ice of low latitude glaciers (e.g. *Favier et al.*, 2004a, 2004b; *Mölg and Hardy*, 2004; *Sicart et al.*, 2005; *Wagnon et al.*, 2009; *Gurgiser et al.*, 2013a, 2013b). Since shortwave radiation is the largest source for energy, the energy balance of tropical glaciers is especially sensitive to parameters related to the shortwave energy budget (e.g. *Favier et al.*, 2004b; *Mölg and Hardy*, 2004; *Gurgiser et al.*, 2013b). A key parameter is surface albedo (ratio of incoming to outgoing shortwave radiation). The albedo of snow is much higher compared to a bare ice glacier surface, especially when there are dust and light-absorbing impurities like mineral dust or black carbon at or near the ice surface. Hence, it is essential to know whether the glacier is covered by snow or bare ice. Generally, the term "snowline" is used to divide the glacier into a snow-covered higher part and a snow free tongue. Surface albedo is determined by different climatic variables such as air temperature during precipitation events (determining the snowfall level and the snowline), mean air temperature and precipitation amount. The snowline can e.g. be used as an indicator of the equilibrium line (*Rabatel et al.*, 2012).

Freezing and snowfall level

In *Paper III* and *Paper IV*, two closely related variables were assessed: the freezing level and the snowfall level during precipitation events. The snowfall level is a critical parameter in hydrological modeling of high-elevation catchments where precipitation phase may be solid (snow and graupel) or liquid (rain). The freezing level is interesting in view of climate change and related glacier shrinkage (e.g. *Wang et al.*, 2014). The freezing level (also called free air 0°C isotherm) is defined as the lowest level in the free-atmosphere where the temperature is 0°C (*American Meteorological Society*, 2016; Figure 3b). The melting level is defined as the top of the melting layer during precipitation events, which is the altitude throughout solid precipitation melts as it descends (*American Meteorological Society*, 2016; Figure 3b). The temperature of the melting layer is

typically 0°C or warmer (*American Meteorological Society*, 2016). The term snowfall level is defined as the altitude above sea level at which precipitation falls as snow which is deposited on the ground, usually some hundreds meters below the freezing level (*EAWS*, 2016). Although, it has to be considered that the transition from solid to liquid precipitation does not happen at a certain altitude but within a layer of several hundred meters (within the melting layer) and solid precipitation frequently occurs as graupel instead of snow in the tropical Andes. According to literature, it is here refered to freezing level height and snowfall level height as the vertical distance between the freezing and snowfall level and the mean sea level, but also the term freezing level altitude is sometimes used and probably more accurate according to the definitions by *McVicar and Körner* (2013).

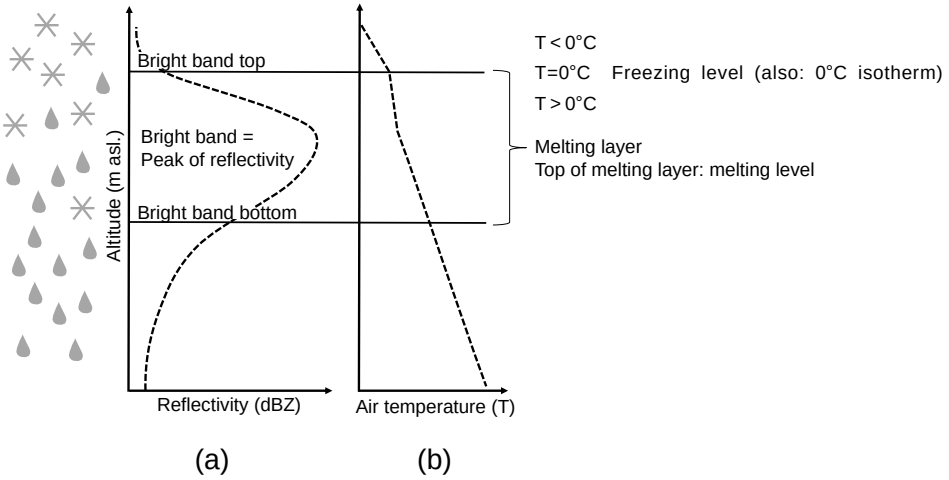

Figure 3 Schematic of vertical profiles of (a) reflectivity and (b) air temperature during a precipitation event and terminology.

The bright band is the radar signature of the melting layer, visible as a narrow horizontal layer of stronger radar reflectivity in precipitation at the altitude in the atmosphere where snow melts to rain (Figure 3a, *American Meteorological Society*, 2016; *Paper III* and *Paper IV*). The bright band typically lies some hundred meters below the freezing level (*Harris et al.*, 2000, *Paper III*, *Paper IV*), due to the dielectric properties during the melting process. Mean melting layer height information might therefore be used as a proxy to estimate the snow/rain transition during particular stratiform precipitation events.

This close link between air temperature during precipitation, albedo and net shortwave radiation leads to a high sensitivity of tropical glaciers to air temperature, especially observable for the inner tropics and Peruvian glaciers (*Kaser*, 2001; *Vuille et al.*, 2008a; *Gurgiser et al.*, 2013a). For example, *Gurgiser et al.* (2013a) showed that the glacier mass balance of Shallap glacier (Cordillera Blanca, Peru) varied significantly within two years due to different air temperature and related snowfall levels, mainly during the wet season. While the mass balance in the accumulation area (>5000 m asl.) was similar in both years due to similar annual total solid precipitation, the

difference in mass balance was considerable for the lower part of the glaciers. The freezing level and the strongly coupled snowfall level are thus crucial variables in accurately determining mass balance and runoff of Peruvian glaciers in hydro-glaciological models. Both parameters - freezing and snowfall level - are important for understanding climate-related glacier surface processes and are therefore here defined as key climate variables.

Other energy fluxes

Mean net longwave radiation is negative and balances out large part of the net shortwave radiation (e.g. *Gurgiser et al.*, 2013a) and it is thus the main sink of energy (*Favier et al.*, 2004b). After net shortwave radiation, sensible heat flux is the next largest source of energy (*Gurgiser et al.*, 2013a). Turbulent sensible heat is countered by the heat sink through sublimation (e.g. *Favier et al.*, 2004b; *Gurgiser et al.*, 2013a), which plays an important role for ablation of tropical glaciers, especially during the dry season (e.g. *Winkler et al.*, 2009). Despite the important role of these energy fluxes, the focus of this work lies mostly on net shortwave radiation.

Inner and outer tropics

In Literature, a distinction between the inner tropics and outer tropics is typically made (e.g. *Troll*, 1941; *Rabatel et al.*, 2013). Glaciers of Ecuador and Colombia (e.g. Antisana 15) lie within the inner tropics, while glaciers in Bolivia (e.g. Zongo) are within the outer tropics. In the inner tropics, there is no clear seasonality in precipitation (e.g. *Francou et al.*, 2004), while the zone of the outer tropics is characterized by a clear wet (austral winter) and dry (austral summer) season, and a clear seasonality in cloud cover and specific humidity. Several studies have shown that temperature sensitivities are greatest in the inner tropics, while, in the outer tropics, the moisture content of the atmosphere (precipitation, cloudiness, specific humidity) becomes more important (e.g. *Favier et al.*, 2004a; *Sagredo et al*., 2014). *Favier et al.* (2004a) found that the interannual variability in ablation on Antisana 15 glacier in the inner tropics was mainly determined by variations in air temperature, determining the snowline altitude. In contrast, in the outer tropics, the freezing level is clearly below the glacier equilibrium line altitude (ELA), which means that liquid precipitation on glaciers is rare and therefore the sensitivity of interannual mass balance is more closely related to the variability in precipitation amount. Glaciers in Peru lie between these two main zones and it is still no consensus in literature, whether these glaciers are more similar to glaciers in the inner or outer tropics. *Rabatel et al.* (2013) classified glaciers in Peru together with glaciers in Bolivia as outer tropics, since there is a clear wet and dry season, similar to Bolivia. A study by *Gurgiser et al.* (2013a) has shed some light on the energy balance of a glacier in the Cordillera Blanca and they found that the glacier mass balance is very sensitive to air temperature and the snow line altitude, which is a feature more similar to the regime of the inner tropics.

2.3 Data

2.3.1 Data scarcity

Many studies are motivated by scarcity or lack of in-situ data in high-mountain environments (e.g. *Bradley et al.*, 2004; *Diaz et al.*, 2006; *Ragettli et al.*, 2013; *Salzmann et al.*, 2013; *Ochoa et al.*, 2014), but the term "scarcity" or "lack" is often not clearly defined and depends on the parameter and research question. While few but homogeneous and long-term records are needed for assessing climate change, a study on the energy balance over a glacier surface requires high spatial and temporal resolution data. In-situ data scarcity can be caused by missing data, but also by poor data quality or inaccessible existing data:

1) No data available

For many mountainous regions or catchments, there are no meteorological in-situ data available or the data density is very low due to various reasons: The access to high mountain regions is often difficult, expensive and time-consuming and it may be dangerous to work in these harsh environments due to low temperatures, rock falls, avalanches or altitude sickness.

2) Data are available but have a limited quality or temporal coverage

For some stations at high elevations, there are inhomogeneities (e.g. implausible jumps or trends) or data gaps due to instrument failure, station relocation and interruption of manual measurements owing to hostile weather or conflicts. Meteorological stations have to be maintained regularly in order to guarantee a high data quality of long duration: instruments need to be calibrated, broken instruments have to be replaced and stations on the glaciers have to be repositioned. The maintenance involves a lot of time and financial resources. However, if a project is funded for only some years, meteorological stations are often abandoned or dismantled after the project duration. Moreover, the purpose meteorological stations can be misinterpreted by local communities or destroyed on purpose, if they feel it represents a threat to them (e.g. *Juen*, 2006).

3) Data are available but not accessible to researchers

For the research community, there may be various obstacles that hinder access to available data in many parts of the world (*Beniston et al.*, 2012). The access to meteorological data from the public sector (e.g. hydropower or mining companies) or public institutions (e.g. national weather services) may be difficult due to administrative, institutional and financial obstacles. Meterological and hydrological data may even be classified as state secret in some regions.

The above named restrictions on data availability may have important impacts on climate and water related research and policy-making (*Beniston et al.*, 2012). Especially researchers from developing countries often face financial and institutional barriers to gather available data and to design new data networks. There are approaches to implement policies aimed at ensuring free and unrestricted access to data, especially to share data that are generated by numerous research projects in high-

mountain regions. Research platforms or data portals are promising tools to foster collaboration among scientists (e.g. *Schwarb et al.*, 2011, *Plataforma de Intercambio Científico*, 2016).

2.3.2 Meteorological station data

In this work, meteorological station data from different networks were used such as from meteorological services and universities as well as METAR weather information.

The national meteorological and hydrological service of Peru (SENAMHI) runs a network of conventional and automatic stations across the country and data are made available through their webpage. Manual measurements at the conventional stations are available at 07:00, 13:00 and 19:00 local time and daily maximum and minimum air temperature and precipitation is registered (used in *Paper II* and *Paper IV*). SENAMHI data have been used in numerous studies on climate and glaciers in the Peruvian Andes (e.g. *Vuille et al.*, 2008b; *Condom et al.*, 2011; *Schwarb et al.*, 2011; *Salzmann et al.*, 2013; *Mantas et al.*, 2015; *Gurgiser et al.*, 2016; *Mourre et al.*, 2016).

A network of 16 stations with hourly data was installed in the framework of the project Centro de Información e Investigación Ambiental de Desarrollo Regional Sostenible (CIIADERS) in the Ancash region of Peru and is now operated by the Universidad Nacional Santiago Antúñez de Mayolo (UNASAM) of Huaraz since 2012. Several parameters are measured, such as air temperature (used for *Paper IV*), precipitation, wind speed, air pressure and radiation. Data can be downloaded via their webpage (*CIIADERS*, 2016). To our knowledge, these data have been used in only one study by *Mourre et al.* (2016) until now.

METAR stands for Meteorological Aerodrome Report and is a format for reporting weather information (*NOAA*, 2016). These data are typically recorded at airports and permanent weather observation stations once every hour or half-hour. METAR data from the Cusco airport (Jorge Velasco International Airport, SPZO) have been used as a complement to SENAMHI stations in various studies (*Scheel et al.*, 2011; *Schwarb et al.*, 2011; *Perry et al.*, 2013) and here, in *Paper IV*.

In the Indian Himalaya, meteorological stations at high elevations are sparse (e.g. *Bolch et al.*, 2012). For the estimation of longwave and shortwave radiation fluxes, we used data from the Pyramid station (27.958°N, 86.813°E) located at an elevation of 5050 m asl. in the Khumbu valley (Nepal), near the Everest base camp. It is recording since 1990 and managed by the Ev-K2-CNR Committee (Italy) in collaboration with the Nepal Academy of Science and Technology. Moreover, we used data from the automated network maintained by the India Meteorological Department (IMD). We used air temperature and wind data from stations in Keylong (32.57°N, 77.03°E, 3119 m asl., *Paper I*) and Srinagar (34.08°N, 74.83°E, 1587 m asl., *Paper III*).

2.3.3 Radiosondes

The India Meteorological Department (IMD) is operating a network of radiosonde stations across the country (e.g. *Mondal et al.*, 2013; *Ansari et al.*, 2015). For *Paper III*, radiosonde data from Srinagar, India (34.08°N, 74.83°E, 1587 m asl.) were analyzed. Radiosondes are released normally

twice a day at 0 and 12 am, recording profiles of air temperature, but also other parameters like e.g. dew point, relative humidity, wind speed and direction.

2.3.4 Micro Rain Radar

For *Paper IV*, we used data from a vertically looking Micro Rain Radar (MRR) which was installed in the city of Cusco (13.5278°S, 71.9508°W) from August 2014 to February 2015 at the SENAMHI office 1 km north from the Airport. The MRR was part of a research project of B. Perry and colleagues from the Appalachian State University. The Micro Rain radar delivers information on the vertical profiles of precipitation and can be used to estimate the melting layer, which appears as a bright band - a layer of enhanced radar reflectivity caused by melting hydrometeors at the level where solid precipitation turns into rain. The Micro Rain Radar outputs include the vertical structure of the radar reflectivity, spectral width and Doppler velocity. The temporal resolution is 1 min and the vertical resolution 150 m.

2.3.5 TRMM Precipitation Radar

In mountainous regions, precipitation is difficult to measure because of the limited access and large spatial and temporal variations in precipitation. Since in-situ information on precipitation is sparse in many countries at high altitudes, space-borne estimations of precipitation are promising data to cope with this gap (e.g. *Condom et al.*, 2010; *Scheel et al.*, 2011; *Ochoa et al.*, 2014; *Mourre et al.*, 2016). The Tropical Rainfall Measuring Mission (TRMM) was a joint mission between NASA and the Japan Aerospace Exploration (JAXA) Agency with different scientific purposes such as advancing our understanding of processes related to precipitation. The TRMM satellite was collecting data during 17 years (1997 – 2015). The orbit of the TRMM satellite ranged between 35° north and south, thus including the tropical Andes and the Himalayas. One orbit lasted a bit longer than 90 minutes, resulting in about 16 orbits per day. The coverage and temporal and spatial resolution of satellite derived rainfall estimations are increasing in the future, as promoted by the International Global Precipitation Program (GPM), which follows the TRMM mission.

The TRMM mission provided different data sets which are not all used and described here. For the estimation of the snow/rain transitions (*Paper III* and *Paper IV*) we used the TRMM product 2A23, which provides the altitude of the bright band. The bright band can only be retrieved when precipitation is present at the time of the satellite overfly, which means that the availability is variable in time and space. Besides the TRMM product 2A23, we also used rainfall rate and type from the 2A25 product (*Paper III*) providing estimations of near-surface rain and rain type, as well as vertical reflectivity profiles. More details on the TRMM satellite can be found in *Kummerow et al.* (2000) and *Kozu et al.* (2001).

2.3.6 Thermal satellite imagery

ASTER surface kinetic temperature images (used in *Paper I*) were acquired from the Land Processes Distributed Active Archive Center (LPDAAC). For most scenes, surface temperature

can be derived within an accuracy and precision of ± 1.5 K (*Gillespie et al.*, 1998) and a spatial resolution of 90 m. From the Landsat 7 ETM+ satellite imagery, we used the thermal band (Band 6), which is acquired at 60-metre resolution and automatically processed to 30-metre pixels. Surface temperature is derived according to *NASA* (2011).

2.3.7 Reanalysis data

A reanalysis is a scientific method for developing a comprehensive record on weather and climate and its change over time. Meteorological reanalysis projects aim to assimilate historical climate observations (from the land surface, ships, rawinsondes, pibals, aircrafts and satellites) using a certain assimilation scheme. Reanalysis products typically extend over several decades and cover the entire globe. The products consist of different surface parameters, upper-air parameters covering the stratosphere and troposphere, vertical integrals of atmospheric fluxes and monthly averages of most of the parameters (e.g. *Dee et al.*, 2011). Table 1 gives an overview over the here used reanalysis products. There are several other reanalysis products which were not used for this work.

Table 1 Overview of the here used global reanalysis products.

Name	Source	Temporal vailability	Reference
ERA-40	ECMWF	1957 - 2002	Uppala et al. (2005)
ERA-Interim	ECMWF	1979 - present	Dee et al. (2011)
NCEP/NCAR	NCEP	1948 - present	Kalnay et al. (1996)
MERRA2	NASA	1980 - present	Rienecker et al. (2011)

2.3.8 Global Climate Models

Global Climate Models (GCMs) were used to assess the change in the freezing level by the end of this century over mountainous regions of Peru (*Paper IV*). Current and future in the freezing levels are taken from models which were part of the Coupled Model Intercomparison Project 5 (CMIP5, *Taylor et al*., 2011). We compared the runs representing present-day climate (1976-2005; “historical” experiment) to the climate by the end of 21st century (2071-2100), taking the most optimistic (low emissions) and pessimistic (high emissions) Representative Concentration Pathways (RCP) 2.6 and 8.5, respectively (*Moss et al.*, 2010). The RCP2.6 is called "peak-to-decay" scenario, in which radiative forcing reaches a maximum near the middle of the 21st century before decreasing to an eventual nominal level of 2.6 Wm^{-2} relative to pre-industrial conditions. Under RCP8.5, the radiative forcing is assumed to increase throughout the 21st century until reaching a level of 8.5 Wm^{-2} at the end of the century relative to pre-industrial conditions (*Taylor et al.*, 2011). We used a 24 member ensemble of CMIP5 model simulations (see *Part II, Section 4.9*).

2.3.9 Glacier outlines and mass balance measurements

For the study regions, few glaciological mass balance measurements based on stake and pit measurements exist (*Zemp et al.*, 2015). In Peru, mass balance measurements are collected on Yanamarey glacier and Artesonraju glacier, both located in the Cordillera Blanca (*WGMS*, 2015 and earlier issues). The existing mass balance data from these two glaciers were made available by the World Glacier Monitoring Service (WGMS, *WGMS*, 1989), and were used in *Paper II*.

Glacier outlines are obtained from the Global Land and Ice Measurements from Space (GLIMS, *Raup et al.*, 2007, see also *Racoviteanu et al.*, 2008), the Randolph Glacier Inventory (RGI, *Pfeffer et al.*, 2014) and the Unidad de Glaciología y Recursos Hídricos (UGRH) glacier database.

3 Summary of research papers

This thesis consists of four research papers, addressing questions on the main climate-driven surface processes on glaciers in the tropical Andes and the Indian Himalaya. *Paper I* is addressing the local and instantaneous energy balance of a debris-covered glacier, *Paper II* is focusing on recent changes in key climate variables and impacts on the glaciers at a regional scale, *Paper III* is focusing on the performance of the snow/rain transition estimations from remote sensing data, leading to *Paper IV*, where data from different sources are gathered to assess regional and interregional freezing and snowfall levels in the present and future. Below, the main aims, methods and results are summarized. The full version of the papers can be found in *Part II*.

3.1 Paper I

Remotely sensed debris thickness mapping of Bara Shigri Glacier, Indian Himalaya

Despite the important role of supraglacial debris in ablation, knowledge of debris thickness on Himalayan glaciers is still sparse. A recently developed approach based on reanalysis data and thermal band satellite imagery has been proven to be potentially suitable for debris thickness estimation without the need of detailed field data (*Foster et al.*, 2012). The main aim of this study was to further develop the approach in view of applying it to a debris-covered glacier in the Himalaya. The approach is based on the energy balance of the debris-atmosphere interface. Radiation and temperature effects are subtracted in order to estimate debris thickness as a function of surface temperature. The uncertainty introduced by single input parameters for debris properties, meteorological variables from reanalysis data and parameterizations of energy fluxes is assessed and the uncertainty of the results is evaluated as a function of debris thickness. Finally, debris thickness is mapped and the underestimation and uncertainty arising through the use of different assumptions is discussed.

Both incoming shortwave and longwave radiation are estimated with a reasonable accuracy when applying parameterizations and reanalysis data. Wind estimations from reanalysis data for the free-atmosphere are not correlated to local wind speed measured at meteorological stations in the Himalayas. A novel approach is therefore presented in this paper to estimate wind speed based on the analysis of meteorological data from a nearby station. The results indicate that an energy

balance approach is a valuable tool to remove effects from radiative fluxes and air temperature on surface temperature, in order to derive debris thickness as a function of surface temperature.

Without the further developed elements, the method would strongly underestimate the thickness of the supraglacial sediment. The improved model likely still underestimates debris thickness, probably due to incorrect representation of vertical debris temperature profiles, the rate of heat stored and the turbulent sensible heat flux. Moreover, the uncertainty of the result was found to increase significantly with thicker debris. This is a promising result, since uncertainty is lower for debris thicknesses below 2cm, which are most relevant for hydrological processes.

3.2 Paper II

Climate trends and glacier retreat in the Cordillera Blanca, Peru, revisited

The aim of this paper was to assess air temperature and precipitation changes in the Cordillera Blanca and to discuss how these key climate variables could have affected the observed glacier shrinkage between the 1980s and the present. Therefore, a unique set of meteorological station data was analyzed in combination with reanalysis air temperature and upper-air zonal wind component. A method to homogenize the data was developed and 30-year running trends were assessed.

Meteorological station data in the region of the Cordillera Blanca show that after a strong air temperature rise of about 0.31°C per decade between 1969 and 1998 with a shift in temperature in the 1970s, the warming was about 0.13°C per decade in the 30 years from 1983 to 2012. The observed recent near-surface air temperature trends are more consistent with NCEP/NCAR reanalysis data than ERA-Interim. In line with the air temperature increase, meteorological station data indicate that the freezing level height during precipitation days has probably not increased significantly in the last 30 years. There is even a cooling trend for maximum daily air temperatures, while the minimum temperature is increasing. Moreover, precipitation has increased by about 60 mm per decade since the early 1980s. The increase in precipitation can be explained by the enhancement of easterly winds, transporting humidity from the Atlantic and the Amazon basin towards the Andes.

The strong increase in precipitation in the last 30 years likely did not balance the effect of increasing temperatures before the 1980s. Moreover, it is suggested that recent changes in temperature and precipitation alone may not explain the glacial recession within the thirty years from the early 1980s to 2012. Measurements and estimates of ice thickness and annual ablation rates on Artesonraju glacier allow estimating a response time on the order of 10 to 40 years for large glaciers with distinct glacier tongues. Hence, the retreat of large glaciers observed over the past three decades may include a signal of the temperature increase before the 1980s. This means that large glaciers in the Cordillera Blanca may be still reacting to the air temperature rise before 1980. Especially small and low-lying glaciers are characterized by a serious imbalance and may disappear in the near future.

3.3 Paper III

Estimation of snowfall limit for the Kashmir Valley, Indian Himalaya, with TRMM PR Bright Band information

Knowing the snowfall level during precipitation events is crucial for understanding the glacier mass and energy balance and for estimating runoff from high mountain catchments. However, knowledge on altitudes of the phase change during precipitation events is limited by the small number of meteorological measurements available at high altitudes, such as the Himalayas. The bright band of satellite based radar data may be used as a proxy for the snow/rain transition during particular stratiform precipitation events over high mountain regions. The specific potential and applicability of Tropical Rainfall Measuring Mission (TRMM) Precipitation Radar (PR) bright band estimations in high mountain regions have not been evaluated so far. To assess the performance of bright band altitudes, we have compared a 17-year data set of bright band estimations detected by the TRMM PR 2A23 algorithm with radiosonde observations and meteorological station data. We first analyzed the spatial and temporal availability of TRMM PR bright band data in a high mountain region in Kashmir, India. Then, we compared bright band data to freezing level data derived from radiosonde records and from extrapolated ground-station data and finally presented seasonal and monthly variability in snow/rain transition and its relation to near-surface rain intensity.

During March to November, the bright band lies about 200 to 800 m below the freezing level recorded by radiosondes. The freezing level height extrapolated from a ground-based station is less strongly correlated with the bright band data than the radiosonde estimates. The correlation between the satellite and the station estimates depends on the timing of the air temperature measurement – an important finding for applying extrapolation techniques to estimate the snow/rain transition altitude in data sparse regions. Large are associated with the timing of the air temperature measurement, especially when the air temperature is measured before the precipitation event. Further on, we found a strong seasonal and monthly variability of the bright band altitude. Comparison with near-surface rain intensity from the TRMM PR product 2A25 indicates that - during intense monsoonal summer precipitation events - the bright band altitude is relatively low and concentrated between about 3500 and 4000 m asl., thus clearly below the mean glacier elevation.

It was concluded that TRMM PR bright band data deliver valuable complementary information for regional or seasonal variability in snow/rain transition in data sparse regions. Bright band data over mountainous regions and during winter are limited, since the snow/rain transition is relatively close to the surface, but bright band data from surrounding lowlands could be used to validate extrapolation approaches to assess the snowfall level for mainly stratiform precipitation events where stations at high elevations are missing.

3.4 Paper IV

The freezing level in the tropical Andes, Peru: an indicator for present and future glacier extents

Along with air temperature, the freezing level has risen over the last decades. The mass balance of tropical glaciers in Peru is highly sensitive to a rise in the freezing level, due to a related decrease of accumulation and increase of energy for ablation via albedo effects. Since in-situ meteorological data are scarce at altitudes where glaciers exist (>4800 m asl.), reliable freezing level and related snowfall level estimates are often missing. To fill this knowledge gap for the two most glaciered mountain ranges in Peru - the Cordillera Blanca and Cordillera Vilcanota - we assessed the present-day freezing and snowfall level and the spatiotemporal variability using multiple data sources. Freezing levels were derived from ERA-Interim and MERRA2 reanalysis data. Snowfall levels were derived from TRMM Precipitation Radar Bright Band data and estimated based on data from a Micro Rain Radar installed in the city of Cusco. Meteorological ground station measurements from both study regions were used to estimate the freezing level height with extrapolation techniques based on either a constant lapse rates or linear regression where several stations were available. Furthermore, we analyzed climate model projections for different Representative Concentration Pathways (RCP2.6 and RCP8.5) to assess the rise in the freezing level under the most optimistic and pessimistic emission scenarios until the end of this century.

The mean annual freezing level lies at 4900 and 5010 m asl., for the Cordillera Blanca and Vilcanota, respectively. During infrequent precipitation events in the dry season, the freezing level can drop significantly below 3500 m asl. During the wet season, the freezing level in the Cordillera Vilcanota lies ca. 150 m higher compared to the Cordillera Blanca, which is in line with the higher glacier terminus elevations. For both study regions, about 15% of the glacier area lies below the present-day wet season freezing level. The projections reveal that by the end of the 21th century, the 0°C level will rise by 230 m (±190 m) for RCP2.6 and 850 m (±390 m) for RCP8.5. The spread between the models is large, pointing to a considerable uncertainty of these model projections.

These results as well as findings from other studies indicate that there is a close relation between freezing and snowfall level, glacier mass and energy balance and consequently glacier extents. Below the mean wet season freezing level, the albedo of the glacier surface is low during the whole year, leading to large ablation rates. Only glaciers with large accumulation areas may form tongues that reach lower elevations. Based on this finding and climate model projections, we suggest that the wet season freezing level can be used as an indicator for glacier extents. Consequently, even under the most optimistic scenario, glaciers may continue shrinking considerably and may lose about half of their area until the end of this century. Under the most pessimistic scenario, glaciers may only remain at the highest summits above approximately 5800 m asl. Factors like response times, changes in other climatic variables or glacier flow dynamics were neglected. Despite the limitations of this experiment, we suggest that our findings are robust and rather optimistic.

4 General discussion

Despite the increasing concern about the future of glaciers and water availability in Peru and the Indian Himalaya, there are still important knowledge gaps in understanding climate-driven glacier surface processes and the response of glaciers to changes in climate. To overcome the limitation of missing data, air temperature and the related freezing and snowfall level as well as precipitation were defined as key climate variables. Approaches were presented that allow studying glacier changes in relation to changes in these key climate variables without the need of detailed in-situ data. A further goal was to apply and evaluate in-situ (meteorological station data, radiosondes) and ex-situ (reanalysis, global climate model and remote sensing) data sets in four studies at different temporal and spatial scales.

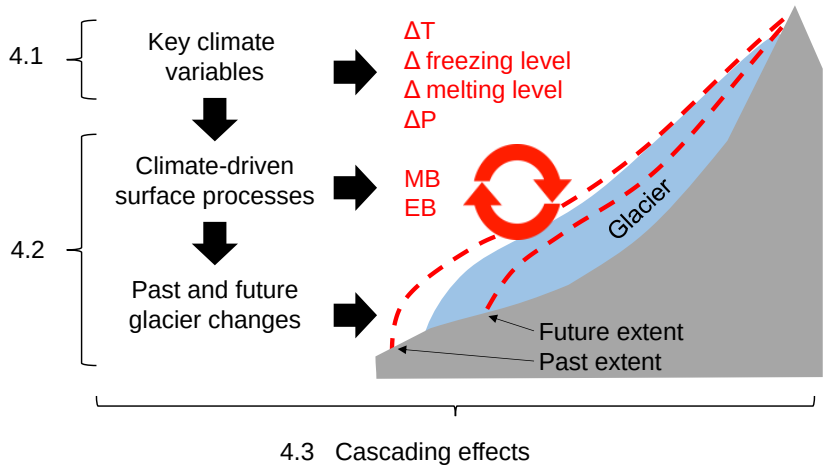

Figure 4 Schematic overview of this section.

In the following section, the main findings from the research questions and articles (summarized in *Chapter 3*) are combined and discussed within the context of the main aims of the thesis. Figure 4 shows a schematic overview of this section. First, the changes in key variables air temperature, precipitation as well as present and future freezing and snowfall levels are discussed (*Section 4.1*). Then, approaches to study climate-driven glacier surface processes and past and future glacier changes in high-mountain regions with poor in-situ data coverage are put into a context and briefly

evaluated (*Section 4.2*). Finally, the importance of the results for the environment and society is discussed using the concept of cascading effects (*Section 4.3*).

4.1 Key climate variables

In the following sections, the key climate variables air temperature, precipitation, freezing and snowfall level are discussed. Some important aspects in estimating temperature and precipitation trends are highlighted and the applicability of different data sets in data poor regions is shown.

4.1.1 Past air temperature and precipitation trends

Air temperature trends

Air temperature is an important variable for the glacier mass and energy balance not only for ablation via sensible heat flux and longwave radiation, but it represents also a decisive variable via the freezing and snowfall level, the snowline, albedo and thus net shortwave radiation (see also *Section 2.2.3*). Therefore, air temperature is defined in this work as a key climate variable. To understand how glaciers react to changes in air temperature, trends for the Cordillera Blanca since the 1960s were analyzed using meteorological station and reanalysis data (*Paper II*). Some important aspects are discussed in the following and some recommendations for future research and applications are given.

- Regional patterns of increasing temperatures were found with a clear difference of warming between the Pacific coast of Peru and the Cordillera Blanca. Air temperature at the coast is cooling, which is consistent with the observed Pacific Decadal Oscillation (PDO, *Mantua and Hare*, 2002) and has been shown before for the Pacific coast of Peru (*Vuille et al.*, 2015) and Chile (*Falvey and Garreaud*, 2009; *Schulz et al.*, 2012). In contrast, warming continues at high elevations according to several studies suggesting that warming may be stronger at high elevations (e.g. *Bradley et al.*, 2006; *Urrutia and Vuille*, 2009). However, the elevation dependence is not yet fully understood since the air below the Pacific inversion level at the coast is separated and complicates an elevation dependent analysis.
- Numerous meteorological stations show a reduced warming in the last 30 years as compared to earlier decades (in line with *Mark and Seltzer*, 2005) and even stagnant temperatures for the first decade of this century. Furthermore, station data indicate that during the 70s, there was a strong increase in temperature, in line with a climatic "jump" or "shift" identified by e.g. *Giese et al.* (2002) or *Jacques-Coper* (2009). Also the pause in warming in the first decade of this century agrees with the global hiatus (e.g. *Trenberth and Fasullo*, 2013). This hiatus in global warming (between 1998 and 2013) is likely part of natural climate variability, tied to a La-Niña-like decadal cooling (*Kosaka and Xie*, 2013). In general, the results indicate that the trend estimations strongly depend on the start and end data of the analysis, especially, when the time series are relatively short (compare to e.g. *Vuille et al.*, 2015). The choice of

the time period should therefore not be arbitrary and could be circumvent by using 30-year running trends and other tools like two-dimensional parameter diagrams that show every possible trend for different start dates and duration (*Liebmann et al.*, 2010).

- Air temperature trends were assessed separately for maximum and minimum temperatures, in order to assess changes in the daily temperature range. It was found that in the last 30 years (1980s – 2010s), minimum temperatures in the Cordillera Blanca were increasing strongly, while maximum temperatures were not changing significantly. This is equivalent to a decrease in the daily temperature range (DTR). This may indicate an increase in specific humidity or cloud cover, as corroborated by *Vuille et al.* (2003) who found a significant increase in relative humidity for the period 1950 to 1995 along the Andean range. Further research would be needed to understand more in-depth the role of humidity and cloud cover in warming over the tropical Andes and the impacts of these parameters on glacier mass balance.

The results showed that air temperature trends are heterogeneous in space but regional patterns can be identified and partly explained by climate variabilities such as the Pacific Decadal Oscillation (PDO). Moreover, trends are non-linear in time and maximum and minimum temperatures are not changing at the same rates. These findings are especially important for communicating climate change to a broad public. After a decade of stagnant temperatures as observed lately, warming could continue even at higher rates than before. Even if temperature is stagnant for some years or a decade, the long-term trend still shows strong warming over the Peruvian region.

Precipitation trends

Changes in precipitation may partly balance an increased ablation due to air temperature rise (e.g. *Zemp et al.*, 2006). To understand changes in glacier mass balance in the past, it is therefore crucial to analyze precipitation changes. Some important aspects can be identified:

- Data from meteorological stations show that the mean annual precipitation over the Cordillera Blanca has strongly increased between the 1980s and 1990s. A significant increase in precipitation has also been observed for northern Peru (1950 to 1994, *Vuille et al.*, 2003) and the Cordillera Huaytapallana (*López-Moreno et al.*, 2014). However, no clear pattern in precipitation changes emerges in Peru (e.g. *Vuille et al.*, 2003; *Rabatel et al.*, 2013, *Salzmann et al.*, 2013, *Mernild et al.*, 2016). In general, the trend in precipitation is minor in most regions of Peru and it is unlikely that precipitation is a dominant driver of glacier shrinkage (*Francou et al.*, 2003; *Vuille et al.*, 2003). Other studies have shown that it is difficult to estimate trends in dry season precipitation and shifts in the start and end of the wet season (e.g. *Gurgiser et al.*, 2016). When precipitation is very low or even close to zero, the monthly precipitation sum is close to the measurement uncertainty and it is therefore almost impossible to estimate a significant trend, or at least, trends have to be interpreted very carefully.

- It was found that the wet season precipitation of the Cordillera Blanca is correlated with the zonal wind flow (according to *Garreaud and Aceituno,* 2001; *Garreaud et al.*, 2003; *Vuille and Keimig,* 2004; *Minvielle and Garreaud,* 2011). The increase of precipitation after 1993 coincides with a shift in strength of the zonal wind towards stronger easterly winds. With the increase of zonal easterly flow, advection of moist air from the Amazon basin is favored. Consequently, the variability of zonal wind explains partly the inter-annual fluctuations of precipitation in the Cordillera Blanca since around 1980.

At the elevation of glaciers, precipitation data are scarce, but with stations from lower elevations, patterns of regional precipitation trends can be identified. It is crucial to put precipitation changes into a larger context of large-scale circulation (e.g. zonal wind flow) in order to check the plausibility of recorded changes and to explain possible causes. Yet, the amount of precipitation at high elevations, especially in the accumulation zones of glaciers, remains largely unknown and should be further investigated in future studies.

Meteorological station data for trend analysis

Meteorological station data were used for analyzing air temperature and precipitation trends. Most of the available records have gaps of different duration and some stations do not operate all the way to the present. Also the data quality is often limited. For a reliable climatic trend analysis, however, long and homogeneous data series of a high quality are required (e.g. *Begert et al.,* 2005) and a respective data homogenization was needed. We found that it was worth to check the data series first visually, looking for outliers, implausible values or trends using a data portal by *Schwarb et al.* (2011). A comparison to neighboring stations often showed whether outliers or breaks are plausible or not. After a first visual check, there are different methods to homogenize station data. The approach developed in *Paper II* was based on so-called base stations, which were stations with relatively long and complete series. These stations were compared to other stations using linear regression, and then the new homogeneized data series are computed using linear relationship between the base stations and the surrounding stations. Other methods like the first difference method could be applied. For instance, *Mark and Seltzer* (2005) homogeneized the same SENAMHI data following the procedure described by *Peterson et al.* (1998) and used by *Vuille and Bradley* (2000).

Reanalysis data for trend analysis

Due to the lack of long-term climate records from the free-atmosphere and increasing concern about climate change, the need for homogeneous reanalysis data to estimate trends is growing. One important goal of reanalysis products is hence to produce homogenous records, free of shifts or other signals. Even if reanalysis data are widely used, there is still a debate on the usefulness to document climatic trends and variability (e.g. *Kalnay et al.*, 1996; *Bengtsson et al.*, 2004; *Simmons et al.*, 2004; *Dee et al.*, 2011). Large uncertainties still come from errors, biases or deficiencies in the observations needed to assimilate the model solutions (*Simmons et al.*, 2004; *Hofer et al.*, 2012). For example, changes in the observing systems or methods of observation (e.g. replacement of

instruments) may cause artificial climate variability and trends (e.g. *Trenberth et al.*, 2001). In line with literature, we found in our study that there might be important limitations in estimating local trends in air temperature based on reanalysis data, requiring awareness on how to interpret the results. In *Paper II*, NCEP/NCAR data agreed best with meteorological station data. In contrast, ERA-Interim data showed much lower trends, deviating especially in the last approximately 15 years from the other two data series. Based on these results, it is not possible to make a general statement about the performance of these two reanalysis products. Over the globe, reanalysis data might represent well air temperature trends (*Bengtsson et al.*, 2004), but for single grid points, the trend might be inaccurate. For a detailed comparison, it would be important to know which data were used for the assimilation. However, until now, there is no information available about the data used for the assimilation, which makes it difficult to assess uncertainties and performance of reanalysis data. An important drawback of reanalysis products is hence that the stations used to assimilate are not known to the users.

4.1.2 Freezing and snowfall level

In *Paper III* and *Paper IV*, two closely related key climate variables were assessed: the freezing and snowfall level. There are different ways to estimate these two parameters. In the following, different approaches and data sets are briefly presented and discussed.

Reanalysis data to estimate the freezing level

The free-atmosphere freezing level is often assessed using reanalysis data, especially when the analysis is performed for large regions (e.g. *Diaz et al.*, 2003; *Bradley et al.*, 2009; *Rabatel et al.*, 2013). The freezing level is estimated from temperature and geopotential height, both classed as "A" variables in the NCEP/NCAR reanalysis (*Kalnay et al.*, 1996). These variables are strongly influenced by observed data, and hence they are the most reliable parameters. On the other hand, biases in observations introduce uncertainty to the reanalysis data, as discussed in *Section 4.1.1*. We found some important biases between the freezing levels from different reanalysis products (*Paper IV, supplementary information*), which are still not understood in detail. For the region of the Andes in Peru, the average freezing level from MERRA2 lies up to 100 m above the ERA-Interim values. However, this bias is not homogeneous over the region of Peru and it is not clear if these biases are caused by using different observations in the respective reanalysis products.

Our results furthermore indicate that the freezing level from reanalysis correlates with the bright band from Micro Rain Radar and TRMM Precipitation Radar data. As expected, the spread is large, since the bright band appears at the level of maximum radar reflectivity, which appears some hundreds of meters below freezing level (e.g. *Harris et al.*, 2000). This means that the uncertainty in estimating the snow/rain transition for a single precipitation event based on reanalysis freezing level may be considerable.

Extrapolated freezing and snowfall level

Freezing and snowfall levels are often estimated using air temperature extrapolation techniques and meteorological station data. Either, the lapse rate is assumed to be constant or the snowfall level is assessed using a simple linear regression when several stations are available. It is assumed that in mountainous regions, altitude is the most important factor determining air temperature. However, for an accurate estimation of surface temperature lapse rates over complex terrain, also topographic information or the seasonal or diurnal variability in lapse rates should be considered (e.g. *Rolland*, 2003; *Minder et al.*, 2010), which was not done here.

Here, it was shown that the extrapolation techniques based on a single station and a constant lapse rate to estimate free-atmosphere freezing or snowfall level has to be applied with caution (*Paper III* and *Paper IV*). Artefacts of air temperature measurements at the ground due to e.g. strong insolation or insufficient ventilation may lead to large uncertainties in estimating snowfall level using temperature extrapolation techniques. At the beginning of a precipitation event, the relatively high temperatures at the meteorological station may lead to an overestimation snowfall level. After ca. 1 h of the onset of the precipitation event, the estimation seems much more reliable.

Moreover, the extrapolation of near-surface air temperature based on several meteorological stations using linear regression gets difficult for regions with few stations available. Additionally, the daily resolution of conventional meteorological stations (from e.g. SENAMHI) hampers the assessment of the snowfall level during precipitation events, since precipitation events in the tropical Andes can be often rather short (minutes to hours). Another uncertainty is introduced by the assumption of the air temperature at the snow/rain transition. A threshold of 1.5°C is often used for near-surface snow/rain transition (e.g. *Klok and Oerlemans*, 2002), however, we found that a threshold of 0°C might be more adequate for the free-air snowfall level in the Central Andes.

TRMM PR bright band to estimate the snowfall level

TRMM PR bright band data have been used to estimate the snow/rain transition in the free-atmosphere over large regions (e.g. *Harris et al.*, 2000). TRMM PR bright band data are reliable estimations for the free-atmosphere snowfall level, but in *Paper III* and *Paper IV*, we found that the data availability of TRMM PR bright band over mountains is limited. Close to the surface, data are masked out, since they are disturbed by ground cluttering. Where the earth surface is low and the snowfall level is high above the surface (e.g. Amazon basin, Kashmir Valley or Indian lowlands), the bright band can thus be detected well. However, over mountainous terrain where the snowfall level might be low and snow can occur down to the valley bottom, the bright band is masked out. From our results we conclude that bright band data from TRMM PR offer a valuable additional data source, particularly in combination with other data products. Despite the small number of data over high mountains, data from greater mountain valleys or the surrounding lowlands provide valuable information, potentially able to provide information on snowfall level where in-situ data are sparse. In the future, satellite derived precipitation estimates will continue to be relevant, especially in the view of a changing climate in complex terrain.

Future freezing level

In the past, the freezing level has increased significantly over the Peruvian Andes (e.g. *Bradley et al.*, 2009; *Rabatel et al.*, 2013; *Paper II*). For the future, global climate models predict a further strong increase in the freezing level. We found that the increase strongly depends on the greenhouse gas emissions scenario and the spread between the single models is very large. The results are in line with other studies on air temperature and freezing level changes in the tropics (*Bradley et al.*, 2004; *Vuille et al.*, 2008a; *Bradley et al.*, 2009; *Diaz et al.*, 2014) and the Himalayas (*Viste and Sorteberg*, 2015). We found that even under the most optimistic emission scenario, the freezing level in the Peruvian Andes will continue increasing at a similar rate as in the last about 5 decades. With RCP8.5, the future increase is extremely high with approximately 90 m per decade, meaning that the increase rate would be three times higher than the observed increase since the 1950s. Parallel to the freezing level, also the snowfall level will increase - likely at a similar rate. Possible impacts on glacier extents are discussed in *Section 4.2.3*.

4.2 Approaches to study climate-driven processes and glacier changes

In *Paper I*, an approach to estimate debris thickness on data poor glaciers was presented. In *Paper II* three simple approaches were applied to understand past and present changes in glaciers and the relation to climate. In *Paper IV*, the future extents of glaciers are projected using the wet season freezing level as an indicator. In the following, the results from these approaches are discussed.

4.2.1 Debris thickness

As shown in *Part I Section 2.2.2*, a layer of debris is altering the energy and mass balance of a glacier surface. Consequently, glacier tongues with thick debris are less sensitive to changes in climate (*Pratap et al.*, 2015). To understand past and future changes it is therefore crucial to consider debris cover thickness, which is still an unsolved problem (*Juen et al.*, 2014). In *Paper I*, we have developed an approach to estimate debris thickness in data scarce environments based on thermal satellite imagery (following other studies by e.g. *Zhang et al.*, 2011; *Foster et al.*, 2012; *Rounce and McKinney*, 2014). As a consequence of working in such remote and data scarce areas, a number of simplifying assumptions about energy fluxes (methods by e.g. *Brunt*, 1932; *Brutsaert*, 1975; *Strasser et al.*, 2004) and debris properties must be made, which leads to considerable uncertainties in the final results.

The study was an important step forward, opening new possibilities to estimate debris thickness on remote glaciers. We found that the uncertainty in the results is relatively small for cool surfaces but it increases significantly with increasing surface temperature. It seems that above roughly 10°C, the method cannot reliably provide accurate results, although it should correctly identify the pixel as relatively thick debris. Moreover, the energy balance approach probably underestimates debris thickness, which is in line with results from other studies (e.g. *Suzuki et al.*, 2007; *Schauwecker*,

2012; *Petersen et al.*, 2013; *Rounce and McKinney*, 2014). We suggest that this underestimation is mainly due to the unknown vertical temperature profile (compare to e.g. *Rounce and McKinney*, 2014), the rate of heat stored and the uncertain turbulent sensible heat flux. Due to both, the large uncertainties and possible underestimation of debris thickness, the method is still not applicable to glaciers without any in-situ measurements. For hydrological models, it is crucial to know debris thickness or at least the effect of debris on ablation of the ice beneath, which can alternatively be expressed by the thermal resistance where thermal conductivity is unknown (e.g. *Mihalcea et al.*, 2006; *Suzuki et al.*, 2007; *Fujita and Sakai*, 2014; *Rounce and McKinney*, 2014).

Where in-situ meteorological data are missing, reanalysis data may deliver valuable information for the conditions above a debris-covered glacier (*Zhang et al.*, 2011). In *Paper I*, we found that air temperature from reanalysis data correlates well with measured air temperature at a meteorological station in the valley. Reanalysis data tend to underestimate local values for air temperature slightly, probably because they represent the free-atmosphere and boundary layer effects are not considered. In contrast, wind speed from reanalysis data is not correlated with in-situ measurements. Local wind systems over debris-covered glaciers are rather driven by thermally developed winds (*Zou* et al., 2008). Thus, reanalysis data have important limitations in complex orographic settings.

4.2.2 Past changes

To understand past glacier shrinkage, we need to understand both components of the glacier mass balance, accumulation and ablation, and assess whether glaciers are in equilibrium or out of balance with the climatic conditions. In *Paper II*, we applied three simple approaches: a) An experiment was conducted to estimate the amount of precipitation needed to balance an increase in the snowline altitude and consequently increased albedo and net shortwave radiation; b) Available mass balance measurements and Equilibrium Line Altitude (ELA) estimations on two glaciers were compiled and compared to the glacier hypsography and a theoretical steady-state ELA, in order to discuss the glacier imbalance; c) The response time of a relatively large glacier was estimated, in order to understand whether the glacier is still reacting to changes in climate that happened some decades ago. These three approaches (illustrated in Figure 5) are simple and only serve to give a rough idea over the past changes in glaciers. Nevertheless, for data scarce regions, they deliver a valuable overview over the state of glaciers and their relation to the climate.

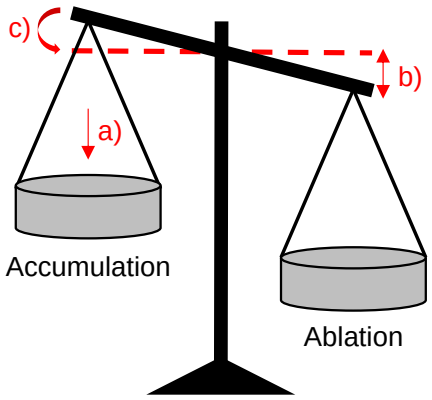

Figure 5 Schematic of the approaches to estimate the glacier state. The approach a) serves to estimate the amount of accumulation increase needed to balance increased ablation due to a higher freezing level and snowline. The approach b) is used to estimate whether the glaciers are in an imbalance with the current climate. The approach c) estimates glacier response times.

a) Precipitation balancing increased ablation due to increased net shortwave radiation

In the first approach, a numerical experiment was applied to Shallap glacier (*Gurgiser et al.*, 2013a). The aim was to estimate the amount of precipitation needed to balance an observed rise in the snowline by 130 m, which corresponds to the observed increase in the freezing level height during precipitation days between 1964/72 and 1973/82. The main assumption of this experiment is that the elevation of the snowline has increased and the elevation band between the former and the current snowline has changed from snow-covered to bare ice. Due to the much lower albedo of this elevation band, the outgoing shortwave radiation is smaller and, consequently, more energy is available for ablation (see *Section 2.2.3*). The increased ablation should be copensated by increased solid precipitation in order to keep the glacier in equilibrium. It was found that the total observed increase in precipitation of about 140 mm between 1964 and 2012 would not compensate the effect of the increased snowline.

This method is very simple and only considers effects of rising temperatures on net shortwave radiation. Other effects (such as increased sensible heat or incoming longwave radiation) are not considered. *Kaser and Osmaston* (2002) even estimated an accumulation increase of ~1200 mm to balance an increase in air temperature of 0.34°C (corresponding to an increase in the freezing level of ~50 m assuming a lapse rate of 0.0065°Cm^{-1}), which is one order of magnitude larger than the observed increase in solid precipitation using the here presented approach. Also other methods (e.g. by *Klok and Oerlemans*, 2004) would likely estimate a much larger accumulation increase. Nevertheless, this method shows the importance of the effect of warming on the glacier mass balance via albedo and net shortwave radiation.

b) Steady state vs. current ELA

For the second approach we used the glacier hypsography which delivers information on the area distribution across elevation. The Accumulation Area Ratio (AAR) describes the ratio of the accumulation to the total glacier area. The theoretical AAR of a glacier in steady state is called steady state AAR. It is assumed that this ratio is constant for different glacier extents, given that the glacier is in equilibrium (*Kerschner*, 1990; *Kaser and Osmaston*, 2002). The steady state AAR for tropical glaciers is suggested to range from 0.75 to 0.82 (*Kaser and Georges*, 1997; *Kaser and Osmaston*, 2002). In *Paper II*, the steady state ELA (derived from the steady state AAR) is compared to estimations of annual ELAs derived by mass balance measurements in the field. We found that currently measured annual ELAs of Artesonraju - a relatively large glacier - mostly lie within the range of the estimated steady state ELA. Probably, the current annual ELAs are still above the steady state ELA, but the rate of area retreat compared to the total area is much lower than for small glaciers. On the other hand, the currently estimated annual ELAs of the low-elevation and small Yanamarey glacier are high compared to the estimated range of the theoretical steady state ELA. These small, low lying glaciers are thus probably strongly unbalanced and are going to shrink further and at a high rate in the next decades. The main limitations of this approach is the uncertainty introduced by deriving a steady state ELA based on the estimated steady state AAR. Furthermore, mass balance measurements are often sparse or incomplete, especially due to the difficult access to the accumulation areas.

c) Response times

Another important aspect in studying glacier changes is the response time of glaciers, defined as the time needed for the volume to change by $(V_2-V_1)(1-e^{-1})$, where e is the base of natural logarithms (*Cogley et al.*, 2011). According to this definition, the response time is the time the glacier takes to reach about 63% of the total volume change. This concept is an idealization, but serves to understand that the glacier change is a reaction to changes in climate that happened some years to decades ago. Often, the response time is estimated by dividing the thickness of a glacier at the equilibrium line by the mass balance rate at the terminus (*Jóhanneson et al.*, 1989). Tropical glaciers in general respond relatively rapidly to changes in atmospheric conditions, typically within a few years, because of their usually small sizes (e.g. *Bahr et al.*, 1998, *Salzmann et al.*, 2013, *Vuille et al.*, 2008a).

For the relatively large Artesonraju glacier, we estimated that the response time is 10-40 years. Especially large glaciers are thus still reacting to changes in air temperature and precipitation that happened few decades ago. Small glaciers have smaller response times and it would be interesting to study if these glaciers have reached a new equilibrium after the few years of probably stagnant temperatures (called hiatus, see *Section 4.1.1*). There are some indications that small glaciers in the Cordillera Blanca (especially at high elevations) might have retreated at a lower rate in the last decade, but detailed studies are still missing.

4.2.3 Future projections

Little is known about the future of glaciers in Peru. In this work, glacier mass and energy balance was not modeled and thus it was not studied how glaciers react to single climatic variables. To overcome this knowledge gap, the wet season freezing level was suggested as an indicator for glacier extents. Glaciers in Peru are most sensitive to air temperature, due to the close relation of air temperature to the snowfall level, albedo and net shortwave radiation (see *Section 2.2.3*) and the small annual variability in air temperature. If we assume that the percentage of glacier area below the wet season freezing level remains similar in the future, we can make rough estimates of the glacier extent by the end of the century. Under this assumption, glaciers will lose about half of their area under the most optimistic scenario RCP2.6. If the temperature increases as much as under RCP8.5, there will likely be only some small glaciers left on the top of the highest mountain peaks in both regions. Especially small, low-elevation glaciers will first disappear, as well as glaciers with low lying accumulation areas. These findings are in the same range as results from *Juen et al.* (2007).

Although this is a very simple experiment, we suggest that it is a robust and rather optimistic estimation for the future glacier extent. The results are related to large uncertainties, which are still difficult to quantify (e.g. changes in other climatic variables, glacier response times and glacier geometries). Furthermore, the exact timing and rate of glacier disappearance is still not known and requires further research.

4.3 Cascading effects

In the following section, the relevance of the results for environment and society is discussed in view of cascading effects. A cascading effect is defined as a sequence of events (or processes) in which each produces the circumstances necessary for the initiation of the next (*Allaby*, 2010). The most widely discussed effect of shrinking glaciers due to climate change is the impact on water availability (amount and seasonality, see *Section 2.1.3*), but also effects on groundwater recharge, natural hazards, biodiversity, ecosystem and human livelihood are often mentioned (e.g. *Xu et al.*, 2009; *Mark et al.*, 2010; *Salzmann et al.*, 2014). A scheme by *Xu et al.* (2009) shows a simplified climate-glacier-water cascade for a mountain region. Based on this scheme it is shown that results from this work are mainly related to the first three steps of the climate-glacier-water cascade, having therefore effects on the entire cascade (Figure 6).

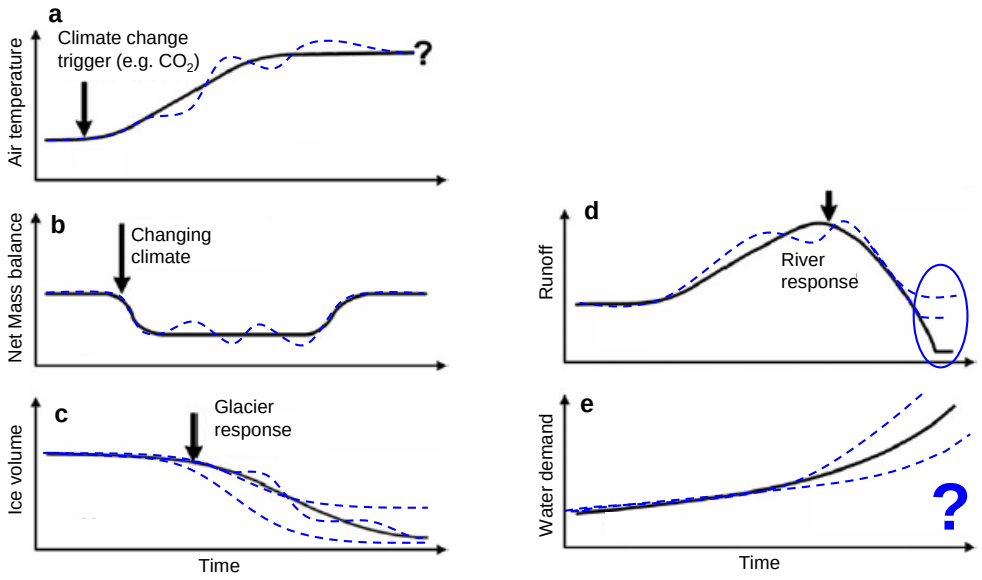

Figure 6 A climate-glacier-water cascade in a mountain region: (a) climate-change affects (b) glacier net mass balance (temporarily negative) which affects (c) ice volume, (d) river runoff and simultaneously (e) demand for water (adapted from *Xu et al.*, 2009, changes in blue color).

a) Climate change

In *Paper II*, it was shown that air temperature in the Cordillera Blanca is not increasing linearly, but rather takes the form of step changes where periods of strong warming alternate with stagnant periods or some years of even decreasing temperatures (schematically shown in Figure 6a). The recorded temperature rise is not only the result of increasing atmospheric greenhouse gas concentrations and anthropogenic forcing, but it is also influenced by decadal or multidecadal natural climate variability (e.g. Pacific Decadal Oscillation, PDO) or year-to-year variability (e.g. El Niño-Southern Oscillation, ENSO, see e.g. *Vuille et al.*, 2008b; *Maussion et al.*, 2015). It is important to communicate to the public and decision makers that climate change is not a linear phenomenon. Otherwise some years of stagnant temperatures could lead to a confusion or even make people believe that climate change is over.

Moreover, climate change is not only a change in air temperature, but also in other climatic variables as e.g. precipitation (*Paper II*) or humidity. Peruvian glaciers are highly sensitive to air temperature changes and it needs a very large change in precipitation or other climatic variables to balance it. Nevertheless, it is crucial to understand whether the already low precipitation during the dry season will decrease or increase in the future. If decreasing discharge during the dry season due to vanished glaciers goes along with less precipitation, the effects on water availability will be even more severe.

b) Glacier net mass balance

It is essential to understand the complex relation between mass balance and climate variables. If e.g. air temperature increases, not only sensible heat is altered, but also incoming longwave and net shortwave radiation increase, the latter indirectly due to an increase in the freezing level and the snowline determining albedo (*Paper III*). Glaciers in Peru are very sensitive to changes in air temperature, since it directly or indirectly determines several energy fluxes, but also the relation to other climatic variables have to be studied. Furthermore, glacier ablation and its relation to climate may be very complex, e.g. due to debris cover (*Paper I*) or ice cliffs (*Molina et al.*, 2015).

The highly complex interplay between glaciers and climate was studied here with some simple approaches. We could show that an increase in air temperature may be balanced by increased precipitation, but the observed precipitation increase in the 1990s in the Cordillera Blanca was likely not sufficiently high to balance the warming in the last decades (*Paper II*). A comparison of current annual ELAs and the steady state ELA showed that the glaciers are not balanced with the current climatic conditions (*Paper II*). Response times of large glaciers of 10-40 years cause delayed response of large glaciers to changes in climate, whereas small glaciers with shorter response times adapt more quickly to climatic changes (*Paper II*). Another experiment assuming a close relation of freezing level and glacier extents allows estimations for future glacier extents (*Paper IV*).

These simple models have the advantage that they need few input data and the results are often robust. However, it is important to continue with both lines of investigation: complex models that are based on physical laws and need detailed in-situ data and simple conceptual models.

c) Ice volume

In the past, glacier volumes have decreased substantially in Peru, as a result of negative mass balances (*Paper II*). But still, the future rate of shrinking and the timing of disappearance remains unknown. Glacier volumes in the Peruvian Andes are very likely further decreasing in the future (*Paper IV*), even under the most optimistic greenhouse gas emission scenario RCP2.6. We could show that the amplitude of warming and glacier shrinkage strongly depends on the emission scenario, and it may be that the glaciers are probably not completely lost (schematically shown in Figure 5c). The fact that glaciers may shrink significantly less under an optimistic scenario is an important finding for future decisions on climate change mitigation.

d) River runoff

In the present work, the impacts of changing glaciers on river runoff were not studied. It is often suggested that annual runoff would increase until reaching a peak, before it decreases leading finally to reduced water availability. However, the timing of the "peak water" is still unknown and after some years of stagnant temperatures, a jump in temperature could even lead to a second peak in runoff (schematically shown in Figure 6d, see also *Paper II* or *Vuille et al.*, 2015). It is therefore important to study non-uniform changes air temperature and changes in air temperature and how glacier mass balance reacts to these variabilities in climate.

Not only annual but also seasonal changes in runoff should be studied, especially for regions with distinct dry and wet seasons like Peru. We showed that observed changes in precipitation are related to easterlies (*Paper II*) in accordance to e.g. *Neukom et al.* (2015). It is suggested that precipitation might experience a reduction in the future (*Neukom et al.*, 2015), which – besides shrinking glacier reservoirs – could have severe impacts on the water cycle. But discharge is not necessarily decreasing for all seasons (schematically shown in Figure 6d). It could increase for the wet season, since precipitation falls as rain and is not stored anymore in glaciers and snow. In this context, it is also crucial to study the influence of groundwater and its role as a seasonal buffer (*Baraer et al.*, 2009; *Mark et al.*, 2010).

e) Water demand

According the scheme by *Xu et al.* (2009), water demand is increasing with decreasing availability. However, this effect is very complex and was not studied here. Water demand is altered as a result of several social, economic, demographic and cultural reasons, which are difficult to predict for the future. Moreover, the demand for water is very heterogeneous in space and difficult to link to climate change and also the dependence of people on water from melting glaciers is spatially variable. To estimate water demand in the future and develop adaptation strategies, it is needed to develop a suit of future scenarios and work towards more integrated water resource management (*Drenkhan et al.*, 2015).

The climate signal decreases from upstream to downstream locations, where non-climatic factors related to human activities are intensifying, e.g. deforestation, hydropower, agriculture or land-cover changes (*Salzmann et al.*, 2014; *Huggel et al.*, 2016). There is an increasing number of so-called "confounding factors" or "confounders" along the cascade (*Salzmann et al.*, 2014), hampering the assessment of climate related changes in water availability at low elevations. The effect of changes in the here defined key climate variables is therefore decreasing along the cascade.

However, for adaptation to climate change, it is important to understand the entire process cascade and unravel and monitor the different climatic and non-climatic factors (*Salzmann et al.*, 2014). Therefore, detailed in-situ measurements and remote sensing and reanalysis data have to be used and combined with approaches as presented in this work. Uncertainties and knowledge gaps should be taken into account when designing adaptation actions (*Buytaert et al.*, 2009). Besides the need for more data and studies, the relevant findings need to be communicated to decision makers and a broad public as simply as possible, but as complex as necessary.

5 Conclusions and perspectives

5.1 Major findings

In this thesis, different approaches were developed and applied in order to further understand climate-driven glacier surface processes in high-mountain regions where data and process understanding are limited. Key climate variables were identified and assessed and past and future glacier changes were related to changes in these variables. Moreover, some insights in using in-situ, remote sensing and model data were given and possibilities and limitations were discussed. In the following, the main conclusions from the research articles are summarized.

Paper I: Remotely sensed debris thickness mapping of Bara Shigri Glacier (Indian Himalayas)

- Long and shortwave radiation could be estimated with a reasonable accuracy, while turbulent heat estimations are associated with more uncertainty. Local wind systems for fair weather situations over debris-covered glaciers are mostly dominated by thermally developed winds, thus supporting the method to estimate wind statistically instead of taking reanalysis data. Thermal conductivity, the vertical temperature profile within the debris and surface albedo are associated to large uncertainties.
- The energy balance approach could be improved, but it still underestimates debris thickness. Uncertainties are strongly increasing with higher surface temperatures, hampering the estimation of debris thickness or total debris volume with a reasonable accuracy. Thin debris is associated to much lower uncertainties than thick debris, which is a promising result from a hydrological perspective.
- It is suggested that an energy balance approach is a valuable tool to remove effects from radiative fluxes or air temperature, in order to derive debris thickness as a function of surface temperature. Although selected field measurements are still needed, remotely sensed data represent an important source of information to map the variability in debris thickness of large and heavily debris-covered glaciers. The high spatial resolution of the surface temperature estimations from thermal band images can hardly be achieved by measurements in the field.

Paper II: Climate trends and glacier retreat in the Cordillera Blanca, Peru, revisited

- Air temperature trends are characterized by large regional differences. For the last 30 years, a slowdown in warming was identified for the Cordillera Blanca, and a cooling for the Pacific coast. The temperature increase may take the form of step changes where periods of strong warming alternate with “stagnant” or even "cooling" periods. Reanalysis data may have limitations to analyze regional trends in air temperature and need careful evaluation.
- The increase in precipitation in the early 1990 could be explained with the strengthening of the upper-tropospheric easterly zonal wind component. The shift in precipitation can probably not balance the negative mass balance caused by a strong increase in air temperature and the related change in freezing level and snowline, which is observed before approximately 1990.
- It is suggested that the strong glacier shrinkage in the Cordillera Blanca during the last 30 years may mainly result from the strongly unbalanced glacier states due to changes in key climate variables that occurred in large part before 1980. Especially small and low-elevation glaciers are extremely sensitive to climate change and may disappear in the near future.

Paper III: Estimation of snowfall limit for the Kashmir Valley, Indian Himalaya, with TRMM PR bright band information

- Our study has shown that bright band data availability in high mountain areas and/or during winter is limited, since the snow/rain transition is relatively close to the surface.
- The TRMM PR bright band altitude is strongly correlated to the freezing level from radiosonde data and less (but still well) correlated to the extrapolated freezing level from a ground station. The correlation depends on the time difference between the ground-based measurement and the TRMM Precipitation Radar overflight.
- Bright band data from greater mountain valleys or the surrounding lowlands provide valuable additional data source particularly in combination with other data products.

Paper IV: The freezing level in the tropical Andes, Peru: an indicator for present and future glacier extents

- Snowfall level estimates of a single precipitation event based on reanalysis data may be associated to large uncertainties. Estimates based on extrapolation techniques have to be applied with caution when relatively high air temperatures are measured at the beginning of the precipitation event.
- Multiple data show that the mean annual freezing level is ~4900 and 5010 m asl. in the Cordillera Blanca and Vilcanota, with a relatively small annual variability but some few precipitation events bringing solid precipitation down to relatively low elevations (<3500 m asl.). The present-day wet season freezing level in the Cordillera Vilcanota lies about 150 m higher than in the Cordillera Blanca, which agrees well with lower glacier termini.

- CMIP5 model data revealed that even under the most optimistic scenario RCP2.6, the freezing level may continue increasing (~230 m ± 190 m) at a similar rate as in the last three decades. For the most pessimistic scenario RCP8.5, the rise in freezing level is very large (~875 m ± 390).
- It is suggested that the present-day wet season freezing level height from reanalysis data is a reasonable indicators for glacier extents. Based on this assumption, even under the most optimistic scenario, at least half of the current glacier area will vanish by the end of this century. Under the mean most pessimistic scenario, only some patches of ice would remain on the summits of the highest peaks.

The findings from these studies concordantly show that simple and robust approaches and well selected key climate variables may be used to further understand climate-driven processes on glaciers in data poor regions. Observed and future glacier shrinkage can be put into a context of a changing climate using these approaches – even if in-situ data are scarce. The results all point to the important role of air temperature through various components of the glacier mass and energy balance, but other variables such as precipitation and humidity cannot be neglected. Glacier shrinkage continues and a monitoring of key climate variables and relevant surface characteristics (like snowline and debris cover) remains crucial in the future.

5.2 Perspectives for future research

Based on the findings presented in this thesis, some important knowledge gaps could be identified. In the following, possible future research steps are proposed.

A new approach to estimate debris thickness was presented in this thesis. It was shown that the method probably still underestimates debris thickness and the uncertainty of the results is considerable, especially for thick debris. Further research is needed to develop more accurate methods. The here presented method was based on remote sensing thermal band images, relating surface temperature to debris thickness. To derive debris thickness as a function of solely surface temperature, all other effects influencing surface temperature (such as the here not considered spatial pattern of albedo, surface inclination and elevation) need to be eliminated. An energy balance approach seems appropriate, but only if all these factors and their spatial variability are accurately estimated. Hence, before applying a method based on a surface temperature image, it is crucial to identify all the relevant factors influencing surface temperature and assess the spatial pattern of these factors.

Besides debris thickness and glacier surface albedo, features like ice cliffs might strongly influence the glacier energy and mass balance. During two field trips in 2014 and 2015 on Suyuparina glacier in the frame of the project Glaciares 513 and Glaciares+, a heterogeneous surface was identified on the glacier tongue (Molina et al., 2015). There are steep ice walls and depressions with diameters of several dozens of meters - some of them forming supgraglacial lakes. Similar patterns can be

identified on other glaciers in the Cordillera Vilcanota. Field observations indicate that these ice cliffs and walls have high back waste rates, while the close-by surface remain almost unchanged in the same period or even shows slight accumulation during the dry season. Due to these highly heterogeneous ablation patterns, it is therefore almost impossible to define a snowline or equilibrium line on the glacier tongue. Furthermore, it is still unclear how these surface features build and evolve. Ice cliffs are currently studied for the Himalayas, but have not been investigated for the tropical Andes. A comparison to glaciers in other tropical regions, e.g. the Kilimanjaro may give more insight (Winkler et al., 2010), but further research should focus on how these surface features influence point and glacier mass balance and how they change over time.

New data products and technologies such as drones are opening completely new fields of research. The big advantage of the drone technology is the relatively low costs for deriving a high resolution Digital Elevation Model (DEM). Large steps forward have been made in flying over high elevation terrain and glaciers above 5000 m asl. This year, for the first time, a successful drone flight over Suyuparina glacier in the Cordillera Vilcanota was conducted. Images from drones could be used to study the seasonal and annual evolution of the glacier surface or surface velocities (see e.g. *Kraaijenbrink et al.*, 2016). High resolution DEMs can also be used to validate mass balance monitoring and to interpret the data. Furthermore, new satellite products with increasing spatial and temporal resolution (provided by e.g. the Sentinel 2 mission) will open new possibilities in e.g. distinguishing between snow-covered and bare ice surfaces or in defining debris-covered areas on the glacier. In line with new remote sensing products, also the quality of reanalysis data is expected to further increase. This is especially interesting for regions with few in-situ meteorological data like the Andes or the Himalayas.

Further investigation may also be directed towards a better understanding of glacier response to variations in air temperature and precipitation and the relation between the freezing level and glacier extents. Moreover, the air temperature hiatus since the beginning of this century is probably already over. It would therefore be interesting to understand the impact of some years with stagnant temperatures on annual glacier mass balance and the reaction of glaciers to a possible increased warming after the hiatus. There are some indications that small glaciers in the Cordillera Blanca might have retreated at a lower rate in the last decade, but detailed studies are still missing. For people living in the vicinity of glaciers it is and will be crucial to be prepared for a possible decrease in water availability related to vanishing glaciers. It is thus also important to develop more detailed models to estimate future glacier volumes and the timing when glaciers disappear.

For studying glaciers and climate in countries like Peru or India, it is crucial to collaborate with local investigators. It is fundamental for these countries to count on researchers that know the current state of investigation and that are familiar with research projects conducted in their region. Important tasks of researchers include conducting own research project, but also translating and communicating findings from science around the world to local policy makers and younger generations.

6 References

Allaby, M. (2010), A Dictionary of Ecology (4 ed.), Oxford University Press.

Allison, E. A. (2015), The spiritual significance of glaciers in an age of climate change, Wiley Interdisciplinary Reviews: Climate Change, 6, 493-508.

American Meteorological Society (2016), Glossary of Meteorology. Available online at http://glossary.ametsoc.org/wiki/, last access: Oktober 2016.

Ames, A., and S. Hastenrath (1996), Diagnosing the imbalance of Glaciar Santa Rosa, Cordillera Raura, Peru, Journal of Glaciology, 42, 212-218.

ANA (2010), Inventario Nacional de glaciares y lagunas, Huaraz, Peru.

Ansari, M. I., R. Madan, and S. Bhatia (2015), Verification of quality of GPS based radiosonde data, Mausam, 66, 367-374.

Azam, M. F., P. Wagnon, C. Vincent, AL. Ramanathan, A. Linda, and V. B. Singh (2014), Reconstruction of the annual mass balance of Chhota Shigri glacier, Western Himalaya, India, since 1969, Annals of Glaciology, 55, 69-80.

Bahr, D. B., W. T. Pfeffer, C. Sassolas, and M. F. Meier (1998), Response time of glaciers as a function of size and mass balance: 1. Theory, Journal of Geophysical Research, 103, 9777-9782.

Baraer, M., J. M. McKenzie, B. G. Mark, J. Bury, and S. Knox (2009), Characterizing contributions of glacier melt and groundwater during the dry season in a poorly gauged catchment of the Cordillera Blanca (Peru), Advances in Geosciences, 22, 41-49.

Baraer, M., B. G. Mark, J. M. McKenzie, T. Condom, J. Bury, K.-I. Huh, C. Portocarrero, J. Gómez, and S. Rathay (2012), Glacier recession and water resources in Peru's Cordillera Blanca, Journal of Glaciology, 58, 134-150.

Barnett, T. P., J. C. Adam, and D. P. Lettenmaier (2005), Potential impacts of a warming climate on water availability in snow-dominated regions, Nature, 438, 303-309.

Barry, R. G., and A. Seimon (2000), Research for mountain area development: Climatic fluctuations in the mountains of the Americas and their significance, Ambio, 29, 364-370.

Begert, M., T. Schlegel, and W. Kirchhofer (2005), Homogeneous temperature and precipitation series of Switzerland from 1864 to 2000, International Journal of Climatology, 25, 65-80.

Bengtsson, L., S. Hagemann, and K. I. Hodges (2004), Can climate trends be calculated from reanalysis data?, Journal of Geophysical Research, 109, D11111.

Beniston, M., M. Stoffel, R. Harding, M. Kernan, R. Ludwing, E. Moors, P. Samuels, and K. Tockner (2012), Obstacles to data access for research related to climate and water: Implications for science and EU policy-making, Environmental Science and Policy, 17, 41-48.

Bhambri, R., T. Bolch, R. K. Chaujar, and S. C. Kulshreshtha (2011), Glacier changes in the Garhwal Himalaya, India, from 1968 to 2006 based on remote sensing, Journal of Glaciology, 57, 543–556.

Bolch, T., M. Buchroithner, T. Pieczonka, and A. Kunert (2008), Planimetric and volumetric glacier changes in the Khumbu Himal, Nepal, since 1962 using Corona, Landsat TM and ASTER data, Journal of Glaciology, 54, 592–600.

Bolch, T., A. Kulkarni, A. Kääb, C. Huggel, F. Paul, J. G. Cogley, H. Frey, J. S. Kargel, K. Fujita, M. Scheel, S. Bajracharya, and M. Stoffel (2012), The state and fate of Himalayan glaciers, Science, 336, 310–314.

Bolin, I. (2009), The glaciers of the Andes are melting: indigenous and anthropological knowledge merge in restoring water resources, in: Anthropology and Climate Change: From Encounters to Actions, pp. 228-239.

Bradley, R. S, F. T. Keimig, and H. F. Diaz (2004), Projected temperature changes along the American cordillera and the planned GCOS network, Geophysical Research Letters, 31, L16210.

Bradley, R. S., M. Vuille, H. F. Diaz, and W. Vergara (2006), Threats to water supplies in the tropical Andes, Science, 312, 1755-1756.

Bradley, R. S., F. T. Keimig, H. F. Diaz, and D. R. Hardy (2009), Recent changes in freezing level heights in the Tropics with implications for the deglacierization of high mountain regions, Geophysical Research Letters, 36, L17701.

Brock, B., A. Rivera, G. Casassa, F. Bown, and C. Acuña (2007), The surface energy balance of an active ice-covered volcano: Villarrica Volcano, southern Chile, Annals of Glaciology, 45, 104–114.

Brock, B.W., C. Mihalcea, M. P. Kirkbride, G. Diolauiuti, M. E. J. Cutler, and C. Smiraglia (2010), Meteorology and surface energy fluxes in the 2005-2007 ablation seasons at the Miage debris-covered glacier, Mont Blanc Massif, Italian Alps, Journal of Geophysical Research, 115, D09106.

Brunt, D. (1932), Notes on radiation in the atmosphere, Quarterly Journal of the Royal Meteorological Society, 58, 389-420.

Brutsaert, W. (1975), On a derivable formula for longwave radiation from clear skies, Water Resources Research, 11, 742–744.

Bury, J. T., F. T. Keimig, H. F. Diaz, and D. R. Hardy (2011), Glacier recession and human vulnerability in the Yanamarey watershed of the Cordillera Blanca, Peru, Climatic Change, 105, 179-206.

Bury, J., B. G. Mark, M. Carey, K. R. Young, J. M. McKenzie, M. Baraer, A. French, and M. H. Polk (2013), New geographies of water and climate change in Peru: Coupled natural and social transformations in the Santa River watershed, Annals of the Association of American Geographers, 103, 363-374.

Buytaert, W., R. Célleri, and L. Timbe (2009), Predicting climate change impacts on water resources in the tropical Andes: Effects of GCM uncertainty, Geophysical Research Letters, 36, L07406.

Carey, M. (2005), Living and dying with glaciers: people's historical vulnerability to avalanches and outburst floods in Peru, Global and Planetary Change, 47, 122-134.

Carey, M. (2007), The history of ice: How glaciers became an endangered species, Environmental History, 12, 497-527.

Carey, M., C. Huggel, J. Bury, C. Portocarrero, and W. Haeberli (2012), An integrated socio-environmental framework for glacier hazard management and climate change adaptation: lessons from Lake 513, Cordillera Blanca, Peru, Climatic Change, 112, 733-767.

Carey, M., M. Baraer, B. G. Mark, A. French, J. Bury, K. R. Young, and J. M. McKenzie (2014), Toward hydro-social modeling: Merging human variables and the social sciences with climate-glacier runoff models (Santa River, Peru), Journal of Hydrology, 518, 60-70.

Chevallier, P., B. Pouyaud, W. Suarez, and T. Condom (2011), Climate change threats to environment in the tropical Andes: glaciers and water resources, Regional Environmental Change, 11, 179-187.

CIIADERS (2016), Centro de Investigación Ambiental para el Desarrollo. Available online at www.ciiaders.com, last access: May 2016.

Cogley, J. G., R. Hock, L. A. Rasmussen, A. A. Arendt, A. Bauder, R. J. Braithwaite, P. Jansson, G. Kaser, M. Möller, L. Nicholson, and M. Zemp (2011), Glossary of Glacier Mass Balance and Related Terms, IHP-VII Technical Documents in Hydrology No. 86, IACS Contribution No. 2, UNESCO-IHP, Paris.

Collier, E., F. Maussion, L. I. Nicholson, T. Mölg, W. W. Immerzeel, and A. B. G. Bush (2015), Impact of debris cover on glacier ablation and atmosphere-glacier feedbacks in the Karakoram, The Cryosphere, 9, 1617-1632.

Condom, T., P. Rau, and J. C. Espinoza (2011), Correction of TRMM 3B43 monthly precipitation data over the mountainous areas of Peru during the period 1998-2007, Hydrological Processes, 25, 1924-1933.

Dee, D. P., S. M. Uppala, A. J. Simmons, P. Berrisford, P. Poli, S. Kobayashi, U. Andrae, M. A. Balmaseda, G. Balsamo, P. Bauer, P. Bechtold, A. C. M. Beljaars, L. van de Berg, J. Bidlota, N. Bormann, C. Delsol, R. Dragani, M. Fuentes, A.J.Geer, L. Haimberger, S. B. Healy, H. Hersbacha, E. V. Hólm, L. Isaksen, P. Kållberg, M. Köhler, M. Matricardi, A.P. McNallya, B. M. Monge-Sanz, J.-J. Morcrette, B.-K. Park, C. Peubey, P. de Rosnay, C.Tavolato, J.-N. Thépaut, and F. Vitart (2011), The ERA-Interim reanalysis: Configuration and performance of the data assimilation system, Quarterly Journal of the Royal Meteorological Society, 137, 553–597.

Diaz, H. F., J. K. Eischeid, C. Duncan, and R. S. Bradley (2003), Variability of freezing levels, melting season indicators, and snow cover for selected high-elevation and continental regions in the last 50 years, Climatic Change, 59, 33-52.

Diaz, H. F., R. Villalba, G. Greenwood, and R. S. Bradley (2006), The impact of climate change in the American Cordillera, EOS Transactions of the American Geophysical Union, 87, 315-316.

Diaz, H. F., R. S. Bradley, and L. Ning (2014), Climatic changes in mountain regions of the American Cordillera and the tropics: historical changes and future outlook, Arctic, Antarctic, and Alpine Research, 46, 735-743.

Drenkhan, F., M. Carey, C. Huggel, J. Seidel, and M. T. Oré (2015), The changing water cycle: climatic and socioeconomic drivers of water-related changes in the Andes of Peru, Wiley Interdisciplinary Reviews: Water, 2, 715-733.

Dutt, G. N. (1961), The Bara Shigri Glacier, Kangra District, East Punjab, India, Journal of Glaciology, 3, 1007–1015.
EAWS (2016), EAWS – European Avalanche Warning Services, Glossary, Available online at http://www.avalanches.org/eaws/en/includes/glossary/glossary_en_all.html, last access: March, 2017.
Emmer, A., E. C. Loarte, J. Klimeš, and V. Vilímek (2015), Recent evolution and degradation of the bent Jatunraju glacier (Cordillera Blanca, Peru), Geomorphology, 228, 345-355.
Fabry, F., and I. Zawadzki (1995), Long-term radar observations of the melting layer of precipitation and their interpretation, Journal of Atmospheric Sciences, 52, 838-851.
Falvey, M., and R. D. Garreaud (2009), Regional cooling in a warming world: Recent temperature trends in the southeast Pacific and along the west coast of subtropical South America (1979–2006), Journal of Geophysical Research, 114, D04102.
Favier, V., P. Wagnon, and P. Ribstein (2004a), Glaciers of the outer and inner tropics: A different behaviour but a common response to climatic forcing, Geophysical Research Letters, 31, L16403.
Favier, V., P. Wagnon, J.-P. Chazarin, L. Maisincho, and A. Coudrain (2004b), One-year measurements of surface heat budget on the ablation zone of Antizana Glacier 15, Ecuadorian Andes, Journal of Geophysical Research, 109, D18105.
Fernández, A., and B. G. Mark (2016), Modeling modern glacier response to climate changes along the Andes Cordillera: A multi-scale review, Journal of Advances in Modeling Earth Systems, 8, 467-495.
Foster, L. A., B. W. Brock, M. E. J. Cutler, and F. Diotri (2012), A physically based method for estimating supraglacial debris thickness from thermal band remote-sensing data, Journal of Glaciology, 58, 677–691.
Francou, B., M. Vuille, P. Wagnon, J. Mendoza, and J.-E. Sicart (2003), Tropical climate change recorded by a glacier in the central Andes during the last decades of the twentieth century: Chacaltaya, Bolivia, 16°S, Journal of Geophysical Research - Atmospheres, 108, n.i..
Francou, B., M. Vuille, V. Favier, and B. Cáceres (2004), New evidence for an ENSO impact on low-latitude glaciers: Antizana 15, Andes of Ecuador, 0°28'S, Journal of Geophysical Research, 109, D18106.
Francou, B., and A. Coudrain (2005), Glacier shrinkage and water resources in the Andes, EOS Transactions of the American Geophysical Union, 43, 415.
Frey, H., F. Paul, and T. Strozzi (2012), Compilation of a glacier inventory for the western Himalayas from satellite data: methods, challenges, and results, Remote Sensing of Environment, 124, 832–843.
Frey, H., H. Machguth, M. Huss, C. Huggel, S. Bajracharya, T. Bolch, A. Kulkarni, A. Linsbauer, N. Salzmann, and M. Stoffel (2014), Estimating the volume of glaciers in the Himalayan-Karakoram region using different methods, The Cryosphere, 8, 2313-2333.
Fujita, K., and A. Sakai (2014), Modelling runoff from a Himalayan debris-covered glacier, Hydrology and Earth System Sciences, 18, 2679-2694.
Gagné, K., M. B. Rasmussen, and B. Orlove (2014), Glaciers and society: attributions, perceptions, and valuation, WIREs Climate Change, 5, 793-808.
Garreaud, R. D., and P. Aceituno (2001), Interannual rainfall variability over the South American Altiplano, Journal of Climate, 14, 2779–2789.
Garreaud, R. D., M. Vuille, and A. C. Clement (2003), The climate of the Altiplano: observed current conditions and mechanisms of past changes, Palaeogeography, Palaeoclimatology, Palaeoecology, 194, 5-22.
Garreaud, R.D., M. Vuille, R. Compagnucci, and J. Marengo (2009), Present-day South American climate, Palaeogeography, Palaeoclimatology, Palaeoecology, 281, 180-195.
GCOS (2003), The second report on the adequacy of the global observing systems for climate in support of the UNFCCC, Reports GCOS - 82 (WMO/TD No. 1143), 85 pp.
Georges, C. (2004), Climate in support of the UNFCCC. Reports GCOS - 82 (WMO/TD No. 1143), Arctic, Antarctic, and Alpine Research, 36, 100-107.
Giese, B. S., S. C. Urizar, and N. S. Fuckar (2002), Southern hemisphere origins of the 1976 climate shift, Geophysical Research Letters, 29, n.i..
Gillespie, A., S. Rokugawa, T. Matsunaga, J. S. Cothern, S. Hook, and A. B. Kahle (1998), A temperature and emissivity separation algorithm for Advanced Spaceborne Thermal Emission and Reflection Radiometer (ASTER) images, IEEE Transactions on Geoscience and Remote Sensing Journal, 36, 1113–1126.
Gurgiser, W., T. Mölg, L. Nicholson, and G. Kaser (2013b), Mass-balance model parameter transferability on a tropical glacier, Journal of Glaciology, 59, 845-858.
Gurgiser, W., B. Marzeion, L. Nicholson, M. Ortner, M., and G. Kaser (2013a), Modeling energy and mass balance of Shallap Glacier, Peru, The Cryosphere, 7, 1787-1802.

Gurgiser, W., I. Juen, K. Singer, M. Neuburger, S. Schauwecker, M. Hofer, and G. Kaser (2016), Comparing peasants' perceptions of precipiation change with precipiation records in the tropical Callejón de Huaylas, Peru, Earth System Dynamics, 7, 499-515.

Haeberli, W. (2005), Changing Views of Changing Glaciers. The Darkening Peaks: Glacial Retreat in Scientific and Social Context, University of California Press.

Han, H., Y. Ding, and S. Liu (2006), A simple model to estimate ice ablation under a thick debris layer, Journal of Glaciology, 52, 528–536.

Harris, G. N., K. P. Bowman, and D.-B. Shin (2000), Comparison of freezing-level altitudes from the NCEP reanalysis with TRMM precipitation radar brightband data, Journal of Climate, 13, 4137–4148.

Hastenrath, S., and A. Ames (1995), Recession of Yamanarey Glacier in Cordillera Blanca, Peru, during the 20th century, Journal of Glaciology, 41, 191–196.

Hegglin, E., and C. Huggel (2008), An integrated assessment of vulnerability to glacial hazards, Mountain Research and Development, 28, 299-309.

Hofer, M., T. Mölg, B. Marzeion, and G. Kaser (2010), Empirical-statistical downscaling of reanalysis data to high-resolution air temperature and specific humidity above a glacier surface (Cordillera Blanca, Peru), Journal of Geophysical Research - Atmospheres, 115, D12120.

Huggel, C., I. Wallimann-Helmer, D. Stone, and W. Cramer (2016), Reconciling justice and attribution research to advance climate policy, Nature Climate Change, 6, 901-908.

Huss, M., M. Zemp, P. C. Joerg, and N. Salzmann (2014), High uncertainty in 21st century runoff projections from glacierized basins, Journal of Hydrology, 510, 35-48.

Immerzeel, W. W., L. P. H. van Beek, and M. F. P. Bierkens (2010), Climate Change will affect the Asian water towers, Science, 328, 1382-1385.

IPCC (2001), Climate Change 2001: The Scientific Basis, Contribution of Working Group I to the Third Assessment Report of the Intergovernmental Panel on Climate Change, edited by J. T. Houghton, Y. Ding, D. J. Griggs, M. Noguer, P. J. van der Linden, X. Dai, K. Maskell, and C. A. Johnson, Cambridge University Press, Cambridge, United Kingdom and New York, NY, USA, 881 pp.

IPCC (2013), Climate Change 2013: The Physical Science Basis, Contribution of Working Group I to the Fifth Assessment Report of the Intergovernmental Panel on Climate Change, edited by T. F. Stocker, D. Qin, G.-K. Plattner, M. Tignor, S. K. Allen, J. Boschung, A. Nauels, Y. Xia, V. Bex and P. M. Midgley, Cambridge University Press, Cambridge, United Kingdom and New York, NY, USA, 1535 pp.

Jacques-Coper, M. (2009), Characterization of the mid-1970's climatic jump in South America. M.S. thesis, Universidad de Chile, Santiago, Chile.

Jóhanneson, T., C. Raymond, and E. Waddington (1989), A simple method for determining the response time of glaciers, in: Glacier Fluctuations and Climatic Change, Kluwer Academic Publishing, Dordrecht, edited by J. Oerlemans, pp. 343–352.

Juen, I. (2006), Glacier mass balance and runoff in the Cordillera Blanca, Perú. Ph.D. thesis, University of Innsbruck, Innsbruck, Austria.

Juen, I., G. Kaser, G., and C. Georges (2007), Modelling observed and future runoff from a glacierized tropical catchment (Cordillera Blanca, Perú), Global and Planetary Change, 59, 37-48.

Juen, M., C. Mayer, A. Lambrecht, H. Han, and S. Liu (2014), Impact of varying debris cover thickness on ablation: a case study for Koxkar Glacier in the Tien Shan, The Cryosphere, 8, 377–386.

Kalnay, E., M. Kanamitsu, R. Kistler, W. Collins, D. Deaven, L. Gandin, M. Iredell, S. Saha, G. White, J. Woollen, Y. Zhu, M. Chelliah, W. Ebisuzaki, W. Higgins, J. Janowiak, K. C. Mo, C. Ropelewski, J. Wang, A. Leetmaa, R. Reynolds, R. Jenne, and D. Joseph (1996), The NCEP/NCAR Reanalysis 40-year Project, Bulletin of the American Meteorological Society, 77, 437–471.

Kaser, G., A. Ames, and M. Zamora (1990), Glacier fluctuations and climate in the Cordillera Blanca, Peru, Annals of Glaciology, 14, 136–140.

Kaser, G. (1995), Some notes on the behaviour of tropical glaciers, Bulletin de l'Institut français d'études andines, 24, 671–681.

Kaser, G., and C. Georges (1997), Changes of the equilibrium-line altitude in the tropical Cordillera Blanca, Peru, 1930–50, and their spatial variations, Annals of Glaciology, 24, 344–349.

Kaser, G. (1999), A review of the modern fluctuations of tropical glaciers, Global and Planetary Change, 22, 93-103.

Kaser, G. (2001), Glacier-climate interaction at low latitudes, Journal of Geophysical Research - Atmospheres, 47, 195-204.

Kaser, G., and H. Osmaston (2002), Tropical Glaciers, Cambridge University Press.

Kaser, G., I. Juen, C. Georges, J. Gómez, and W. Tamayo (2003), The impact of glaciers on the runoff and the reconstruction of mass balance history from hydrological data in the tropical Cordillera Blanca, Peru, Journal of Hydrology, 282, 130-144.

Kaser, G., M. Grosshauser, and B. Marzeion (2010), Contribution potential of glaciers to water availability in different climate regimes, Proceedings of the National Academy of Sciences of the United States of America, 107, 20223-20227.

Kayastha, R., Y. Takeuchi, M. Nakawo, and Y. Ageta (2000), Practical prediction of ice melting beneath various thickness of debris cover on Khumbu Glacier, Nepal, using a positive degree-day factor, in: Debris-Covered Glaciers, IAHS Publication, Seattle, Washington, USA, pp. 71–151.

Kellerer-Pirklbauer, A., G. K. Lieb, M. Avian, and J. Gspurning (2008), The response of partially debris-covered valley glaciers to climate change: the example of the Pasterze Glacier (Austria) in the period 1964 to 2006, Geografiska Annaler, 4, 269–285.

Kerschner, H. (1990), Methoden der Schneegrenzbestimmung, in: Eiszeitforschung, Wissenschaftliche Buchgesellschaft, Darmstadt, edited by H. Liedtke, pp. 299–311.

Klok, E. J., and J. Oerlemans (2002), Model study of the spatial distribution of the energy and mass balance of Morteratschgletscher, Switzerland, Journal of Geophysical Research - Atmospheres, 48, 505-518.

Kobayashi, S., and T. Iguchi (2003), Variable pulse repetition frequency for the global Precipitation Measurement Project (GPM), IEEE Transactions on Geoscience and Remote Sensing Journal, 41, 1714–1718.

Kosaka, Y., and S.-P. Xie (2013), Recent global-warming hiatus tied to equatorial Pacific surface cooling, Nature, 501, 403-407.

Kozu, T., T. Kawanishi, H. Kuroiwa, M. Kojima, K. Oikawa, H. Kumagai, K. Okamoto, M. Okumura, H. Nakatsuka, and K. Nishikawa (2001), Development of precipitation radar onboard the Tropical Rainfall Measuring Mission (TRMM) satellite, IEEE Transactions on Geoscience and Remote Sensing Journal, 39, 102–116.

Kraaijenbrink, P., S. W. Meijer, J. M. Shea, F. Pellicciotti, S. M. De Jong, and W. W. Immerzeel (2016), Seasonal surface velocities of a Himalayan glacier derived by automated correlation of unmanned aerial vehicle imagery, Annals of Glaciology, 57, 103-113.

Kuhn, M. (1981), Climate and glaciers. International Association of Hydrological Sciences Publication 131, Symposium at Canberra 1979, Sea Level, Ice and Climatic Change, pp. 3-20.

Kumar, S., H. Rai, K.K. Purohit, B. R. S. Rawat, and A. K. Mundepi (1987), Multi disciplinary glacier expedition to Chhota Shigri Glacier, Department of Science and Technology, Government of India, New Delhi, Technical Report Number 1, 219 pp.

Kumar, V., and S. K. Jain (2010), Trends in seasonal and annual rainfall and rainy days in Kashmir Valley in the last century, Quaternary International, 212, 64–69.

Kummerow, C., W. Barnes, T. Kozu, J. Shiue, and J. Simpson (1998), The Tropical Rainfall Measuring Mission (TRMM) Sensor Package, Journal of Atmospheric and Oceanic Technology, 15, 809–817.

Lambrecht, A., C. Mayer, W. Hagg, V. Popovnin, A. Rezepkin, N. Lomidze, and D. Svanadze (2011), A comparison of glacier melt on debris-covered glaciers in the northern and southern Caucasus, The Cryosphere, 5, 525-538.

Lejeune, Y., J.-M. Bertrand, P. Wagnon, and S. Morin (2013), A physically based model of the year-round surface energy and mass balance of debris-covered glaciers, Journal of Glaciology, 59, 327–344.

Liebmann, B., R. M. Dole, C. Jones, I. Blade, and D. Allured (2010), Influence of choice of time period on global surface temperature trend estimates, Bulletin of the American Meteorological Society, 91, 1485-1491.

Lliboutry, L. (1977), Glaciological problems set by the control of dangerous lakes in Cordillera Blanca, Peru. II. Movement of a overed glacier embedded within a rock glacier, Journal of Glaciology, 18, 255-273.

Lliboutry, L. (1986), Discharge of debris by glaciar Hatunraju, Cordillera Blanca, Peru, Journal of Glaciology, 32, 133-133.

López-Moreno, J. I., S. Fontaneda, J. Bazo, J. Revuelto, C. Azorin-Molina, B. Valero-Garcés, E. Morán-Tejeda, S. M. Vicente-Serrano, R. Zubieta, and J. Alejo-Cochachín (2014), Recent glacier retreat and climate trends in Cordillera Huaytapallana, Peru, Global and Planetary Change, 112, 1-11.

Lutz, A. F., W. W. Immerzeel, A. B. Shrestha, and M. F. P. Bierkens (2014), Consistent increase in High Asia's runoff due to increasing glacier melt and precipitation, Nature Climate Change, 4, 587-592.

Lynch, B. (2012), Vulnerabilities, competition and rights in a context of climate change toward equitable water governance in Peru's Rio Santa Valley, Global Environmental Change, 22, 364-373.

Mantas, V. M., Z. Liu, C. Caro, and A. J. S. C. Pereira (2015), Validation of TRMM multi-satellite precipitation analysis (TMPA) products in the Peruvian Andes, Atmospheric Research, 163, 132-145.

Mantua, N. J., and S. R. Hare (2002), The Pacific Decadal Oscillation, Journal of Oceanography, 58, 35-44.

Mark, B. G., and G. O. Seltzer (2003), Tropical glacier meltwater contribution to stream discharge: a case study in the Cordillera Blanca, Peru, Journal of Glaciology, 49, 271-281.
Mark, B. G., J. M. McKenzie, and J. Gómez (2005), Hydrochemical evaluation of changing glacier meltwater contribution to stream discharge: Callejon de Huaylas, Peru, Hydrological Sciences Journal, 50, 975-987.
Mark, B. G., and G. O. Seltzer (2005), Evaluation of recent glacier recession in the Cordillera Blanca, Peru (AD 1962-1999): spatial distribution of mass loss and climatic forcing, Quaternary Science Reviews, 24, 2265-2280.
Mark, B. G., J. Bury, J. M. McKenzie, A. French, A., and M. Baraer (2010), Climate change and tropical andean glacier recession: Evaluating hydrologic changes and livelihood vulnerability in the Cordillera Blanca, Peru, Annals of the Association of American Geographers, 100, 794–805.
Mattson, L. E., J. S. Gardner, and G. J. Young (1993), Ablation on debris covered glaciers: an example from the Rakhiot Glacier, Punjab, Himalaya, in: Snow and Glacier Hydrology, IAHS Publication, Kathmandu, pp. 289–296.
Maussion, F., W. Gurgiser, M. Grosshauser, G. Kaser, and B. Marzeion (2015), ENSO influence on surface energy and mass balance at Shallap Glacier, Cordillera Blanca, Peru, The Cryosphere, 9, 1663-1683.
Mernild, S. H., G. E. Liston, C. A. Hiemstra, J. K. Malmros, J. C. Yde, and J. McPhee (2016), The Andes Cordillera. Part I: snow distribution, properties and trends (1979-2014), International Journal of Climatology, n.i., n.i..
McVicar, R. R., and C. Körner (2013), On the use of elevation, altitude, and height in the exological and climatological literature, Oecologia, 171, 335-337.
Mihalcea, C., C. Mayer, G. Diolaiuti, A. Lambrecht, C. Smiraglia, and G. Tartari (2006), Ice ablation and meteorological conditions on the debris-covered area of Baltoro glacier, Karakoram, Pakistan, Annals of Glaciology, 43, 292–300.
Mihalcea, C., C. Mayer, G. Diolaiuti, C. D'Agata, C. Smiraglia, A. Lambrecht, E. Vuillermoz, and G. Tartari (2008b), Spatial distribution of debris thickness and melting from remote-sensing and meteorological data, at debris-covered Baltoro glacier, Karakoram, Pakistan, Annals of Glaciology, 48, 49–57.
Minder, J. R., P. W. Mote, and J. D. Lundquist (2010), Surface temperature lapse rates over complex terrain: Lessons from the Cascade mountains, Journal of Geophysical Research - Atmospheres, 115, D14122.
Minveille, M., and R. D. Garreaud (2011), Projecting rainfall changes over the South American Altiplano, Journal of Climate, 24, 4577-4583.
Mölg, T., and D. R. Hardy (2004), Ablation and associated energy balance of a horizontal glacier surface on Kilimanjaro, Journal of Geophysical Research - Atmospheres, 109, n.i..
Molina, E., S. Schauwecker, C. Huggel, W. Haeberli, A. Cochachin, T. Condom, F. Drenkhan, C. Giráldez, N. Salzmann, L. Jiménez, N. Montoya, M. Rado, N. Chaparro, J. Samata, W. Suarez, S. Arias, and F. Sikos (2015), Iniciación de un monitoreo del balance de masa en el glaciar Suyuparina, Cordillera Vilcanota, Perú, Climate Change in the Tropical Andes, 2, 1-14.
Mondal, N. C., and S. K. Sarkar (2003), Rain height in relation to 0°C isotherm height for satellite communication over the Indian Subcontinent, Theoretical and Applied Climatology, 76, 89–104.
Moss, R. H., J. A. Edmonds, K. A. Hibbard, M. R. Manning, S. K. Rose, D. P. van Vuuren, T. R. Carter, S. Emori, M. Kainuma, T. Kram, G. A. Meehl, J. F. B. Mitchell, N. Nakicenovic, K. Riahi, S. J. Smith, R. J. Stouffer, A. M. Thomson, J. P. Weyant, and T. J. Wilbanks (2010), The next generation of scenarios for climate change research and assessment, Nature, 463, 747-756.
Mourre, L., T. Condom, C. Junquas, T. Lebel, J. E. Sicart, R. Figueroa, and A. Cochachin (2016), Spatio-temporal assessment of WRF, TRMM and in situ precipitation data in a tropical mountain environment (Cordillera Blanca, Peru), Hydrology and Earth System Sciences, 20, 125-141.
Nakawo, M., and G. J. Young (1981), Field experiments to determine the effect of a debris layer on ablation of glacier ice, Annals of Glaciology, 2, 85–91.
Nakawo, M., S. Iwata, O. Watanabe, and M. Yoshida (1986), Processes which distribute supraglacial debris on the Khumbu Glacier, Nepal Himalaya, Annals of Glaciology, 8, 129–131.
NASA (2011), National Aeronautics and Space Administration: Landsat 7 Science Data Users Handbook, Available at: http://landsathandbook.gsfc.nasa.gov/.
Natural Earth (2016), Free vector and raster map data at 1:10m, 1:50m, and 1:110m scales. Available online at www.naturalearthdata.com, last access: September 2016.
Neukom, R., M. Rohrer, P. Calanca, N. Salzmann, C. Huggel, D. Acuña, D. A. Christie, and M. S. Morales (2015), Facing unprecedented drying of the Central Andes? Precipitation variability over the period AD 1000–2100, Environmental Research Letters, 10, 84017.
Nicholson, L., and D. I. Benn (2006), Calculating ice melt beneath a debris layer using meteorological data, Journal of Glaciology, 52, 463–470.
NOAA (2016), Available online at ftp://tgftp.nws.noaa.gov/data/observations/metar, last access: May 2016.

Ochoa, A., L. Pineda, P. Crespo, and P. Willems (2014), Evaluation of TRMM 3B42 precipitation estimates and WRF retrospective precipitation simulation over the Pacific-Andean region of Ecuador and Peru, Hydrology and Earth System Sciences, 18, 3179-3193.

Östrem, G. (1959), Ice melting under a thin layer of moraine, and the existence of ice cores in moraine ridges, Geografiska Annaler, 41, 228–230.

Perry, L. B., A. Seimon, A., and G. M. Kelly (2014), Precipitation delivery in the tropical high Andes of southern Peru: new findings and paleoclimatic implications, International Journal of Climatology, 34, 197-215.

Peterson, T. C., T. R. Karl, P. F. Jamason, R. Knight, and D. R. Easterling (1998), First difference method: maximizing station density for the calculation of long-term global temperature change, Journal of Geophysical Research - Atmospheres, 103, 25967–25974.

Petersen, L., S. Schauwecker, B. W. Brock, W. Immerzeel, and F. Pellicciotti (2013), Deriving supraglacial debris thickness using satellite data on the Lirung Glacier in the Nepalese Himalayas, In: Geophysical Research Abstracts, EGU General Assembly.

Pfeffer, W. T., A. A. Arendt, A. Bliss, T. Bolch, J. G. Cogley, A. S. Gardner, J.-O. Hagen, R. Hock, G. Kaser, C. Kienholz, E. S. Miles, G. Moholdt, N. Mölg, F. Paul, V. Radić, P. Rastner, B. H. Raup, J. Rich, M. J. Sharp, and the Randolph Consortium (2014), The Randolph Glacier Inventory: a globally complete inventory of glaciers, Journal of Glaciology, 60, 537-552.

Plataforma de Intercambio Científico (2016), Investigación en los Andes peruanos. Available online at http://investigacioninter.wixsite.com/andes, last access: September 2016.

Poremba, R. J., L. B. Perry, A. Semon, D. T. Martin, and A. Tupayachi (2015), Meteorological characteristics of heavy snowfall in the Cordillera Vilcanota, Peru, 72nd Eastern Snow Conference, Sherbrooke, Québec, Canada.

Pratap, B., D. P. Dobhal, M. Mehta, and R. Bhambri (2015), Influence of debris cover and altitude on glacier surface melting: a case study on Dokriani Glacier, central Himalaya, India, Annals of Glaciology, 56, 9-16.

Rabatel, A., A. Bermejo, E. Loarte, A. Soruco, J. Gomez, G. Leonardini, C. Vincent, and J. E. Sicart (2012), Can the snowline be used as an indicator of the equilibrium line and mass balance for glaciers in the outer tropics?, Journal of Glaciology, 58, 1027–1036.

Rabatel, A., B. Francou, A. Soruco, J. Gomez, B. Cáceres, J. L. Ceballos, R. Basantes, M. Vuille, J. E. Sicart, C. Huggel, M. Scheel, Y. Lejeune, Y. Arnaud, M. Collet, T. Condom, G. Consoli, V. Favier, V. Jomelli, R. Galarraga, P. Ginot, L. Maisincho, J. Mendoza, M. Ménégoz, E. Ramirez, P. Ribstein, W. Suarez, M. Villacis, and P. Wagnon (2013), Current state of glaciers in the tropical Andes: a multicentury perspective on glacier evolution and climate change, The Cryosphere, 7, 81–102.

Racoviteanu, A. E., Y. Arnaud, M. W. Williams, and J. Ordonez (2008), Decadal changes in glacier parameters in the Cordillera Blanca, Peru, derived from remote sensing, Journal of Glaciology, 54, 499–510.

Radić, V., and R. Hock (2011), Regionally differentiated contribution of mountain glaciers and ice caps to future sea-level rise, Nature Geoscience, 4, 91-94.

Ragettli, S., G. Cortés, J. McPhee, and F. Pellicciotti (2013), An evaluation of approaches for modelling hydrological processes in high-elevation, glacierized Andean watersheds, Hydrological Processes, 28, 5674-5695.

Rasul, G., and B. Sharma (2015), The nexus approach to water–energy–food security: an option for adaptation to climate change, Climate Policy, 16, 682-702.

Raup, B., A. Racoviteanu, S. J. S. Khalsa, C. Helm, R. Armstrong, and Y. Arnaud (2007), The GLIMS geospatial glacier database: A newtool for studying glacier change, Global and Planetary Change, 56, 101–110.

Reid, T. D., and B. W. Brock (2010), An energy-balance model for debris-covered glaciers including heat conduction through the debris layer, Journal of Glaciology, 56, 903–916.

Reid, T. D., M. Carenzo, F. Pellicciotti, and B. W. Brock (2012), Including debris cover effects in a distributed model of glacier ablation, Journal of Geophysical Research, 117, D18105.

Reynolds, J. M. (1992), The identification and mitigation of glacier-related hazards: examples from the Cordillera Blanca, Peru, in: Geohazards, Springer Netherlands, pp. 143-157.

Richardson, S. D., and J. M. Reynolds (2000), An overview of glacial hazards in the Himalayas, Quaternary International, 65, 31-47.

Rienecker, M. M., M. J. Suarez, R. Gelaro, R. Todling, J. Bacmeister, E. Liu, M. G. Bosilovich, S. D. Schubert, L. Takacs, G.-K. Kim, S. Bloom, J. Chen, D. Collins, A. Conaty, A. da Silva, W. Gu, J. Joiner, R. D. Koster, R. Lucchesi, A. Molod, T. Owens, S. Pawson, P. Pegion, C. R. Redder, R. Reichle, F. R. Robertson, A. G. Ruddick, M. Sienkiewicz, and J. Woollen (2011), MERRA2: NASA's modern-era retrospective analysis for research and applications, Journal of Climate, 24, 3624-3648.

Rolland, C. (2003), Spatial and seasonal variations of air temperature lapse rates in Alpine regions, Journal of Climate, 16, 1032-1046.

Rounce, D. R., and D. C. McKinney (2014), Debris thickness of glaciers in the Everest area (Nepal Himalaya) derived from satellite imagery using a nonlinear energy balance model, The Cryosphere, 8, 1317–1329.

Rounce, D. R., D. J. Quincey, and D. C. McKinney (2015), Debris-covered glacier energy balance model for Imja-Lhotse Shar Glacier in the Everest region of Nepal, The Cryosphere, 9, 2295-2310.

Sagredo, E. A., S. Rupper, and T. V. Lowell (2014), Sensitivities of the equilibrium line altitude to temperature and precipitation changes along the Andes, Quaternary Reserach, 81, 355-366.

Salzmann, N., C. Huggel, P. Calanca, A. Díaz, T. Jonas, T. Konzelmann, P. Lagos, M. Rohrer, W. Silverio, and M. Zappa (2009), Integrated assessment and adaptation to climate change impacts in the Peruvian Andes, Advances in Geosciences , 22, 35-39.

Salzmann, N., C. Huggel, M. Rohrer, W. Silverio, B. G. Mark, P. Burns, and C. Portocarrero (2013), Glacier changes and climate trends derived from multiple sources in the data scarce Cordillera Vilcanota region, southern Peruvian Andes, The Cryosphere, 7, 103–118.

Salzmann, N., C. Huggel, M. Rohrer, and M. Stoffel (2014), Data and knowledge gaps in glacier, snow and related runoff reserach - A climate change adaptation perspective, Journal of Hydrology, 518, 225-234.

Schaner, N., N. Voisin, B. Nijssen, and D. P. Lettenmaier (2012), The contribution of glacier melt to streamflow, Environmental Research Letters, 7, 34029.

Schaub, Y., C. Huggel, and A. Cochachin (2015), Ice-avalanche scenario elaboration and uncertainty propagation in numerical simulation of rock-/ice-avalanche-induced impact waves at Mount Hualcán and Lake 513, Peru, in: Landslides, Springer, Berlin Heidelberg.

Schauwecker, S. (2012), Mapping supraglacial debris thickness on mountain glaciers using satellite data: validation of a new, physically-based method. M.S. thesis, ETH Zürich, Zürich, Switzerland.

Scheel, M. L. M., M. Rohrer, Ch. Huggel, D. Santos Villar, E. Silvestre, and G. J. Huffman (2011), Evaluation of TRMM Multi-satellite Precipitation Analysis (TMPA) performance in the Central Andes region and its dependency on spatial and temporal resolution, Hydrology and Earth System Sciences, 15, 2649-2663.

Scherler, D., B. Bookhagen, and M. R. Strecker (2011), Spatially variable response of Himalayan glaciers to climate change affected by debris cover, Nature Geoscience, 4, 156–159.

Schmidt, S., and M. Nüsser (2009), Fluctuations of Raikot Glacier during the past 70 years: a case study from the Nanga Parbat massif, northern Pakistan, Journal of Glaciology, 55, 949–959.

Schneider, D., C. Huggel, A. Cochachin, S. Guillén, and J. García (2014), Mapping hazards from glacier lake outburst floods based on modelling of process cascades at Lake 513, Carhuaz, Peru, Advances in Geosciences, 35, 145-155.

Schulz, N., J. P. Boisier, and P. Aceituno (2012), Climate change along the arid coast of northern Chile, International Journal of Climatology, 32, 1803-1814.

Schwanghart, W., R. Worni, C. Huggel, M. Stoffel, and O. Korup (2016), Uncertainty in the Himalayan energy–water nexus: estimating regional exposure to glacial lake outburst floods, Environmental Research Letters, 11, 074005.

Schwarb, M., D. Acuña, T. Konzelmann, M. Rohrer, N. Salzmann, B. Serpa Lopez, and E. Silvestre (2011), A data portal for regional climatic trend analysis in a Peruvian High Andes region, Advances in Sciences and Technology, 6, 219–226.

Shukla, A., R. P. Gupta, and M. K. Arora (2009), Estimation of debris cover and its temporal variation using optical satellite sensor data: a case study in Chenab basin, Himalaya, Journal of Glaciology, 55, 444–452.

Sicart, J. E., P. Wagnon, and P. Ribstein (2005), Atmospheric controls of the heat balance of Zongo Glacier (16°S, Bolivia), Journal of Geophysical Research, 110, D12106.

Sicart, J. E., R. Hock, P. Ribstein, M. Litt, and E. Ramirez (2011), Analysis of seasonal variations in mass balance and meltwater discharge of the tropical Zongo Glacier by application of a distributed energy balance model, Journal of Geophysical Research, 116, D13105.

Silverio, W. and J. M. Jaquet (2005), Glacial cover mapping (1987–1996) of the Cordillera Blanca (Peru) using satellite imagery, Remote Sensing of Environment, 95, 342–350.

Simmons, A. J., P. D. Jones, V. da Costa Bechtold, A. C. M. Beljaars, P. W. Kållberg, S. Saarinen, S. M. Uppala, P. Viterbo, and N. Wedi (2004), Comparison of trends and low-frequency variability in CRU, ERA-40, and NCEP/NCAR analyses of surface air temperature, Journal of Geophysical Research - Atmospheres, 109, D24115.

Strasser, U., J. Corripio, F. Pellicciotti, P. Burlando, B. Brock, and M. Funk (2004), Spatial and temporal variability of meteorological variables at Haut Glacier d'Arolla (Switzerland) during the ablation season 2001: Measurements and simulations, Journal of Geophysical Research, 109, D03103.

Suzuki, R., K. Fujita, and Y. Ageta (2007), Spatial distribution of thermal properties on debris-covered glaciers in the Himalayas derived from ASTER data, Bulletin of glaciological Research, 24, 13-22.

Takeuchi, Y., R. B. Kayastha, and M. Nakawo (2000), Characteristics of ablation and heat balance in debris-free and debris-covered areas on Khumbu Glacier, Nepal Himalayas in the pre-monsoon season, in: Debris-Covered Glaciers, IAHS Publication, Seattle, Washington, USA, pp. 53–61.

Taylor, K. E., R. J. Stouffer, and G. A. Meehl (2011), An overview of CMIP5 and the experiment design, Bulletin of the American Meteorological Society, 93, 485-498.

Tiwari, R. K., R. P. Gupta, R. Gens, and A. Prakash (2012), Use of optical, thermal and microwave imagery for debris characterization in Bara-Shigri Glacier, Himalayas, India, IEEE 4422–4425.

Trenberth, K. E., and J. T. Fasullo (2013), An apparent hiatus in global warming?, Earth's Future, 1, 19-32.

Troll (1941), Studien zur vergleichenden Geographie der Hochgebirge der Erde, Bonner Mitteilungen, Bonn, Germany.

Uppala, S. M., P. W. Kållberg, A. J. Simmons, U. Andrae, V. Bechtold, M. Fiorino, and J. Woollen (2005), The ERA-40 re-analysis, Quarterly Journal of the Royal Meteorological Society, 131, 961–3012.

Urrutia, R., and M. Vuille (2009), Climate change projections for the tropical Andes using a regional climate model: Temperature and precipitation simulations for the end of the 21st century, Journal of Geophysical Research, 114, D02108.

Vergara, W., A. M. Deer, M. Valencia, R. S. Bradley, B. Francou, A. Zarzar, A. Grünwaldt, and S. M. Haeussling (2007), Economic impacts of rapid glacier retreat in the Andes, EOS, Transactions, American Geophysical Union, 88, 261-268.

Vilímek, V., J. Klimeš, A. Emmer, and M. Benešová (2015), Geomorphologic impacts of the glacial lake outburst flood from Lake No. 513 (Peru), Environmental Earth Sciences, 73, 5233-5244.

Viste, E., and A. Sorteberg (2015), Snowfall in the Himalayas: an uncertain future from a little-known past, The Cryosphere, 9, 1147-1167.

Viviroli, D., D. R. Archer, W. Buytaert, H. J. Fowler, G. B. Greenwood, A. F. Hamlet, Y. Huang, G. Koboltschnig, M. I. Litaor, J. I. López-Moreno, S. Lorentz, B. Schädler, H. Schreier, K. Schwaiger, M. Vuille, and R. Woods (2011), Climate change and mountain water resources: overview and recommendations for reserach, management and policy, Hydrology and Earth System Sciences, 15, 471-504.

Vuille, M., and R. S. Bradley (2000), Mean annual trends and their vertical structure in the tropical Andes, Geophysical Research Letters, 27, 3885–3888.

Vuille, M., R. Bradley,M. Werner, and F. Keimig (2003), 20th century climate change in the Tropical Andes: Observations and model results, Climatic Change, 59, 75–99.

Vuille, M., and F. Keimig (2004), Interannual variability of summertime convective cloudiness and precipitation in the Central Andes derived from ISCCP-B3 Data, Journal of Climate, 17, 3334-3348.

Vuille, M. (2006), Climate change in the tropical Andes - observations, models, and simulated future impacts on glaciers and streamflow, Mountain Research and Development, 26, 3.

Vuille, M., B. Francou, P. Wagnon, I. Juen, G. Kaser, B. G. Mark, and R. S. Bradley (2008a), Climate change and tropical Andean glaciers: Past, present and future, Earth Science Reviews, 89, 79-96.

Vuille, M., G. Kaser, and I. Juen (2008b), Glacier mass balance variability in the Cordillera Blanca, Peru and its relationship with climate and the large-scale circulation, Global and Planetary Change, 62, 14-28.

Vuille, M., E. Franquist, R. Garreaud, W. S. Lavado Casimiro, and B. Cácares (2015), Impact of the global warming hiatus on Andean temperature, Journal of Geophysical Research - Atmospheres, 120, 3745-3757.

Wagnon, P., P. Ribstein, G. Kaser, and P. Berton (1999), Energy balance and runoff seasonality of a Bolivian glacier, Global and Planetary Change, 22, 49-58.

Wagnon, P., A. Linda, Y. Arnaud, R. Kumar, P. Sharma, C. Vincent, J. G. Pottakkal, E. Berthier, AL. Ramanathan, S. I. Hasnain, and P. Chevallier (2007), Four years of mass balance on Chhota Shigri Glacier, Himachal Pradesh, India, a new benchmark glacier in the western Himalaya, Journal of Glaciology, 53, 603–611.

Wagnon, P., M. Lafaysse, Y. Lejeune, L. Maisincho, M. Rojas, and J. P. Chazarin (2009), Understanding and modeling the physical processes that govern the melting of snow cover in a tropical mountain environment in Ecuador, Journal of Geophysical Research, 114, D19112.

Wang, S., M. Zhang, N. C. Pepin, Z. Li, M. Sun, X. Huang, and Q. Wang (2014), Recent changes in freezing level heights in High asia and their impacts on glacier changes, Journal of Geophysical Research - Atmospheres, 119, 1753-1765.

WGMS (2015): Global Glacier Change Bulletin No. 1 (2012-2013). Zemp, M., I. Gärtner-Roer, S. U. Nussbaumer, F. Hüsler, H. Machguth, N. Mölg, F. Paul, and M. Hoelzle (eds.), ICSU(WDS) / IUGG(IACS)/ UNEP / UNESCO / WMO, World Glacier Monitoring Service, Zurich, Switzerland, 230.

WGMS (1989), World glacier inventory – Status 1988. W. Haeberli, H. Bösch, K. Scherler, G. Østrem, and C. C. Wallén (eds.), IAHS (ICSI) / UNEP / UNESCO, World Glacier Monitoring Service, Zurich, Switzerland: 458 pp.

Williams, P., and D. Nash (2006), Sighting the Apu: a GIS analysis of Wari imperialism and the worship of mountain peaks, World Archaeology, 38, 455-468.

Winkler, M., I. Juen, T. Mölg, P. Wagnon, J. Gómez, and G. Kaser (2009), Measured and modelled sublimation on the tropical Glaciar Artesonraju, Perú, The Cryosphere, 3, 21-30.

Winkler, M., G. Kaser, N. J. Cullen, T. Mölg, D. R. Hardy, and W. T. Pfeffer (2010), Land-based marginal ice cliffs: focus on Kilimanjaro, Erdkunde, 64, 179-193.

Xu, J., R. E. Grumbine, A. Shreshta, M. Eriksson, X. Yang, Y. Wang, and A. Wilkes (2009), The melting Himalayas: cascading effects of climate change on water, biodiversity, and livelihoods, Conservation biology: the journal of the Society for Conservation Biology, 32, 520-530.

Zemp, M., W. Haeberli, M. Hoelzle, and F. Paul (2006), Alpine glaciers to disappear within decades?, Geophysical Research Letters, 33, L13504.

Zhang, Y., K. Fujita, S. Liu, Q. Liu, and T. Nuimura (2011), Distribution of debris thickness and its effect on ice melt at Hailuogou glacier, southeastern Tibetan Plateau, using in situ surveys and ASTER imagery, Journal of Glaciology, 57, 1147–1157.

Zou, H., L. Zhou, S. Ma, P. Li, W. Wang, A. Li, J. Jia, and D. Gao (2008), Local wind system in the Rongbuk Valley on the northern slope of Mt. Everest, Geophysical Research Letters, 35, L13813.

Part II Research papers

S. Schauwecker

1 Paper I

Schauwecker, S., M. Rohrer, C. Huggel, A. Kulkarni, AL. Ramanathan, N. Salzmann, M. Stoffel, and B. Brock (2015). Remotely sensed debris thickness mapping of Bara Shigri Glacier, Indian Himalaya. *Journal of Glaciology*, 61(228), 675-688.

On the debris-covered tongue of Lirung glacier, Nepal (S. Schauwecker)

Contributions of the PhD candidate:

Conception and design of the work, further developing the method presented by *Foster et al.* (2012), developing methods to estimate wind speed and energy fluxes as well as vertical temperature profiles, analysis and interpretation of meteorological data, model implementation in MATLAB, designing and conducting sensitivity and uncertainty analyses, drafting and writing the article

Remotely sensed debris thickness mapping of Bara Shigri Glacier (Indian Himalayas)

Simone Schauwecker[1,2], Mario Rohrer[1], Christian Huggel[2], Anil Kulkarni[3], AL. Ramanathan[4], Nadine Salzmann[2,5], Markus Stoffel[6,7], Ben Brock[8]

1 Meteodat GmbH, Technoparkstrasse 1, 8005 Zurich, Switzerland
2 Physical Geography Division, Department of Geography, University of Zurich - Irchel, Winterthurerstr. 190, CH-8057 Zurich, Switzerland
3 Divecha Center for Climate Change, Centre for Atmospheric & Oceanic Sciences, Indian Institute of Science, Bangalore, Karnataka 560012, India
4 School of Environmental Sciences, Jawaharlal Nehru University, New Delhi 110067, India
5 Unit of Geography, Department of Geosciences, University of Fribourg, Chemin du Musée 4, CH-1700 Fribourg, Switzerland
6 Institute for Environmental Sciences, University of Geneva, route de Drize 7, CH-1227 Carouge-Geneva, Switzerland
7 Institute of Geological Sciences, University of Bern, Baltzerstrasse 1+3, CH-3012 Bern, Switzerland
8 Geography Department, Northumbria University, Newcastle upon Tyne, UK

Despite the important role of supraglacial debris in ablation, knowledge of debris thickness on Himalayan glaciers is sparse. A recently developed approach based on reanalysis data and thermal band satellite imagery has been proven to be potentially suitable for debris thickness estimation without the need of detailed field data. In this study, we further develop the method and discuss possibilities and limitations, arising in its application to a glacier in the Himalayas with scarce *in-situ* data. Surface temperature patterns are consistent for thirteen scenes of ASTER and Landsat 7 imagery and correlate well with incoming shortwave radiation and air temperature. We use an energy balance approach to subtract these radiation or air temperature effects, in order to estimate debris thickness patterns as a function of surface temperature. Both incoming shortwave and longwave radiation are estimated with a reasonable accuracy when applying parameterizations and reanalysis data. However, the model likely underestimates debris thickness, probably due to incorrect representation of vertical debris temperature profiles, the rate of heat stored and turbulent sensible heat flux. Moreover, the uncertainty of the result was found to increase significantly with thicker debris, a promising result, though, since ablation is enhanced for thin debris of 1-2 cm.

Keywords: Debris-covered glacier; Surface energy balance; glacier mapping; Remote sensing; Glacier surface temperature; Debris thickness estimation; Bara Shigri Glacier; Indian Himalayas

1.1 Introduction

Glaciers with extensive mantles of supraglacial debris on their ablation areas are widely present in many high mountain ranges including the Himalayas (e.g. *Scherler et al.*, 2011; *Bolch et al.*, 2012; *Frey et al.*, 2012). In this region, an expansion of sediment and rock covered areas has been observed in recent decades, due to glacier surface lowering and unstable adjacent slopes, processes which are likely associated with climate change (*Bolch et al.*, 2008; *Schmidt and Nüsser*, 2009; *Shukla et al.*, 2009; *Bhambri et al.*, 2011). Improved knowledge of debris-covered glaciers and their response to climate change is not only interesting from a scientific perspective focused on process understanding, but also essential for the quantification of glacier runoff as well as for present and future water availability (*Wagnon et al.*, 2007; *Brock et al.*, 2010; *Zhang et al.*, 2011; *Reid et al.*, 2012; *Juen et al.*, 2014). Several studies (*Brock et al.*, 2010; *Kayastha et al.*, 2000; *Lambrecht et al.*, 2011; *Mattson et al.*, 1993; *Mihalcea et al.*, 2006; *Nakawo and Young*, 1981; *Nicholson and Benn*, 2006; *Östrem*, 1959; *Reid and Brock*, 2010) have shown relations between debris thickness and ablation rates of the ice beneath. Where ice is covered with very thin debris (1-2 cm), melt is enhanced compared to clean ice as a result of increased absorption of solar radiation and the related rapid heat transfer. On the other hand, melt rates are reduced where debris is thicker than a few centimeters, as less surface heat will be conducted through the debris layer and transferred to the ice as compared to clean ice. Hence, from a hydrological perspective, it is crucial to know where debris is thin enough to enhance melt or above a critical thickness to reduce melt compared to a bare-ice surface. This is why both, the debris-covered area and debris thickness, are critical variables for melt. While the extent of debris can be delineated manually using satellite images (*Paul et al.*, 2013; *Frey et al.*, 2012), thickness estimations are difficult to achieve over larger areas. At the local scale, in-situ measurements of debris thickness have been conducted on several glaciers at individual points, such as e.g. at Haut Glacier d'Arolla (Swiss Alps; *Reid et al.*, 2012), Pasterze Glacier (Austrian Alps; *Kellerer-Pirklbauer et al.*, 2008), Miage Glacier (Italian Alps; *Mihalcea et al.*, 2008a), Hailuogou Glacier (Tibetan Plateau; *Zhang et al.*, 2011), Koxkar Glacier (Central Tien Shan; *Juen et al.*, 2014), Lirung Glacier (Nepalese Himalayas; *Petersen et al.*, 2013), Khumbu Glacier (Nepalese Himalayas; *Nakawo et al.*, 1986), and Imja-Lhotse Shar Glacier (Nepalese Himalayas; *Rounce and McKinney*, 2014).

Recent studies have confirmed a good correlation between debris thickness d and surface temperature T_s for values of d ranging between 1 and 40 cm (*Mihalcea et al.*, 2008a) and therefore confirmed the feasibility of estimating debris thickness based on surface temperature. Empirical relationships have been developed to map d based on thermal band imagery for glaciers for which extensive field measurements exist (*Mihalcea et al.*, 2008a; *Mihalcea et al.*, 2008b). Since these models account for a known relationship between d and T_s, extensive field measurements of debris thickness and surface temperature are needed for the date at which the satellite image was taken. The transferability to other images or glaciers is therefore limited. To overcome the limitations of empirical relationships, *Foster et al.* (2012) developed an energy balance model approach to map debris thickness on Miage glacier, using meteorological data in conjunction with ASTER thermal band imagery. Methods such as these, which are based on satellite imagery along with climate

reanalysis data, have the advantage to map debris thickness of remote glaciers without the need of detailed *in-situ* data. They provide valuable tools for distributed ablation modelling, since *in-situ* debris thickness measurements are very time-consuming and the sites often difficult to access. In fact, for large debris-covered glaciers, it is often impossible to measure debris thickness directly by extensive *in-situ* measurements as e.g. in a 90 m x 90 m grid. The approach F12, here named after the publication of *Foster et al.* (2012), has been applied to an alpine glacier. The method was further developed by *Rounce and McKinney* (2014) and applied to a glacier in the Khumbu region with meteorological data from a nearby meteorological station, and showed promising results to map debris thickness without detailed field measurements. A common limitation of energy balance model approaches is the underestimation of mapped supraglacial sediment (e.g. *Schauwecker*, 2012; *Petersen et al.*, 2013; *Rounce and McKinney*, 2014; *Suzuki et al.*, 2007), and hence calls for further research. The underestimation has in some cases been related to the mixed-pixel effect of poor-resolution DEMs (*Suzuki et al.*, 2007; *Rounce and McKinney*, 2014) and will be discussed here in view of the single energy balance components. A further limitation arises from unknown meteorological conditions on widely debris-covered tongues, here assessed through testing the performance of reanalysis data and parameterizations.

The main aim of this study is to further develop the F12 approach in view of applying it in the Himalayas and by evaluating the performance and uncertainty that arises when applying the approach to a debris-covered glacier where detailed field measurements are sparse. The evaluation is performed by (i) assessing the spatial distribution of surface temperature for different satellite scenes and sensors, (ii) estimating introduced uncertainty by single input parameters for debris properties, meteorological variables from reanalysis data and parameterizations of energy fluxes; and finally by (iii) mapping debris thickness and discussing the underestimation and uncertainty arising through the use of different assumptions.

1.2 Study site

Bara Shigri glacier (32.21°N, 77.63°E) is the largest glacier in the Indian state of Himachal Pradesh (Figure 1-1), in which about 16% of the glacier area in this region is covered by debris (*Frey et al.*, 2012). The glacierized area of Bara Shigri glacier extends from 3920 m asl. at the terminus to around 6000 m asl., comprising an area of ca. 131 km^2 in 2002 and a glacier length of 28 km. The glacier flows in northwest direction and is fed by several tributaries. The Bara Shigri glacial stream feeds its waters into the Chandra River some 3 km below the present-day glacier terminus. About 14% of the total glacier surface of Bara Shigri is extensively debris-covered. At around 4900 m asl., where the main glacier tributaries confluence (‘Konkordiaplatz’), debris appears in the form of medial moraines. Further down, the glacier tongue is continuously covered by moraine material. *Tiwari et al.* (2012) have characterized the tongue of Bara Shigri as covered by widespread and fine-grained debris with variable water content. Various lakes of diameters comprised between 20 and 170 m were identified using optical-thermal images (ASTER) and radar (*Tiwari et al.*, 2012). Based on manual digitalization of a SPOT image taken in June 2014, we identified around 60 to

70 supraglacial lakes with an area larger than 500 m^2 on the lower part of the glacier tongue (Figure 1-1).

The Bara Shigri Glacier lies on the northern slopes of the main Pir Panjal Range, a crystalline axis composed mostly of metamorphites, migmatites, and gneisses (*Kumar et al.*, 1987). *Dutt* (1961) reports that bedrock and moraines of Bara Shigri are mainly dark brown mica-schist with occasional Haimanta (Cambrian) conglomerates. Farther up-glacier and over a distance of several kilometres bedrock is formed by granite, gneiss, muscovite-quartzite and schist (*Singh et al.*, 2015).

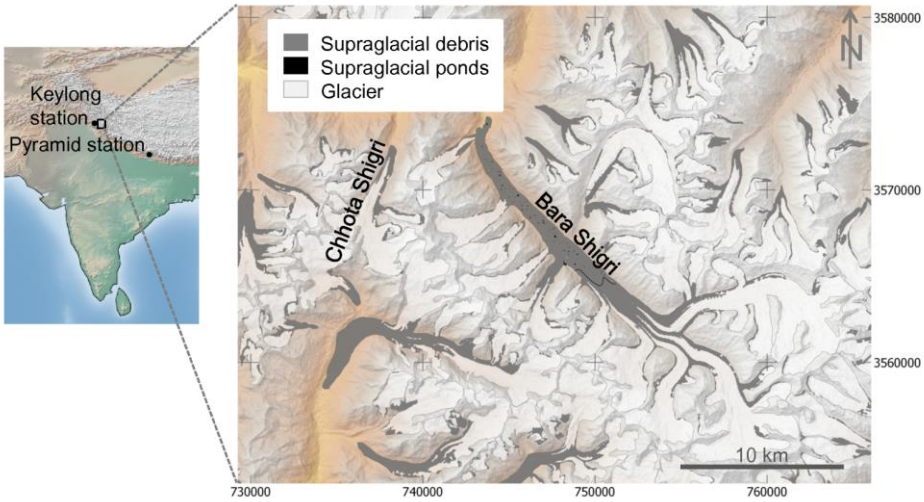

Figure 1-1 Left: Location of the study area and the two meteorological stations Keylong (India, 3119 m asl.) and Pyramid (Nepal, 5050 m asl.). Right: Overview map with the Bara Shigri glacier investigated here and the adjacent Chhota Shigri benchmark glacier to the West (*Wagnon et al.*, 2007). Debris outlines were provided by *Frey et al.* (2012) and glacier outlines are made available by GLIMS (*Raup et al.*, 2007). Supraglacial ponds on the lower part of the glacier tongue (below black line) are manually digitized based on a SPOT image taken in June 2014.

1.3 Data

The method applied in this study requires a combination of remotely sensed estimates of surface temperatures, meteorological data as well as data on debris properties.

ASTER surface kinetic temperature images (AST08) were acquired from the Land Processes Distributed Active Archive Center (LPDAAC). For most scenes, surface temperature can be derived within an accuracy and precision of ± 1.5 K (*Gillespie et al.*, 1998) and a spatial resolution of 90 m. From the Landsat 7 ETM+ satellite imagery, we used the thermal band (Band 6), which is acquired at 60-metre resolution and automatically processed to 30-metre pixels. Surface temperature is derived according to NASA (2011). Seven ASTER and six Landsat 7 images were analyzed for clear-sky days during the dry season (September to November) with snow-free ablation areas (Table 1-1). For the estimation of debris thickness, only images with more than 10 percent of debris-covered area exceeding 0°C were considered, since the model used cannot map

debris thickness for cells with negative surface temperature values. On homogeneous areas, *in-situ* thermistor measurements and ASTER surface temperature estimations have been found in the past to correlate reasonably well (*Mihalcea et al.*, 2008a).

Table 1-1 Date, time and percent of debris-covered area with surface temperature below 0°C for 13 acquired satellite images. Only images with less than 10% of the debris-covered area below 0°C were used for the estimation of debris thickness.

Para-meter	Unit	Value	Site	Region	Literature
α	-	0.27	Changri Nup	Nepal Himal.	Lejeune et al. (2013)
		0.21	Khumbu	Nepal Himal.	Takeuchi et al. (2000)
		0.12 - 0.16	Miage	Alps	Brock et al. (2010)
		0.2	Ngozumpa	Nepal Himal.	Nicholson and Benn (2012)
K	$Wm^{-1}K^{-1}$	0.7	Changri Nup	Nepal Himal.	Lejeune et al. (2013)
		0.85 ± 0.2	Base Camp, Khumbu	Nepal Himal.	Conway and Rasmussen (2000)
		1.28 ± 0.15	Lobuche, Khumbu	Nepal Himal.	Conway and Rasmussen (2000)
		0.96 ± 0.33	Imja-Lhotse Shar	Nepal Himal.	Rounce and McKinney (2014)
		1.36 ± 0.14	Ngozumpa	Nepal Himal.	Nicholson and Benn (2012)
ε	-	0.95	Changri Nup	Nepal Himal.	Lejeune et al. (2013)
		0.95	Imja-Lhotse Shar	Nepal Himal.	Rounce and McKinney (2014)
		0.94	Miage	Alps	Brock et al. (2010)
z_0	m	0.05	Changri Nup	Nepal Himal.	Lejeune et al. (2013)
		0.016	Miage	Alps	Brock et al. (2010)
		0.0063	Khumbu	Nepal Himal.	Takeuchi et al. (2000)
a	°C	7	Miage	Alps	Foster et al. (2012)
		2.8	Haut Glacier d'Arolla	Alps	Schauwecker (2012)
		4.5 - 8.1	Lirung	Nepal Himal.	Petersen et al. (2013)
b	-	0.32	Miage	Alps	Foster et al. (2012)
		0.32	Haut Glacier d'Arolla	Alps	Schauwecker (2012)
		0.2	Lirung	Nepal Himal.	Petersen et al. (2013)

Reanalysis data for air temperature T_a, wind speed *u*, relative humidity *rh* and precipitable water *pw* are used as inputs for the estimation of local meteorological variables. We compare temperature and wind speed of reanalysis data with measurements of two meteorological stations to estimate the accuracy of the gridded climate data in the Himalayan region. The first meteorological station Keylong (32.57°N, 77.03°E) is part of the automated network maintained by the India Meteorological Department (IMD). The station is located close to a small village, about 70 km to the Northwest of the study site at an elevation of 3119 m asl. The Pyramid station (27.958°N, 86.813°E) is located at an elevation of 5050 m asl. in the Khumbu valley (Nepal). We used the two most widely used reanalysis products, namely the NCEP/NCAR (*Kalnay et al.*, 1996) and ERA-Interim Reanalysis (*Dee et al.*, 2011) datasets. Comparison of reanalysis data with meteorological field data was performed for clear sky days of the dry season (September to November) at 06:00 UTC, the approximate time of the satellite overpass at Bara Shigri glacier. We used data for the

700 hPa (approximately 3100 m asl.) and 500 hPa (approximately 5800 m asl.) for comparison with the observed meteorological records, respectively. For the debris thickness estimation, reanalysis values for air temperature and relative humidity from NCEP/NCAR were used for the 600 hPa level (approximately 4360 m asl.).

Parameter values for albedo α, thermal conductivity K, emissivity ε, surface roughness z_0 and parameters are taken from field measurements and published literature on Himalayan and alpine glaciers (*Conway and Rasmussen*, 2000; *Takeuchi et al.*, 2000; *Brock et al.*, 2010; *Nicholson and Benn*, 2012; *Schauwecker*, 2012; *Foster et al.*, 2012; *Lejeune et al.*, 2013; *Petersen et al.*, 2013; *Rounce and McKinney*, 2014). Glacier and debris masks were used to restrict debris thickness maps to the debris-covered areas of the glacier. The outline of debris extent was reconstructed based on debris outlines compiled for a glacier inventory for the western Himalaya from satellite data (*Frey et al.*, 2012). Glacier outlines were obtained from the Global Land and Ice Measurements from Space (GLIMS).

1.4 Methods

1.4.1 Energy balance to compute debris thickness (model F12)

The F12 approach is described briefly in the following, as it was used and further developed in view of its application to Himalayan glaciers. Debris thickness d is mapped for every pixel of the spaceborne debris surface temperature T_s by solving the energy balance for the debris-covered glacier surface with d as a residual. The energy balance equation describes that the change in heat stored within a defined volume of debris is equal to the sum of all fluxes towards the debris volume, given by:

$$\Delta D = S_{net} + L_{net} + H + G$$

where (ΔD) is the rate of change in heat stored within debris, S_{net} is net shortwave radiation, L_{net} is net longwave radiation, H is the sensible turbulent heat flux and G the conductive heat flux. Energy contribution provided by rain and latent heat are neglected, assuming that the debris layer is dry at the time of satellite image acquisition (*Brock et al.*, 2007; *Brock et al.*, 2010). Fluxes are considered positive when directed towards the debris layer.

Energy transfer within debris is reduced here to conductive heat flux G, neglecting other transfer energy sources and sinks like e.g., convection, advection, phase changes or ventilation. The one-dimensional conductive heat flux G is estimated from the Fourier's law, as a function of the effective conductivity K of the debris material and the temperature gradient within the layer dT/dz. Assuming a linear temperature gradient within the debris surface and temperature of the ice-debris interface to be at melting point:

$$G = -K\frac{dT}{dz} \approx -K\frac{T_s}{d}$$

where T_s debris surface temperature and d debris thickness. Conductivity K is strongly influenced by the moisture content of the debris surface. Here, we assume that the uppermost level of the debris layer is dry and use a spatially constant value for the conductivity of dry material.

The rate of change in heat stored ΔD at the time of the image acquisition results from the morning warming of the debris layer. This heat flux depends on the density and specific heat of the debris layer, the rate of temperature change and debris thickness. Stored heat cannot be determined precisely in this approach as satellite thermal band imagery has a daily resolution and does not represent a sequence of images. *Foster et al.* (2012) therefore assumed that the rate of change in heat stored is a fraction F (hereafter referred as "stored heat factor F") of the conductive heat flux in the form:

$$\Delta D = -F \cdot G$$

Using these assumptions, debris thickness is given by:

$$d = \frac{(1+F)K\,T_s}{S_{net} + L_{net} + H}$$

Net shortwave radiation S_{net} is calculated from $S_{in}(1\text{-}albedo)$, using a spatially constant value for albedo, according to *Rounce and McKinney* (2014). *Foster et al.* (2012) proposed to take a spatially constant value for albedo for Miage glacier due to minor measured spatial variation Incoming shortwave radiation S_{in} is computed using the equations of *Strasser et al.* (2004) for a clear sky situation. Incoming longwave radiation can be estimated through parameterizations as described by *Brunt* (1932) or *Brutsaert* (1975). Outgoing longwave radiation L_{out} is computed based on the Stefan-Boltzmann law, using surface temperature T_s from the satellite images and spatially constant emissivity. The sensible heat flux H is calculated using the bulk aerodynamic approach:

$$H = Du(T_a - T_s)$$

Where u is wind speed, T_a and T_s air and debris surface temperatures, respectively, and D is a bulk exchange coefficient. D can be calculated using a stability correction based on the bulk Richardson number (*Brutsaert*, 1975; *Oke*, 1987).

Air temperature T_a distribution over glaciers is commonly extrapolated from station data by applying a spatially constant lapse rate, which may not hold for debris-covered glaciers. *Foster et al.* (2012) proposed that air temperature is strongly related to surface temperature T_s in the morning hours with strong insolation and low wind speed. At this time of the day, under strong insolation, above debris-covered surfaces, sensible as well as longwave heat fluxes are upwardly directed transferring heat to the near-surface air (*Reid and Brock*, 2010). *Foster et al.* (2012) computed an empirical relationship based on data from Miage glacier in the form:

$$T_a = a + b \cdot T_s$$

where T_a is air temperature, T_s surface temperature and a, b are empirical parameters that can be derived based on measurements of air temperature and surface temperature on debris-covered

glaciers. Table 1-2 shows values for the linear regression of air temperature against surface temperature for three sites in the Alps and the Himalayas with different elevation and debris cover. Here we take values from Lirung and Miage glaciers to extrapolate air temperature across the glacier surface.

Table 1-2 Values from literature for albedo, thermal conductivity, emissivity, surface roughness and parameters *a* and *b*.

Satellite	Year	Day	Time (UTC)	Area of T_s < 0°C (%)
ASTER	2003	8 Oct	05:41	1
ASTER	2004	17 Sep	05:34	0
ASTER	2005	7 Nov	05:34	37
ASTER	2006	17 Nov	05:41	48
ASTER	2007	20 Nov	05:41	54
ASTER	2011	30 Oct	05:41	24
ASTER	2012	23 Sep	05.35	6
Landsat 7	1999	13 Oct	05:17	11
Landsat 7	2000	29 Sep	05:14	4
Landsat 7	2000	15 Oct	05:14	2
Landsat 7	2001	18 Oct	05:12	5
Landsat 7	2002	5 Oct	05:11	16
Landsat 7	2002	22 Nov	05:12	67

1.4.2 Extension of the F12 approach

In view of the different regional context and comparably limited number of existing field-based data, we modified the F12 approach to make it applicable to an extensively debris-covered glacier in the Indian Himalayas. The modifications, illustrated schematically in Figure 1-2, are mainly related to (i) the vertical temperature gradient within the debris layer, which is possibly not linear within the debris layer in the morning hours and (ii) the energy balance, which has been closed in this application for the uppermost layer (uppermost 10%) rather than for the entire debris cover.

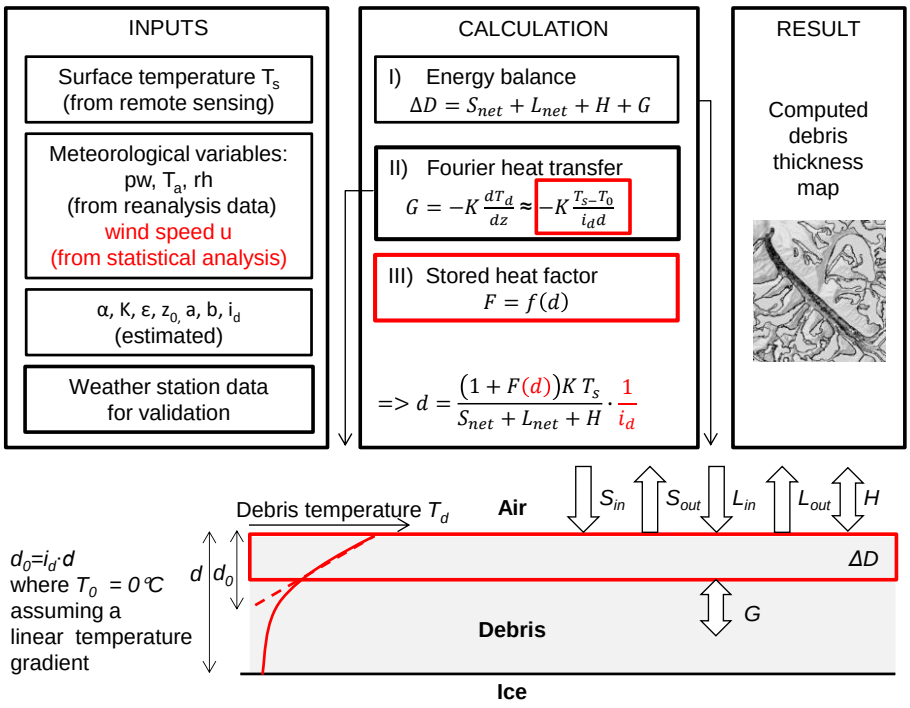

Figure 1-2 Schematic view of changes added to the F12 approach presented by *Foster et al.* (2012) to map debris thickness with reanalysis data and thermal band surface temperature. Additions to the original approach are highlighted in red.

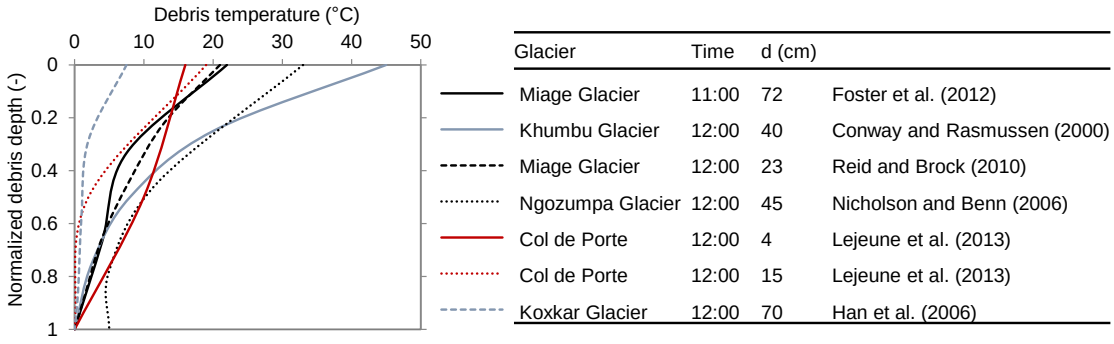

Glacier	Time	d (cm)	
Miage Glacier	11:00	72	Foster et al. (2012)
Khumbu Glacier	12:00	40	Conway and Rasmussen (2000)
Miage Glacier	12:00	23	Reid and Brock (2010)
Ngozumpa Glacier	12:00	45	Nicholson and Benn (2006)
Col de Porte	12:00	4	Lejeune et al. (2013)
Col de Porte	12:00	15	Lejeune et al. (2013)
Koxkar Glacier	12:00	70	Han et al. (2006)

Figure 1-3 Temperature profiles within the supraglacial debris at about noon local time as published in literature.

Observations have shown that temperature gradients within a debris layer are not linear at around 10 to 12 AM local time, as illustrated in Figure 1-3 (*Conway and Rasmussen*, 2000, *Han et al.*, 2006; *Nicholson and Benn*, 2006; *Reid and Brock*, 2010; *Lejeune et al.*, 2013). Taking a linear gradient within the entire debris leads to a large underestimation of debris thickness. Recently published results by *Rounce and McKinney* (2014) also indicate that accounting for a nonlinear temperature gradient is crucial. Here, instead of taking a linear gradient, we estimate the depth d_0

at which the linear temperature gradient would reach 0°C. Based on field measurements, the 0°C depth is estimated to be half of the total debris depth ($d_0 = i_d \cdot d$). Conductive heat flux is then computed by:

$$G \approx -K \frac{T_s - T_0}{i_d d}$$

where T_0 is 0°C, and the factor i_d is 0.5.

We assume that F is a function of debris thickness and thus should be represented by a dependent stored heat factor $F(d)$. In case of a thin debris cover, we assume that the surface is close to an equilibrium temperature and is not warming up strongly in the morning hours. The energy from the surface is conducted through the debris layer and melts the ice beneath, leading to a linear temperature gradients and a small F (small fraction $\Delta D/G$). Where debris is thick, the diurnal temperature maxima of the debris surface increases. Energy from the surface is used to heat up the debris layer, resulting in a larger F (large fraction $\Delta D/G$). This relationship can be expressed based on data found in literature (*Conway and Rasmussen*, 2000; *Nicholson and Benn*, 2006; *Reid and Brock*, 2010; *Foster et al.*, 2012; *Lejeune et al.*, 2013) by a polynomial function of the order 2 with an R^2 of 0.97 (Figure 1-4). However, we found that the iterated result converges to 0 for $F<1$. Therefore, the assumption of a linear relationship with $F=1$ where $d=0$ is necessary. Debris thickness d is finally derived by rearranging the energy balance and the Fourier's law in order to get the result by iterating

$$d = \frac{(1+F(d))K\,T_s}{S_{net}+L_{net}+H} \cdot \frac{1}{i_d}, \qquad F = m \cdot d(F) + n$$

where the parameters m and n are taken from the linear regression in (Figure 1-4). The debris thickness d is first evaluated for a neutral F, and this value is used to make an initial estimate of F. This initial estimate is then used to recalculate d and this procedure is repeated until the value of d is unchanged.

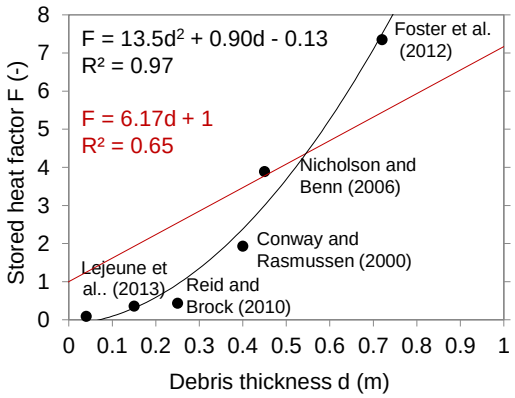

Figure 1-4 Stored heat factor F for the upper ca. 10 to 50% of the debris layer at around noon as a function of debris thickness using vertical temperature profiles published in literature. Note that F increases clearly with larger debris thickness.

1.5 Model Application

1.5.1 Satellite derived surface temperatures

The F12 model is transferable in time (applicable to different satellite images), given that the pattern and distribution of computed d are consistent for different satellite images. Since d is calculated as a function of T_s – with increasing computed debris thickness for warmer surfaces – spatial patterns of T_s are required as well to be consistent among different satellite images. Hence, an important test for the model performance and transferability consists in comparing the spatial distribution of remotely sensed surface temperatures between different satellite scenes.

Figure 1-5 and Figure 1-6 show that the distribution and the pattern of the standardized surface temperatures are highly consistent for different scenes and sensors (ASTER and Landsat 7), despite of differences in mean surface temperatures. Relatively high surface temperatures are observed for the medium moraine and the eastern edge of the glacier tongue, as well as across the lowest part of the tongue. Figure 1-7 shows that mean surface temperature is clearly correlated to modelled incoming shortwave radiation at the time of satellite image acquisition with an R^2 of 0.75 and to air temperature from reanalysis data (for 32.5N/77.5E at 600hPa) with an R^2 of 0.74.

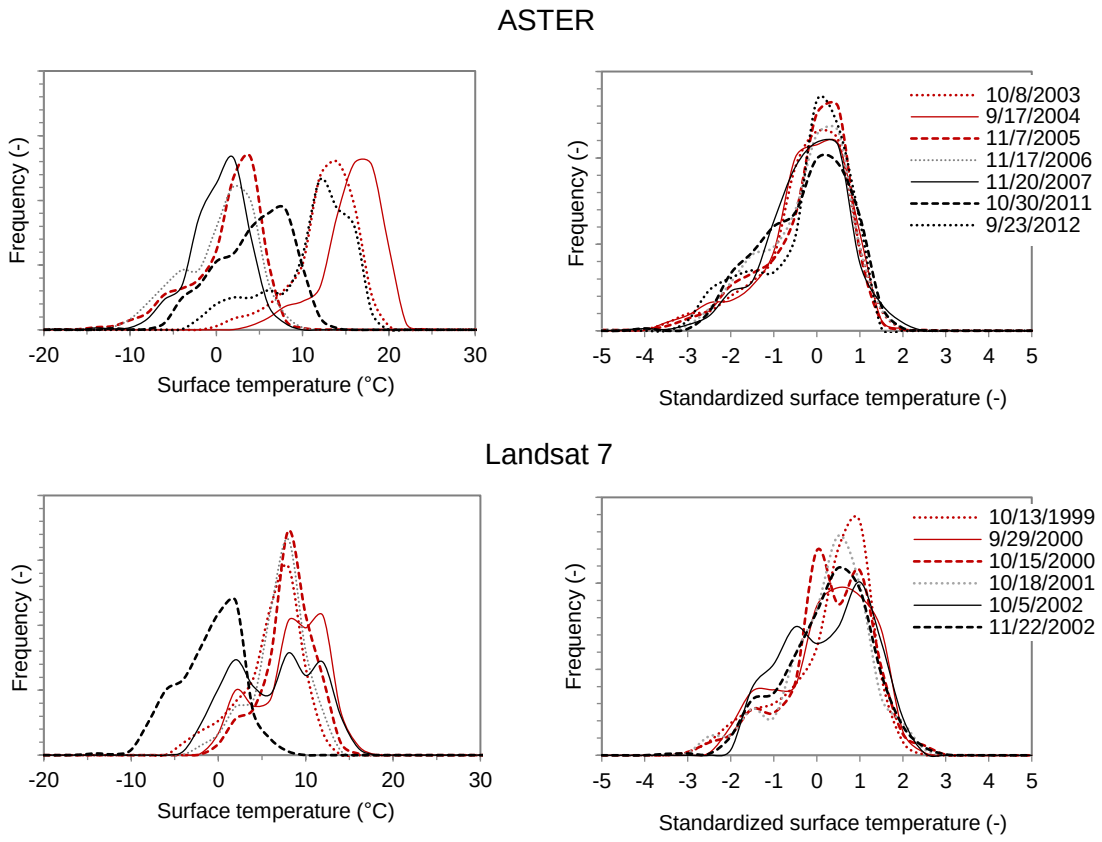

Figure 1-5 Histograms of surface temperature and standardized surface temperature for the debris-covered part of Bara Shigri, based on seven ASTER and six Landsat 7 satellite images, taken in dry season conditions between 1999 and 2012 on clear-sky days.

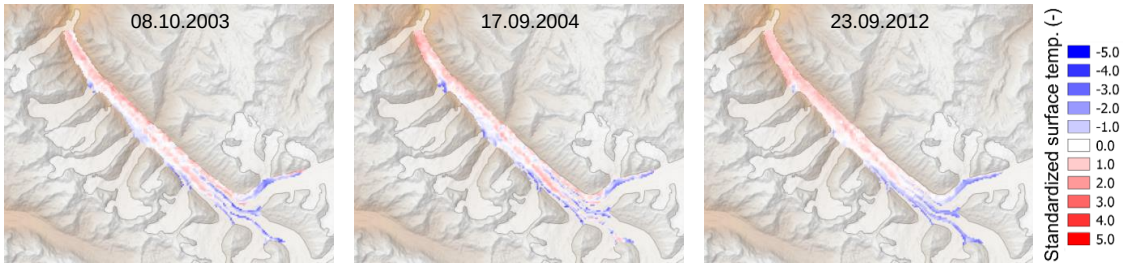

Figure 1-6 Maps of standardized surface temperature for Bara Shigri based on three ASTER thermal band satellite images. Relatively high surface temperatures are observed for the medium moraine and the eastern edge of the glacier tongue, as well as across the lowermost part of the tongue.

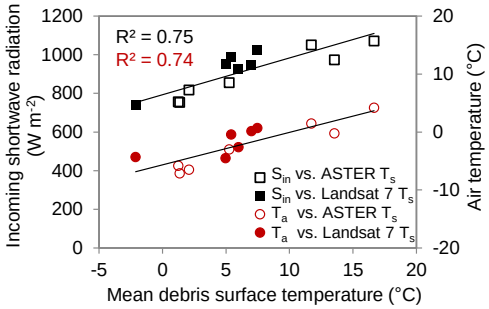

Figure 1-7 Incoming shortwave radiation (using the approach described in *Strasser et al.*, 2004) and NCEP/NCAR air temperature versus mean ASTER (hollow) and Landsat 7 (filled) surface temperature of the debris-covered glacier area of Bara Shigri.

1.5.2 Reanalysis data versus station data

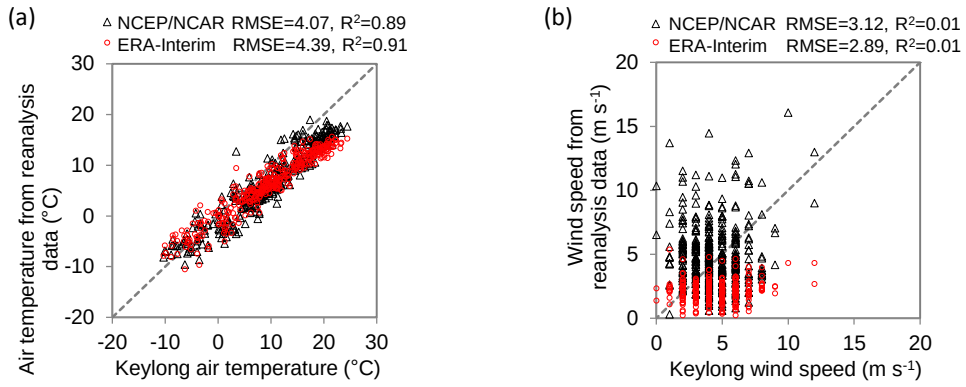

Figure 1-8 Reanalysis (ERA-Interim and NCEP/NCAR) 700 hPa level data versus station measurements at Keylong for (a) air temperature and (b) wind speed.

Reanalysis data, including wind speed, air temperature, relative humidity and precipitable water, are used to compute shortwave and longwave radiation and turbulent sensible heat flux. We compare reanalysis data for wind speed and air temperature from both ERA-Interim and NCEP/NCAR to the Keylong station data to check for their representativeness within the Himalayan region.

700 hPa level air temperature from NCEP/NCAR and ERA-Interim has been used for the computation of downwelling longwave radiation and correlates well to measured air temperature from Keylong station (Figure 1-8a). Reanalysis data tends to underestimate local values for air temperature slightly, probably because it represents free-atmosphere and does not consider boundary layer effects.

Wind speed from reanalysis data, used for the computation of turbulent fluxes, is not correlated with measurements of meteorological stations (Figure 1-8b). To overcome the low quality in input variables for wind speed, we conducted a statistical analysis of the Keylong and Pyramid station data. The analysis shows that wind speed for clear sky days from September to November at 06:00 UTC is mostly between 1 to 4 m s^{-1} for the Keylong (Figure 1-9a), and 3 to 7 m s^{-1} for Pyramid (Figure 1-9b) stations, whereas the distribution is much more scattered for the entire period including all time steps. Given the lack of correlation between reanalysis wind speed and measured, we used measured wind speed at the adjacent station and assumed that wind speed on Bara Shigri is close to 3 m s^{-1} at the time of satellite overpass.

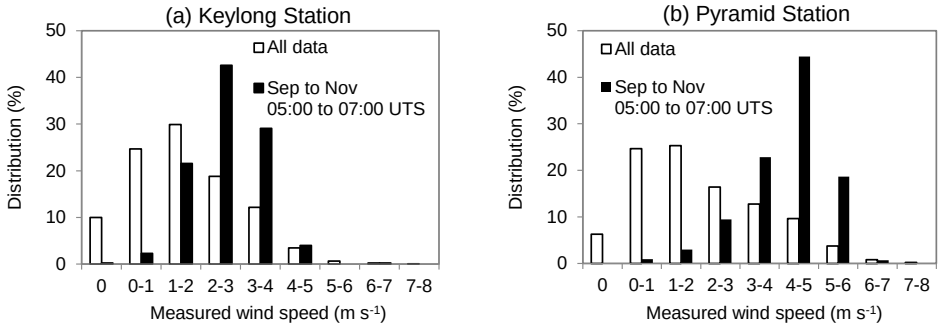

Figure 1-9 Histograms of wind speed measured at the (a) Keylong and (b) Pyramid meteorological station during all seasons and times (grey bars) as well as for September to November from 05:00 to 07:00 UTC for clear-sky conditions with incoming shortwave radiation > 800 Wm^{-2} (black bars).

1.5.3 Parameterisation of radiative fluxes

Longwave radiation fluxes are computed for the Khumbu region using the empirical relationships introduced by *Brunt* (1932) and *Brutsaert* (1975). The parameterization by *Brunt* (1932) relates clear-sky emissivity to screen-level measurements of air temperature and humidity, using

empirically determined coefficients. *Brutsaert* (1975) developed a more physically based approach based on the Schwarzschild's transfer equations for simple atmospheric profiles of a certain air temperature and vapour pressure. Parameterizations of downwelling longwave radiation L_{in} are compared to meteorological station data from Pyramid station under clear sky conditions (S_{in} > 800 Wm^{-2}) from September to November at about noon. In addition, we compared ERA-Interim downwelling longwave radiation to the station measurements. ERA-Interim is overestimating incoming longwave radiation by an average of about 60 W m^{-2} as compared to station measurements (Figure 1-10a). Both parameterizations are accurate for measured longwave below around 230 W m^{-2}, whereas an underestimation is found for the higher end of measured high longwave radiation. For the purpose of this study, the method of *Brutsaert* (1975) seems to be more accurate with a RMSE of 5.9 W m^{-2} (compared to RMSE=11.2 W m^{-2}) for situations with measured incoming longwave radiation below 230 W m^{-2}.

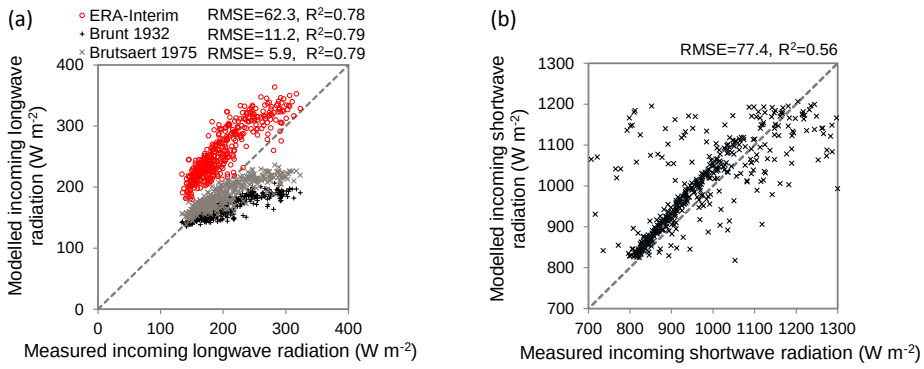

Figure 1-10 Modelled versus measured radiation fluxes for the Pyramid station at 06:00 UTC between September and November 2002 to 2008 where incoming shortwave radiation was above 800 Wm^{-2} (a) downwelling longwave radiation and (b) incoming shortwave radiation. For longwave radiation, RMSE and R^2 are given for measured incoming longwave radiation below 230 Wm^{-2}.

Shortwave radiation was computed using the parameterization proposed by *Strasser et al.* (2004) accounting for the total transmittance of the atmosphere, given as the product of the individual transmittances. Precipitable water is taken from ERA-Interim reanalysis data and a spatially constant value for incoming shortwave radiation is assumed. Direct solar radiation under clear-sky conditions is assumed to vary only slightly within the elevation range of 3900 m asl. to about 5000 m asl. for Bara Shigri. In addition, the surface of debris-covered glacier tongues is assumed to be flat, which may not be the case for ice cliffs and steep moraines, but any improvement in model performance including the slope resulted to be questionable, at least for the European Alps (*Foster et al.*, 2012). As the local time of image acquisition is almost midday, spatial variations due to horizon obstruction and reflections are neglected. The parameterization of incoming shortwave radiation is compared to the Pyramid data for the months September to November for 06:00 UTC

time in order to validate the approach developed by *Strasser et al.* (2004) for clear-sky conditions at about noon in the Himalayan region. As can be seen from Figure 1-10b, the parameterization of shortwave radiation tends to strongly over- and underestimate measured values in some cases. Nevertheless, the performance proves to be good (RMSE=77.4, R^2= 0.56) for the range of measured shortwave radiation of 800 to 1300 Wm^{-2} and corresponds to the approximate range of clear-sky situations.

1.5.4 Sensitivity analysis

In a next step we introduce a sensitivity analysis to see how the uncertainty of modelled debris thickness can be apportioned to energy fluxes, input variables and parameters. We therefore run the model 10^3 times for each variable and parameter by varying one parameter while keeping the others constant. Input variables for wind speed were assumed to be normally distributed. Parameters were varied uniformly within a range of plausible values taken from literature or normally distributed with estimated mean values and standard deviations (Table 1-3). Longwave and shortwave radiation fluxes were computed with the parameterizations introduced by *Brutsaert* (1975) and *Strasser et al.* (2004), respectively, and varied by the standard deviation, which was derived by comparing computation to station data. The sensitivity analysis was based on the satellite image taken on September 23, 2012, assuming that the uncertainty of the parameters and variables is transferable to other images. The uncertainty of the results is evaluated as a function of debris thickness.

Table 1-3 Standard deviation of estimated heat fluxes and ranges of input parameters and variables used for the sensitivity analysis. The right column explains for which components of the energy balance the input values and parameters are used for.

Heat flux	Range	
Incoming longwave rad. L_{in}	μ computed, δ= 6 Wm^{-2}	
Incoming shortwave rad. S_{in}	μ computed, δ= 77 Wm^{-2}	
Parameters and variables	**Range**	**Used for:**
Albedo α	0.1 - 0.3	S_{out}
Emissivity ε	0.94 - 0.98	L_{out}
Surface temperature T_s	μ from ASTER/Landsat, δ=1K	L_{out}, T_s, H
Surface roughness z_0	0.001 - 0.01m	H
Parameter a	μ=0.3, δ=0.05	H
Parameter b	μ=6°C, δ=2°C	H
Wind speed u	μ=3 ms^{-1}, δ=1ms^{-1}	H
Conductivity K	0.7 - 1.3 $Wm^{-1}K^{-1}$	K
Stored heat factor F	δ=1	F
0°C depth factor i_d	μ=0.5, δ=0.1	i_d

The parameters introducing most uncertainty are related to the unknown temperature profile within the debris at the time of satellite image acquisition (Figure 1-11a). Highest uncertainty is introduced by the estimation of a linear temperature gradient within the debris (expressed by the 0°C depth factor i_d) and the relation of stored heat to conducted heat (expressed by the stored heat factor F). Moreover, thermal conductivity introduces remarkable uncertainty, followed by surface temperature T_s. In this context, surface temperature estimation T_s from the satellite image leads to notable uncertainties for low debris thickness.

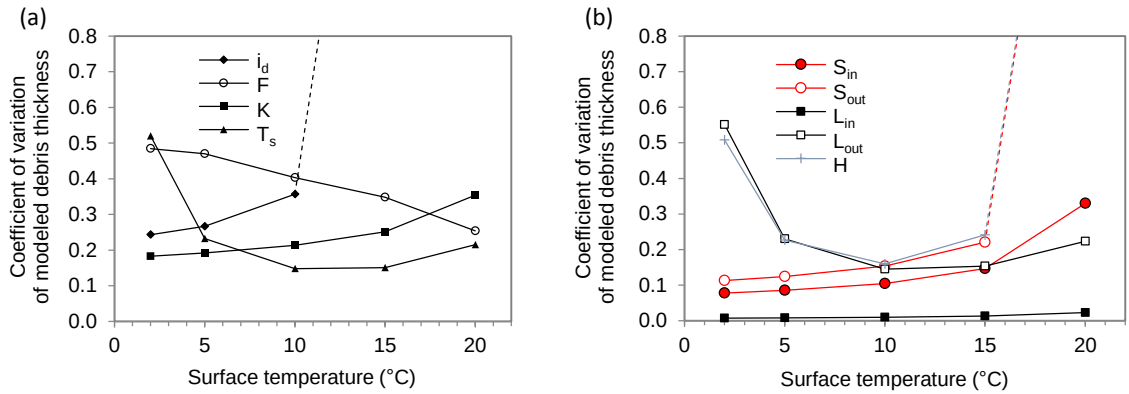

Figure 1-11 Coefficient of variation of modelled debris thickness as a function of surface temperature T_s (a) for different parameters (0°C depth factor i_d, stored heat factor F, conductivity K, surface temperature T_s); and (b) for different heat fluxes (incoming and outgoing shortwave, S_{in}, S_{out}, and longwave radiation, L_{in}, L_{out}, and turbulent sensible heat flux H).

Generally, the single energy fluxes present smaller uncertainty than the characteristics of the debris (Figure 1-11). For low temperatures, L_{out} and H are important, whereas H and S_{out} (through albedo) are important for warm surfaces. For warm surfaces, the uncertainty of H becomes very high mainly due to the unknown air temperature, followed by surface roughness z_0 and wind speed u.

1.5.5 Debris thickness

The total uncertainty of model results that arises in estimating physical parameters and taking meteorological variables from reanalysis data was assessed by running the model several times and by varying randomly and simultaneously input variables and parameters. Figure 1-12 shows that uncertainty is small for cool surfaces but it increases significantly with increasing surface temperature, especially for temperature above ca. 10°C for which debris thickness cannot be estimated with reasonable certainty. Even though i_d and F were hold constant in this Figure, the uncertainties are remarkable. It seems that above roughly 10°C, the method cannot be relied on to give an accurate results, although it should correctly identify the pixel as relatively thick debris. The spread in results is small for relatively cool surfaces, which means that thin debris can be identified with a lower uncertainty.

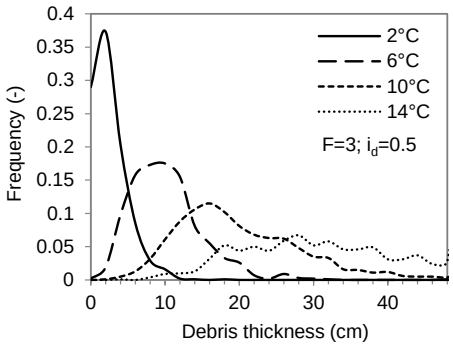

Figure 1-12 Distribution of the modelled debris thickness (varying the energy fluxes, input parameters and variables) for different surface temperatures as analyzed for the ASTER scene taken on September 23, 2012, assuming constant 0°C depth (i_d=0.5) and stored heat factor (F=3).

A final debris thickness map was calculated for the entire debris-covered area, including each of the satellite imagery scenes (Figure 1-13). The final debris thickness values of every pixel represent the mean of six satellite images, whereas the values of every image are from the median value of the 10^3 runs. In their work conducted in the Alps and based on extensive field data, *Foster et al.* (2012) concluded that the F12 model is able to properly identify areas with thick debris cover (>50 cm). By analogy and assuming comparable system behavior, we can assume that debris cover passes this threshold at the medial moraine of the heavily debris-covered tongue of Bara Shigri by visual inspection of SPOT satellite imagery and the analysis of photographs taken at the glacier tongue. However, the here computed debris thickness values remain below 30 cm in most cells and the model thus seems to underestimate debris thickness. The modelled result reveals relatively thick debris on medial moraines, the eastern edge and on the lower tongue. The thick debris on the eastern edge is probably deposited from the steep slopes on the East with likely higher erosion activity than on the opposite slopes. Thin debris of a few centimetres thickness is observed at the edges of the medial moraines at the confluence and on the western edge of the tongue.

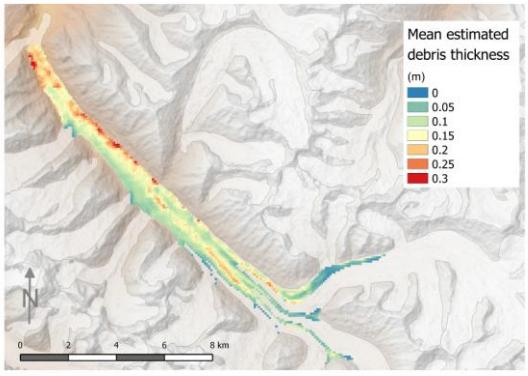

Figure 1-13 Mean debris thickness from three ASTER and three Landsat 7 scenes.

1.6 Discussion

In this study we have applied an approach developed for debris thickness analysis in the Alps and further developed it to be used in data scarce environments such as the Indian Himalayas. As a consequence of working in such remote and data scarce areas, a number of simplifying assumptions about energy fluxes and debris properties must be made, which leads to higher uncertainties in the final results. In the following, we evaluate some of the emerging limitations of the method, which may partly explain the underestimation of debris thickness found in this study. We divide the discussion into subsections where we assess separately the uncertainties associated to the different elements of F12.

1.6.1 Surface temperature

The aim of the energy balance method is to account for all effects determining surface temperature so as to consider exclusively the effect of debris thickness on surface temperature. Figure 1-7 shows that mean surface temperature is clearly correlated to modelled incoming shortwave radiation and air temperature from reanalysis data. This finding is in line with previous work from the Alps where T_s was shown to correlate well with global radiation on debris-covered areas (*Mihalcea et al.*, 2006). The effect for instance of air temperatures and incoming shortwave radiation on surface temperature should be considered and subtracted by the energy balance approach. It is controlled by the denominator via S_{in}, L_{in}, and H. For situations with low air temperature and low solar radiation, the denominator is lower, thus resulting in higher debris thickness for a pixel of a certain surface temperature T_s, than for a situation with warm temperatures and high radiation. The high correlation between T_s and shortwave radiation as well as T_s and air temperature thus supports the use of an energy balance to estimate debris thickness based on remote sensing.

The spaceborne surface temperature is provided with a spatial resolution of 90 m and 30 m for ASTER and Landsat 7 imagery, respectively, and every pixel represents a mean temperature over an assumable inhomogeneous surface. The surface temperature at a certain point depends on various factors which are neglected in the model like shading, aspect, elevation, humidity of debris material, snow cover on debris, cooling during night, and influence of supraglacial ponds and ice cliffs. Where debris is patchy or characterized by a mix of fine material and large boulders, pixels will yield a mean temperature, which may not be representative of adequate heterogeneous surface conditions. However, for large glaciers with continuous debris cover such as Bara Shigri, spaceborne satellite data may well represent surface conditions.

Where surface temperature of debris is below 0°C, the F12 approach cannot be applied properly, as pixels with negative surface temperatures will be classified as debris-free. The presence of snow or morning shadows as well as the strong cooling during the night may thus well lead to relatively low surface temperatures at the time of overflight and therefore to an underestimation of debris thickness. It is therefore important to consider only satellite images with clearly positive surface temperatures across the debris-covered area.

1.6.2 Parameterizations of radiative fluxes

The computation of downwelling longwave radiation is based on an input value for air temperature. The parameterization of incoming longwave radiation as defined by *Brutsaert* (1975) is performing well and shows higher correlation than the values derived by the approach introduced by *Brunt* (1932) or from the ERA-Interim data. The underestimation of longwave radiation by these two parameterizations for situations with relatively high downwelling longwave radiation is probably due to variations in cloudiness. In the Bara Shigri region and elsewhere in the Indian Himalayas, convective clouds are typically forming around noon, thereby leading to increased downwelling longwave radiation. Without measurements of cloud cover, it is not possible to model the increase of radiation due to cloudiness. Nevertheless, at the time of satellite image acquisition and the scenes selected, sky is cloud free and longwave and shortwave radiation can be expected to be modelled reasonably. The uncertainty in outgoing longwave radiation resulted to be higher than for downwelling longwave radiation. The uncertainty stems from the error in surface temperature as derived from satellite imagery and estimated to be in the order of 1 to 1.5 K.

The uncertainty introduced through the parameterizations of incoming shortwave radiation is larger than that for downwelling longwave radiation. Outgoing shortwave radiation is a function of surface albedo, which adds additional uncertainty to this heat flux. We conclude that for a large glacier like Bara Shigri, the spatial variable value for albedo adds remarkable uncertainty to the model result and should be assessed more in-depth using for example Multispectral Landsat Thematic Mapper (TM) satellite data or geological maps.

1.6.3 Turbulent sensible heat flux

Brock et al. (2010) showed that turbulent sensible heat flux is a very large and crucial component of the surface energy balance of a debris-covered glacier and should not be neglected. We suggest that sensible heat flux may be the most uncertain component of the energy balance and constitutes an important source of model error. Uncertainty is mainly due to the uncertainties in surface temperature for surfaces close to 0°C and uncertainties in estimated 2 m air temperature, followed by surface roughness and wind speed. Whereas *Foster et al.* (2012) found that model results are quite sensitive to surface roughness, we found that in our case the uncertainty introduced as a result of unknown surface roughness is relatively small.

For the estimation of turbulent sensible fluxes, a spatial extrapolation of air temperature is needed. *Foster et al.* (2012) showed that the relationship between surface temperature and 2m air temperature is well correlated. This correlation could be confirmed by measurements at Haut Glacier d'Arolla (Swiss Alps) and Lirung Glacier (Nepalese Himalaya). The value *b* is similar for all glaciers, whereas the value *a* is much lower for Haut Glacier d'Arolla glacier. Miage and Lirung glaciers are both extensively debris-covered, whereas Haut Glacier d'Arolla glacier is only partly debris-covered. Based on the results of this study, we assume that the relation of air temperature to surface temperature may depend on the degree of debris-cover of the glacier surface. Where a glacier surface is only partly debris-covered, air temperature is less governed by a heating of the

debris surface, which would be expressed by a lower parameter *a*, as measured for Haut Glacier d'Arolla glacier. On this glacier, air temperature might by influenced strongly by katabatic wind associated with low ice surface temperatures, which may explain the relatively low value for *a*. Since data only exists for one Himalayan glacier, more measurements are clearly needed here to determine this relationship at other debris-covered glaciers and to understand how this relation is influenced by e.g. wind speed and direction as well as the degree of debris cover.

Moreover, wind speed is an important input value for turbulent sensible heat flux. Reanalysis data are not correlated to local wind speed estimations, calling for improved near-surface wind speed estimations as input values to the model. *Zou et al.* (2008) observed that the wind over the debris-covered tongue of Rongbuk glacier is dominated by thermally developed winds, i.e. valley and mountain winds or katabatic winds. Local wind systems over glaciers in this region may be poorly influenced by synoptic winds as a result of topographic shielding effects. We therefore suggest that wind speed over Bara Shigri is dominated by local valley-mountain winds in the morning hours on clear-sky days, rather than by synoptic scale meteorology. As a consequence, quality of input data for wind speed could be improved remarkably by taking statistically derived wind speed instead of reanalysis data, and by selecting clear-sky situations in the morning hours from September to November. As we did not have *in-situ* wind data from at least one nearby station, the application of the F12 approach can be seen as somewhat limited in this particular respect.

1.6.4 Vertical profile of temperature and rate of change in heat stored

Temperature gradients are assumed to be linear in the uppermost debris layers with a gradient defined by the 0°C depth of 50% of the total debris thickness, which can be confirmed by data found in literature and results from *Rounce and McKinney* (2014). Also the assumption of the fraction *F* dependent on *d* is supported by *in-situ* data from other glaciers. Without these new assumptions, the estimated debris thickness would result in much lower values and consequently be strongly underestimated. However, the unknown local vertical gradient as well as the rate of change in heat stored *(ΔD)* lead to remarkable uncertainties in model result which cannot be improved unless field data of vertical temperature gradients will become available for heavily debris-covered glaciers such as Bara Shigri.

1.6.5 Thermal conductivity

Conductivity depends on factors such as e.g., debris composition, lithology, water saturation, and density. Both the increase of water saturation or density of the material will result in increased thermal conductivity. As these characteristics are spatially heterogeneous across the glacier, conductivity may be highly variable in space and a single value does not represent well the conditions of supraglacial debris. As the model does not account for the spatial variability of thermal conductivity *K*, we assessed the uncertainty of the model result introduced by the assumption of a spatially constant *K*. We found that uncertainty is important but smaller than uncertainties caused by the unknown temperature profile of the debris. Again, field measurements are needed to assess the spatial distribution of thermal conductivity on a Himalayan glacier.

1.7 Conclusions

In this paper we further developed and applied the F12 approach presented by *Foster et al.* (2012) to a heavily debris-covered glacier in the Himalayas using satellite thermal band imagery and reanalysis data. Without the further developed elements, the method would strongly underestimate the thickness of the supraglacial sediment.

The spatial pattern of surface temperature was found to be consistent among different satellite images, which is an important requirement to estimate debris thickness based on remote sensing. Mean surface temperature correlates well with estimated incoming shortwave radiation and air temperature at the time of the image acquisition, thus supporting the assumption to estimate debris thickness based on a surface energy balance. We suggest that an energy balance approach (considering shortwave, long wave and sensible heat fluxes) is a valuable tool to remove effects from e.g. radiative fluxes or air temperature on surface temperature, in order to derive debris thickness as a function of surface temperature.

Incoming shortwave and downwelling and outgoing longwave radiation fluxes were estimated with reasonable accuracy in this study by taking parameterizations and input values from reanalysis data, whereas turbulent sensible heat flux is associated with more uncertainty. The distribution, evolution and driving forces of local wind systems over debris-covered glaciers are mostly dominated by thermally developed winds, the “mountain-valley wind” and “glacier wind” (*Zou et al.*, 2008) for fair weather situations. This is why wind estimations from reanalysis data for the free-atmosphere are not correlated to local wind speed measured by meteorological stations in the Himalayas. We therefore present a novel approach in this paper to estimate wind speed based on the analysis of meteorological data from a nearby station.

The energy balance approach probably underestimates debris thickness, which is in line with results from other studies. We suggest that this underestimation is mainly due to the unknown vertical temperature profile and the rate of heat stored, and the uncertain turbulent sensible heat flux. Within the upper debris layers, probably both the vertical gradient of debris temperature and the rate of change of heat stored in the debris in are much higher than assumed, thus leading to an underestimation of debris. Only detailed debris temperature measurements at different depths could help to improve the knowledge on thermal processes within the supraglacial debris. As mentioned by *Rounce and McKinney* (2014), also mixed-pixel effects may lead to an underestimation of debris thickness, however, would probably not explain an overall underestimation across the tongue.

Moreover, thermal conductivity and surface albedo are associated to large uncertainties, since values from measurements on other glaciers span wide ranges and a spatially constant value is assumed for a probably very heterogeneous surface. Uncertainties are strongly increasing with higher surface temperatures, hampering the estimation of debris thickness or total debris volume with a reasonable accuracy. Thin debris is related to much lower uncertainties than thick debris, which is a promising result from a hydrological perspective. For hydrological modelling, it is important to map thin debris of 1-2 cm, where ablation is enhanced, and critical debris thickness

(up to 5 cm), beyond which ablation decreases. This could be observed for the upper tongue on the edges of the medial moraines where the main glacier tributaries confluence. On the lower tongue, debris may be thick enough to insulate the glaciers, causing the ablation rate to decrease in comparison to a bare-ice surface. However, other factors like thermokarst, absorbed heat of supraglacial ponds or ice cliffs could lead to very high downwasting rates despite insulation by debris cover (e.g., *Bolch et al.*, 2008; *Kääb et al.*, 2012).

We suggest that selected field measurements on representative sites on the glacier with different debris thickness and a nearby meteorological station would improve remarkably the model results. Nevertheless, although selected field measurements are needed, remotely sensed data still represent an important source of information to map variability in debris thickness of large and heavily debris-covered glaciers. The high spatial resolution of the consistent surface temperature estimations from thermal band images can hardly be achieved by measurements in the field. Especially for a large debris-covered glacier such as Bara Shigri, where extensive debris measurements are almost impossible to realize, the improved F12 approach presented here could provide important information.

In future studies, the factors governing surface temperature like net shortwave radiation (via albedo, aspect, shading), supraglacial ponds and ice cliffs but also the meteorological variables like air temperature or wind will need to be assessed more in-depth. Only a method able to estimate and subtract all the factors controlling surface temperature may reliably relate debris thickness to surface temperature. If all the effects except for debris thickness can be eliminated, the remaining pattern of surface temperature is thus governed by debris thickness and might be a good indicator for the depth of the supraglacial sediment.

1.8 Acknowledgements

This study was funded by the Swiss Agency for Development and Cooperation (SDC) under the Indian Himalayas Climate Adaptation Programme (http://ihcap.in). The authors are grateful to Ev-K2-CNR committee and the SHARE project for providing open meteorological data from the Pyramid Observatory Laboratory (Khumbu Valley, Nepal). We acknowledge the use of station data provided by IMD. NCEP/NCAR reanalysis data were obtained from US National Oceanic and Atmospheric Administration/Office of Oceanic and Atmospheric Research/Earth and Space Research Laboratory/Physical Sciences Division (NOAA/OAR/ESRL/PSD), Boulder, CO, USA. ERA-interim data were provided by ECMWF, and GLIMS data from the National Snow and Ice Data Center. F. Paul and two anonymous reviewers provided helpful comments that greatly improved the manuscript.

1.9 References

Bhambri, R., T. Bolch, R. K. Chaujar, and S. C. Kulshreshtha (2011), Glacier changes in the Garhwal Himalaya, India, from 1968 to 2006 based on remote sensing, Journal of Glaciology, 57, 543–556.

Bolch, T., M. Buchroithner, T. Pieczonka, and A. Kunert (2008), Planimetric and volumetric glacier changes in the Khumbu Himal, Nepal, since 1962 using Corona, Landsat TM and ASTER data, Journal of Glaciology, 54, 592–600.

Bolch, T., A. Kulkarni, A. Kääb, C. Huggel, F. Paul, J. G. Cogley, H. Frey, J. S. Kargel, K. Fujita, M. Scheel, S. Bajracharya, and M. Stoffel (2012), The state and fate of Himalayan glaciers, Science, 336, 310–314.

Brock, B., A. Rivera, G. Casassa, F. Bown, and C. Acuña (2007), The surface energy balance of an active ice-covered volcano: Villarrica Volcano, southern Chile, Annals of Glaciology, 45, 104–114.

Brock, B.W., C. Mihalcea, M. P. Kirkbride, G. Diolauiuti, M. E. J. Cutler, and C. Smiraglia (2010), Meteorology and surface energy fluxes in the 2005-2007 ablation seasons at the Miage debris-covered glacier, Mont Blanc Massif, Italian Alps, Journal of Geophysical Research, 115, D09106.

Brunt, D. (1932), Notes on radiation in the atmosphere, Quarterly Journal of the Royal Meteorological Society, 58, 389-420.

Brutsaert, W. (1975), On a derivable formula for longwave radiation from clear skies, Water Resources Research, 11, 742–744.

Conway, H., and L. A. Rasmussen (2000), Summer temperature profiles within supraglacial debris on Khumbu Glacier, Nepal, in: Debris-Covered Glaciers, IAHS Publication, Seattle, Washington, USA, pp. 89–97.

Dee, D. P., S. M. Uppala, A. J. Simmons, P. Berrisford, P. Poli, S. Kobayashi, U. Andrae, M. A. Balmaseda, G. Balsamo, P. Bauer, P. Bechtold, A. C. M. Beljaars, L. van de Berg, J. Bidlota, N. Bormann, C. Delsol, R. Dragani, M. Fuentes, A.J.Geer, L. Haimberger, S. B. Healy, H. Hersbacha, E. V. Hólm, L. Isaksen, P. Kållberg, M. Köhler, M. Matricardi, A.P. McNallya, B. M. Monge-Sanz, J.-J. Morcrette, B.-K. Park, C. Peubey, P. de Rosnay, C.Tavolato, J.-N. Thépaut, and F. Vitart (2011), The ERA-Interim reanalysis: Configuration and performance of the data assimilation system, Quarterly Journal of the Royal Meteorological Society, 137, 553–597.

Dutt, G. N. (1961), The Bara Shigri Glacier, Kangra District, East Punjab, India, Journal of Glaciology, 3, 1007–1015.

Foster, L. A., B. W. Brock, M. E. J. Cutler, and F. Diotri (2012), A physically based method for estimating supraglacial debris thickness from thermal band remote-sensing data, Journal of Glaciology, 58, 677–691.

Frey, H., F. Paul, and T. Strozzi (2012), Compilation of a glacier inventory for the western Himalayas from satellite data: methods, challenges, and results, Remote Sensing of Environment, 124, 832–843.

Gillespie, A., S. Rokugawa, T. Matsunaga, J. S. Cothern, S. Hook, and A. B. Kahle (1998), A temperature and emissivity separation algorithm for Advanced Spaceborne Thermal Emission and Reflection Radiometer (ASTER) images, IEEE Transactions on Geoscience and Remote Sensing Journal, 36, 1113–1126.

Han, H., Y. Ding, and S. Liu (2006), A simple model to estimate ice ablation under a thick debris layer, Journal of Glaciology, 52, 528–536.

Juen, M., C. Mayer, A. Lambrecht, H. Han, and S. Liu (2014), Impact of varying debris cover thickness on ablation: a case study for Koxkar Glacier in the Tien Shan, The Cryosphere, 8, 377–386.

Kääb, A., E. Berthier, C. Nuth, J. Gardelle, and Y. Arnaud (2012), Contrasting patterns of early twenty-first-century glacier mass change in the Himalayas, Nature, 488, 495–498.

Kalnay, E., M. Kanamitsu, R. Kistler, W. Collins, D. Deaven, L. Gandin, M. Iredell, S. Saha, G. White, J. Woollen, Y. Zhu, M. Chelliah, W. Ebisuzaki, W. Higgins, J. Janowiak, K. C. Mo, C. Ropelewski, J. Wang, A. Leetmaa, R. Reynolds, R. Jenne, and D. Joseph (1996), The NCEP/NCAR Reanalysis 40-year Project, Bulletin of the American Meteorological Society, 77, 437–471.

Kayastha, R., Y. Takeuchi, M. Nakawo, and Y. Ageta (2000), Practical prediction of ice melting beneath various thickness of debris cover on Khumbu Glacier, Nepal, using a positive degree-day factor, in: Debris-Covered Glaciers, IAHS Publication, Seattle, Washington, USA, pp. 71–151.

Kellerer-Pirklbauer, A., G. K. Lieb, M. Avian, and J. Gspurning (2008), The response of partially debris-covered valley glaciers to climate change: the example of the Pasterze Glacier (Austria) in the period 1964 to 2006, Geografiska Annaler, 4, 269–285.

Kumar, S., H. Rai, K.K. Purohit, B. R. S. Rawat, and A. K. Mundepi (1987), Multi disciplinary glacier expedition to Chhota Shigri Glacier, Department of Science and Technology, Government of India, New Delhi, Technical Report Number 1, 219 pp.

Lambrecht, A., C. Mayer, W. Hagg, V. Popovnin, A. Rezepkin, N. Lomidze, and D. Svanadze (2011), A comparison of glacier melt on debris-covered glaciers in the northern and southern Caucasus, The Cryosphere, 5, 525-538.

Lejeune, Y., J.-M. Bertrand, P. Wagnon, and S. Morin (2013), A physically based model of the year-round surface energy and mass balance of debris-covered glaciers, Journal of Glaciology, 59, 327–344.

Mattson, L. E., J. S. Gardner, and G. J. Young (1993), Ablation on debris covered glaciers: an example from the Rakhiot Glacier, Punjab, Himalaya, in: Snow and Glacier Hydrology, IAHS Publication, Kathmandu, pp. 289–296.

Mihalcea, C., C. Mayer, G. Diolaiuti, A. Lambrecht, C. Smiraglia, and G. Tartari (2006), Ice ablation and meteorological conditions on the debris-covered area of Baltoro glacier, Karakoram, Pakistan, Annals of Glaciology, 43, 292–300.

Mihalcea, C., B. W. Brock, G. Diolaiuti, C. D'Agata, M. Citterio, M. P. Kirkbride, M. E. J. Cutler, and C. Smiraglia (2008a), Using ASTER satellite and ground-based surface temperature measurements to derive supraglacial debris cover and thickness patterns on Miage Glacier (Mont Blanc Massif, Italy), Cold Regions Science and Technology, 52, 341–354.

Mihalcea, C., C. Mayer, G. Diolaiuti, C. D'Agata, C. Smiraglia, A. Lambrecht, E. Vuillermoz, and G. Tartari (2008b), Spatial distribution of debris thickness and melting from remote-sensing and meteorological data, at debris-covered Baltoro glacier, Karakoram, Pakistan, Annals of Glaciology, 48, 49–57.

Nakawo, M., and G. J. Young (1981), Field experiments to determine the effect of a debris layer on ablation of glacier ice, Annals of Glaciology, 2, 85–91.

Nakawo, M., S. Iwata, O. Watanabe, and M. Yoshida (1986), Processes which distribute supraglacial debris on the Khumbu Glacier, Nepal Himalaya, Annals of Glaciology, 8, 129–131.

NASA (2011), National Aeronautics and Space Administration: Landsat 7 Science Data Users Handbook, Available at: http://landsathandbook.gsfc.nasa.gov/.

Nicholson, L., and D. I. Benn (2006), Calculating ice melt beneath a debris layer using meteorological data, Journal of Glaciology, 52, 463–470.

Nicholson, L., and D. I. Benn (2012), Properties of natural supraglacial debris in relation to modelling sub-debris ice ablation, Earth Surface Processes and Landforms 435 pp., Earth Surface Processes and Landforms, 38, 490-501.

Oke, T. R. (1987), Boundary Layer Climates, Routledge, London.

Östrem, G. (1959), Ice melting under a thin layer of moraine, and the existence of ice cores in moraine ridges, Geografiska Annaler, 41, 228–230.

Paul, F., N. E. Barrand, S. Baumann, E. Berthier, T. Bolch, K. Casey, H. Frey, S. P. Joshi, V. Konovalov, R. Le Bris, N. Mölg, G. Nosenko, C. Nuth, A. Pope, A. Racoviteanu, P. Rastner, B. Raup, K. Scharrer, S. Steffen, and S. Winsvold (2013), On the accuracy of glacier outlines derived from remote-sensing data, Annals of Glaciology, 54, 171-182.

Petersen, L., S. Schauwecker, B. W. Brock, W. Immerzeel, and F. Pellicciotti (2013), Deriving supraglacial debris thickness using satellite data on the Lirung Glacier in the Nepalese Himalayas, In: Geophysical Research Abstracts, EGU General Assembly.

Raup, B., A. Racoviteanu, S. J. S. Khalsa, C. Helm, R. Armstrong, and Y. Arnaud (2007), The GLIMS geospatial glacier database: A newtool for studying glacier change, Global and Planetary Change, 56, 101–110.

Reid, T. D., and B. W. Brock (2010), An energy-balance model for debris-covered glaciers including heat conduction through the debris layer, Journal of Glaciology, 56, 903–916.

Reid, T. D., M. Carenzo, F. Pellicciotti, and B. W. Brock (2012), Including debris cover effects in a distributed model of glacier ablation, Journal of Geophysical Research, 117, D18105.

Rounce, D. R., and D. C. McKinney (2014), Debris thickness of glaciers in the Everest area (Nepal Himalaya) derived from satellite imagery using a nonlinear energy balance model, The Cryosphere, 8, 1317–1329.

Schauwecker, S. (2012), Mapping supraglacial debris thickness on mountain glaciers using satellite data: validation of a new, physically-based method. M.S. thesis, ETH Zürich, Zürich, Switzerland.

Scherler, D., B. Bookhagen, and M. R. Strecker (2011), Spatially variable response of Himalayan glaciers to climate change affected by debris cover, Nature Geoscience, 4, 156–159.

Schmidt, S., and M. Nüsser (2009), Fluctuations of Raikot Glacier during the past 70 years: a case study from the Nanga Parbat massif, northern Pakistan, Journal of Glaciology, 55, 949–959.

Shukla, A., R. P. Gupta, and M. K. Arora (2009), Estimation of debris cover and its temporal variation using optical satellite sensor data: a case study in Chenab basin, Himalaya, Journal of Glaciology, 55, 444–452.

Singh, V., AL. Ramanathan, and T. Kuriakose (2015), Hydrogeochemical assessment of meltwater quality using major ion chemistry: A case study of Bara Shigri glacier, Western Himalaya, India, National Academy Science Letters: 1-5.

Strasser, U., J. Corripio, F. Pellicciotti, P. Burlando, B. Brock, and M. Funk (2004), Spatial and temporal variability of meteorological variables at Haut Glacier d'Arolla (Switzerland) during the ablation season 2001: Measurements and simulations, Journal of Geophysical Research, 109, D03103.

Suzuki, R., K. Fujita, and Y. Ageta (2007), Spatial distribution of thermal properties on debris-covered glaciers in the Himalayas derived from ASTER data, Bulletin of glaciological Research, 24, 13-22.

Takeuchi, Y., R. B. Kayastha, and M. Nakawo (2000), Characteristics of ablation and heat balance in debris-free and debris-covered areas on Khumbu Glacier, Nepal Himalayas in the pre-monsoon season, in: Debris-Covered Glaciers, IAHS Publication, Seattle, Washington, USA, pp. 53–61.

Tiwari, R. K., R. P. Gupta, R. Gens, and A. Prakash (2012), Use of optical, thermal and microwave imagery for debris characterization in Bara-Shigri Glacier, Himalayas, India, IEEE 4422–4425.

Wagnon, P., A. Linda, Y. Arnaud, R. Kumar, P. Sharma, C. Vincent, J. G. Pottakkal, E. Berthier, AL. Ramanathan, S. I. Hasnain, and P. Chevallier (2007), Four years of mass balance on Chhota Shigri Glacier, Himachal Pradesh, India, a new benchmark glacier in the western Himalaya, Journal of Glaciology, 53, 603–611.

Zhang, Y., K. Fujita, S. Liu, Q. Liu, and T. Nuimura (2011), Distribution of debris thickness and its effect on ice melt at Hailuogou glacier, southeastern Tibetan Plateau, using in situ surveys and ASTER imagery, Journal of Glaciology, 57, 1147–1157.

Zou, H., L. Zhou, S. Ma, P. Li, W. Wang, A. Li, J. Jia, and D. Gao (2008), Local wind system in the Rongbuk Valley on the northern slope of Mt. Everest, Geophysical Research Letters, 35, L13813.

2 Paper II

Schauwecker, S., M. Rohrer, D. Acuña, A. Cochachin, L. Dávila, H. Frey, C. Giráldez, J. Gómez, C. Huggel, M. Jacques-Coper, E. Loarte, N. Salzmann, and M. Vuille (2014). Climate trends and glacier retreat in the Cordillera Blanca, Peru, revisited. *Global and Planetary Change*, 119, 85-97.

Artesonraju Glacier in July 2014, Cordillera Blanca, Peru (S. Schauwecker)

Contributions of the PhD candidate:

Conception and design of the work, developing the homogenization method, data analysis and interpretation, developing approaches to discuss the glacier imbalance and shrinkage, drafting and writing the article

Climate trends and glacier retreat in the Cordillera Blanca, Peru, revisited

Simone Schauwecker[1,4], Mario Rohrer[1], Delia Acuña[2], Alecho Cochachin[3], Luzmila Dávila[3], Holger Frey[4], Claudia Giráldez[4], Jesús Gómez[5], Christian Huggel[4], Martín Jacques-Coper[6], Edwin Loarte[7], Nadine Salzmann[4,8], Mathias Vuille[9]

1 Meteodat GmbH, Technoparkstr. 1, 8005 Zurich, Switzerland
2 SENAMHI, av. Las Palmas s/n, Lima, Peru
3 ANA, UGRH, Huaraz, Peru
4 Department of Geography, University of Zurich, Winterthurerstr. 190, 8057 Zurich, Switzerland
5 SERNANP, ANP Huascarán, Huaraz, Peru
6 Institute of Geography, University of Berne, Hallerstr. 12, 3012 Berne, Switzerland
7 Facultad de Ciencias del Ambiente, Universidad Santiago Antúnez de Mayolo, Huaraz, Peru
8 Department of Geosciences, University of Fribourg, Chemin du Musée 4, 1700 Fribourg, Switzerland
9 Department of Atmospheric and Environmental Sciences, University at Albany, State University of New York, 1400 Washington Ave., Albany, NY 12222, USA

The total glacial area of the Cordillera Blanca, Peru, has shrunk by more than 30% in the period of 1930 to the present with a marked glacier retreat also in the recent decades. The aim of this paper is to assess local air temperature and precipitation changes in the Cordillera Blanca and to discuss how these variables could have affected the observed glacier retreat between the 1980s and present. A unique data set from a large number of stations in the region of the Cordillera Blanca shows that after a strong air temperature rise of about 0.31°C per decade between 1969 and 1998, a slowdown in the warming to about 0.13°C per decade occurred for the 30 years from 1983 to 2012. Additionally, based on data from a long-term meteorological station, it was found that the freezing level height during precipitation days has probably not increased significantly in the last 30 years. We documented a cooling trend for maximum daily air temperatures and an increase in precipitation of about 60 mm/decade since the early 1980s. The strong increase in precipitation in the last 30 years probably did not balance the increase of temperature before the 1980s. It is suggested that recent changes in temperature and precipitation alone may not explain the glacial recession within the thirty years from the early 1980s to 2012. Glaciers in the Cordillera Blanca may be still reacting to the positive air temperature rise before 1980. Especially small and low-lying glaciers are characterized by a serious imbalance and may disappear in the near future.

Keywords: Cordillera Blanca; glacier change; climate change; equilibrium-line altitude (ELA); precipitation; air temperature

2.1 Introduction

The tropical Andes - and especially the Cordillera Blanca (CB) - have been recognized as a region highly vulnerable to climate change and the related glacier recession (e.g. *Bury et al.*, 2011; *Mark et al.*, 2010; *Lynch*, 2012). Glaciers in this region act as a temporal water storage for precipitation falling as snow at high elevations in the wet season from about October to April. The stored water is partly released during the dry season, compensating for the lack of water due to scarce precipitation events between May and September (*Kaser et al.*, 2003). The discharge from the glaciated catchments is used in the downstream settlements particularly for mining, agriculture, domestic consumption and hydropower (*Vuille et al.*, 2008a). The disappearance of these natural reservoirs has a dominant impact on the water availability in the Rio Santa valley particularly during the dry season (*Juen et al.*, 2007; *Baraer et al.*, 2012). As outlined by *Lynch* (2012), rural communities and poor urban neighbourhoods in the Santa watershed, which drains the western part of the CB, face a threat of losing access to clean water, adequate to meet their basic domestic and livelihood needs. It is therefore indispensable to understand the response of glaciers to a changing climate in order to develop and implement related adaptation measures.

This study focuses on climatic trends and related glacier changes in the CB in the Peruvian Andes. Glaciers in the tropical Andes have witnessed a strong retreat during the last decades (e.g. *Kaser*, 1990; *Hastenrath and Ames*, 1995; *Kaser and Georges*, 1997; *Georges*, 2004; *Mark and Seltzer*, 2005; *Silverio and Jaquet*, 2005; *Raup et al.*, 2007; *Vuille et al.*, 2008a; *Rabatel et al.*, 2013; *Salzmann et al.*, 2013). Small glaciers in the tropical Andes at low altitudes show a more pronounced retreat, as the current equilibrium line altitude (ELA) climbed up towards the upper reaches causing a reduction or even loss of the accumulation area (*Rabatel et al.*, 2013).

Based on a large number of stations along the tropical Andes between 1°N and 23°S, *Vuille and Bradley* (2000) and later *Vuille et al.* (2008a) observed a significant warming of approximately 0.1°C per decade between 1939 and 2006. They included station data from the network maintained by SENAMHI, however, they did not analyze temperature and precipitation trends for the region of the CB specifically. For the area of the CB, *Mark and Seltzer* (2005) reported a temperature increase of 0.39°C per decade between 1951 and 1999 and 0.26°C per decade between 1962 and 1999. They used data from the SENAMHI network from 29 and 45 stations for temperature and precipitation respectively, until 1998. They used temperature data to compute a trend for two time periods (1951-1999 and 1962-1999) and did not consider 30-year running trends as in the present work.

Precipitation changes are more difficult to document than temperature trends because of missing station records (*Rabatel et al.*, 2013). In southern Peru and the Bolivian Altiplano, precipitation has decreased in the period 1950 to 1994, while station data indicate a slight increase for northern Peru for the same period (*Vuille et al.*, 2003). Since precipitation is characterized by a large spatial variability, no clear pattern of increasing or decreasing precipitation can be found on a regional scale for the tropical Andes (*Vuille et al.*, 2003). The understanding of local trends in meteorological variables is crucial to examine the glacier retreat in the CB. Therefore, trends of

precipitation and air temperature in the CB are identified based on an extensive and unique in-situ data base. It is assessed how these local trends differ from general trends along the tropical Andes as published in e.g. *Vuille et al.* (2003) or *Rabatel et al.* (2013). The results are related to existing studies about linear temperature change in the CB such as from e.g. *Mark and Seltzer* (2005) and it is assessed how running 30-year trends varied in time.

The main objectives of this study can be summarized as follows: (i) Assessing recent trends in precipitation and near-surface as well as 500 hPa air temperature in the CB based on extensive in-situ measurements and reanalysis data with a focus on differences to the general trends in the tropical Andes. Additionally, it is examined how the running 30-year linear trends have changed in time since the 1960s and meteorological variables are compared to the upper-air zonal wind component during the austral summer and the Pacific Decadal Oscillation (PDO). (ii) Applying a novel approach to assess the increase in the freezing level during precipitation days and to estimate the amount of precipitation needed to balance such an increase. (iii) Analysing the relation of precipitation and air temperature trends to observed glacier change using available mass balance measurements.

2.2 Study area

The CB is located between approximately 8°S and 10°S in the Ancash Region of Peru (Figure 2-1), spanning roughly 180 km in length and 20 km in width. The highest peak in this mountain range is the southern summit of the glaciated Nevado Huascarán with an elevation of 6768 m asl. Although the distance to the Pacific Ocean is only about 100 km and more than 4000 km to the Atlantic, this range marks the continental divide. The Rio Santa drains the western part of the CB, flows to the northwest into the Pacific and separates the CB from the Cordillera Negra in the west, which reaches altitudes of about 5200 m asl. The western foothills of the Cordillera Negra descend to the Pacific coast.

The study site lies in the outer tropical zone and exhibits a typical climate for this region with a pronounced seasonality mainly in precipitation, cloud cover and specific humidity. The pronounced dry season spans from May to September, while the wet season is dominant in austral summer (*Kaser and Georges,* 1997). About 70 to 80% of the total annual precipitation falls within the pronounced wet season (*Kaser et al.,* 1990). The seasonal distribution of precipitation is caused by the onset and demise of the South American monsoon system (*Garreaud et al.,* 2009). During the wet season, precipitation mainly results from easterly winds transporting moisture from the Amazon Basin (*Garreaud et al.,* 2003). During the dry months, precipitation in the valley bottom is almost zero, as plotted in Figure 2-2a. Precipitation at high elevations in the CB is more abundant. In contrast to the strong differences in seasonal precipitation, the area is characterized by small seasonal temperature variability (Figure 2-2b). Air temperature shows stronger diurnal than seasonal variability. The diurnal variability is higher in the dry season due to the lower humidity and cloud cover.

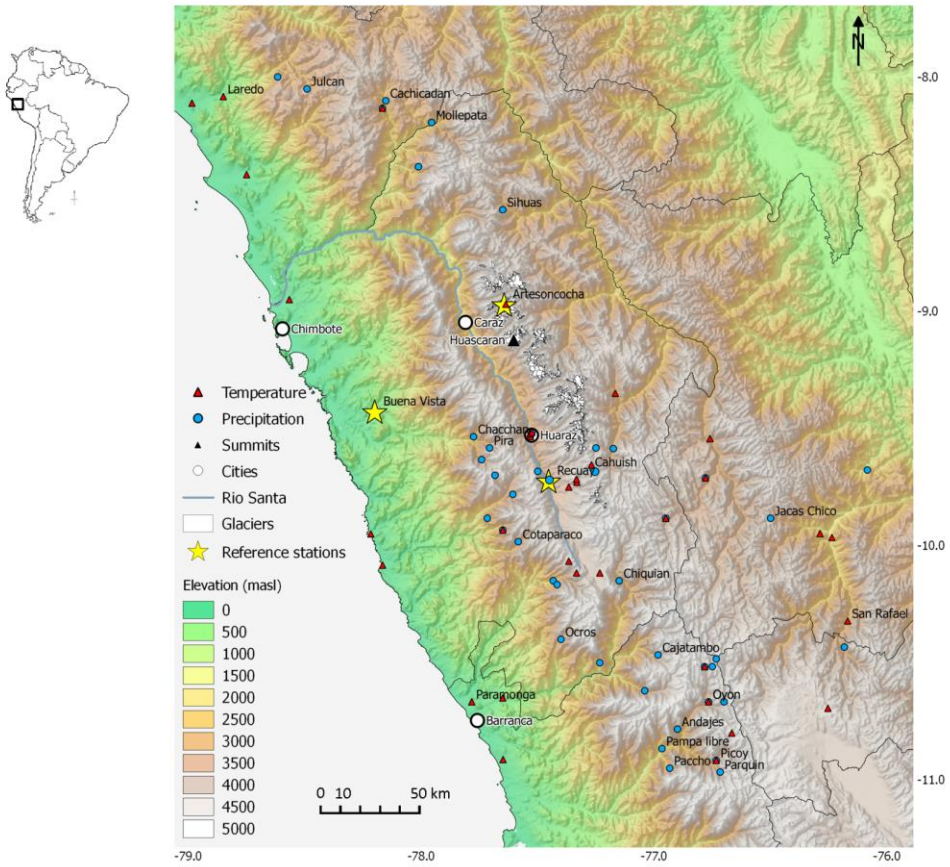

Figure 2-1 Map of the glaciers in the Cordillera Blanca and the location of the here considered meteorological stations measuring temperature (red triangle) and precipitation (blue circle). Stations used as reference stations are marked with yellow stars. Stations with labels were used as base stations, due to relatively long and complete time series.

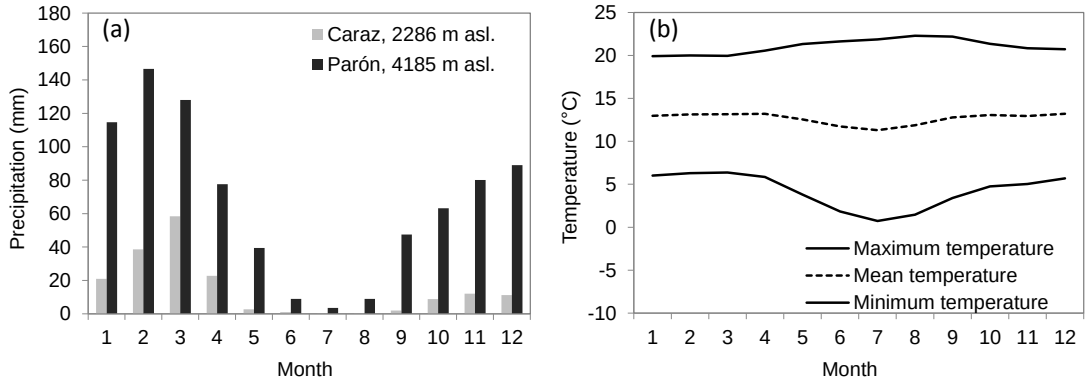

Figure 2-2 Monthly precipitation and air temperature in the Cordillera Blanca. (a) Multi-annual monthly mean precipitation registered at Caraz in the valley bottom (grey) and near Laguna Parón at over 4000 m asl. (black) between 1953 and 1995. (b) Multi-annual monthly mean of daily maximum, minimum and mean temperature for the station Recuay at 3444 m asl. for the period 1980 to 2011.

The mountain range of the CB is the largest glacierized area in the tropics, containing about one quarter of all tropical glaciers (*Kaser and Osmaston*, 2002). Several studies about glacier retreat in the CB have been published and they show consistently that total glacier area diminished heavily since 1930, as compiled in Figure 2-3. For 2003, *Racoviteanu et al.* (2008) document an area of 596.6 $km^2 \pm 21$ km^2, whereas in 1930 the glacierized area was still around 800 to 850 km^2 (*Georges*, 2004).

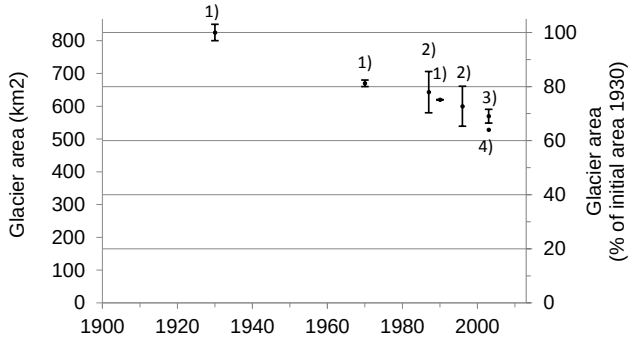

Figure 2-3 Total glacier area and uncertainty ranges for glaciers in the Cordillera Blanca between 1930 and 2003, compiled based on *Georges* (2004), *Silverio and Jaquet* (2005), *Racoviteanu et al*. (2008) and *ANA* (2010).

2.3 Data

2.3.1 Meteorological station data

Station data were provided by the National Meteorological and Hydrological Service of Peru (SENAMHI), which maintains a national network of climate stations. The network consists of over 100 stations in the Ancash and the surrounding regions of which several are located in the CB. Additional daily time series are available from a network of six stations maintained by the Glaciology and Water Resources Unit (UGRH) of the National Water Authority (ANA) in Huaraz. The latter time series are available only since early 2000, which is too short of a period to compute climatically meaningful trends. However, this set provides important and unique information about air temperature in the last decade at high altitudes of more than 4000 m asl. Mean monthly precipitation data are used from the network of Electroperú S.A. to calculate vertical precipitation gradients.

The available variables are daily mean, minimum and maximum temperature and total daily precipitation. Some stations also provide other variables like dew point, relative humidity, air pressure, wind speed and direction. Due to the large uncertainty associated with the data, these variables have not been considered in the present study. The data are available through a data portal, originally developed in the framework of the Swiss-Peruvian initiative for Climate Change Adaptation in Cusco and Apurimac (Programa de Adaptación al Cambio Climático en el Perú, PACC) from the Swiss Agency for Development and Cooperation (SDC), as described in *Schwarb*

et al. (2011). For the present study, the data portal has been modified and contains now also data of the CB now.

Table 2-1 List of all stations used as "base stations" in the analysis with the respective zone, altitude, variables, measuring period and data gaps. A gap in annual precipitation appears here where precipitation data are missing for at least one day. A gap in annual temperature appears where more than 10% of the daily data are missing. Asteriks indicate stations used as a basis for reference stations.

Station Name	Zone	Altitude (m asl.)	Variables	Period	Gaps (years missing)
Recuay*	CB	3532	Tmax	1965-2010	1971/72, 1974-78, 2000/01, 2005/06
			Tmin	1966-2012	1970-72, 1974-78, 1980, 1986/87, 1991, 2005/06, 2011
Oyon	CB	3676	Tmax	1964-2012	1983-1986, 1997, 2004-07, 2011
			Tmin	1964-2012	1983-86, 1992-94, 2006/07, 2011
San Rafael	CB	3060	Tmax	1966-2012	1974-81, 1983-89, 1991-93
			Tmin	1966-2012	1974, 1983-89, 1991-94
Buena Vista*	Coast	216	Tmax	1967-2012	1970, 2011
			Tmin	1967-2012	1970, 2011
Laredo	Coast	253	Tmax	1965-2002	1978/79, 1985-87, 1989
			Tmin	1965-2002	1978, 1985-87
Paramonga	Coast	120	Tmax	1971-2007	1972,1974,1978-84, 2004/05
			Tmin	1971-2007	1972, 1974, 1978-1984, 2004/05
Artesoncocha*	CB >4000 masl	4838	Tmean	2002-2011	only 2004 and 2006 are complete
Andajes	CB	2725	P	1964-2012	11
Cachicadan	CB	2890	P	1964-2010	12
Cajatambo	CB	3325	P	1968-2012	23
Chacchan	CB	2285	P	1964-2012	9
Chiquian	CB	3382	P	1965-2012	29
Cotaparaco	CB	3170	P	1964-2009	13
Jacas Chico	CB	3673	P	1975-2012	11
Julcan	CB	3460	P	1965-2012	13
Mollepata	CB	2580	P	1964-2010	10
Ocros	CB	3179	P	1965-2012	7
Oyon	CB	3676	P	1968-2012	27
Paccho	CB	3110	P	1966-2010	7
Pampa libre	CB	1960	P	1976-2012	13
Parquin	CB	3590	P	1970-2009	10
Picoy	CB	3075	P	1982-2012	10
Pira	CB	3625	P	1965-2009	13
Recuay*	CB	3444	P	1965-2010	19
Sihuas	CB	3375	P	1965-2012	29

Figure 2-1 shows the locations of the available stations and Table 2-1 provides the details. The three highlighted stations Recuay, Artesoncocha and Buena Vista in Figure 2-1 were used to reconstruct reference stations. For the trend analyses in this work, the area is separated into two zones: Coast and Cordillera. The coastal region is defined for elevations up to 400 m asl. For the Cordillera Region, only stations with a high correlation to the final reference station are considered. The lowest station with temperature data is Huari (3025 m asl.) and the lowest with precipitation data is Pampa Libre (1960 m asl.).

2.3.2 Reanalysis data from NCEP/NCAR and ERA-Interim

Three of the most widely used reanalysis products are the ones from the National Centers for Environmental Prediction and the National Center for Atmospheric Research (NCEP/NCAR) and from the European Centre for Medium-Range Weather Forecasts (ECMWF), described briefly in Table 2-2. Here, air temperature of the 500 hPa pressure level is used to derive trends of air temperature over the tropical Andes. The pressure level at 500 hPa corresponds to an average elevation range of about 5865 m asl. The aim is to depict significant seasonal trends in air temperature between 1979 and 2012 at high elevations and to embed the results from station data into a larger framework of temperature changes along the tropical Andes. Additionally, zonal wind data were used from both ERA-Interim and NCEP/NCAR at the 250 hPa level for a 2.5° x 2.5° grid box (7.5 to 10°S and 75° to 77.5°W).

Table 2-2 Details of the three reanalysis products.

Name	Spatial coverage	Pressure levels	Temporal coverage	Institution	Citation
NCEP/NCAR	2.5°	17	1948 to present	NCEP/NCAR	Kalnay et al. (1996)
ERA-Interim	1.5°	37	1979 to present	ECMWF	Dee et al. (2011)
ERA-40	2.5°	23	1957 to 2002	ECMWF	Uppala et al. (2005)

2.3.3 Present and historical glacier data

There are several field measurements of mass balance and estimations of ELAs used here to discuss the current state of glaciers in the CB. (i) The Glaciology and Water Resources Unit (UGRH) conducts mass balance measurements on Artesonraju and Yanamarey glaciers. For the hydrological year 2011 to 2012, they derived an actual ELA of 4975 m asl. for Artesonraju, and 4915 m asl. for Yanamarey (*Dávila,* 2013). (ii) *Gurgiser et al.* (2013a) published field measurements from Shallap glacier. They document an actual ELA of 4985 m asl. for the season 2006/07 with a specific mass balance of -0.32 m w.e. and an actual accumulation area ratio (AAR) of 0.70. For 2007/08, they observed an actual ELA of 4953 m asl. with a specific mass balance of 0.56 m w.e. and an actual AAR of 0.74. Consequently, mass balance is zero when the steady state AAR is approximately 0.72 with a steady state ELA of 4973 m asl. (iii) Mass balance data from Yanamarey and

Artesonraju glaciers for the period 2005 to 2010 were made available by the World Glacier Monitoring Service (WGMS) (*WGMS,* 2012). (iv) *Rabatel et al.* (2012) documented ELAs of Artesonraju for each year between 2000 and 2010.

2.4 Methods

2.4.1 Quality check and homogenisation of climate data for trend analyses

In order to characterize spatial patterns of running 30-year temperature and precipitation trends, we analyzed a large data set from stations along the Ancash coast and the mountainous region of the CB. Some of the stations from SENAMHI are operating since the early 1960s, but due to political and economic reasons, observations have been frequently interrupted or even shut down at times. This is why most records have gaps of different duration and some do not operate all the way to the present. Other stations have been in operation for the past 10 to 20 years.

In addition to missing data, there are other limitations of which one should be aware. Common limitations are inhomogeneities which may result from changes in a station's geographic location, instruments, averaging techniques or observers. A reliable climatic trend analysis, however, requires long and homogeneous data series (e.g. *Begert et al.*, 2005) and respective data treatment prior to trend analyses is needed. The main aim of a homogenization is to identify and adjust implausible patterns, erroneous values or breaks caused by non-climatic factors, in order to create datasets suitable for climate change analyses.

As a first step, the available data series were checked regarding implausible values. A comparison with neighboring stations shows whether outliers or breaks are plausible or not. Values classified as evidently erroneous are then deleted from the data series. For a climate change analysis of a region, air temperature and precipitation data of a complete and homogeneous long-term reference station are needed. However, in the CB and the time period from about 1960 to 2012, there is no homogeneous and complete time series available which could be utilized directly as reference station. To overcome this limitation, ensembles/clusters of available station series are used to substitute for one single reference station. This procedure is described in e.g. *Schwarb et al.* (2011) or *Salzmann et al.* (2013). We created temporally complete temperature time series for a reference station in every zone (Cordillera region, the Cordillera region above 4000 m asl. and the coast) using a number of data series available. The following steps describe the approach applied here, relying on data homogenization and correction, with the aim of deriving one reference station for every region with an enhanced data quality.

- Relatively long and homogeneous data series were selected, which are henceforth referred to as "base stations": Laredo, Paramonga and Buena Vista for the coast; Recuay, Oyon and San Rafael for the Cordillera; Artesoncocha for the Cordillera zone above 4000 m asl. (See Figure 2-1).

- Next, the correlation between these base stations and each station in the zone was computed based on daily values for maximum and minimum air temperatures. Only stations with a high correlation (R^2>0.6) to the base station were used in these further steps. Additionally, the pairs of station data were inspected visually and the Craddock test (*Craddock*, 1979) was applied in order to find inhomogeneous patterns between pairs of stations.
- Then, linear regressions were calculated between the measured maximum and minimum air temperature of the base station and each of the selected stations from the former step. Every linear regression is defined by a slope *m* and an intersect *q*.
- These linear regressions were used to create a new a time series for maximum and minimum air temperature for each base station $T_{base,sim}$ as follows:

$$\mathrm{T_{base,sim}} = \frac{1}{\mathrm{n}}\sum_{\mathrm{i=1}}^{\mathrm{n}}(\mathrm{T_{i,meas}} \cdot \mathrm{m_i} + \mathrm{q_i})$$

- with $T_{base,sim}$ being the simulated temperature of every base station, n is the number of stations with a high correlation (R^2>0.6) to the base station, m and q defining the linear regression between the base station and the selected stations in the zone. Figure 2-5 shows the new substituted time series for the three base stations for the Cordillera region and the Cordillera region above 4000 m asl.
- Finally, one reference station was selected for each zone. The final reference stations are Buena Vista for the coast and Recuay for the Cordillera region. These stations are highlighted in Figure 2-1. As described before, the linear regression between the reference station and every base station was computed on a daily basis. The time series of the final reference stations was derived using linear regression with the base stations as predictors, corresponding to the former steps.

In addition to creating a reference station of temperature data, a representative time series of precipitation for the Cordillera region was also derived based on the Recuay station with a cluster of 18 base stations (Figure 2-1) using a monthly time step. In contrast to the approach for air temperature, only gaps of missing precipitation data of base stations are filled:

$$P_{base,sim} = \begin{cases} \frac{1}{n}\sum_{i=1}^{n}(P_{i,meas} \cdot m_i + q_i) & P_{base,meas} = n.i. \\ P_{base,meas} & P_{base,meas} =\geq 0 \end{cases}$$

with $P_{base,sim}$ being the simulated precipitation of every base station, *n* is the number of stations with a high correlation (R^2>0.8) to the base station, *m* and *q* defining the linear regression between the base station and the selected stations in the zone.

Running 30-year trends of air temperature were computed for the reference stations applying linear regressions. Seasonal trends were computed for the standard 3-monthly means (DJF, MAM, JJA,

SON). The commonly used Mann-Kendall trend test is applied with a significance level of 0.05 to assess the significance of trends.

The transition from snow to rain during precipitation events is closely related to air temperature. The precipitation partitioning is crucial for the glacier surface albedo and the net shortwave radiation budget. Therefore, it is important to know how air temperature changed during precipitation events. As a novel approach, we here computed the change in freezing level for precipitation days. The analysis was based on station data from Recuay - the only station that provides long-term daily air temperature and precipitation records. The freezing level for precipitation days is computed by extrapolating air temperature from Recuay, using a constant temperature lapse rate. Additional precipitation and air temperature records for 10 years from two high-elevation stations (Yanamarey, 4698 m asl. and Querococha, 4087 m asl.) are used to derive a lapse rate of -0.80°C/100m (standard deviation: 0.11°C/100m) for precipitation days at all three stations. This lapse rate corresponds to the one suggested by *Carey et al.* (2012), based on stations between around 3000 and 5000 m asl. The lapse rate represents a mean daily lapse rate for days with precipitation. On average, precipitation occurs during 5 h (standard deviation: 3.2 h) on precipitation days. The lapse rate is therefore rather high for a moist adiabatic lapse rate and may lead to an underestimation of the freezing level. However, the gradient does not influence the relative change in time of the freezing level

The CB is an orographic barrier between the humid Amazon basin and the extremely dry Peruvian coastal region (*Kaser et al.*, 2003). Precipitation over the CB mainly results from an easterly advection of moist air masses from the Amazon Basin and locally induced convective cells (*Kaser and Georges*, 1997). In order to understand how precipitation is linked to the large-scale circulation, the role of zonal flow in the interannual variability of precipitation is documented. Therefore, austral summer (DJF) precipitation is compared to the upper-air zonal wind component at 250 hPa, used as an index for advection of moist air masses from the interior of the continent. The actual advection of humidity, however, does not occur at that level. These winds only serve to entrain easterly momentum through downward mixing – the actual moisture influx occurs through near-surface level upslope flow.

Additionally, the annual precipitation and air temperature is compared to the Pacific Decadal Oscillation (PDO, *Mantua and Hare*, 2002). The PDO index is provided by National Oceanic and Atmospheric Administration (NOAA) web-site and compared to annual precipitation and temperature data at the reference station Recuay.

2.4.2 Glacier characteristics

Glacier characteristics and glacier-climate-interactions are discussed based mainly on two approaches. First, a simple experiment is conducted with the aim to estimate the amount of precipitation needed to balance an increase in the snowline altitude during precipitation events. Second, available mass balance measurements and ELA estimations on two glaciers are compiled and compared to the glacier hypsography, in order to discuss the glacier imbalance.

In the first approach, a simple numerical experiment is applied to Shallap glacier. The aim is to estimate the amount of precipitation needed to balance an observed rise in the snowline during precipitation events. The sensitivity of the glacier mass balance to albedo changes is estimated similar to *Klok and Oerlemans* (2004). The main assumption of this experiment is that the elevation of the snowline has increased and the elevation band between the former and the current snowline has changed from snow-covered to bare ice. Due to the much lower albedo of a bare ice surface of the elevation band, the outgoing shortwave radiation is smaller and, consequently, more energy is available for ablation. The estimations are based on data from *Gurgiser et al.* (2013a) and the glacier hypsography from the year 2003. Seasonal mean values of energy fluxes and surface are utilized, assuming that all fluxes (except for outgoing shortwave radiation) are constant and the fraction of sublimation to total ablation is 12.5% and 75% for the wet and dry season, respectively (*Winkler et al.*, 2009).

For the second approach we used the glacier hypsography at different stages which delivers information on the area distribution across elevation. The hypsography measured at different points of time indicates the rate of area lost within different elevation bands. The hypsography is derived using glacier boundary outlines combined with an Advanced Spaceborne Thermal Emission and Reflection Radiometer (ASTER) Global Digital Elevation Map (GDEM) at a resolution of 30 m (released in October 2011). Outlines from 2003, based on Satellite Pour l'Observation de la Terre (SPOT) images, are freely available through Global Land and Ice Measurements from Space (GLIMS) glacier database (*Racoviteanu et al.*, 2008). The contemporary positions have been drawn visually based on the high-resolution SPOT images from 2011 and 2012, available through GoogleEarth.

The Accumulation Area Ratio (AAR) describes the ratio of the accumulation to the total glacier area. It is assumed that this ratio is constant for different glacier extents, given that the glacier is in equilibrium (*Kerschner*, 1990; *Kaser and Osmaston*, 2002b). Here, we distinguish between the actual AAR of an unbalanced glacier and the theoretical steady state AAR for a glacier in equilibrium. Different values for AAR in the CB are given in the literature: A steady state AAR of 0.82 is suggested by *Kaser and Osmaston* (2002) and *Kaser and Georges* (1997) estimated a steady state AAR of 0.75. The steady state ELA is here defined as the altitude of the equilibrium line, assuming a steady state AAR ranging from 0.75 to 0.82. Under certain conditions, a mean ELA of a stationary glacier can be determined by the application of an AAR to the hypsographic curve (*Kerschner*, 1990). This hypothetical steady state ELA corresponds to glacier mass conservation. The steady state ELA is compared to estimations of actual ELAs derived by mass balance measurements in the field. If the steady state ELA lies below the actual ELA, the glacier is unbalanced and it is assumed that the glacier will retreat until the theoretical and the actual ELA coincide.

2.5 Results

2.5.1 Temperature and precipitation changes

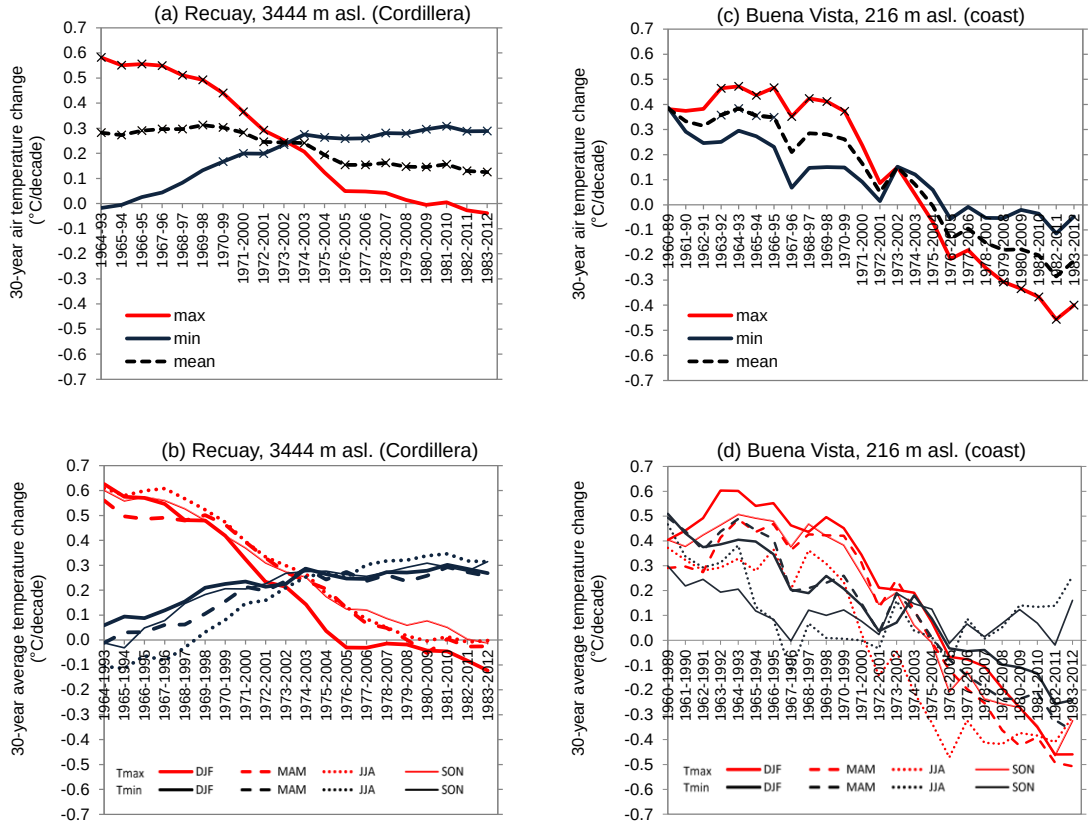

Figure 2-4 Running 30-year air temperature trends between 1964 and 2012 for the reference station Recuay in the CB and between 1960 and 2012 for the reference station Buena Vista at the coast for (a) and (c) annual maximum, mean and minimum air temperature; (b) and (d) seasonal maximum and minimum temperature. Black crosses in (a) and (c) indicate significant 30-year trends at the 5% level (according to the Mann-Kendall test) based on annual data.

Temperature changes are analyzed by calculating 30-year running mean changes for maximum, minimum and mean air temperatures (Figure 2-4). Significant trends are highlighted in Figure 2-4according to the Mann-Kendall test at the 0.05 level based on annual mean air temperature. Our results show that there is a notable difference between air temperature trends for the CB and the coast. In the Cordillera region, the running 30-year mean annual air temperature increase has slowed down during the recent decades from a maximum of significant 0.31°C/decade in the period 1969 to 1998 to significant 0.13°C/decade in the past thirty years from 1983 to 2012 (Figure 2-4a). In this period, the minimum temperature has increased significantly by almost 0.29°C/decade, while maximum temperature has cooled insignificantly by about -0.04°C/decade. Accordingly, the daily temperature range (DTR) has decreased over the period 1974 - 2003. In contrast to the

decelerated but still increasing daily mean air temperatures in the Cordillera, a general cooling of air temperature at coastal stations is observed for the 30-year period of 1983 to 2012 of -0.22°C per decade (Figure 2-4c). The negative trend is found for minimum and maximum daily temperatures, however, only the maximum temperature is decreasing significantly. For stations above 4000 m asl., air temperature was "stagnant" between 2002 and 2012 (Figure 2-5). The temperature decrease is not significant with a trend of -0.04°C for this decade. Figure 2-5 shows the annual times series of the four reference stations for the CB (San Rafael, Recuay, Oyon and Artesoncocha) and the final reference station Recuay.

Running 30-year air temperature trends for seasonal values were computed for both Cordillera and coastal stations between the 1960s and 2012. For air temperature in the CB, the highest increase was found for minimum temperatures during the dry season JJA and in the transition season SON (Figure 2-4b). Also for the coastal stations, minimum air temperature is increasing for these two seasons JJA and SON (Figure 2-4d).

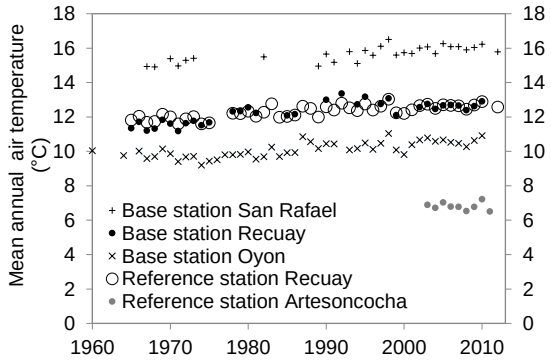

Figure 2-5 Mean annual air temperature for the base stations San Rafael, Recuay and Oyon, the reference station Recuay and the reference station Artesoncocha.

In order to compare the trends in the CB to the general trends of the tropical Andes, we computed seasonal trends of 500 hPa temperature for the period 1979–2012 based on reanalysis data. Figure 2-6 seasonal trends over the tropical Andes, based on ERA-Interim and NCEP/NCAR data. For both ERA-Interim and NCEP/NCAR the strongest warming is found for the season JJA over the Andes at around 20°S. The warming trends are strong and significant over the southern Andes in almost all seasons in both reanalysis products. In contrast, over the tropical Andes between approximately 10°N and 10°S (northern Peru, Ecuador, Colombia), temperatures tend to decrease. However, the cooling trends in the north are weak and less significant. The CB is located within the transition zone between the areas displaying a significant warming trend over southern Peru and Bolivia and the regions showing a slight cooling over northern Peru. Despite of the generally similar patterns of air temperature trends, there are large regional differences between ERA-Interim and NCEP/NCAR reanalysis data, particularly for the study site. ERA-Interim data show negative trends for all seasons for the cell of the CB, however the trend is not significant. In contrast to this,

NCEP/NCAR reanalysis data show a warming for the grid cell of the CB. The 500 hPa temperature is increasing significantly by more than 0.2°C per decade for the austral winter and spring between 1979 and 2012.

Figure 2-7 illustrates the standardized mean annual air temperature from the reference station Recuay, the mean annual 500 hPa air temperature from NCEP/NCAR reanalysis and the average of mean annual 500 hPa air temperature from ERA-40 and ERA-Interim for the grid cell of the CB. NCEP/NCAR air temperature increases by 0.16°C per decade in the period from 1983 to 2012. In contrast, ERA-Interim temperature does not change significantly in the same period. The observed recent near-surface air temperature trends of about 0.13°C per decade are more consistent with NCEP/NCAR reanalysis data than ERA-Interim.

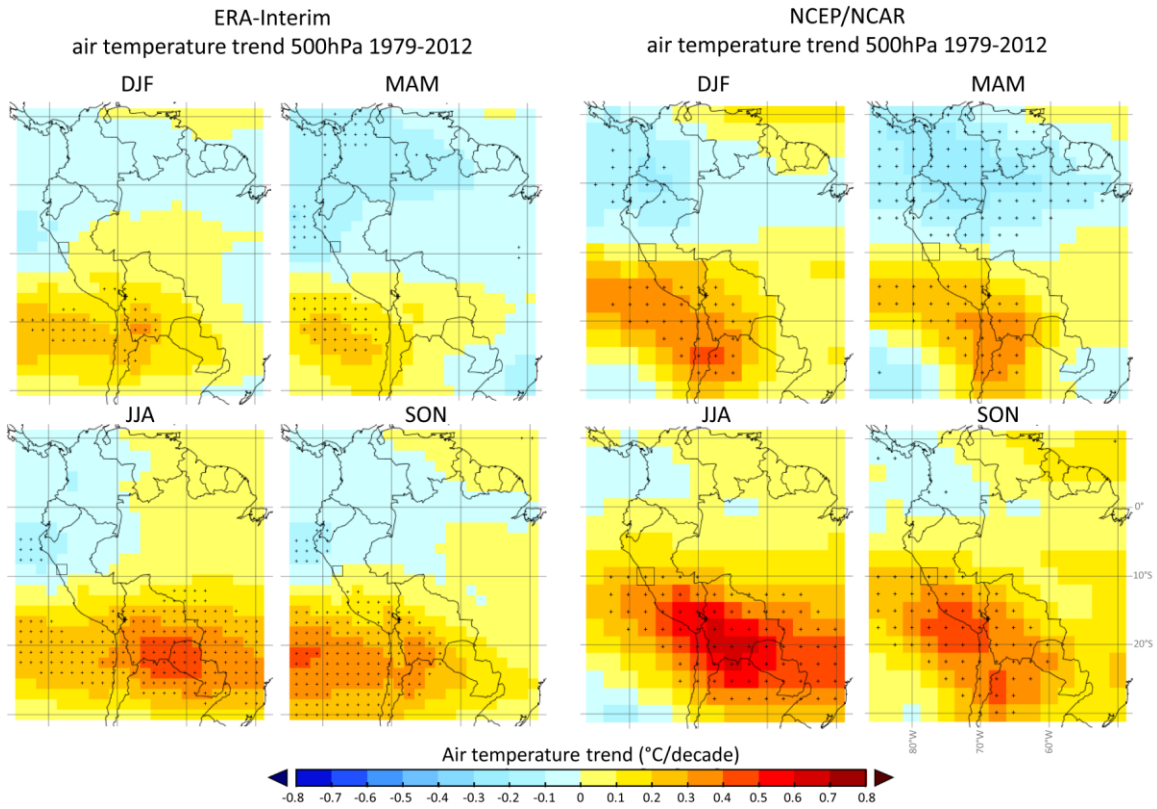

Figure 2-6 Trends in air temperature between 1979 and 2012 at the 500 hPa level from (left) ERA-Interim and (right) NCEP/NCAR reanalysis data for DJF, MAM, JJA and SON. Black crosses indicate statistically significant trends (according to the Mann-Kendall test at the 0.05 level). The grid representing the CB is marked with a black box.

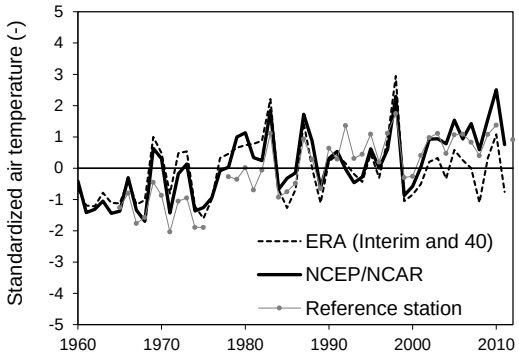

Figure 2-7 Standardized annual values for 500 hPa air temperature from reanalysis data for the grid cell of Cordillera Blanca (ERA-40, ERA-Interim, NCEP/NCAR) and standardized annual values for air temperature at the final reference station Recuay at 3444 m asl.

Figure 2-8 highlights that 1993 was characterized by a large annual precipitation total. After this event, mean decadal precipitation remained at a higher level than before 1993. The increase of precipitation for the reference station Recuay is about 60 mm/decade for the 30 years between 1983 and 2012. Figure 2-9 shows boxplots of decadal means of annual and seasonal precipitation for a set of eight stations in the CB in order to show the range of precipitation among different stations. Between the decade of the 1980s and 1990s, the increase in annual precipitation was more than 200 mm and is observed by all stations. The shift in precipitation affects annual values and all seasons, except for the dry season JJA where precipitation is decreasing. For the dry season, the decade 1993 to 2002 - including the wet year 1993 was even the driest decade of the entire observation period.

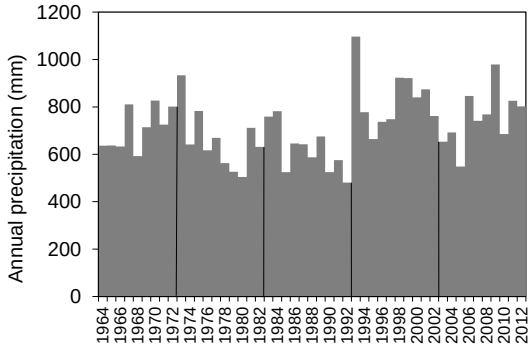

Figure 2-8 Annual precipitation for the reconstructed final reference station Recuay at 3444 m asl. The decades are marked by black lines.

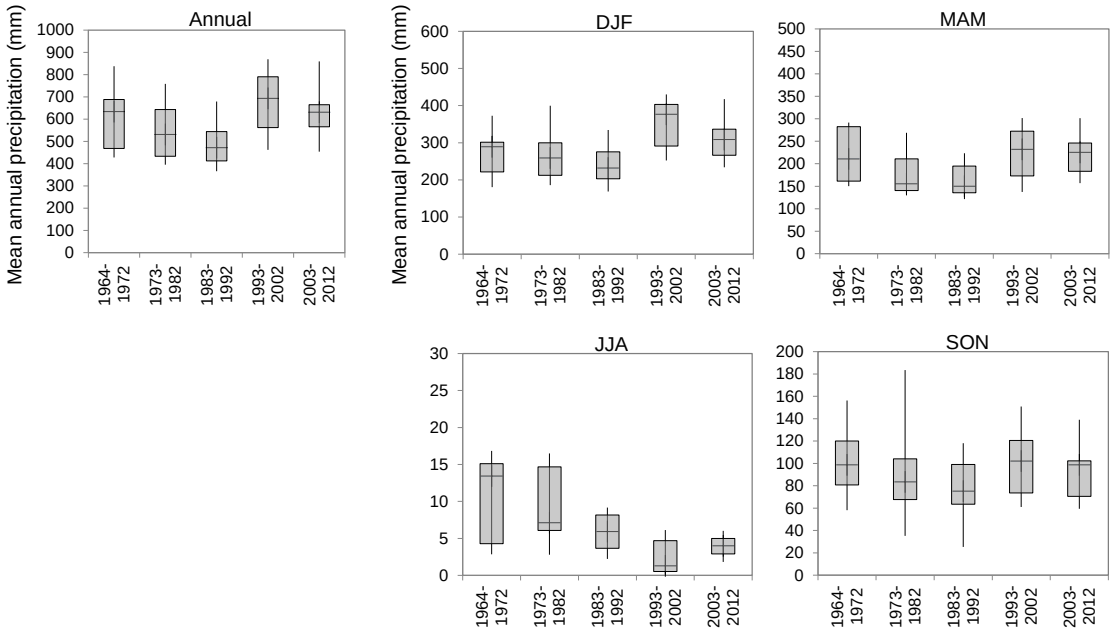

Figure 2-9 Boxplots of decadal mean of annual and seasonal precipitation. Each boxplot consists of a set of data measured by eight stations in the Cordillera Blanca (Andajes, Cajamarquilla, Ocros, Oyon, Paccho, Parquin, Picoy, Pira).

In Figure 2-10, the standardized zonal wind at 250 hPa and the standardized precipitation for the month DJF exhibit a clear negative relationship between 1980 and 2012. Stronger (lower) easterly winds are related to wetter (drier) rainy seasons. A shift is identified towards larger precipitation and a stronger easterly wind component after 1993. Hence, this shift to larger precipitation may be influenced by a change in the upper tropospheric wind patterns. The correlation between the seasonal precipitation and seasonal zonal wind is relatively low with coefficients of determination of R^2=0.23 and R^2=0.28, for reanalysis data from NCEP/NCAR and ERA-Interim, respectively.

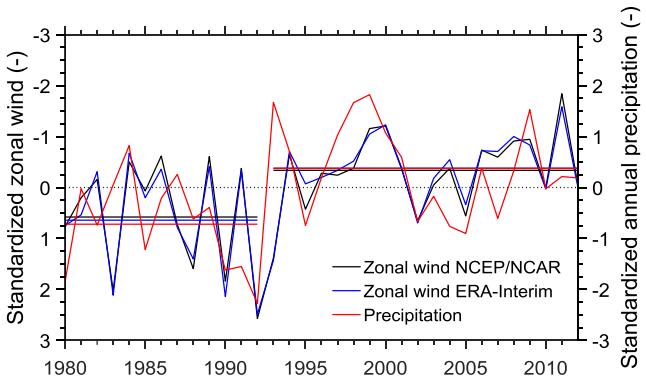

Figure 2-10 Standardized DJF precipitation for the reference station Recuay and standardized DJF zonal wind from NCEP/NCAR and ERA-Interim between 1980 and 2012 for the 250 hPa level. Horizontal lines indicate mean values for the two periods 1980-1992 and 1993-2012. Note that scale on left-side y-axis is reversed. Positive (negative) zonal wind means westerly (easterly) winds.

Annual precipitation at the reference station Recuay is not correlated with the Pacific Decadal Oscillation (PDO), with R^2=0.05. The correlation between the PDO and mean annual air temperature is approximately 0.5 for the 30-year period between the 1960s and 1990s. Then the correlation decreases and is below 0.1 for the 30-year period from the late 1970s to the late 2000s.

An increase in the freezing level during precipitation days of about 160 m is observed between the two decades 1964/72 and 1983/92 based on meteorological data from Recuay station (Figure 2-11). In contrast to this strong increase, the height of the freezing level for precipitation days has not changed significantly in the last 2 decades.

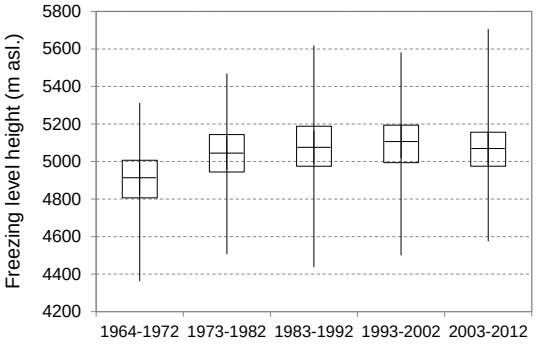

Figure 2-11 Boxplots of freezing level for days with precipitation. Each boxplot consists of a set of daily values. The 0°-level height was extrapolated based on daily air temperature data from Recuay (original time series) for days with registered precipitation. The temperature lapse rate is assumed to be -0.8°C/100m.

2.5.2 Glaciers states

Figure 2-12 shows the hypsography for 2003 and 2011 of two glaciers with mass balance measurements available: a relatively small, low elevation glacier (Yanamarey) and a relatively large glacier with elevations extending up to about 5900 m asl. (Artesonraju). There is a distinct areal retreat of Yanamarey characterized by areal losses on the front, but also on the lateral edges until the upper reaches of the glacier. The percent of area lost is much lower for Artesonraju glacier, where areal retreat is observed essentially along the tongue. Vertical lines indicate measured ELAs since 2000 for Artesonraju and 2005 for Yanamarey (*Rabatel et al.*, 2012; *Zemp et al.*, 2012; *Dávila*, 2013). Grey horizontal bars indicate the approximate range of Ablation Area Ratio (AAR), assuming steady state. For Yanamarey, all measured ELAs are above the range of the theoretical steady state ELAs, with the measured ablation area between about 50% to 70%. For Artesonraju, the measured ELAs lie mostly within the range of steady state ELAs. With one exception (2009/10 from WGMS), all measured AAR exceed 70%.

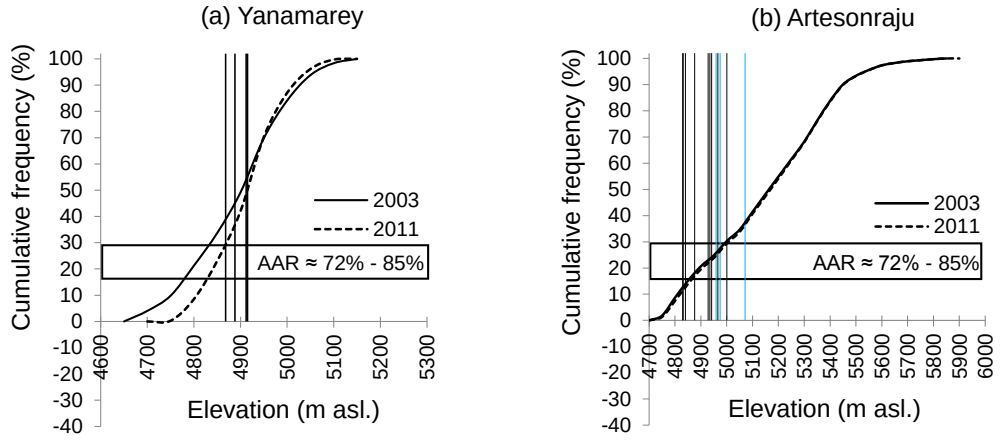

Figure 2-12 Cumulative frequencies of glacier surface area for (a) Yanamarey and (b) Artesonraju glaciers for 2003 and 2011 as a function of elevation. An AAR of 0.72 to 0.85 is assumed and describes the ratio of accumulation area to total area of a glacier in equilibrium (grey horizontal bar). The AAR allows estimating a range of steady state ELAs, which are needed to conserve the glacier mass. The actual, measured ELAs are indicated by single vertical lines (black: *WGMS*, 1989, blue: *Rabatel et al.*, 2012) and include measurements since 2005 for Yanamarey and 2000 for Artesonraju.

2.6 Discussion

2.6.1 Climatic trend

Temperature records from numerous stations in the CB show a reduced warming in the last 30 years as compared to earlier decades. The trends computed for the 30-year period before 1999 are consistent with the results by *Mark and Seltzer* (2005). They observed a slightly reduced warming for 29 stations in the CB in an analysis of temperature trends in the period 1962 to 1999 as compared to the earlier period 1951 to 1999, which agrees with the reduced warming until 2012 observed here. Despite of the reduced warming trends, the temperature is still increasing at a rate of approximately 0.13°C per decade during the last three decades.

In contrast to the reduced warming observed in the CB, an actual cooling was observed in the last 30 years for coastal stations of the Ancash region. This is consistent with results from *Falvey and Garreaud* (2009) and *Jacques-Coper* (2009) who similarly observed a decreasing air temperature trend after the 1970s along the west coast of Chile and southern Peru, respectively. These studies linked the cooling along the west coast of South America with the intensification of the Southeast Pacific Anticyclone (SEPA), and thus an enhancement of the Humboldt Current System, after the abrupt weakening of this system in mid 1970s. This previous SEPA weakening seems to have played a major role in the climate shift registered as sudden warming in sea surface temperature in the Southeastern Pacific and in surface air temperature in many stations across South America (*Giese et al.*, 2002; *Jacques-Coper*, 2009).

The rise in temperature in the CB is the result of daily minimum temperature increasing at a larger rate than the decreasing daily maximum, which is equivalent to a decrease in the daily temperature range (DTR). The decrease in DTR is apparent after 1974 (analysing 30-year periods) at both Cordillera and coastal stations and may indicate an increase in specific humidity or cloud cover, as corroborated by *Vuille et al.* (2003) who found a significant increase in relative humidity for the period 1950 to 1995 along the Andean range. Additionally, *Salzmann et al.* (2013) reported a significant increasing trend in specific humidity in the southern Peruvian Altiplano over the past 50 years based on reanalysis data from NCEP/NCAR. Further research would be needed to understand more in-depth the trends in humidity and cloud cover over the tropical Andes.

Our data based on meteorological stations show that mean annual precipitation has strongly increased between the 1980s and 1990s. The increase in precipitation has also been observed by *Vuille et al.* (2003) for northern Peru between 5°S and 11°S (1950 to 1994). However, for general precipitation changes in the tropical Andes no clear pattern emerges (e.g. *Vuille et al.*, 2003; *Rabatel et al.*, 2013). A decreasing trend is observed, for example, over the Vilcanota region in the period 1965-2009 (*Salzmann et al.*, 2013) and for southern Peru in the period 1950-1994 (*Vuille et al.*, 2003). Figure 2-10 indicates that the austral summer precipitation (about 40% of the total annual precipitation) is correlated with the zonal wind flow. The shift in strength of the zonal wind towards stronger easterly winds coincides with the increase of precipitation after 1993. With the increase of zonal easterly flow, advection of moist air from the Amazon basin is favored. Consequently, the variability of zonal wind explains partly the inter-annual fluctuations of precipitation in the CB since around 1980. The mechanism between ENSO years and mass balance of glaciers in the CB has been discussed previously (*Vuille et al.*, 2008b). Changes in the upper-tropospheric zonal flow are associated with ENSO-related tropical Pacific SST (*Vuille et al.*, 2008b). This mechanism is inducing westerly (El Niño) or easterly (La Niña) wind anomalies with reduced (El Niño) or enhanced (La Niña) moisture flux from the east, producing anomalously dry or wet conditions, respectively. This teleconnection mechanism is spatially incoherent and affects the CB in most, but not all years. Inter-annual variability of the seasonal-mean zonal wind is more pronounced and relevant for the variance of summertime convection over the Altiplano (*Garreaud and Aceituno*, 2001).

Results show that annual precipitation in the CB has a low correlation with the PDO. The relatively high correlation between air temperature and PDO for the 30-year period before about 1995 indicates a teleconnection. However, in the recent two decades, this correlation was very low. The increase in temperature in the late 1970s is correlated with the shift in the PDO and consistent with the well-known 1976 climate regime shift (e.g. *Giese et al.*, 2002). This circulation shift clearly affects the observed 30-year air temperature trends.

The freezing level during days with precipitation is estimated based on station data from Recuay at 3444 m asl. An increase in the freezing level of about 130 m is found between the two decades 1964/72 and 1973/82, but no significant increase in the freezing level occurred after about 1983, which is at odds with many other studies that have noted a clear and significant increase of the 0°C-isotherm (e.g. *Bradley et al.*, 2009 or *Rabatel et al.*, 2013). *Bradley et al.* (2009) found that

over the 30 years between about 1979 and 2009, freezing level across the Tropics have risen by about 45 m on average. More recently, *Rabatel et al.* (2013) calculated an increase of the freezing level of 28.9 m per decade over the CB for the period 1955-2011 based on NCEP/NCAR reanalysis data. However, our results cannot be directly compared to the findings by *Bradley et al.* (2009) or *Rabatel et al.* (2013), since we only considered days with precipitation and our analysis is based on an extrapolation of only one station (Recuay). More work on this topic may be warranted to analyze whether these discrepancies are due to a regional anomaly or problems with the Recuay data.

2.6.2 Glacier retreat

Despite the slowdown of the temperature rise and an increase in precipitation, glacier retreat has continued at a high rate over the last 30 years. Here, it is discussed how the observed trends of meteorological variables may affect the glacier mass balance through changes in accumulation or ablation processes. In a second step, the glacier imbalance is discussed and differences in glacier retreat between large and small glaciers are highlighted.

Both, precipitation and temperature changes may affect the accumulation process. The precipitation increase observed during the wet and transition seasons SON, DJF and MAM would lead to an increase of solid precipitation in the accumulation area and thus, a more positive (or less negative) annual mass balance if precipitation is falling as snow. *Vuille et al.* (2008b) e.g. found that on interannual timescales, precipitation variability appears to be the main driver for glacier mass balance fluctuations in the CB. On the other hand, increasing air temperatures during precipitation events lead to a rise of the snowline. However, the increase of air temperature in the last 30 years is particularly dominant in the relatively dry seasons JJA and SON (Figure 2-4), where precipitation events are rather scarce. Additionally, the freezing level during precipitation days has probably not increased significantly since the early 80s, as shown by data from Recuay station.

The ablation process of a glacier is controlled by the energy balance at the glacier surface. Since incoming shortwave radiation is the dominant energy source all over the year (e.g. *Sicart et al.*, 2008; *Gurgiser et al.*, 2013a), glacier melt in the tropics depends to a large degree on the surface albedo (*Rabatel et al.*, 2013) and the sensitivity of glaciers to albedo changes is high. The glacier surface albedo is largely influenced by the state of aggregation of precipitation (and ice surface having a much lower albedo compared to a snow surface), and the transition of snow to rain is closely related to air temperature. From the 1960s to the 1980s, the freezing level height - and thus the snowline altitude - during precipitation events increased. Consequently, net radiation absorption was higher where the glacier was snow-free and more energy was available for melt. If we assume an albedo of 0.2 for ice and 0.75 for snow (taken from *Gurgiser et al.*, 2013a) under constant conditions, about 3.2 times more energy from net shortwave radiance is available for the ablation process of an ice surface. The height of the freezing level during precipitation events is therefore crucial for the ablation process.

Additionally, higher air temperatures may lead to an increased sensible heat flux, which also results in increased ablation. However, the sensible heat flux is generally small compared to the energy supplied by shortwave and longwave radiation (*Wagnon et al.*, 1999; *Sicart et al.*, 2010; *Gurgiser et al.*, 2013a). An unknown remains the role of humidity and cloud cover. The decreased daily temperature range may indicate higher humidity and cloud cover in the last decades (as observed e.g. by *Salzmann et al.*, 2013 for the Cordillera Vilcanota). An increase in cloud cover would result in lowered incoming shortwave and increased incoming longwave radiation (*Sicart et al.*, 2010). Specific humidity, on the other hand, is crucial in the process of latent heat fluxes, since it determines the fraction of sublimation. In the CB, sublimation consumes 60 to 90% of the total available energy during the dry season (*Sicart et al.*, 2005; *Winkler et al.*, 2009). Since sublimation of ice needs 8.5 times more energy than melt, a decrease in the fraction of sublimation may lead to drastically increased ablation rates. As an example, a decreasing fraction of sublimation from 75% to 50% on a clear sky day in July would theoretically almost double total ablation.

Our results show that precipitation has increased significantly between the 1980s and 2012, which would lead to a more positive (or less negative) mass balance if precipitation is falling as snow. Additionally, while the freezing level height during precipitation days increased before the 1980s it did probably not increase significantly during the past 30 years. Glaciers have continued retreating since the 1980s which may be a contradiction at first sight. In order to get additional insights, a simple numerical experiment, described in the Methods section is conducted based on energy flux data from *Gurgiser et al.* (2013a). Based on the available data, the increase of precipitation over the accumulation area of Shallap glacier is estimated, which would be needed to balance the increase in ablation in the elevation band between the former and the current freezing level height due to a decrease of albedo. The needed increase in annual precipitation was found to be 240 mm and 530 mm for data from 2007/08 and 2006/07, respectively. The total observed increase in precipitation of about 140 mm between 1964 and 2012 for the reference station Recuay would thus not compensate the increase of the snowline before about 1980. At Cahuish station at an elevation of 4550 m asl., annual precipitation is about 30% higher than at Recuay station at about 3400 m asl. Assuming that the precipitation increase is proportional to the annual precipitation, the increase would be about 180 mm between 1964 and 2012 at an elevation of about 4500 m asl. and still not enough to balance the increased ablation due to the shift in the snowline. This example based on Shallap glacier is very simple and the sensitivity of glaciers to changes in temperature and precipitation depends on several factors. For example, glaciers with a large accumulation area are more sensitive to changes in precipitation and would benefit more from an increase (*Klok and Oerlemans*, 2004).

In a second step, we focus on the glacier hypsography and mass balance measurements, which allows comparing actual ELAs to theoretical steady state ELAs and discussing if glaciers are unbalanced. The decrease in glacier area (in percent of the total area) is particularly high for small, low-lying and isolated glaciers like Yanamarey and Pastoruri. A certain shift of the ELA (as a result of a combination of climatic parameters involved, *Kaser*, 1995) has a much stronger effect on the AAR of a small glacier than the one of a large glacier (*Paul et al.*, 2007), which makes small

glaciers more sensitive to climate change (e.g. *Rabatel et al.*, 2013). In other words, a shift in the ELA would lead to a much higher percentage of area lost for small glaciers than for large ones, but the total area lost might be larger for large glaciers. We found that actual measured ELAs of Artesonraju - a relatively large glacier - mostly lie within the range of estimated steady state ELAs. Probably, the actual ELA is still above the steady state ELA, but the rate of area retreat compared to the total area is much lower than for small glaciers. On the other hand, the actual ELAs of the low-elevation and small Yanamarey glacier are high compared to the estimated range of theoretical steady state ELAs. These small, low lying glaciers are thus probably strongly unbalanced and are going to shrink further and at a high rate in the next decades even if temperature was stagnant. These findings are in line with a recent study that reports different retreat scenarios for small glaciers with maximum elevations below 5400 m asl. and large glaciers with maximum elevation above 5400 m asl. (*Racoviteanu et al.*, 2008; *Rabatel et al.*, 2013). *Rabatel et al.* (2013) also showed that the annual mass balance of large glaciers ranges between negative (-2 m w.e. per year) to positive mass balance. Also *Gurgiser et al.* (2013a) observed a positive mass balance on Shallap glacier in 2007/08. In contrast to this, small glaciers experienced a permanently negative mass balance, indicating their strongly unbalanced condition.

Temperature and precipitation changes since the 1980s may probably not completely explain the strong glacier retreat during the past 30 years. Here, we suggest that the recent glacier retreat may still occur in response to the strong temperature rise of more than 0.3°C per decade before 1980, especially in the 1970s. To further discuss the response of glaciers in the CB to a changing climate in the last decades, it is necessary to estimate the response time, a measure for the time taken for a glacier to adjust the its geometry to a new climate regime. Until now, little is known about the response times of CB glaciers (*Kaser and Georges*, 1997). A simple method for determining the response time of glaciers was developed by *Jóhanneson et al.* (1989) and applied e.g. in *Hoelzle et al.* (2003), based on maximum ice thickness at the equilibrium line and annual ablation at the glacier tongue. Generally, glaciers with low ice thickness at the equilibrium line and large annual ablation at the glacier tongue have smaller response times to climate perturbations than large glaciers. Measurements and estimates of ice thickness and annual ablation rates exist for some glaciers in the CB (e.g. Artesonraju) and allow estimating a response time on the order of 10 to 40 years. Hence, the strong glacier retreat observed over the past three decades may include a signal of the temperature increase before the 1980s, depending on the glacier. The moderate temperature rise over the past 30 years may have induced additional forcing. However, the interpretation of glacier responses to climatic forcing is challenging, since some climatic fluctuations happen at time scales shorter than reaction times and, consequently, the observed response of a glacier can be a reaction to a large number of overlapping causes (*Kaser and Osmaston*, 2002). In order to discuss more in-depth the response of glaciers in the CB to changes in meteorological variables in the last three decades, a more detailed assessment of factors such as ice dynamics or response time of glaciers of different characteristics like size, slope or orientation would be needed.

2.7 Conclusions

Here we presented air temperature and precipitation trends since the 1960s based on reanalysis and station data of a relatively dense station network in the region of the CB. The main aim was to identify changes in temperature and precipitation patterns and to relate these changes to the glacier retreat during the last 30 years until 2012. We summarize as follows:

- Air temperature trends are characterized by large regional differences. A slowdown in temperature increase was identified for the CB, as was a cooling of air temperature for the coast. These findings are in line with recent studies. Climate warming may be spatially heterogeneous and temporally discontinuous. The increase may rather take the form of step changes where periods of strong warming alternate with "stagnant" periods.
- Reanalysis data were compared to in-situ air temperature data acquired from regional networks of climate stations. The present study underlines that global climate products (NCEP/NCAR and ERA-Interim reanalysis data) may have limitations to analyze regional trends in air temperature and need careful evaluation.
- Precipitation has increased in the CB with a clear shift observed in the early 1990s. The increase in wet season precipitation is correlated with the strengthening of the upper-tropospheric easterly zonal wind component. The shift in precipitation can probably not balance the negative mass balance caused by a strong increase in air temperature and the related change in freezing level and snowline, which is observed before approximately 1990.
- The observed decrease in the daily temperature range may indicate an increase in specific humidity or cloud cover. This finding is in line with recent studies, however, reliable station data are missing and the effect of increasing humidity and cloud cover remains a missing piece to fully understand the interactions between climate and glacier retreat in the CB. Detailed and long-term field measurements are needed to assess how humidity changes influence the radiation budget and turbulent latent heat fluxes.
- The freezing level height during precipitation days has increased by about 160 m between the 1960s and the 1980s, based on data of Recuay station. Our analysis does not show significant change after this period. The large increase before 1980 probably caused a significant shift in the ELA, since ablation is governed by net shortwave radiation via surface albedo.
- We suggest that the strong glacier shrinkage in the CB during the last 30 years may result from the strongly unbalanced glacier states in relation with changes in meteorological variables that occurred in large part before 1980. Especially small and low-elevation glaciers are extremely sensitive to climate change and may disappear in the near future.

If the already scarce water resources of the poor population of the Santa valley further diminish, water conflicts could exacerbate dramatically in the near future. Consequently, adaptation measures for CB's population should be planned, incorporating the knowledge of climate-glacier

interactions in order to properly estimate possible advantages and changes but also disadvantages and risks of the respective options.

2.8 Acknowledgements

This research was developed in the framework of Proyecto Glaciares, a program financed by the Swiss Agency for Development and Cooperation SDC. We acknowledge also the use of data from the SENAMHI and the UGRH. NCEP/NCAR reanalysis data are provided by the NOAA/OAR/ESRL PSD Boulder, Colorado, USA. ERA-40 and ERA-interim data are obtained from the ECMWF. GLIMS data are provided by the National Snow and Ice Data Center and the ASTER DEM is obtained through the DAAC Global Data Explorer, a product of METI and NASA. We are grateful for the comments by two anonymous reviewers, who helped to substantially improve this paper.

2.9 References

ANA (2010), Inventario Nacional de glaciares y lagunas, Huaraz, Peru.

Baraer, M., B. G. Mark, J. M. McKenzie, T. Condom, J. Bury, K.-I. Huh, C. Portocarrero, J. Gómez, and S. Rathay (2012), Glacier recession and water resources in Peru's Cordillera Blanca, Journal of Glaciology, 58, 134-150.

Begert, M., T. Schlegel, and W. Kirchhofer (2005), Homogeneous temperature and precipitation series of Switzerland from 1864 to 2000, International Journal of Climatology, 25, 65-80.

Bradley, R. S., F. T. Keimig, H. F. Diaz, and D. R. Hardy (2009), Recent changes in freezing level heights in the Tropics with implications for the deglacierization of high mountain regions, Geophysical Research Letters, 36, L17701.

Bury, J. T., F. T. Keimig, H. F. Diaz, and D. R. Hardy (2011), Glacier recession and human vulnerability in the Yanamarey watershed of the Cordillera Blanca, Peru, Climatic Change, 105, 179-206.

Carey, M., C. Huggel, J. Bury, C. Portocarrero, and W. Haeberli (2012), An integrated socio-environmental framework for glacier hazard management and climate change adaptation: lessons from Lake 513, Cordillera Blanca, Peru, Climatic Change, 112, 733-767.

Craddock, J. M. (1979), Methods of comparing annual rainfall records for climatic purposes, Weather, 34, 332-346.

Dávila, L. (2013), Memoria anual de glaciares - 2012, Unidad de Glaciología y Recursos Hídricos (UGRH), Huaraz, Peru.

Dee, D. P., S. M. Uppala, A. J. Simmons, P. Berrisford, P. Poli, S. Kobayashi, U. Andrae, M. A. Balmaseda, G. Balsamo, P. Bauer, P. Bechtold, A. C. M. Beljaars, L. van de Berg, J. Bidlota, N. Bormann, C. Delsol, R. Dragani, M. Fuentes, A.J.Geer, L. Haimberger, S. B. Healy, H. Hersbacha, E. V. Hólm, L. Isaksen, P. Kållberg, M. Köhler, M. Matricardi, A.P. McNallya, B. M. Monge-Sanz, J.-J. Morcrette, B.-K. Park, C. Peubey, P. de Rosnay, C.Tavolato, J.-N. Thépaut, and F. Vitart (2011), The ERA-Interim reanalysis: Configuration and performance of the data assimilation system, Quarterly Journal of the Royal Meteorological Society, 137, 553–597.

Falvey, M., and R. D. Garreaud (2009), Regional cooling in a warming world: Recent temperature trends in the southeast Pacific and along the west coast of subtropical South America (1979–2006), Journal of Geophysical Research, 114, D04102.

Garreaud, R. D., and P. Aceituno (2001), Interannual rainfall variability over the South American Altiplano, Journal of Climate, 14, 2779–2789.

Garreaud, R. D., M. Vuille, and A. C. Clement (2003), The climate of the Altiplano: observed current conditions and mechanisms of past changes, Palaeogeography, Palaeoclimatology, Palaeoecology, 194, 5-22.

Garreaud, R.D., M. Vuille, R. Compagnucci, and J. Marengo (2009), Present-day South American climate, Palaeogeography, Palaeoclimatology, Palaeoecology, 281, 180-195.

Georges, C. (2004), Climate in support of the UNFCCC. Reports GCOS - 82 (WMO/TD No. 1143), Arctic, Antarctic, and Alpine Research, 36, 100-107.

Giese, B. S., S. C. Urizar, and N. S. Fuckar (2002), Southern hemisphere origins of the 1976 climate shift, Geophysical Research Letters, 29, n.i..

Gurgiser, W., B. Marzeion, L. Nicholson, M. Ortner, M., and G. Kaser (2013a), Modeling energy and mass balance of Shallap Glacier, Peru, The Cryosphere, 7, 1787-1802.

Hastenrath, S., and A. Ames (1995), Recession of Yamanarey Glacier in Cordillera Blanca, Peru, during the 20th century, Journal of Glaciology, 41, 191–196.

Hoelzle, M., W. Haeberli, M. Dischl, and W. Pescke (2003), Secular glacier mass balances derived from cumulative glacier length changes, Global and Planetary Change, 36, 295–306.

Jacques-Coper, M. (2009), Characterization of the mid-1970's climatic jump in South America. M.S. thesis, Universidad de Chile, Santiago, Chile.

Jóhanneson, T., C. Raymond, and E. Waddington (1989), A simple method for determining the response time of glaciers, in: Glacier Fluctuations and Climatic Change, Kluwer Academic Publishing, Dordrecht, edited by J. Oerlemans, pp. 343–352.

Juen, I., G. Kaser, G., and C. Georges (2007), Modelling observed and future runoff from a glacierized tropical catchment (Cordillera Blanca, Perú), Global and Planetary Change, 59, 37-48.

Kalnay, E., M. Kanamitsu, R. Kistler, W. Collins, D. Deaven, L. Gandin, M. Iredell, S. Saha, G. White, J. Woollen, Y. Zhu, M. Chelliah, W. Ebisuzaki, W. Higgins, J. Janowiak, K. C. Mo, C. Ropelewski, J. Wang, A. Leetmaa, R. Reynolds, R. Jenne, and D. Joseph (1996), The NCEP/NCAR Reanalysis 40-year Project, Bulletin of the American Meteorological Society, 77, 437–471.

Kaser, G., A. Ames, and M. Zamora (1990), Glacier fluctuations and climate in the Cordillera Blanca, Peru, Annals of Glaciology, 14, 136–140.

Kaser, G. (1995), Some notes on the behaviour of tropical glaciers, Bulletin de l'Institut français d'études andines, 24, 671–681.

Kaser, G., and C. Georges (1997), Changes of the equilibrium-line altitude in the tropical Cordillera Blanca, Peru, 1930–50, and their spatial variations, Annals of Glaciology, 24, 344–349.

Kaser, G., and H. Osmaston (2002), Tropical Glaciers, Cambridge University Press.

Kaser, G., I. Juen, C. Georges, J. Gómez, and W. Tamayo (2003), The impact of glaciers on the runoff and the reconstruction of mass balance history from hydrological data in the tropical Cordillera Blanca, Peru, Journal of Hydrology, 282, 130-144.

Kerschner, H. (1990), Methoden der Schneegrenzbestimmung, in: Eiszeitforschung, Wissenschaftliche Buchgesellschaft, Darmstadt, edited by H. Liedtke, pp. 299–311.

Klok, E. J., and J. Oerlemans (2002), Model study of the spatial distribution of the energy and mass balance of Morteratschgletscher, Switzerland, Journal of Geophysical Research - Atmospheres, 48, 505-518.

Lynch, B. (2012), Vulnerabilities, competition and rights in a context of climate change toward equitable water governance in Peru's Rio Santa Valley, Global Environmental Change, 22, 364-373.

Mantua, N. J., and S. R. Hare (2002), The Pacific Decadal Oscillation, Journal of Oceanography, 58, 35-44.

Mark, B. G., and G. O. Seltzer (2003), Tropical glacier meltwater contribution to stream discharge: a case study in the Cordillera Blanca, Peru, Journal of Glaciology, 49, 271-281.

Mark, B. G., J. M. McKenzie, and J. Gómez (2005), Hydrochemical evaluation of changing glacier meltwater contribution to stream discharge: Callejon de Huaylas, Peru, Hydrological Sciences Journal, 50, 975-987.

Mark, B. G., J. Bury, J. M. McKenzie, A. French, A., and M. Baraer (2010), Climate change and tropical andean glacier recession: Evaluating hydrologic changes and livelihood vulnerability in the Cordillera Blanca, Peru, Annals of the Association of American Geographers, 100, 794–805.

Paul, F., M. Maisch, C. Rothenbühler, M. Hoelzle, and W. Haeberli (2007), Calculation and visualisation of future glacier extent in the Swiss Alps by means of hypsographic modelling, Global and Planetary Change, 55, 343–357.

Rabatel, A., A. Bermejo, E. Loarte, A. Soruco, J. Gomez, G. Leonardini, C. Vincent, and J. E. Sicart (2012), Can the snowline be used as an indicator of the equilibrium line and mass balance for glaciers in the outer tropics?, Journal of Glaciology, 58, 1027–1036.

Rabatel, A., B. Francou, A. Soruco, J. Gomez, B. Cáceres, J. L. Ceballos, R. Basantes, M. Vuille, J. E. Sicart, C. Huggel, M. Scheel, Y. Lejeune, Y. Arnaud, M. Collet, T. Condom, G. Consoli, V. Favier, V. Jomelli, R. Galarraga, P. Ginot, L. Maisincho, J. Mendoza, M. Ménégoz, E. Ramirez, P. Ribstein, W. Suarez, M. Villacis, and P. Wagnon (2013), Current state of glaciers in the tropical Andes: a multicentury perspective on glacier evolution and climate change, The Cryosphere, 7, 81–102.

Racoviteanu, A. E., Y. Arnaud, M. W. Williams, and J. Ordonez (2008), Decadal changes in glacier parameters in the Cordillera Blanca, Peru, derived from remote sensing, Journal of Glaciology, 54, 499–510.

Raup, B., A. Racoviteanu, S. J. S. Khalsa, C. Helm, R. Armstrong, and Y. Arnaud (2007), The GLIMS geospatial glacier database: A newtool for studying glacier change, Global and Planetary Change, 56, 101–110.

Salzmann, N., C. Huggel, M. Rohrer, W. Silverio, B. G. Mark, P. Burns, and C. Portocarrero (2013), Glacier changes and climate trends derived from multiple sources in the data scarce Cordillera Vilcanota region, southern Peruvian Andes, The Cryosphere, 7, 103–118.

Schwarb, M., D. Acuña, T. Konzelmann, M. Rohrer, N. Salzmann, B. Serpa Lopez, and E. Silvestre (2011), A data portal for regional climatic trend analysis in a Peruvian High Andes region, Advances in Sciences and Technology, 6, 219–226.

Sicart, J. E., P. Wagnon, and P. Ribstein (2005), Atmospheric controls of the heat balance of Zongo Glacier (16°S, Bolivia), Journal of Geophysical Research, 110, D12106.

Sicart, J. E., R. Hock, and D. Six (2008), Glacier melt, air temperature, and energy balance in different climates: The Bolivian Tropics, the French Alps, and northern Sweden, Journal of Geophysical Research, 113, D24113.

Sicart, J. E., R. Hock, P. Ribstein, and J. P. Chazarin (2010), Sky longwave radiation on tropical Andean glaciers: parameterization and sensitivity to atmospheric variables, Journal of Glaciology, 56, 854–860.

Silverio, W. and J. M. Jaquet (2005), Glacial cover mapping (1987–1996) of the Cordillera Blanca (Peru) using satellite imagery, Remote Sensing of Environment, 95, 342–350.

Uppala, S. M., P. W. Kållberg, A. J. Simmons, U. Andrae, V. Bechtold, M. Fiorino, and J. Woollen (2005), The ERA-40 re-analysis, Quarterly Journal of the Royal Meteorological Society, 131, 961–3012.

Vuille, M., and R. S. Bradley (2000), Mean annual trends and their vertical structure in the tropical Andes, Geophysical Research Letters, 27, 3885–3888.

Vuille, M., R. Bradley, M. Werner, and F. Keimig (2003), 20th century climate change in the Tropical Andes: Observations and model results, Climatic Change, 59, 75–99.

Vuille, M., B. Francou, P. Wagnon, I. Juen, G. Kaser, B. G. Mark, and R. S. Bradley (2008a), Climate change and tropical Andean glaciers: Past, present and future, Earth Science Reviews, 89, 79-96.

Vuille, M., G. Kaser, and I. Juen (2008b), Glacier mass balance variability in the Cordillera Blanca, Peru and its relationship with climate and the large-scale circulation, Global and Planetary Change, 62, 14-28.

Wagnon, P., P. Ribstein, G. Kaser, and P. Berton (1999), Energy balance and runoff seasonality of a Bolivian glacier, Global and Planetary Change, 22, 49-58.

WGMS (1989), World glacier inventory – Status 1988. W. Haeberli, H. Bösch, K. Scherler, G. Østrem, and C. C. Wallén (eds.), IAHS (ICSI) / UNEP / UNESCO, World Glacier Monitoring Service, Zurich, Switzerland: 458 pp.

WGMS (2012), Fluctuations of Glaciers 2005-2010, vol. X, in: ICSU(WDS)/IUGG(IACS)/UNEP/UNESCO/WMO, World Glacier Monitoring Service, Zurich, Switzerland, edited by M. Zemp, H. Frey, I. Gärtner-Roer, S. U. Nussbaumer, M. Hoelzle, F. Paul.

Winkler, M., I. Juen, T. Mölg, P. Wagnon, J. Gómez, and G. Kaser (2009), Measured and modelled sublimation on the tropical Glaciar Artesonraju, Perú, The Cryosphere, 3, 21-30.

3 Paper III

Schauwecker, S., M. Rohrer, M. Schwarb, C. Huggel, A. P. Dimri, and N. Salzmann (2016), Estimation of snowfall limit for the Kashmir Valley, Indian Himalayas, with TRMM PR Bright Band information, *Meteorologische Zeitschrift*, 25, 501-509.

Camp after a snow and graupel event, Lirung Glacier, Nepal (S. Schauwecker)

Contributions of the PhD candidate:

Conception and design of the work, analysis and interpretation of TRMM Precipitation Radar and meteorological station data, drafting and writing the article

Estimation of snowfall limit for the Kashmir Valley, Indian Himalayas, with TRMM PR Bright Band information

Simone Schauwecker[1,2], Mario Rohrer[1], Manfred Schwarb[1], Christian Huggel[2], A. P. Dimri[3], Nadine Salzmann[4]

1 Meteodat GmbH, Technoparkstrasse 1, 8005 Zurich, Switzerland
2 Department of Geography, University of Zurich - Irchel, Winterthurerstr. 190, CH-8057 Zurich, Switzerland
3 School of Environmental Sciences, Jawaharlal Nehru University, New Delhi, India
4 Department of Geosciences, University of Fribourg, Chemin du Musée 4, 1700 Fribourg, Switzerland

Knowing the height of the snowfall level during precipitation events is crucial for better understanding a number of hydro-climatic processes, for instance glacier-climate interactions or runoff from high mountain catchments. However, knowledge on heights of the phase change during precipitation events is limited by the small number of meteorological measurements available at high altitudes, such as the Himalayas. The bright band (BB) of satellite based radar data may be a promising proxy for the snow/rain transition during particular stratiform precipitation events over high mountain regions. The BB is a horizontal layer of stronger radar reflectivity caused by the melting of hydrometeors at the level where solid precipitation turns into rain. Here, we present BB heights detected by the Tropical Rainfall Measuring Mission (TRMM) Precipitation Radar (PR) 2A23 algorithm over a mountainous area. To assess the performance of BB heights, we have compared a 17-year data set of BB estimations of the TRMM PR with radiosonde observations and meteorological station data from Srinagar, Kashmir Valley, India. During March to November, the BB lies mostly about 200 to 800 m below the freezing level (FL) recorded by radiosondes. The correlation between BB and FL heights extrapolated from a ground-based station is smaller and depends on the timing of the air temperature measurement – an important finding for applying extrapolation techniques in data sparse regions. Further on, we found a strong seasonal and monthly variability of the BB height, e.g. extending in summer months from about 2700 m to almost 6000 m asl. Comparison with near-surface rain intensity from the TRMM PR product 2A25 indicates that - during intense monsoonal summer precipitation events - the BB height is concentrated between about 3500 and 4000 m asl. We can conclude that TRMM PR BB data deliver valuable complementary information for regional or seasonal variability in snow/rain transition in data sparse regions and, further on, BB data from surrounding lowlands could be used to validate extrapolation approaches to assess snowfall level for mainly stratiform precipitation events where stations at high elevations are missing.

Keywords: Bright band; TRMM PR 2A23; snow/rain transition; freezing level; snowfall limit; melting layer

3.1 Introduction

The height of the snowfall level, being the altitude where the transition from snow to rain occurs, is a critical variable to understand fundamental glacier-hydro-climatic processes. In modelling mass balance of seasonal snow cover and glaciers, snowfall level is a decisive variable since solid precipitation is contributing to accumulation and rain is contributing to runoff and additionally enhancing ablation via higher albedo and other processes. Further on, variations in the snowline altitude on glaciers (defined as the line separating snow surfaces from ice or firn surfaces) and related albedo effects, are among the most crucial factors to explain for instance differences in annual energy balance and thus glacier mass balance (e.g. *Benn and Lehmkuhl*, 2000; *Bolch et al.*, 2012) or to model runoff processes (*Immerzeel et al.*, 2009; *Rohrer et al.*, 2013). Nevertheless, the related information is typically lacking in many mountainous regions due to missing in-situ measurements. Remote sensing data are thus promising information sources to fill these gaps. Here, we assess the applicability of bright band (BB) height estimations from space for its use as a proxy for the snow/rain transition height, as suggested by *Rohrer et al.* (2013).

The BB is a zone of enhanced radar reflectivity, which is commonly observed in precipitation radar (PR) images during precipitation events. This zone of intensified echoes is caused by a horizontal melting layer in the atmosphere, at the height where ice or snow particles are transformed into liquid raindrops (e.g. *Battan*, 1973). Above this layer, precipitation is mostly solid and does not much attenuate radar signals. The enhanced reflectivity may lead to large positive biases in precipitation estimates from PR. The identification of the BB is therefore an important step in correcting precipitation data (*Kitchen*, 1997; *Pfaff et al.*, 2014). Since the magnitude of the BB peak in the reflectivity profile is dependent on the precipitation type, it can also be used for rain-type classification (*Awaka et al.*, 2007).

While numerous studies have been published about BB from ground based precipitation radars (e.g. *Austin and Bemis*, 1950; *Cluckie et al.*, 2000; *Fabry and Zawadzki*, 1995; *Klaassen*, 1988; *Pfaff et al.*, 2014; *Smith*, 1986; *Smyth and Illingworth*, 1998), an increasing number of studies recently also presented BB heights from the space-borne PR of the Tropical Rain Measuring Mission (TRMM) by the National Aeronautics and Space Administration (NASA) and the Japanese Aerospace Exploration Agency (JAXA). The TRMM precipitation radar (PR) was the first weather radar to estimate precipitation over the tropics and subtropics from space. Launched in 1997, TRMM produced over 17 years of scientific data, until the satellite was turned off in April 2015. Some studies have shown the performance and statistical properties of the BB measured by the TRMM PR at a global scale (*Awaka et al.*, 2009; *Harris et al.*, 2000; *Shin et al.*, 2000; *Thurai et al.*, 2005). *Wen et al.* (2013) incorporated TRMM 3D reflectivity structures from five overpasses to correct for the vertical profile of reflectivity (VPR) in a mountainous region with complex terrain, where a reliable estimation of surface precipitation from ground-based radar is difficult. *Das et al.* (2011) used monthly mean melting layer heights from the data product 3A25 over the Indian region and found that the height of the BB observed by TRMM and a ground-based vertically looking Micro Rain Radar are in good agreement. They furthermore suggest that TRMM 3A25 5x5 degree grid

data can be a good information source for average melting layer characteristics where local data are scarce. Despite numerous studies evaluating TRMM melting layer information over large areas, to our knowledge, the specific potential and applicability of TRMM PR BB estimations in high mountain regions have not been further evaluated so far.

In the following we i) analyze the spatial and temporal availability of TRMM PR BB data in a high mountain region in Kashmir, India; ii) compare BB data to freezing level (FL) data derived from radiosonde records and from extrapolated ground-station data; and iii) present seasonal and monthly variability in snowfall levels (TRMM PR product 2A23) and its relation to near-surface rain intensity (TRMM PR product 2A25).

3.2 Study site and data

For this study, we focus on the region of Kashmir valley in the Indian state of Jammu and Kashmir, a broad, open valley located between the central Himalayan ranges in the north and the Pir Panjal in the south-west (cf. Figure 3-1a for an overview). The study area meets the criteria to be representative for a mountainous region with a complex terrain on the one hand, and disposes of long-term meteorological station and radiosonde data (Srinagar) for comparison with the TRMM BB data on the other hand. Mountainous regions with higher data availability as for instance the European Alps lie outside the TRMM extent.

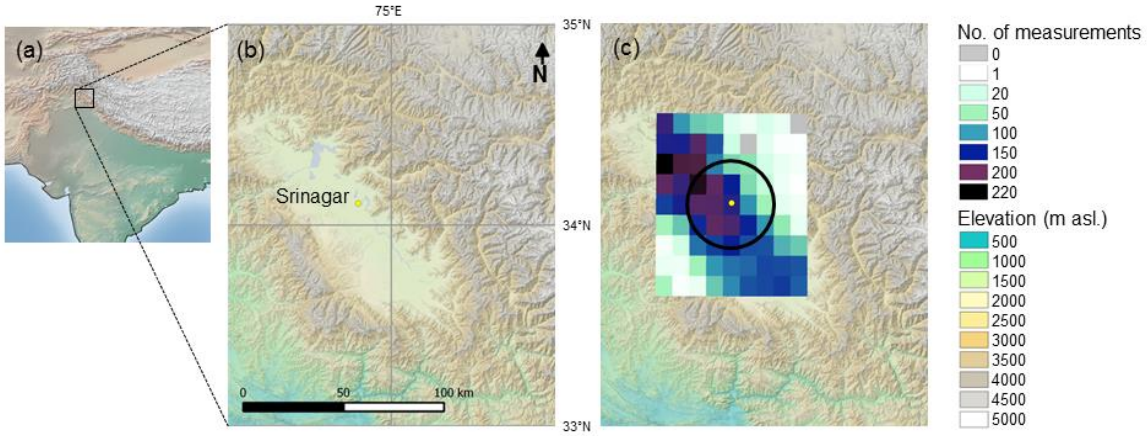

Figure 3-1 Overview of the Study area. (a) Overview map with the location of the Kashmir valley; (b) Topographic map of the Kashmir valley; (c) Number of measurements of TRMM PR BB during the 17-years of measurements on a 0.1 x 0.1° grid. The black circle indicates the 20 km distance to Srinagar.

The average altitude of the Kashmir valley is 1600 m asl. and the surrounding mountains rise higher than 4000 m asl. (cf. Figure 3-1b, which shows the topography of the study area). The climate of Kashmir Valley is temperate and characterized by wet and cold winters (mean air temperatures of 2 to 4°C in December to February at the meteorological station in Srinagar) and relatively dry and moderate hot monsoon seasons (mean air temperatures of about 21°C in July and August at the

meteorological station in Srinagar). On average, a total annual precipitation sum of about 710 mm was recorded between 2008 and 2014 at the meteorological station in Srinagar at 1587 m asl. The relatively high amount of rain and snowfall in winter (about 40% of total precipitation falling between December and March) is due to the western disturbances, while summer precipitation events are caused by the southwestern monsoon (*Kumar and Jain*, 2010). The FL height in Srinagar varies strongly during a year. Radiosonde observations show that the 0°C isotherm ranges from 2300 to 5500 m asl. during monsoon and from 250 to 1600 m asl. during winter (*Mondal and Sarkar*, 2003).

Radiosonde and meteorological station data from Srinagar, India (34.08°N, 74.83°E, 1587 m asl.), are operated by the India Meteorological Department (IMD). Radiosonde data are released normally twice a day at 0 and 12 UTC. The meteorological station is recording in 3-hour intervals.

Figure 3-2 schematically shows vertical profiles of reflectivity, air temperature and melting rate during a precipitation event. The BB appears as a layer of enhanced reflectivity where the phase changes from solid to liquid precipitation (Figure 3-2a). Melting particles have an effect on electromagnetic wave propagation, because of the strongly changing dielectric properties during the melting process. Melting starts when hydrometeors fall into a zone of 0°C (Figure 3-2b). A nearly isothermal layer with a very small lapse rate is formed close to the 0°C zone down to the level of maximum melting rate (Figure 3-2c, *Szyrmer and Zawadzki*, 1999). The peak of reflectivity is slightly below the bottom of this quasi-isothermal layer (*Szyrmer and Zawadzki*, 1999; *Willis and Heymsfield*, 1989).

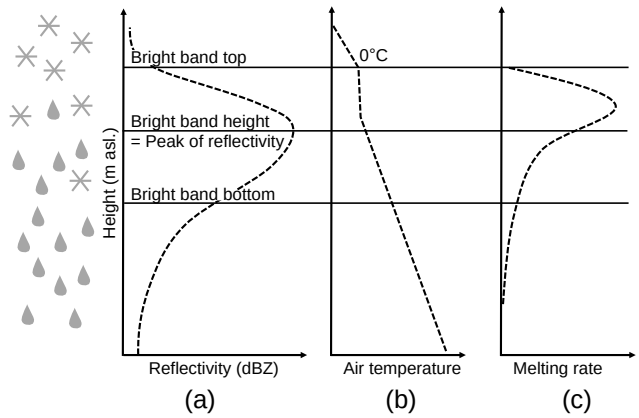

Figure 3-2 Schematic of vertical profiles of (a) reflectivity; (b) air temperature; and (c) melting rate during a precipitation event (based on *Szyrmer and Zawadzki*, 1999).

The BB data from TRMM are available for the 17 years (1997 – 2015) of active TRMM measurements. The orbit of the TRMM satellite ranges between 35° north and south. The satellite overflies a certain location on the Earth's surface at a different local time each day. One orbit lasts a bit more than 90 minutes, resulting in about 16 orbits per day. Further on, the swath width is about 250 km with 49 rays, corresponding to a horizontal resolution (footprint) of about 4 to 5 km.

The vertical resolution of the BB is 250 m at nadir. The BB can only be retrieved when precipitation is present at the time of the satellite overfly, which means that registered BB is variable in time and space. More details on the TRMM satellite and PR can be found in e.g. *Kummerow et al.* (1998) and *Kozu et al.* (2001).

The BB (defined in meters above sea level) is detected by the algorithm 2A23, which uses a spatial filter method (*Awaka et al.*, 2007). This method searches for the BB peak, as a maximum reflectivity in a window defined by the FL ± 2.5 km. The FL is computed using the operational global analysis of the Global Analysis data (GANAL) from the Japan Meteorological Agency. The outputs of 2A23 are then used by another algorithm 2A25, which estimates rainfall rates (*Iguchi et al.*, 2000). Additionally, the BB height information is used for the rain-type classification (*Awaka et al.*, 2007). The echo from the surface (surface clutter) is determined by the TRMM PR 1B21 algorithm and given by a ground clutter flag of -88.88 in the 2A23 product. While the determination of the surface echo is relatively easy for flat terrain, it gets more difficult over mountainous areas, since the surface height smears within the footprint of a radar beam and broadens the peak shape of the surface clutter (*Awaka et al.*, 2007).

For this study, we use the BB heights from the 2A23 product ("height of bright band"). Additionally, we took the rainfall rate and type from 2A25 product ("near surface rain", "rain type flag") for a comparison between the BB height and rainfall intensity as well as the vertical profiles of reflectivity ("corrected reflectivity factor *Z*").

3.3 Results and Discussion

3.3.1 Evaluation of available BB measurements

As recording and thus the availability of BB data by TRMM PR depends on various factors, in a first step, we examined the 17-years of BB records in view of the spatial and temporal data availability. Figure 3-1c shows the number of registered TRMM PR BB measurements closer than 4 km to every grid point for the entire record period. The data availability is considerably higher in the valley compared to the surrounding mountain ranges. In the centre of the valley, data availability is highest with up to 220 measurements per grid cell during the 17 years of measurements. Over the mountain ranges, data availability is much lower with a maximum of only 20 records or even no data for some grid cells.

In the following, we analyze the BB measurements that were registered within a 20km distance to Srinagar (Figure 3-1c, black circle). For the 17-year time record, there are 196 days with available measurements, with a total number of measurements is 3620. The reason for this high total amount of measurements is that the number of daily measurements for the area ranges between 1 to over 100 data points per day. One satellite overpass can take up to around 60 measurements within the 20 km distance to Srinagar, but, in most cases, the number of measurements is relatively small (<10

per day). Very high numbers of measurements (with more than 100 per day) are produced by two overlapping overpasses - with a time difference of about 96 to 98 minutes.

Figure 3-3 shows two examples for vertical reflectivity profiles (2A25) and BB heights (2A23) for precipitation events on 13 September 2002 and 2 August 2003 within 20 km distance to Srinagar. The BB is clearly visible in the vertical profiles and seems to be detected well by the algorithm 2A23. From Figure 3-3 we can also see that the ground clutter zone was masked out by the TRMM algorithms within the first 500 to 1500 m above ground (Figure 3-3, see right axis for height in meters above ground). It can be assumed that for mountain areas in the Himalayas, reflectivity values are masked out for considerably high elevations. Ground clutter masking is thus an important limitation for the BB detection over high elevation, mountainous regions.

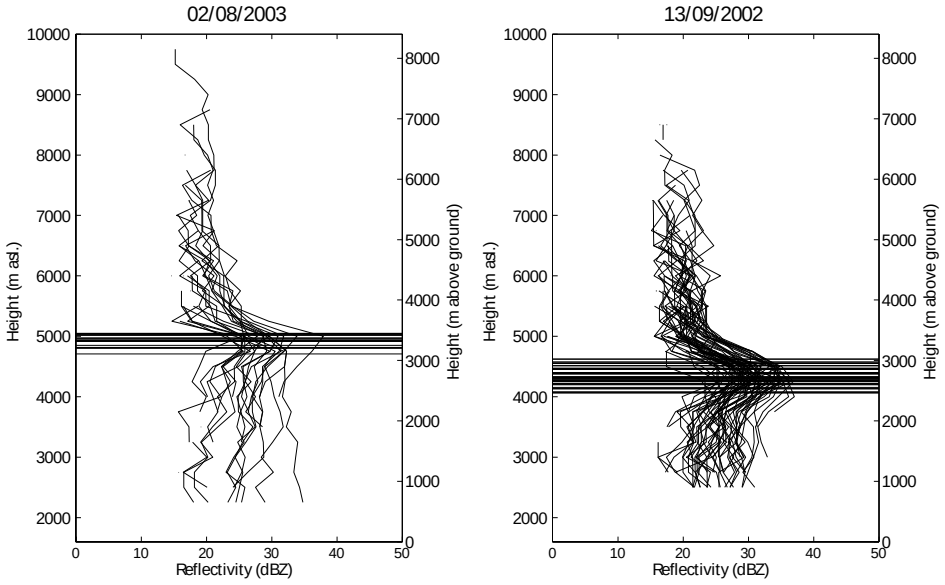

Figure 3-3 Vertical reflectivity profiles (2A25) for two precipitation events on 13 September 2002 and 2 August 2003 within 20 km distance to Srinagar (black circle in Figure 3-1c). Horizontal lines represent BB heights (2A23) and do not relate to the x-axis. The right y-axes show BB height in m above ground (the ground being at 1600 m asl.).

The classification of the rain type is given in the TRMM PR product 2A25. For the available vertical profiles within 20 km distance to Srinagar, 88% are classified as “certainly stratiform”, the other 12% are “maybe stratiform”. No BB is available for convective precipitation events, which represents a limitation for assessing snow/rain transition for this type of precipitation.

3.3.2 Bright band height versus freezing level

The relation between BB and FL height is important for using BB as a proxy for snow/rain transition. In a next step, we thus analyzed the correlation between BB and radiosonde FL and FL extrapolated based on ground-based air temperature data from Srinagar. We only considered

radiosonde measurements that are separated by less than 6 hours from a TRMM satellite overflight. The extrapolated FL heights are from measurements one hour before, after or at the time of the TRMM overflight.

We found that BB heights and radiosonde FL heights are clearly correlated, with a coefficient of determination of R^2=0.71 (Figure 3-4a). Only in a few cases, the BB height is higher than the FL, mostly the BB height is below the FL by about 100 - 900 m. This finding is in line with a number of previous studies. *Harris et al.* (2000) who found differences between TRMM PR BB height and NCEP (National Centers for Environmental Prediction) reanalysis FL to range typically between about 300 to 900 m for the tropics. Also *Awaka et al.* (2009) found that the BB height is on average about 500 m below the FL derived from NCEP reanalysis data, which is similar to 470 m from our analysis. Accordingly, *Thurai et al.* (2003) found that BB heights typically occur 300 m below the FL heights with 90% of the cases having differences ranging within 0 to 600 m.

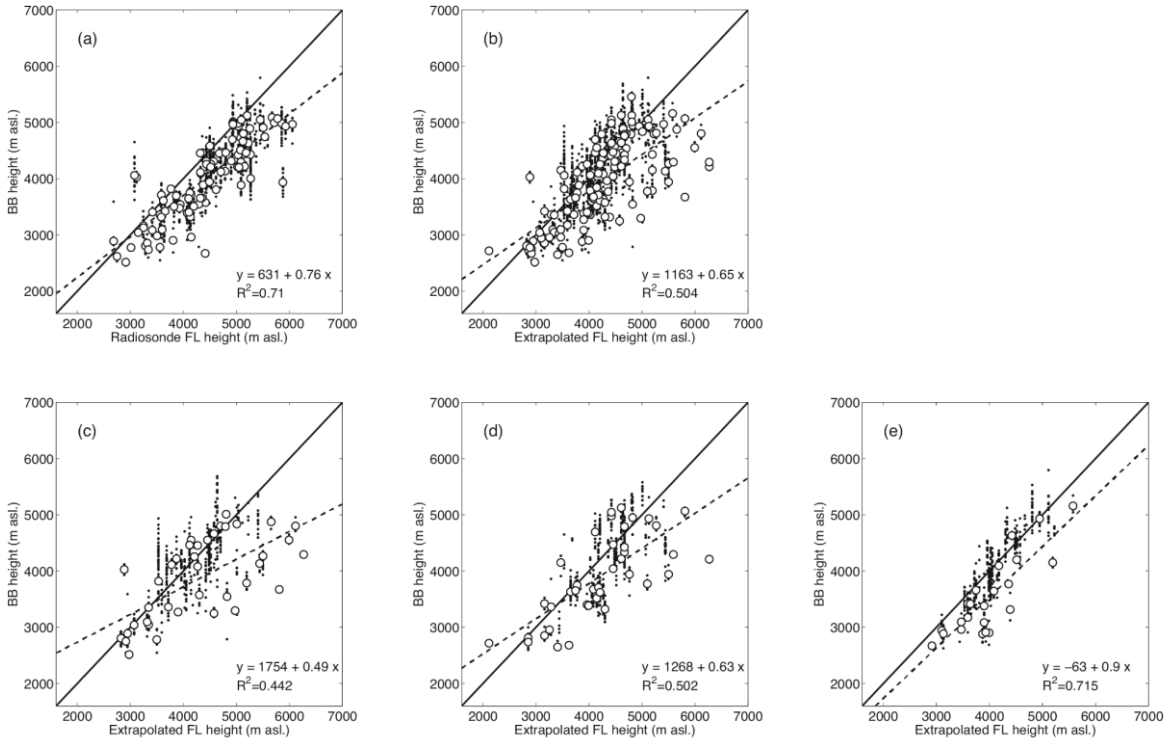

Figure 3-4 (a) TRMM BB height vs. radiosonde FL height. (b) TRMM BB height vs. extrapolated FL height from ground-based meteorological station data in Srinagar. The three figures (c) to (e) show the same as (b), but separated into ground-based station data measured (c) one hour before, (d) at the time and (e) one hour after the TRMM BB height record. Black dots show single BB height records; white circles are mean BB values per event. Dashed lines are linear least squares regression fits to data points. The equations, regression lines and coefficients of determination R^2 are computed for the mean values (white circles).

Figure 3-4b shows TRMM PR BB against extrapolated FL heights based on data from the meteorological station in Srinagar, using a lapse rate of 0.65°C/100m. The correlation is lower (R^2=0.50) and, in some cases, the snowfall level lies more than 1 km below the extrapolated FL. In order to identify these outliers, we compared the difference between BB and FL height to near-

surface rain intensity (TRMM PR product 2A25) and precipitation intensity measured at the meteorological station in Srinagar. We found that the outliers in Figure 3-4b are not related to high precipitation rates. In contrast, large precipitation intensities are generally related to small BB and FL differences. It can be thus suggested that the large differences between FL and BB heights may not be caused by valley effects, where latent heat required for melting falling snow particles is removed from the valley air until the snowline reaches the valley bottom (described e.g. *Unterstrasser and Zängl*, 2006). Figure 3-4c, Figure 3-4d and Figure 3-4 show that these outliers are rather related to precipitation events where air temperature was recorded 1 hour before (Figure 3-4c) or at the time of the TRMM overflight (Figure 3-4d). In contrast, the correlation of BB and FL heights is higher when air temperature is measured 1 hour after the BB record (R^2=0.72, Figure 3-4e). Interestingly, the time of the air temperature record seems crucial in estimating appropriately the melting layer with simple air temperature extrapolation techniques. If air temperature is measured before e.g. frontal precipitation, relatively high air temperature records could lead to an overestimation of the FL during the following precipitation event. In these cases, the snowfall level may be strongly overestimated. It also seems striking that the correlation is relatively high in Figure 3-4a for the radiosonde FL heights, despite a larger time difference between the satellite overflight and radiosonde records of up to 6 hours. Also this observation indicates that artefacts of air temperature measurements (due to e.g. strong insolation) at the ground may lead to large uncertainties in estimating melting layers using temperature extrapolation techniques.

3.3.3 Seasonal and monthly variability

In a last step, we analyzed the seasonal and monthly variability of BB height for Srinagar. Figure 3-5 shows monthly boxplots of the 17-year BB record and the radiosonde FL of the same dates. There is a clear seasonal variability in the BB heights with maximum heights in August (Figure 3-5a). A similar seasonal variability is found in the radiosonde FL heights (Figure 3-5b). *Saikranthi et al.* (2013) detected similar monthly mean TRMM-derived BB heights for Patiala (around 430 km in the NNE), with the exception of some months of considerably higher BB heights in Patiala (June, July and October). Also monthly mean melting layer heights presented by *Das et al.* (2011) based on the TRMM product 3A25 for the grid cell closest to Srinagar are similar to our results.

We found that a considerably larger number of BB data are recorded during summer (April to September, Figure 3-5c). The low number of data registered during winter (December to February) cannot be explained by fewer precipitation events only, because precipitation events are frequently observed during these months. A possible explanation for the low data availability in winter might be that the BB is not detected by the algorithm within the first 1000 m above ground, due to masked ground clutter. Figure 3-5a clearly shows that the BB is only available if it appears higher than about 1000 m above ground (corresponding to 2600 m asl.; see right axes in Figure 3-5a and b for BB and FL height in meters above ground). This means that the melting layer is probably close to the surface in winter in Srinagar, but not detected by the TRMM algorithm. This assumption stands in line with results by e.g. *Saikranthi et al.* (2013) who found BB heights lower than 2500 m asl. for Patiala, around 430 km in the NNE at an elevation of 250 m asl. Due to the low altitude of

Patiala, the ground clutter was only masked out up to approximately 1250 m asl., thus not affecting data availability of the BB heights.

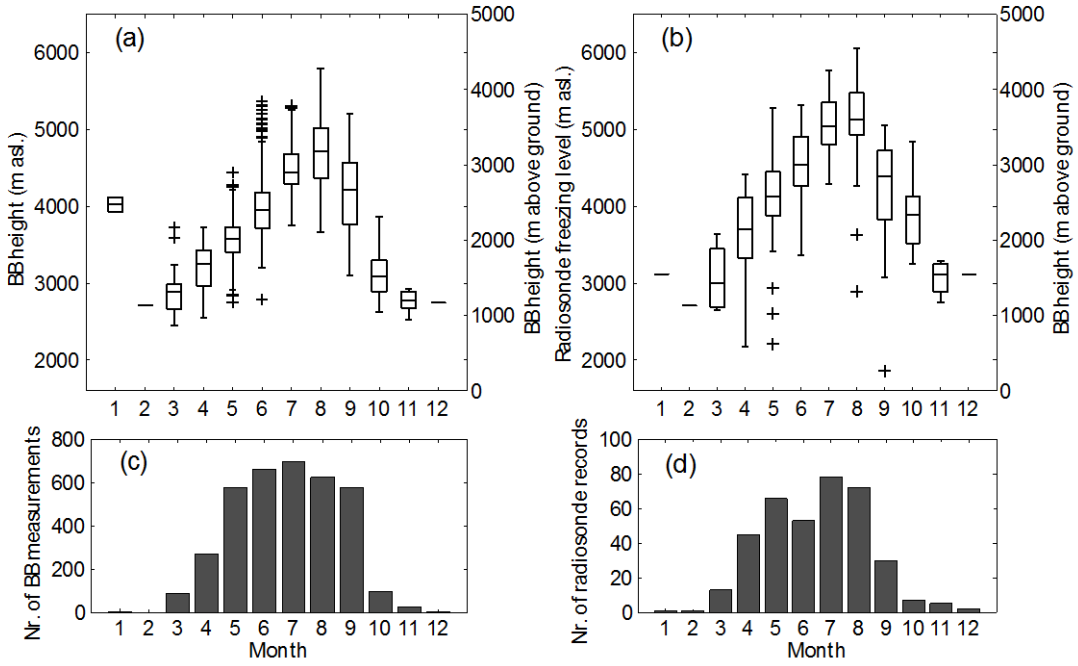

Figure 3-5 (a) Monthly BB heights during the observation period 1998 – 2014; (b) Monthly radiosonde FL heights for days with BB data available. Boxplots represent the 25th, 50th, and 75th percentiles, whiskers represent 1.5 standard deviation and outliers are plotted with crosses; (c) Available TRMM BB estimations per month (1997 - 2015); and (d) Available radiosonde records for days with TRMM BB estimations available. The right y-axes of plots (a) and (b) show BB height in m above ground (the ground being at 1600 m asl.).

Moreover, it can be seen from Figure 3-5a that the variability of the BB height during a single month is considerably large. For example, in August, BB height ranges between 3700 to almost 6000 m. Figure 3-5a also indicates that the BB height may be low in March and April in some cases, with snowfalls at elevations below 3000 m asl. This finding is confirmed by daily snowfall data collected from November to April by the Snow and Avalanche Study Establishment (SASE) at four locations in the region of the Kashmir valley (*Dimri and Mohanty*, 1999).

3.3.4 Bright band height versus near-surface rain intensity

Figure 3-6 shows BB heights against near-surface rain intensity (from TRMM PR product 2A25) for the seasons MAM, JJA and SON. The winter season is not shown here, due to the low data availability (5 registered BB heights, see also Figure 3-5c). As already shown in Figure 3-5, the BB climbs up during the summer months (JJA). While there is a large scatter of BB heights for low-to-medium rainfall intensities, relatively high rainfall intensities (> 15-20 mm/h) are predominantly related to relatively low BB heights of 3500 to 4000 m asl, and occur during summer.

A similar pattern is observed in MAM and SON, where relatively large rainfall intensities are also related to BB heights of around 3500 m asl. However, rainfall intensity from the TRMM 2A25 product is subject to considerable uncertainties, as evaluated by e.g. *Kirstetter et al.* (2012). Therefore, the absolute values of rainfall intensities should be evaluated carefully when used for further analyses.

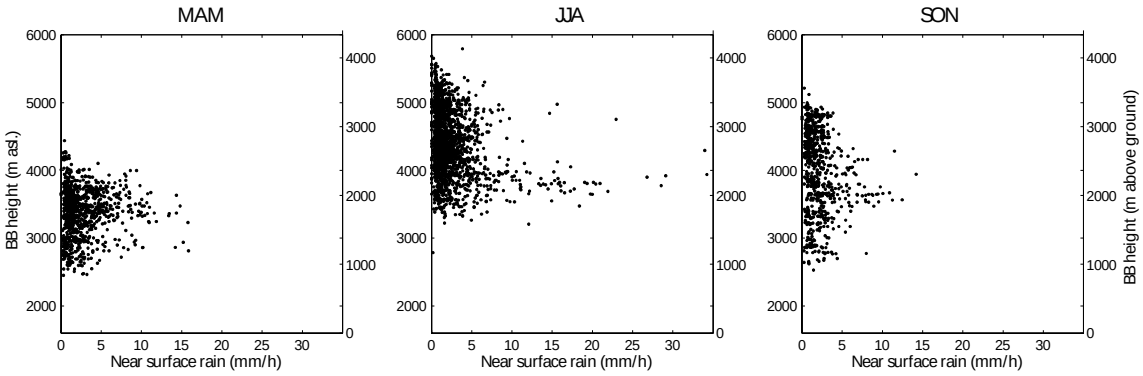

Figure 3-6 BB height against near-surface rain intensity (mm/h) from the TRMM PR product 2A25 for the seasons MAM, JJA and SON. The right y-axes show BB height in m above ground (the ground being at 1600 m asl.).

It is often mentioned in the literature that the thickness of BB strongly depends on precipitation intensity (e.g. *Klaassen*, 1988). Based on over 4000 radar scans in Southern France, the Swiss Alps and Iowa, USA, *Wolfensberger et al.* (2015) found that the thickness of the melting layer is strongly correlated with the intensity of the BB (reflectivity factor Zh), the vertical velocity of the hydrometeors and the presence of rimed particles (c.f. also *Zawadzki et al.*, 2005 for a detailed analysis and model). The presence of larger hydrometeors was somewhat less correlated with the depth of the BB, but the relative importance of this correlation is also mentioned e.g. in *Barthazy Meier* (1998). *Wolfensberger et al.* (2015) also indicate that an increased hydrometeor concentration can lead to an increase in the diabatic cooling of the surrounding air during the melting process, which can increase the thickness of the melting layer, as particle melting takes more time. They did not find a significant correlation between the rainfall intensity and the altitude of the BB. However, for tropical conditions *Durden et al.* (1997) did find a clear dependence which is more in line with our findings for the summer season in India (Figure 3-6).

Our data suggest that the snowfall level drops during intense large monsoonal precipitation events (> 10 mm/h) in summer. It seems that only during relatively low precipitation intensities, the snowfall level rises above about 5000 m asl. The low snowfall level during high intensity precipitation events has a large influence for instance on the hydrology and glacier mass balance in this region. This means, for example, that after intense precipitation events on Nanga Parbat (8126 m asl., located 130 km to the north of Srinagar), the snowline may lie clearly below the mean glacier elevation (5140 and 4720 m asl. on the north and south side of the mountain, respectively,

Shroder et al., 2000). A low snowline after a summer precipitation event has a positive (or less negative) effect on glacier mass balance due to both, increased accumulation and lower melt energy via albedo effects. The snowfall level has also a large influence on runoff generation, since the height of the snowline determines the portion of precipitation leading to direct runoff – hence an important quantity for runoff prediction.

3.4 Conclusions

This study presents an evaluation of TRMM PR BB data and seasonal variability over a mountainous region in the Indian Himalaya. Moreover, BB heights were compared to radiosonde data as well as to extrapolated FL heights from a ground station in Srinagar, Kashmir Valley, India.

Our study has shown that BB data availability in high mountain area may be limited. It requires that there is a stratiform precipitation event during the satellite overpass and that the zone of the enhanced reflectivity is high enough above the surface. Especially, BB data over mountainous regions and/or during winter are limited, since the snow/rain transition is relatively close to the surface. Despite the small number of data over high mountains, data from greater mountain valleys or the surrounding lowlands provide valuable information, potentially able to provide information on snowfall level where in-situ data are sparse.

Our findings are basically in line with previous studies showing that the TRMM PR BB height is strongly correlated to the FL from radiosonde data. The BB height does not directly correspond to the FL but in most cases rather lies around 200 to 800 m below the 0°C line. The difference between the snowfall level and the FL may depend on various factors like precipitation intensity, stability of the atmosphere, topographical influences and others. Further on, we found that the BB altitude is less (but still well) correlated to the extrapolated FL from a ground station. Interestingly, the correlation depends on the time difference between the ground-based measurement and the TRMM PR overflight. This means that large uncertainties could appear when we extrapolate snowfall level from ground-based air temperature measurements, especially when the air temperature is measured before the precipitation event. In conclusion, for a particular stratiform precipitation event where BB data are available, the extrapolation approach could be validated, and hopefully even be calibrated, and thus represents a promising application for data sparse regions.

The 17-year set of BB data could be used to assess statistical properties of e.g. seasonal or regional snow/rain transition. We found a strong seasonal and even monthly variability of the snowfall level. Intense precipitation events are related to relatively low snowfall levels during summer - an important finding in view of TRMM PR BB application for studies on e.g. glacier mass balance or mountain hydrology.

From our results we conclude that BB data from TRMM PR offer a valuable additional data source particularly in combination with other data products. The TRMM mission has come to an end in 2015, but the new Global Precipitation Measurement (GPM) was initiated in 2014 and is now operating. It is a joint mission between JAXA and NASA, as well as other international space

agencies, building upon the success of TRMM. A new core satellite carries a Dual-frequency Precipitation Radar (DPR, *Kobayashi and Iguchi*, 2003). Since the horizontal and vertical resolution of the GPM PR are similar, the here presented information of 17-year BB data for mountainous regions will be useful for further analyses of future BB data.

3.5 Acknowledgements

This study was funded by the Swiss Agency for Development and Cooperation (SDC) under the Indian Himalayas Climate Adaptation Programme (http://ihcap.in). We acknowledge the use of station and radiosonde data provided by the India Meteorological Department (IMD). TRMM PR 2A23 and 2A25 data are obtained from the Japan Aerospace Exploration Agency (JAXA) and the National Aeronautics and Space Administration (NASA). We are grateful for the comments by the editor by an anonymous reviewer, who helped to substantially improve this paper.

3.6 References

Austin, P. M., and A. C. Bemis (1950), A quantitative study of the "bright band" in radar precipitation echoes, Journal of Meteorology, 7, 145-151.

Awaka, J., T. Iguchi, and K. Okamoto (2007), Rain Type Classification Algorithm TRMM PR 2A23 V6, 2nd TRMM International Science Conference, extended abstract.

Awaka, J., T. Iguchi, and K. Okamoto (2009), TRMM PR standard algorithm 2A23 and its performance on bright band detection, Journal of the Meteorological Society of Japan, 87A, 31–52.

Barthazy Meier, E. J. (1998), Microphysical properties of the melting layer. Ph.D. thesis, ETH Zürich, Zürich, Switzerland.

Battan, L. J. (1973), Radar observation of the atmosphere, The University of Chicago Press, 324 pp.

Benn, D. I., and F. Lehmkuhl (2000), Mass balance and equilibrium-line altitudes of glaciers in high-mountain environments, Quaternary International, 65, 15-29.

Bolch, T., A. Kulkarni, A. Kääb, C. Huggel, F. Paul, J. G. Cogley, H. Frey, J. S. Kargel, K. Fujita, M. Scheel, S. Bajracharya, and M. Stoffel (2012), The state and fate of Himalayan glaciers, Science, 336, 310–314.

Cluckie, I. D., R. J. Griffith, A. Lane, and K. A. Tilford (2000), Radar hydrometeorology using a vertically pointing radar, Hydrology and Earth System Sciences, 4, 565–580.

Das, S., A. Maitra, and A. K. Shukla (2011), Melting layer characteristics at different climatic conditions in the Indian region: Ground based measurements and satellite observations, Atmospheric Research, 101, 78–83.

Dimri, A. P., and U. C. Mohanty (1999), Snowfall statistics of some SASE field stations in J&K, Defence Science Journal, 49, 437-445.

Durden, S. L., A. Kitiyakara, E. Im, A. B. Tanner, Z. S. Haddad, F. K. Li, and W. J. Wilson (1997), ARMAR observations of the melting layer during TOGA COARE, IEEE Transactions on Geoscience and Remote Sensing Journal, 35, 1453–1456.

Fabry, F., and I. Zawadzki (1995), Long-term radar observations of the melting layer of precipitation and their interpretation, Journal of Atmospheric Sciences, 52, 838-851.

Harris, G. N., K. P. Bowman, and D.-B. Shin (2000), Comparison of freezing-level altitudes from the NCEP reanalysis with TRMM precipitation radar brightband data, Journal of Climate, 13, 4137–4148.

Iguchi, T., T. Kozu, R. Meneghini, J. Awaka, and K. Okamoto (2000), Rain-profiling algorithm for the TRMM precipitation radar, Journal of Applied Meteorology and Climatology, 39, 2038–2052.

Immerzeel, W. W., P. Droogers, S. M. De Jong, and M. F. P. Bierkens (2009), Large-scale monitoring of snow cover and runoff simulation in Himalayan river basins using remote sensing, Remote Sensing of Environment, 113, 40–49.

Kirstetter, P.-E., Y. Hong, J. J. Gourley, M. Schwaller, W. Petersen, and J. Zhang (2013), Comparison of TRMM 2A25 Products, Version 6 and Version 7, with NOAA/NSSL Ground Radar–Based National Mosaic QPE, Journal of Hydrometeorology, 14, 661–669.

Kitchen, M. (1997), Towards improved radar estimates of surface precipitation at long range, Quarterly Journal of the Royal Meteorological Society, 123, 145-163.

Klaassen, W. (1988), Radar observations and simulation of the melting layer of precipitation, Journal of Atmospheric Sciences, 45, 3741–3753.

Kobayashi, S., and T. Iguchi (2003), Variable pulse repetition frequency for the global Precipitation Measurement Project (GPM), IEEE Transactions on Geoscience and Remote Sensing Journal, 41, 1714–1718.

Kozu, T., T. Kawanishi, H. Kuroiwa, M. Kojima, K. Oikawa, H. Kumagai, K. Okamoto, M. Okumura, H. Nakatsuka, and K. Nishikawa (2001), Development of precipitation radar onboard the Tropical Rainfall Measuring Mission (TRMM) satellite, IEEE Transactions on Geoscience and Remote Sensing Journal, 39, 102–116.

Kumar, V., and S. K. Jain (2010), Trends in seasonal and annual rainfall and rainy days in Kashmir Valley in the last century, Quaternary International, 212, 64–69.

Kummerow, C., W. Barnes, T. Kozu, J. Shiue, and J. Simpson (1998), The Tropical Rainfall Measuring Mission (TRMM) Sensor Package, Journal of Atmospheric and Oceanic Technology, 15, 809–817.

Mondal, N. C., and S. K. Sarkar (2003), Rain height in relation to 0°C isotherm height for satellite communication over the Indian Subcontinent, Theoretical and Applied Climatology, 76, 89–104.

Pfaff, T., A. Engelbrecht, and J. Seidel (2014), Detection of the bright band with a vertically pointing k-band radar, Meteorologische Zeitschrift, 23, 527–534.

Rohrer, M., N. Salzmann, M. Stoffel, and A. V. Kulkarni (2013), Missing (in-situ) snow cover data hampers climate change and runoff studies in the Greater Himalayas, Science of the Total Environment, 468-470 (Suppl.), S60-S70.

Saikranthi, K., T. Narayana Rao, B. Radhakrishna, and S. Vijaya Bhaskara Rao (2013), Impact of misrepresentation of freezing-level height by the TRMM algorithm on shallow rain statistics over India and adjoining oceans, Journal of Applied Meteorology and Climatology, 52, 2001–2008.

Shin, D.-B., G. R. North, and K. P. Bowman (2000), A summary of reflectivity profiles from the first year of TRMM radar data, Journal of Climate, 13, 4072–4086.

Shroder, J.F., M. P. Bishop, L. Copland, and V. F. Sloan (2000), Debris-covered glaciers and rock glaciers in the Nanga Parbat Himalaya, Pakistan, Geografiska Annaler, 82, 17–31.

Smith, C. J. (1986), The reduction of errors caused by Bright Bands in quantitative rainfall measurements made using radar, Journal of Atmospheric and Oceanic Technology, 3, 129-141.

Smyth, T. J., and A. J. Illingworth (1998), Radar estimates of rainfall rates at the ground in bright band and non-bright band events, Quarterly Journal of the Royal Meteorological Society, 124, 2417–2434.

Szyrmer, W., and I. Zawadzki (1999), Modeling of the Melting Layer. Part I: Dynamics and Microphysics, Journal of Atmospheric Sciences, 56, 3573–3592.

Thurai, M., E. Deguchi, T. Iguchi, and K. Okamoto (2003), Freezing height distribution in the tropics, International Journal of Satellite Communications and Networking, 21, 533–545.

Thurai, M., E. Deguchi, K. Okamoto, and E. Salonen (2005), Rain height variability in the Tropics, 152, 17-23.

Unterstrasser, S., and G. Zängl (2006), Cooling by melting precipitation in Alpine valleys: An idealized numerical modelling study, Quarterly Journal of the Royal Meteorological Society, 132, 1489–1508.

Wen, Y., Q. Cao, P.-E. Kirstetter, Y. Hong, J. J. Gourley, J. Zhang, G. Zhang, and B. Yong (2013), Incorporating NASA spaceborne radar data into NOAA national mosaic QPE system for improved precipitation measurement: A physically based VPR identification and enhancement method, Journal of Hydrometeorology, 14, 1293–1307.

Willis, P. T., and A. J. Heymsfield (1989), Structure of the Melting Layer in Mesoscale Convective System Stratiform Precipitation, Journal of Atmospheric Sciences, 46, 2008-2025.

Wolfensberger, D., D. Scipion, and A. Berne (2015), Detection and characterization of the melting layer based on polarimetric radar scans, Quarterly Journal of the Royal Meteorological Society.

Zemp, M., H. Frey, I. Gärtner-Roer, S. U. Nussbaumer, M. Hoelzle, F. Paul, W. Haeberli, F. Denzinger, A. P. Ahlstrøm, B. Anderson, S. Bajracharya, C. Baroni, L. N. Braun, B. E. Cáceres, G. Casassa, M. N. Demuth, L. Espizua, A. Fischer, K. Fujita, B. Gadek, A. Ghazanfar, J. O. Hagen, P. Holmlund, N. Karimi, Z. Li, M. Pelto, P. Pitte, V. V. Popovnin, C. A. Portocarrero, R. Prinz, C. V. Sangewar, I. Severskiy, O. Sigurdsson, A. Soruco, R. Usubaliev, and C. Vincent (2015), Historically unprecedented global glacier decline in the early 21st century, Journal of Glaciology, 61, 745-761.

Zawadzki, I., W. Szyrmer, C. Bell, and F. Fabry (2005), Modeling of the melting layer. Part III: The density effect, Journal of Atmospheric Sciences, 62, 3705–3723.

4 Paper IV

Schauwecker, S., M. Rohrer, C. Huggel, J. Endries, N. Montoya, R. Neukom, B. Perry, N. Salzmann, M. Schwarb, and W. Suarez. (2016). The freezing level in the tropical Andes, Peru: an indicator for present and future glacier extents. *Journal of Geophysical Research – Atmospheres*, in review.

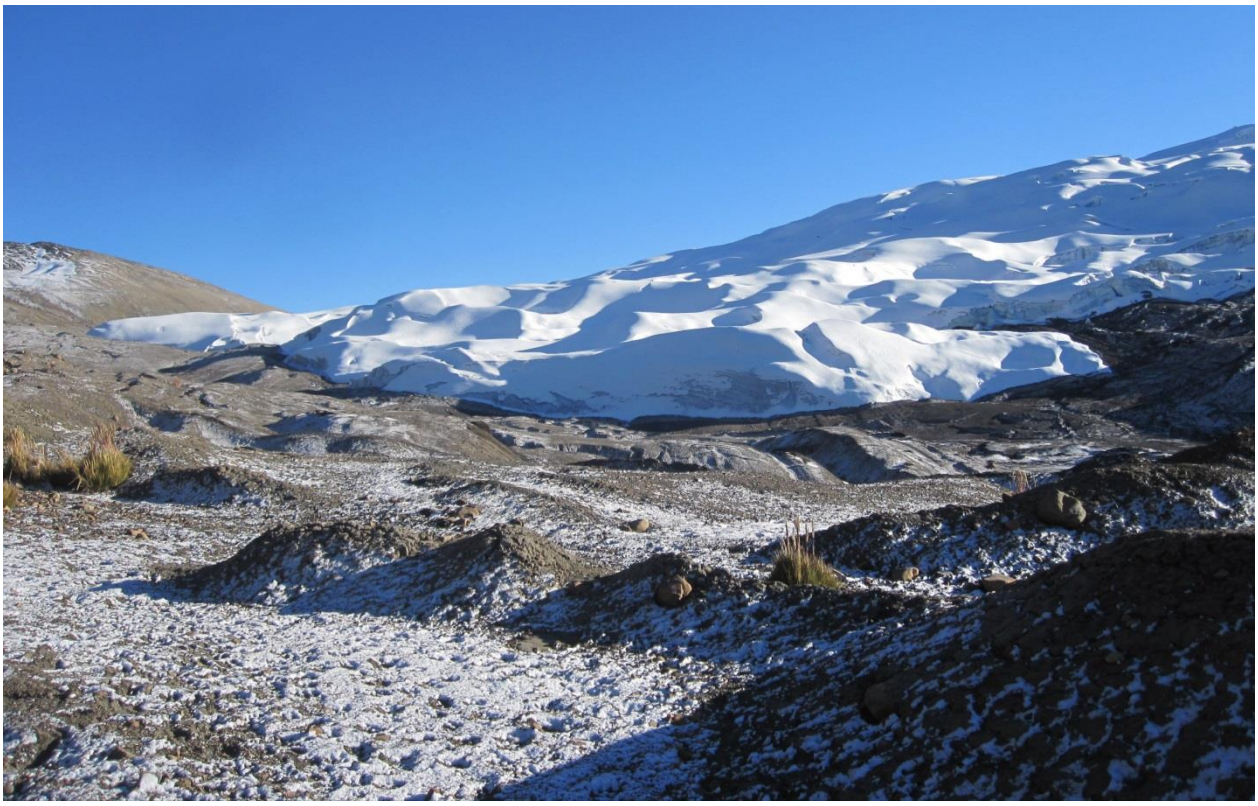

Suyuparina Glacier in the morning after a graupel event, Cordillera Vilcanota (S. Schauwecker)

Contributions of the PhD candidate:

Conception and design of the work, analysis and interpretation of multiple data sets, developing an experiment to relate freezing level height to glacier extents, drafting and writing the article

The freezing level in the tropical Andes, Peru: an indicator for present and future glacier extents

Simone Schauwecker[1,2], Mario Rohrer[1], Christian Huggel[2], Jason Endries[3], Nilton Montoya[4], Raphael Neukom[5], Baker Perry[3], Nadine Salzmann[6], Manfred Schwarb[1], Wilson Suarez[7]

1 Meteodat GmbH, Technoparkstr. 1, 8005 Zurich, Switzerland
2 Department of Geography, University of Zurich, Winterthurerstr. 190, 8057 Zurich, Switzerland
3 Department of Geography and Planning, Appalachian State University, Boone, NC 28608, USA
4 Professional School of Agronomy, National University of San Antonio Abad at Cusco, Cusco, Peru
5 Oeschger Centre for Climate Change Research and Institute of Geography, University of Bern, Erlachstrasse 9a, 3012 Bern, Switzerland
6 Department of Geosciences, University of Fribourg, Chemin du Musée 4, 1700 Fribourg, Switzerland
7 Servicio Nacional de Meteorología e Hidrología del Peru SENAMHI, av. Las Palmas s/n, Lima, Peru

Along with air temperatures, the freezing level height (FLH) has risen over the last decades. The mass balance of tropical glaciers in Peru is highly sensitive to a rise in the FLH, mainly due to a decrease in accumulation and increase of energy for ablation caused by reduced albedo. Knowledge of future changes in the FLH is thus crucial to estimating changes in glacier extents. Since in-situ data are scarce at altitudes where glaciers exist (above ca. 4800 m asl.), reliable FLH estimates must be derived from multiple data types. Here, we assessed the FLHs and their spatiotemporal variability, as well as the related snow/rain transition in the two largest glacier-covered regions in Peru by combining ERA-Interim and MERRA2 reanalysis, TRMM Precipitation Radar Bright Band, Micro Rain Radar data and meteorological ground station measurements. The mean FLH lies at 4900 and 5010 m asl., for the Cordillera Blanca and Vilcanota, respectively. During the wet season, the FLH in the Cordillera Vilcanota lies ca. 150 m higher compared to the Cordillera Blanca, which is in line with the higher glacier terminus elevations. CMIP5 climate model projections reveal that by the end of the 21st century, the FLH will rise by 230 m (±190 m) for RCP2.6 and 850 m (±390 m) for RCP8.5. Even under the most optimistic scenario, glaciers may continue shrinking considerably, assuming a close relation between FLH and glacier extents. Under the most pessimistic scenario, glaciers may only remain at the highest summits above approximately 5800 m asl.

Keywords: Freezing level height, snow/rain transition, glacier shrinkage, climate change, CMIP5 climate scenarios, Peruvian glaciers

4.1 Introduction

Observations show that the retreat of glaciers in the 21st century is unprecedented on a global scale for the time period observed and probably also for the recorded history (*Zemp et al.*, 2015). Glaciers play an important role in many regions in Peru, particularly because 1) there is a strong seasonality in precipitation with a considerable contribution of glacier melt to total river discharge during the dry season (e.g. *Kaser et al.*, 2003; *Mark et al.*, 2005; *Kaser et al.*, 2010); 2) people use river water for irrigation, hydropower, tourism or domestic consumption (e.g. *Drenkhan et al.*, 2015; *Gurgiser et al.*, 2016) and 3) discharge from glaciers is expected to change in the future due to glacier shrinkage (*Ames and Hastenrath*, 1996; *Kaser and Georges*, 1997; *Mark and Seltzer*, 2003; *Juen et al.*, 2007; *Vuille et al.*, 2008; *Baraer et al.*, 2012; *Rabatel et al.*, 2013). The consequences of vanishing glaciers are especially severe where people have only limited capacity to adapt to changes in the water availability due to, for instance, lack of financial resources and knowledge or/and where competition for water is intensifying (*Lynch*, 2012). Various studies have shown that glaciers in Peru are rapidly shrinking since they are out of equilibrium with current climatic conditions (*Vuille et al.*, 2008; *Rabatel et al.*, 2013; *Salzmann et al.*, 2013). Especially small glaciers at lower elevations will almost certainly disappear in a few years to decades (*Vuille et al.*, 2008; *Schauwecker et al.*, 2014). Also large glaciers with response times of 10-40 years (*Schauwecker et al.*, 2014) will continue retreating during the coming decades.

A crucial step to projecting future glacier shrinkage is understanding the dominant processes of glacier ablation and how these processes will change in future. Several studies have identified the net shortwave radiation budget as the main energy source for ablation of tropical glaciers (e.g. *Favier et al.*, 2004a; *Favier et al.*, 2004b; *Gurgiser et al.*, 2013a; *Gurgiser et al.*, 2013b). Net shortwave radiation is largely determined by albedo, which is strongly affected by the snowline, the snowfall level height (SLH) and thereby the temperature during precipitation events (*Francou et al.*, 2004). This close link between the air temperature during precipitation events, albedo and net shortwave radiation together with the fact that glacier tongues are constantly close to melting conditions, leads to a high sensitivity of tropical glaciers to air temperature which is described in several studies (e.g. *Kaser*, 2001; *Vuille et al.*, 2008; *Gurgiser et al.*, 2013a). For example, *Gurgiser et al.* (2013a) showed that the glacier mass balance of the Shallap Glacier (Cordillera Blanca, Peru) varied significantly between two years due to different air temperatures and related SLHs, mainly during the wet season. While the mass balance in the accumulation area (>5000 m asl.) was similar in both years due to similar annual total solid precipitation, the difference in mass balance was considerable for the lower part of the glaciers. *Gurgiser et al.* (2013a) suggest that the Shallap Glacier is characterized by a high sensitivity of mass balance to air temperature, and is thus more similar to glaciers in the inner tropics (Ecuador) than the outer tropics (Bolivia) (*Favier et al.*, 2004a; *Favier et al.*, 2004b).

The SLH (also called snow/rain transition height or melting level) is thus a crucial variable in accurately determining mass balance and runoff for tropical glaciers The SLH is defined as the top of the melting layer during precipitation events, which is the altitude throughout solid precipitation

melts as it descends (*American Meteorological Society*, 2016). The temperature of the melting layer is typically 0°C or warmer (*American Meteorological Society*, 2016). The freezing level height (FLH, or also called freezing height or free air 0°C isotherm) is defined as the lowest level in the free atmosphere where the temperature is 0˚C (*American Meteorological Society*, 2016). Since melting of solid precipitation starts approximately where air temperature is over 0°C, the FLH during precipitation events and the SLH are closely related. It is thus crucial to study the seasonal and regional variability of the FLH, past and future changes and how the FLH during precipitation events is linked to the SLH.

The FLH is on average within about 4500-5000 m asl. in tropical regions between 20°N – 20°S (*Harris et al.*, 2000). NCEP/NCAR reanalysis data show that over the last 30 years, the FLH has increased by 10-20 m per decade over the tropics (1977-2007, *Bradley et al.*, 2009) and by about 30 m per decade over the Cordillera Blanca (1960-2010, *Rabatel et al.*, 2013). Also *Diaz et al.* (2003) found that the tropical (20°N – 20°S) FLH increased by about 14 m per decade from 1948-2000 and by 12 m per decade between 1958-2000. In addition to reanalysis data, station data indicate that the FLH during precipitation days has risen by about 200 m during the 5 decades between the 1960s and 2012 in the Cordillera Blanca (*Schauwecker et al.*, 2014). In the recent years, large efforts have been made to monitor air temperature and precipitation at high altitudes in order to assess the snow/rain transition and precipitation type (e.g. *Poremba et al.*, 2015, *Hellström et al.*, 2017). However, meteorological measurements at the elevation of glaciers (>4800 m asl.) are still very sparse and often limited to short time periods, thus limiting the estimation of the FLH and SLH. This calls for studies based on data from multiple sources, e.g. radiosondes, precipitation radar, reanalysis data or remote sensing. The first objective of this article is therefore to assess the spatial and temporal variability of the FLH and the link to the SLH over the two largest glacierized mountain ranges in Peru, the Cordillera Blanca (CB, Figure 4-1) and the Cordillera Vilcanota (CV, Figure 4-1), using remote sensing, reanalysis as well as in-situ data.

Our second objective is to assess future FLHs by the end of this century, using global climate model (GCM) outputs. Model projections indicate a continued warming of the tropical troposphere throughout the 21st century, but to our knowledge, the future FLH has not yet been assessed for the mountainous regions of Peru. GCMs driven by the SRES A2 emission scenarios indicate an increase in mean air temperature on the order of 4.5 to 5°C (*Bradley et al.*, 2006; *Vuille et al.*, 2008; *Urrutia and Vuille*, 2009) over Peru, whereas for B2 scenarios, a smaller warming of around 3 to 3.5°C results (*Urrutia and Vuille*, 2009). *Bradley et al.* (2004; 2006) found that warming particularly affects high mountain regions and suggested that these changes could likely result in the complete disappearance of glaciers in many regions.

A third objective of this article is to discuss possible future glacier extents under different Representative Concentration Pathways (RCPs; *Moss et al.*, 2010). While several studies have focused on future air temperature, little is known about future glacier extents in the Peruvian Cordilleras. For glaciers in High Asia, a rise of 10 m in summer FLH causes a strong decrease in mass balance and increase in the equilibrium line altitude (ELA) of up to 10 m (*Wang et al.*, 2014). But, to our knowledge this relationship has not been investigated for glaciers in Peru. Studies on

the future of Peruvian glaciers have mostly been motivated by future runoff from glaciated catchments (e.g. *Juen et al.*, 2007, *Lopez-Moreno et al.*, 2014), but future glacier shrinkage and the response of tropical glaciers to temperature rise has still not been analyzed in detail nor fully understood. The glacier-climate interactions are complex because temperature not only affects the sensible heat flux, but also influences other energy fluxes like incoming longwave radiation and net shortwave radiation via the SLH and albedo (see e.g. *Vuille et al.*, 2008). We discuss here the future glacier extents based on a simple experiment, assuming a strong and stable relation between the FLH during precipitation events, the closely connected SLH and glacier extents (as already indicated by e.g. *Rabatel et al.*, 2013).

4.2 Study site

In our study we focus on the two largest glacier covered tropical mountain ranges in Peru (Figure 4-1): The CB (9.0°S / 77.5°W) and the CV (13.7°S / 71.0°W). The termini of glaciers are currently located at around 4200 to 4800 m asl. in the CB (*Racoviteanu et al.*, 2008) and 4600 to maximum 5400 m asl. in the CV (*Salzmann et al.*, 2013).

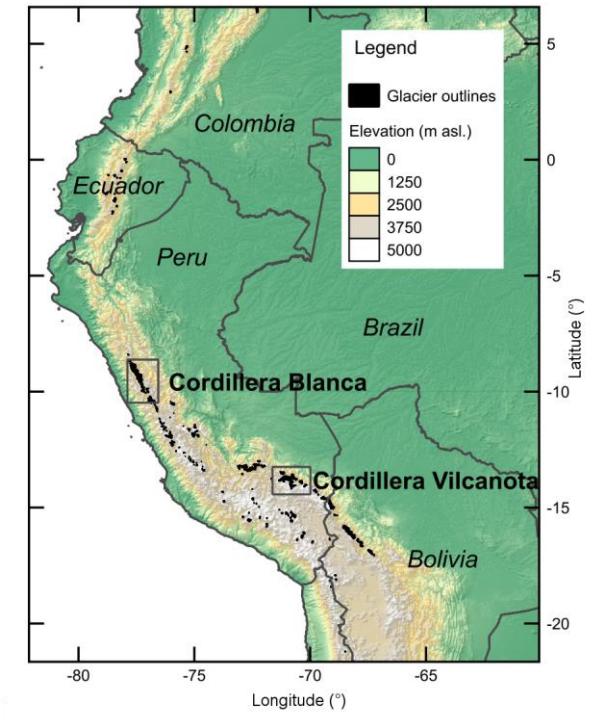

Figure 4-1 Overview map of the study areas CB and CV.

The climate of the Peruvian Cordilleras is characterized by a distinct dry and wet season, defined by the global circulation patterns of the Intertropical Convergence Zone (ITC) and the trade winds.

Station data from the Servicio Nacional de Meteorología e Hidrología de Perú (SENAMHI) indicate that over 90% of the precipitation in the CB falls during the wet season from October to April, but some precipitation also occurs during the dry season, especially at high elevations (*Schauwecker et al.*, 2014). Precipitation events are predominantly graupel at the elevation of the glacier tongues in the CV (*Poremba at al.*, 2015), similar to other tropical high mountain regions in the world (e.g. on Mt. Kenya, *Prinz et al.*, 2016). Since the bulk of the moisture advection is coming from the tropical Atlantic and the Amazon basin, interannual precipitation correlates well with easterly winds of the upper troposphere (e.g. *Garreaud et al.*, 2003; *Minvielle and Garreaud*, 2011; *Schauwecker et al.*, 2014; *Neukom et al.*, 2015). In contrast to the strong seasonal variation in precipitation, the Peruvian Cordilleras are characterized by small seasonal temperature variability. During the dry season, the diurnal variation in air temperature is more pronounced and mean daily air temperatures are lower compared to the wet season (*Schauwecker et al.*, 2014).

Several studies show that the climate in the tropical Andes has changed significantly over the last century (*Vuille and Bradley*, 2000; *Mark and Seltzer*, 2005; *Vuille et al.*, 2008; *Schauwecker et al.*, 2014). Warming has slowed down slightly in the last 30 years (compared to the three decades from the 60s to the 90s) to approximately -0.04 for minimum (T_{min}) and 0.29°C for maximum (T_{max}) per decade daily air temperature between 1983 and 2012 in the CB (*Schauwecker et al.*, 2014) and -0.2 and 0.23°C per decade for T_{min} and T_{max}, respectively between 1980 and 2009 in the CV (*Salzmann et al.*, 2013).

4.3 Data and methods

Since in-situ meteorological data are relatively sparse along the Peruvian Cordilleras and at high elevations in particular, we assessed FLHs and SLHs using a combination of multiple data sets. These data products have different temporal and spatial resolution and coverage, as schematically shown in Figure 4-2. An overview of the data types is presented in Table 4-1. Reanalysis data are first used to assess seasonal and regional patterns in FLH over Peru. Furthermore, we compared reanalysis FLH as well as extrapolated FLH from the METAR station at the airport of Cusco to the SLH derived from the Micro Rain Radar (MRR). The SLH data derived by the MRR for all events are then compared to reanalysis data and to the extrapolated FLH. In addition, we estimated monthly FLH and SLH for all available data sets.

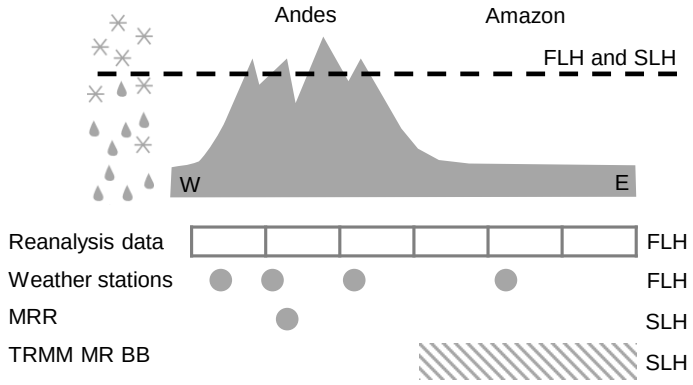

Figure 4-2 Schematic of the FLH and SLH over the Peruvian Cordillera from the West to the East and spatial availability of different data types, used for deriving SLH and FLH (indicated on the right). The boxes representing reanalysis data illustrate that the data are provided for a regular global grid. Weather stations and MRR data are available as point measurements. TRMM MR BB data are available for a variable spatial and temporal resolution, and limited over mountainous regions (e.g. *Schauwecker et al.*, 2016).

Table 4-1 Data types used for assessing FLH and SLH and used variables (P: Precipitation, T: Air temperature, H: geopotential height, BB: Bright band height).

Data Type	Variable	Selected time period for analysis	Spatial resolution	Temporal resolution	Used for
ERA-Interim reanalysis	P, T, H	1980-2015	0.75° (~82 km)	6h	FLH
MERRA2 reanalysis	T, H	1980-2015	0.5° (~56 km)	3h	FLH
Ground stations SENAMHI	P, T	1964-2015 **	Point meas.	daily	FLH
Ground stations UNASAM	P, T	2012-2015	Point meas.	1h	FLH
Ground stations METAR	T	1996-2015	Point meas.	1h	FLH
TRMM 2A23 PR	BB	1997-2015	variable*	variable*	SLH
MRR	Doppler velocities and reflectivity	Aug 2014 – Feb 2015	Point meas.	1 min	SLH

*see e.g. *Schauwecker et al.* (2016) **depending on station

4.3.1 Reanalysis data

Our study is based on two reanalysis products: ERA-Interim (interim reanalysis of the European Centre of Medium-range Weather Forecasts, ECMWF, *Dee et al.*, 2011) and MERRA2 (reanalysis of the Modern Era Retrospective-Analysis for Research and Applications by the National Aeronautics and Space Administration, NASA, *Rienecker et al.*, 2011). Large warm daily maximum air temperature biases of MERRA over southern America have largely been removed in MERRA2 (*Bosilovitch et al.*, 2015). *Hofer et al.* (2010) found that the skill of MERRA as predictor for daily air temperature on high altitudes in Peru is considerably higher than for other reanalysis products. Reanalysis data cover the entire globe and in our study serve to assess the FLH in the free atmosphere using air temperature from different geopotential heights. The levels around the FLH (500, 550, 600, 650 hPa) were examined for a transition from a positive to a negative

temperature (similar to *Bradley et al.*, 2009). Free-air FLHs were then linearly interpolated from the geopotential heights of the transition levels. The high spatial resolution of MERRA2 (0.5°) may for some cases be a disadvantage in assessing FLH over mountainous terrain. In comparison to ERA-Interim, values lying below the topography are masked out in MERRA2. Due to the higher resolution, there are more grid points with the FLH lying below the earth surface, which leads to difficulties in interpolating a FLH. We did not consider the topography and extrapolated to a FLH even if the resulting FLH lay below the surface, as a potential future temperature rise may lead to an FLH that lies above the surface.

4.3.2 Meteorological station data

Meteorological ground-based measurements are provided by the Servicio Nacional de Meteorología e Hidrología de Perú (SENAMHI) and the Universidad Nacional Santiago Antúnez de Mayolo (UNASAM). A list of the stations is given in the supporting information (Table 4-3). The SENAMHI operated a relatively dense national network of meteorological stations since 1964. Air temperature is provided as daily T_{max} and T_{min} (and additionally measured at 07:00, 13:00 and 19:00 local time) and precipitation is measured once a day, which makes it difficult to estimate the FLH only during precipitation events. The UNASAM runs a network of 16 meteorological stations located in the region of the CB (Ancash) since 2012. The hourly resolution allows distinguishing between the FLH for all hours and during precipitation events. Additionally, we used data from the METAR station located at the airport in Cusco (71.97°W / 13.55°S). METAR-records can be downloaded e.g. from the National Oceanic and Atmospheric Administration (*NOAA*, 2016).

Station data are scarce at high elevations, but lower elevation stations can be used to assess the FLH and SLH using simple extrapolation techniques with either constant lapse rates (assuming e.g. -0.0065°C/m, Figure 4-4 and Figure 4-5) or by linearly extrapolating where several stations are recording (Figure 4-6). For the analyses in Figure 4-6, we considered stations located at elevations above 3500 (3000) m asl. in the area of the CV (CB). We only considered station data from days (SENAMHI data) or hours (UNASAM data) where precipitation was registered, in order to assess the FLH for wet conditions. The FLH was then extrapolated on a daily (hourly) basis from these stations using linear regression, but only where data of at least 4 (3) stations were available for SENAMHI (UNASAM) data. Table 4-3 in the supporting information provides information on the utilized SENAMHI and UNSAM stations used.

4.3.3 TRMM Precipitation Radar Bright Band data

In addition, we used Bright Band (BB) heights from the Tropical Rainfall Measuring Mission (TRMM) by the National Aeronautics and Space Administration (NASA) and the Japan Aerospace Exploration Agency (JAXA) to assess the snow/rain transition height. The BB is a zone of enhanced radar reflectivity, which is commonly observed in precipitation radar (PR) images during precipitation events. This zone of intensified echoes is caused by a horizontal melting layer in the atmosphere, at the height where ice or snow particles are transformed into liquid raindrops (e.g. *Battan*, 1973). TRMM BB heights are given in the product 2A23 and are available for the 17 years

of active TRMM measurements (1997 – 2015). The possibilities and limitations of using TRMM 2A23 BB heights for mountainous regions are described in e.g. *Schauwecker et al.* (2016), who found for instance that the data availability is generally limited over high mountain regions. Over the CB and CV, the BB is too close to the surface, and thus disturbed by the ground echo (*Schauwecker et al.*, 2016). However, over the Amazon lowlands, TRMM 2A23 BB heights have the potential to provide valuable information on the seasonal variability of the SLH.

4.3.4 Micro Rain Radar data

From August 2014 to February 2015, a MRR was installed in the city of Cusco, (13.5278°S, 71.9508°W) at the SENAMHI office (at a distance of ca. 1 km from the Airport, see also *Perry et al.*, 2017). We estimate the altitude of the melting layer using the minute-resolution MRR data and an algorithm that includes several checks to filter unrealistic values. The first removes periods of positive velocity and reflectivity gradients (from lower altitudes to higher altitudes) due to the fact that melting layers will always involve negative gradients of these two values. Periods of virga are then discarded to prevent the algorithm from utilizing gradients at the bottom of the precipitation. Time periods when the most negative gradient in reflectivity is not within 300 m above the most negative gradient in velocity are then discarded. This is to ensure that unrealistically thick melting layers are not processed by the rest of the algorithm. Once the data are run through these filters, aspects of the melting layer are calculated. As a snowflake falls through the atmosphere from temperatures below freezing to above freezing, water droplets form on the outside of the flake. This increases the radar-detected reflectivity due to the higher dielectric constant of water than of ice. Once melting is complete, the denser rain drop will fall at a higher velocity than the previous snowflake. Using these principles, the algorithm identifies the bottom of the melting layer as the most negative gradient in velocity in the profile and the top of the melting layer as the most negative gradient in reflectivity. The SLH is then computed as the most negative gradient in velocity plus the average melting layer thickness for the respective hour of the storm. Finally, the results of the algorithm are passed through two more checks. The first discards values above 6000 m, since the FLH rarely exceeds this altitude even in the tropics. The second discards any values outside of one standard deviation of the mean for the hour in which it lies. The values that are used in this study are the hourly median SLHs which are computed from the original minute-resolution values.

4.3.5 Global Climate Model data

To assess the FLH by the end of this century over the mountainous regions of Peru, we analyzed GCM simulations. The resolution of most GCMs does not adequately resolve the complex topography of the Andes. We therefore analyzed FLH changes of the free troposphere (according to e.g. *Bradley et al*. (2004); *Bradley et al.*, 2009). The FLH change is taken from models which were part of the Coupled Model Intercomparison Project 5 (CMIP5, *Taylor et al*., 2011). We compared the runs representing present-day climate (1976-2005; "historical" experiment) to the climate by the end of 21st century (2071-2100), taking the most optimistic (low emissions) and pessimistic (high emissions) Representative Concentration Pathways (RCP) 2.6 and 8.5,

respectively (*Moss et al.*, 2010). The RCP2.6 is called "peak-to-decay" scenario, in which radiative forcing reaches a maximum near the middle of the 21st century before decreasing to an eventual nominal level of 2.6 Wm^{-2} relative to pre-industrial conditions. Under RCP8.5, the radiative forcing is assumed to increase throughout the 21st century until reaching a level of 8.5 Wm^{-2} at the end of the century relative to pre-industrial conditions (*Taylor et al.*, 2011). We use a 24 member ensemble of CMIP5 model simulations. A list of the models used is given in the supporting information (Text S1). Similar to the analysis of reanalysis data, we estimated the FLH based on the temperature of different pressure levels (400, 500, 600, 700 hPa). The increase of the FLH is then estimated as the difference between the historical runs (average over 1976-2005) and the end-of-century projections (2081-2100).

4.3.6 Glacier and elevation data

To assess whether regional differences in glacier extents are linked to the FLH, we computed glacier hypsographies in 100 m elevation bins, using glacier outlines from the Global Land and Ice Measurements from Space (*GLIMS*, 2005) and the Unidad de Glaciología y Recursos Hídricos (UGRH) glacier database and ASTER digital elevation models (DEM) (*NASA JPL*, 2009). We do not consider any potential vertical error of the ASTER DEM in this study. Outlines are based on satellite images from 2003 and 2005 for the CB (*Racoviteanu et al.*, 2008) and from 2000 (GLIMS inventory) and 2009 (UGRH inventory) for the CV. Based on the hypsographies we then assessed the median elevation of glaciers as well as the fraction of glacier area below the present-day wet season (DJF) FLH from reanalysis data. The present-day wet season FLH is then illustrated in a map, as well as the FLH by the end of this century under RCP2.6 and RCP8.5.

4.4 Results

4.4.1 Present-day freezing and snowfall level height from multiple data types

First, we present an overview of the FLHs and the regional and seasonal variability derived from reanalysis data. Seasonal present-day (1980-2015) FLHs over Peru based on ERA-Interim and MERRA2 reanalysis data are shown in Figure 4-3. The MERRA2 FLH generally lies higher than the ERA-Interim FLH over the study areas and the Andes (see also Figure 4-12 in the supporting information). Both data sets have similar regional pattern: the FLH is higher over Southern Peru and Bolivia, as well as at the Peruvian coast, compared to the lower FLH over Northern Peru and the Amazon basin. According to the overall pattern, the FLH is higher over the CV than the CB. The results further show that the FLH is lowest during the dry season (JJA) and highest during the wet season (DJF).

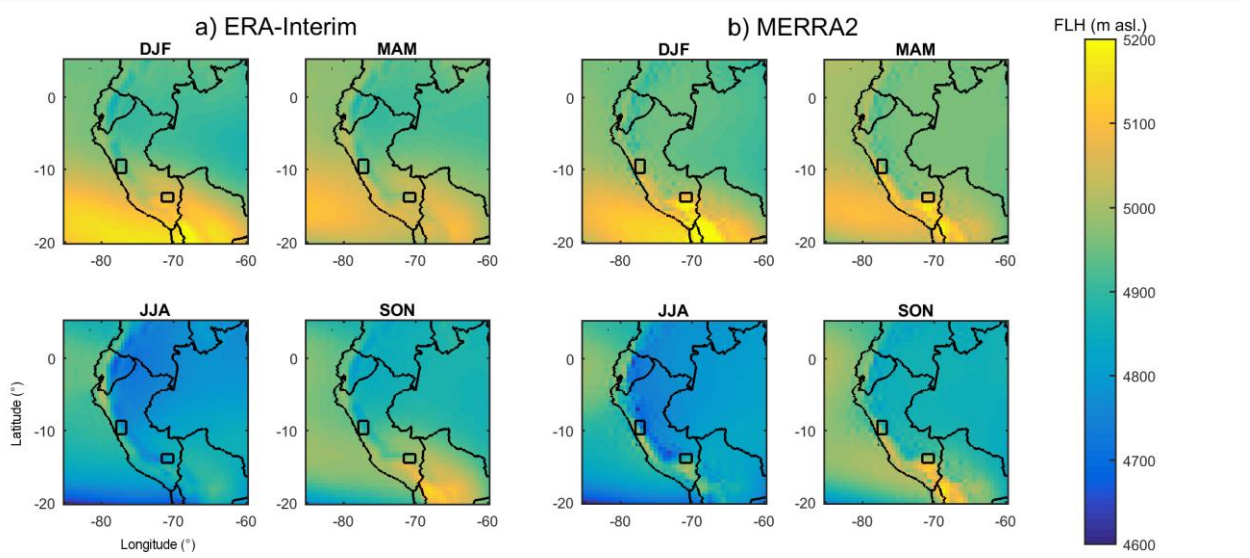

Figure 4-3 Mean present-day (1980-2015) seasonal (a) ERA-Interim and (b) MERRA2 FLH (m asl.). The areas of the CB and CV are marked with black boxes.

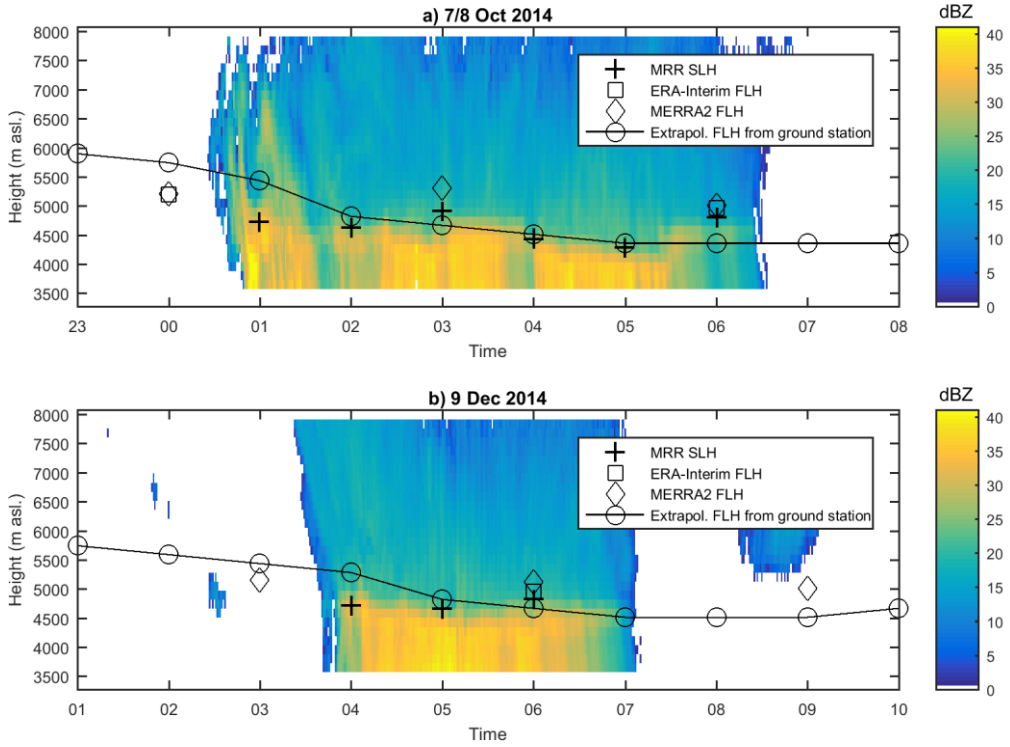

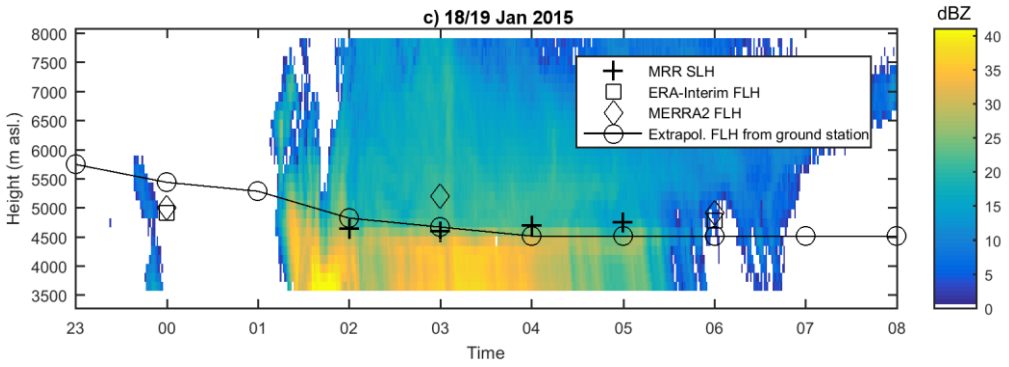

Figure 4-4 MRR reflectivity of three precipitation events over the city of Cusco registered on 7/8 October 2014, 9 December 2014 and 18/19 January 2015. Indicated are simulated SLHs from MRR and FLHs from ERA-Interim and MERRA2 reanalysis, as well as extrapolated FLH from the meteorological ground station.

Figure 4-4 shows the reflectivity of three rainfall events from different months during the transition and wet season (7/8 October 2014, 9 December 2014 and 18/19 January 2015). We selected these events, because the duration was at least 3 hours and the transition from solid to liquid precipitation was clearly visible. Figure 4-4 further shows the estimated SLH based on the MRR data, as well as the ERA-Interim and MERRA2 FLH and the extrapolated FLH based on data from one meteorological station, using a constant lapse rate (-0.0065°C/m). The three figures show that at the beginning of the precipitation events, the extrapolated FLH clearly lies above the SLH derived from the MRR data. After approximately the first hour of strong precipitation, the extrapolated FLH drops and approaches the SLH derived from MRR data. These results illustrate that the accuracy of the snow/rain transition estimation based on air temperature extrapolation strongly depends on the time of the measurements and likely improves after the first few hours of the precipitation event. The reanalysis FLHs lie in all cases above the SLH, whereas the MERRA2 FLH is found at higher altitudes than the ERA-Interim FLH, according to Figure 4-3.

We then compared the MRR SLH data from all recorded precipitation events to FLH obtained from ERA-Interim and MERRA2 reanalysis data (Figure 4-5a) as well to the extrapolated FLH (Figure 4-5b). The MRR SLH ranges in 95% of the cases between 4430 and 5160 asl. ($\mu \pm 2\delta$, Figure 4-5a). As expected, the correlation between the SLH and reanalysis FLH is rather low (R^2=0.26 and R^2=0.10, for ERA-Interim and MERRA2, respectively). The radar derived SLH lies on average 220 m below the ERA-Interim FLH and 240 m below the MERRA2 FLH. The spread is considerable (δ = 172 and 202 m, for ERA-Interim and MERRA2, respectively). Only in few cases was the SLH higher than the FLH, indicating that liquid precipitation rarely occurs above the reanalysis FLH. In Figure 4-5b we see that the extrapolated FLH represents relatively well the SLH for relatively low air temperatures at the ground (below approximately 15°C). In contrast, the extrapolated FLH strongly overestimates the SLH for high temperatures above approximately 15°C. Figure 4-5b indicates that high temperatures are in most cases occurring within the first 5 hours of the precipitation events, as shown in Figure 4-4.

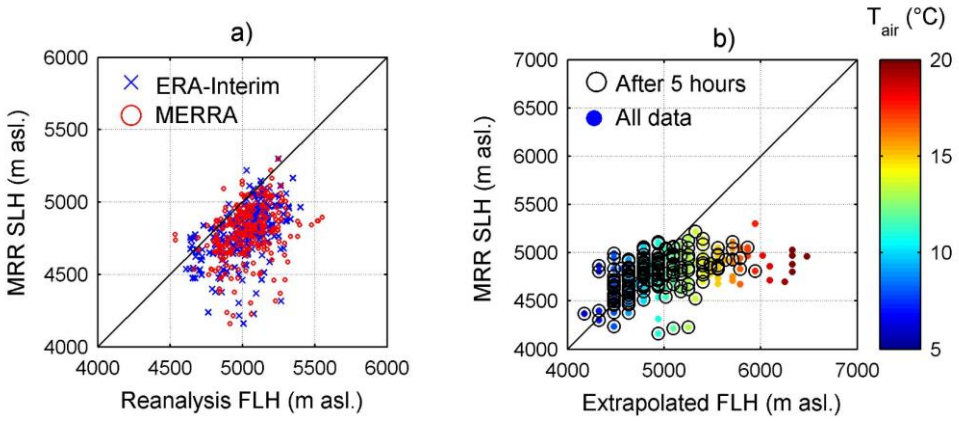

Figure 4-5 a) MRR SLH estimations vs. ERA-Interim and MERRA2 FLH; b) MRR SLH estimation vs. extrapolated FLH based on air temperature measured at the METAR station in Cusco. The colour scale in b) expresses air temperature measured at the METAR meteorological station.

Figure 4-6 presents FLHs and SLHs for the CB and CV based on multiple data types. All data sets show a clear seasonal variability with lower FLHs and SLHs during the dry season (JJA). The different data types indicate that the seasonal variability is stronger for the CV than the CB. The stronger seasonality is especially visible for the extrapolated FLH from station measurements (Figure 4-6h). The extrapolated FLH in the CB (Figure 4-6c) shows a much lower annual variability compared to reanalysis data (Figure 4-6a and Figure 4-6b). In contrast, the FLH based on UNASAM station data (Figure 4-6d) have a much larger variability and spread compared to the SENAMHI data (Figure 4-6c), probably due to the hourly resolution of the UNASAM data (compared to the daily resolution of SENAMHI data). The difference between the extrapolated FLH from ground stations (Figure 4-6c and h) and the free atmosphere FLH from reanalysis data (Figure 4-6a, b, f and g) is about 310 m for the CB and 220 m for the CV. For the dry season (JJA) in the CV, the extrapolated FLH (Figure 4-6h) lies up to 390 m below the reanalysis free atmosphere FLH (Figure 4-6f and g). There seems to be a regional difference in FLH between the CV and CB. The FLH from reanalysis data lies on average about 110 m higher for the CV (Figure 4-6f and g) than for the CB (Figure 4-6a and b), with a larger difference of 150 m during the wet season. During the dry season (JJA) this difference is much smaller or even negligible (approximately 50 m). During the wet season, the mean FLH from reanalysis is around 4950 (5090) m asl. for the CB (CV), in line with the overall pattern identified in Figure 4-4.

ERA-Interim reanalysis data (Figure 4-6b and g) show that the FLH during precipitation events agrees well with the FLH for all days during the wet season and the transition periods. Except during the dry season (JJA), the event-based FLH lies below the mean FLH of all days, the difference being larger for the CV. Also the extrapolated FLH of all hours and wet hours agrees well (Figure 4-6d). As expected, due to few precipitation events during the dry season and the relatively short measuring period, it was not possible to assess accurately the dry season FLH during precipitation events.

TRMM PR BB data are only available for the Amazon basin and the foothills adjacent to the mountain regions, which makes a direct comparison to the MRR data difficult. Compared to the reanalysis FLH over the study areas (Figure 4-6a, b, f and g), the SLHs derived from BB heights from TRMM over the Amazon basin lie approximately 500 m (CB) to 600 m (CV) lower (Figure 4-6e and j). This difference is comparable to results from other studies from the Himalaya (e.g. *Thurai et al.*, 2003; *Awaka et al.*, 2009; *Schauwecker et al.*, 2016).

Hence, these multiple data types show a clear but - compared to mid-latitudes - low seasonality in the FLH and indicate a regional difference between the CB and the CV. However, the difference of the FLH among the different data products is considerable and points to the need of multiple data analyses to get a reliable FLH assessment.

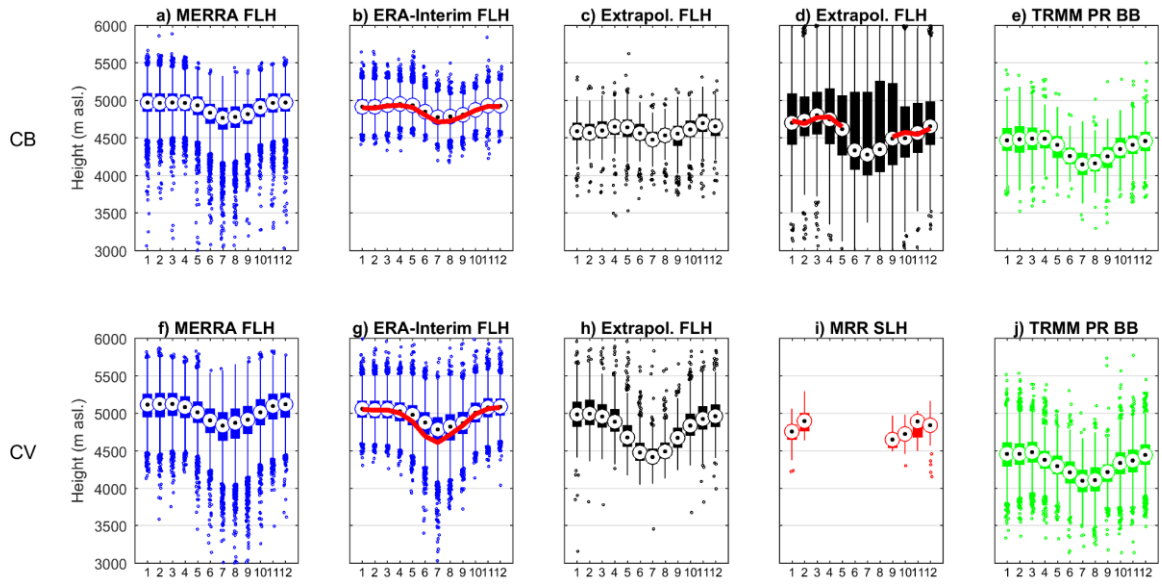

Figure 4-6 Monthly FLHs and SLHs (January to December) for the CB a) to e) and CV f) to j) from different data sources: a) and f) MERRA2 FLH (1980-2015), b) and g) ERA-Interim FLH (1980-2015), c) and h) FLH extrapolated from SENAMHI stations (1994-2015, CV and 1998-2015, CB) as well from d) UNASAM stations, i) SLH estimated with MRR data (September 2014 – February 2015), e) and j) TRMM BB heights (1997-2015). Red lines in b), d) and g) represent the median of the FLH during precipitation events. Circles represent the median, boxes represent the 25th and 75th percentiles, whiskers represent 1.5 standard deviations and outliers are plotted with points.

4.4.2 Future freezing height from CMIP5 model results

We used CMIP5 model results to assess the expected FLH changes by the end of this century (2071-2100). For both regions, the CMIP5 models project a strong FLH increase (Figure 4-7). The model results show a remarkable difference between the two scenarios. While the multi-model median FLH increase is on average 230 m for RCP2.6, it is 850 m for the most pessimistic scenario RCP8.5. The spread between the single model results is considerable, ranging within

approximately 40 to 420 m for RCP2.6 (μ±2δ, 2δ=190 m) and 460 to 1240 m (μ±2δ, 2δ=390m) for RCP8.5. The increase is strongest during the dry season (JJA) for most models under the emission scenario RCP8.5. The stronger climb in the dry season is not visible under RCP2.6.

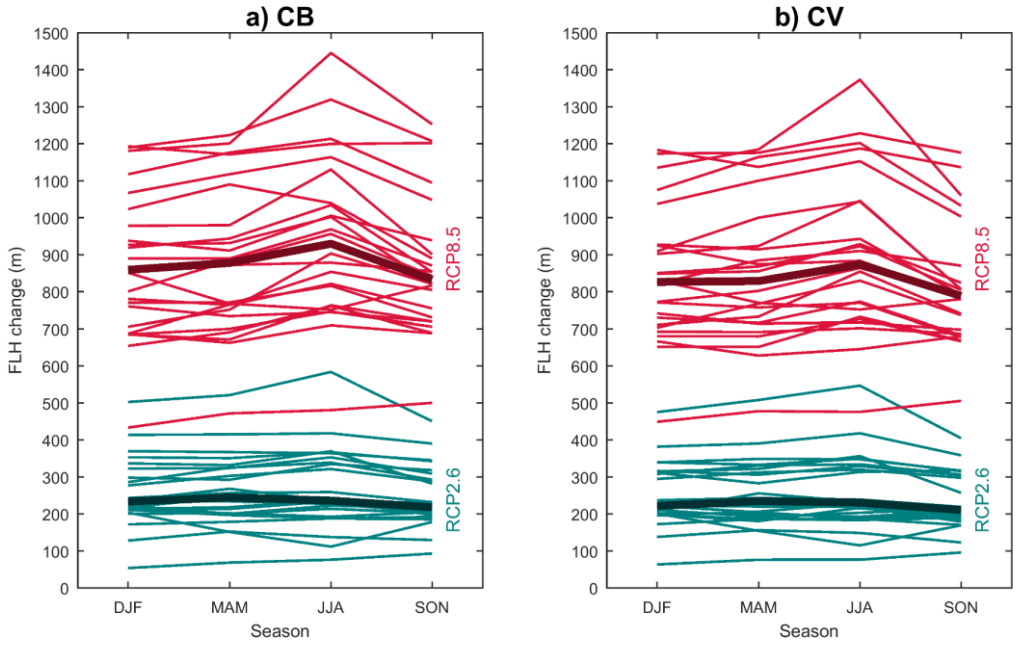

Figure 4-7 Projected future FLH change for the grid cell closest to the (a) CB and (b) CV for RCP2.6 (green) and RCP8.5 (red). Each line represents the results of one model (see list in supporting information) and thick dark lines represent the median of all model results.

Slight regional differences for the projected FLH increases are visible in Figure 4-8. The multi-model results for RCP8.5 indicate that the FLH is predicted to increase by ca. 900 m over Ecuador, especially during the dry season (JJA). Over the Altiplano in Southern Peru, the increase is slightly smaller but still over 700 m.

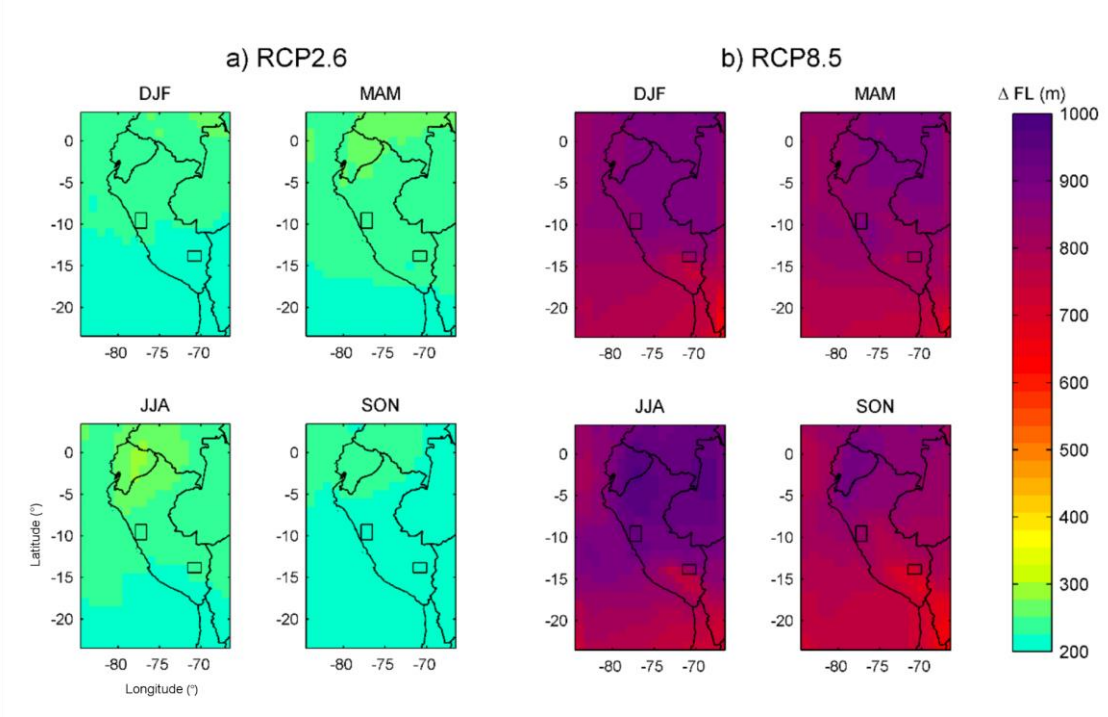

Figure 4-8 Multi-model median of projected future FLH level change for the region of the Peruvian Andes during DJF, MOM, JJA, SON for a) RCP2.6 and b) RCP8.5 between 1976-2005 and 2081-2100. The areas of the CB and CV are marked with black boxes.

Glacier hypsographies provide valuable information on glacier elevation distribution and allow relating the glacier covered area to the observed regional differences in the FLH. Both regions show a similar pattern of altitudinal distribution, but the elevation of glaciers in the CB is shifted down to lower elevations compared to glaciers in the CV (Figure 4-9). The median elevation of glaciers in the CB is 126 m lower compared to the CV, respectively. In Figure 4-9, we also plotted the mean wet season (DJF) FLH and SLH from ERA-Interim and MERRA2 data. From the results in Figure 4-5, we suggest that the SLH lies on average about 220 m and 240 m below the ERA-Interim and MERRA2 FLH, respectively, so the mean wet season SLH lies at about 4700 and 4900 m asl., for the CB and CV, respectively. For both regions, the SLH is the approximate altitude below which no glaciers exist. According to the glacier inventory data used only 4% (1%) of the total glacier area of CB (CV) lies below this elevation. Both reanalyses clearly show that the wet season FLH lies about 150 m higher in the CV compared to the CB. It can be seen from the hypsographies that the wet season FLH approximately corresponds to the 17% (15%) quantile of the elevation distribution for the CB (CV), meaning that only ca. 17% (15%) of the total glacier area is below the wet season FLH, indicating a relation between the wet season FLH and glacier extents.

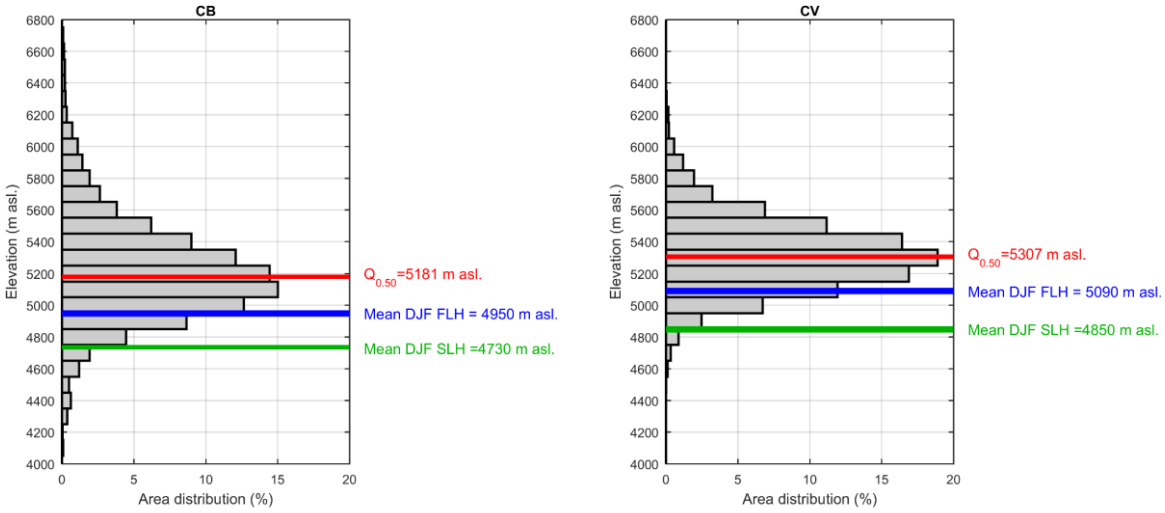

Figure 4-9 Glacier hypsographies for (a) CB and (b) CV. Red lines show the median elevation of the glacier-covered area; blue lines show the present-day wet season (DJF) FLH based on ERA-Interim and MERRA2 reanalysis data; green lines show the mean estimated present-day wet season (DJF) SLH.

Figure 4-10 and 4-11 show the present-day glacier extent as well as the present-day and end-of-century wet season FLH under RCP8.5 and RCP2.6. Mainly tongues of relatively large glaciers, some of them debris-covered, exist below the altitude of the present-day wet season FLH, especially for the CB. On the Southern side of CV, around the Sibinacocha lake, many glaciers tongues are ending at altitudes higher than the present-day FLH. The map also shows that in some areas around Sibinacocha lake there are no glaciers at all above the FLH, probably due to limited maximum elevation (ca. 5300 m asl) in these areas implying insufficient accumulation areas for the existence of glaciers. The green areas show the area above the projected wet season FLH under the RCP2.6 scenario. The area above the projected FLH under RCP2.6 is about 40% of the area above the present-day wet season FLH (Table 4-2). In contrast, the area above the RCP8.5 FLH is very small and consists only of the highest peaks in the region (e.g. Huascarán in the CB and Ausangate in the CV, Table 4-2).

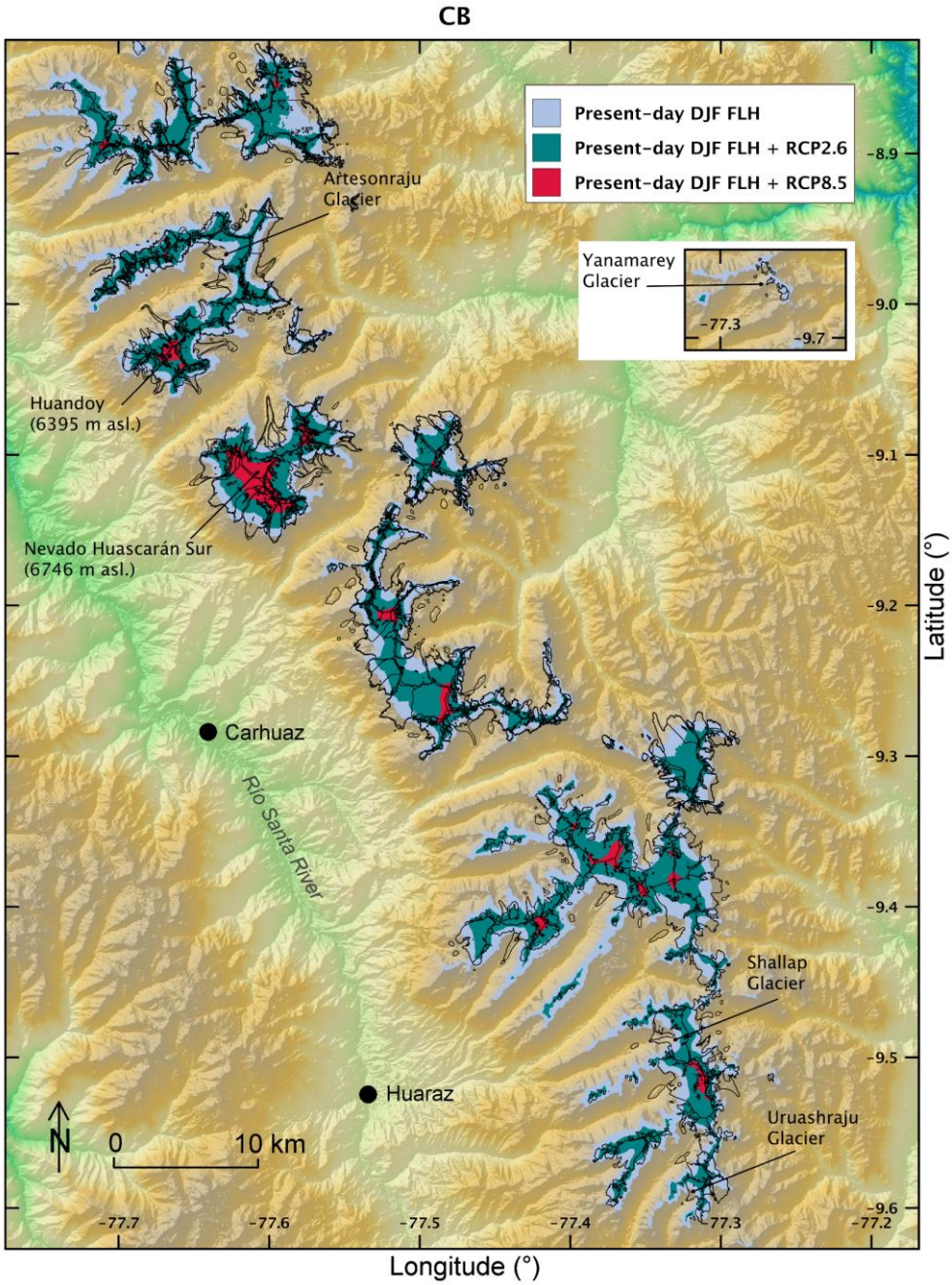

Figure 4-10 Glaciers in the CB with the area above the present-day FLH (light blue), and the area above the mean end-of-century FLH from the multi-model median model runs under emission scenarios RCP2.6 (green) and RCP8.5 (red). Black lines represent modern glacier extents.

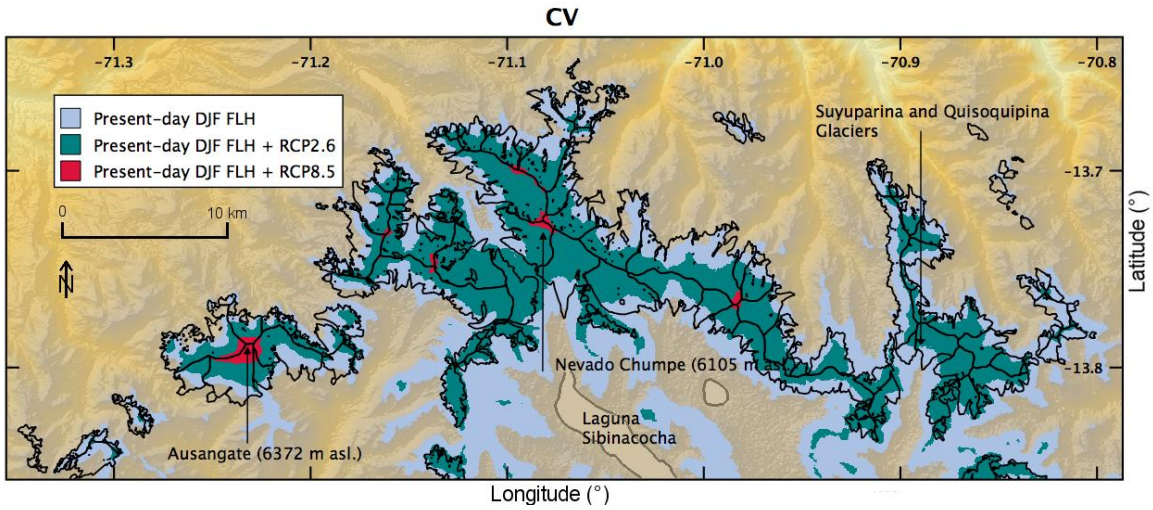

Figure 4-11 Glaciers in the CV (black lines) with the area above the present-day FLH (light blue), and the area above the mean end-of-century FLH from the multi-model median model runs under emission scenarios RCP2.6 (green) and RCP8.5 (red). Black lines represent modern glacier extents.

Table 4-2 Current glacier extents and areas above the current wet season FLH (respective to the current area above the wet season FLH) and the mean end-of-century FLH under RCP2.6 and RCP8.5 (CB: 13.4°S to 13.86°S / 70.79°W to 71.37°W, UGRH inventory; CV: 8.74°S to 9.88°S and 77.14°W to 77.86°W, GLIMS inventory).

	Cordillera Blanca		Cordillera Vilcanota	
	(km^2)	(%)	(km^2)	(%)
Current glacier extent	457	-	223	-
Area above the current wet season FLH	614	100	374	100
Area above mean end-of-century FLH under RCP2.6	260	42	155	41
Area above mean end-of-century FLH under RCP8.5	7	1	13	3

4.5 Discussion

In the following section, we discuss the spatial and seasonal variability of the FLH derived from different data types (reanalysis data, extrapolation of meteorological station data and TRMM PR BB estimations). Further on, the change in FLH by the end of this century and possible impacts on glacier extents are discussed.

4.5.1 Present-day freezing and snowfall level height

Reanalysis data are easily applicable tools to assess regional and seasonal variabilities in the FLH. Despite local biases between ERA-Interim and MERRA2 (supporting information, Figure 4-12), the overall pattern of both reanalysis products consistently shows highest FLHs occurring in the wet season (DJF) and lowest FLHs during the dry season (JJA). This follows from the nature of

the annual air temperature cycle with cooler mean air temperature during the dry period (see for instance *Schauwecker et al*., 2014). We assume that the higher FLH over Southern Peru may be a result of the Bolivian high pressure system, present in the upper troposphere during austral summer (DJF). The higher FLH over the coast and Southern Peru is in agreement with the FLH observed by *Bradley et al.* (2009) based on NCEP/NCAR data. *Diaz et al.* (2014) found a mean FLH of ~4500 m asl. over the tropics, based on NCEP/NCAR reanalysis data from 1973-2002. Therefore, our results indicate that the mean FLH of about 4900 and 5010 m asl. in the CB and CV, respectively, may lie above the mean tropical FLH. These results are consistent with *Rabatel et al.* (2013), that found annual FLHs in the CB in the range of 4830 to 5000 m asl., with individual values of up to 5100 m asl.. ERA-Interim data indicate that the FLH is on average lower during precipitation events. This difference is only visible during the dry season. The FLH can drop to considerably low altitudes (<3500 m asl.) during the infrequent dry season precipitation events. Additionally, we found a correlation between reanalysis FLH and radar derived SLH. The SLH lies generally below the reanalysis FLH. Other studies have also shown that the SLH (derived by TRMM PR BB) lies some hundreds of meters below the reanalysis FLH (*Harris et al.*, 2000; *Thurai et al.*, 2003; *Awaka et al.*, 2009) or the radiosonde FLH (*Schauwecker et al.*, 2016). We conclude that reanalysis data are useful tools to assess the SLH, assuming that in our study region the SLH lies on average about 220 m and 240 m below the ERA-Interim and MERRA2 FLH, respectively. At single glacier, various factors (e.g. katabatic winds, aspect, insolation) may influence local lapse rates. The here presented regional estimation of FLH and SLH is therefore associated with considerable uncertainties for a single precipitation event or at a certain point in time.

We found a relatively good agreement between radar derived SLH and FLH estimation using extrapolation techniques (based on air temperature from a single meteorological station and a constant lapse rate of -0.0065°C/m). However, the bias increases significantly with higher air temperatures at the station, and the SLH is often strongly overestimated using extrapolation techniques above a near-surface temperature of around 15°C. Our results further indicate that the extrapolation is not very accurate if the air temperature is measured at the beginning of the rainfall event when the near-surface air temperatures are still high, similar to the conditions in the Indian Himalayas (*Schauwecker et al.*, 2016). The extrapolation based on several meteorological stations using linear regression gets difficult for regions with few stations available. Additionally, the temporal resolution of conventional meteorological stations hampers the assessment of the FLH and SLH during precipitation events, since precipitation events in this region can be often rather short (minutes to hours). Another uncertainty exists in the estimation of the air temperature at the snow/rain transition. A threshold of 1.5°C is often used (e.g. *Klok and Oerlemans*, 2002), however, we found that a threshold of 0°C might be more adequate for the Central Andes if compared to the radar derived SLH of the free atmosphere.

We found that the TRMM PR BB lies on average about 500 to 600 m below the FLH from reanalysis which agrees with other studies (e.g. *Harris et al.*, 2000; *Schauwecker et al.*, 2016). We also found a limited TRMM PR BB data availability over the high mountain regions in Peru, as already described in *Schauwecker et al.* (2016) for the Indian Himalayas. However, the data provided over

the foothills of the Andes and the Amazon basin serve as a complementary information source to assess for example the annual variability of the SLH. The variability of the BB height agrees well with the annual variability of the FLH derived by reanalysis data in these regions.

Our findings agree with more anecdotal evidence, such as observations of the snow/rain transition at the elevation of glaciers in the CB and the CV. For instance, it has been observed that during the wet season, there was almost exclusively rain on the tongue of Yanamarey glacier located at around 4680 m asl. (according to the GLIMS inventory, *Racoviteanu et al.*, 2008). In contrast, during the dry period, solid precipitation frequently occurred below the glacier terminus (Ames, 1995, personal communication in *Kaser and Osmaston*, 2002). Also the tongue of Suyuparina glacier (CV) at approximately 5100 m asl. was covered by a relatively thick layer of compact snow or firn in July 2011, August 2014 and 2015 (observations made by the authors), indicating low snow/rain transition levels during the dry season. Moreover, present weather sensor measurements indicate that in the CV at 5050 m asl., precipitation is predominantly solid (94% of all precipitation hours during July 2012 – June 2014, *Poremba et al.*, 2015).

4.5.2 Future freezing height

We found that under RCP2.6, the mean future increase of the FLH is approximately 24 m per decade (±20 m, 2δ), agreeing with the observed 30 m per decade between 1955 and 2011 by e.g. *Rabatel et al.* (2013), but being higher than the observed ca. 14 m per decade for the entire tropics (1958-2000, *Diaz et al.*, 2003). This means that even under the most optimistic scenario, the FLH in the Peruvian Andes will continue increasing at a similar rate as in the last about 5 decades. With RCP8.5, the future increase is extremely high with approximately 89 m per decade (±41 m, 2δ), meaning that the increase rate would be three times higher than the observed increase since the 1950s.

The results from Figure 4-8 show that the expected rise in the FLH over the Peruvian Cordilleras is rather homogeneous in space, probably a result of the spatial model resolution. However, the warming at the elevation of glaciers may be stronger than at low altitudes (e.g. *Bradley et al.*, 2004), which we could not show based on the FLH of the free atmosphere. *Diaz et al.* (2014) found similar increases in the FLH by the end of this century for the latitude of 10-15°S with about 900 m for DJF and 1000 m for JJA. *Bradley et al.* (2006) and *Vuille et al.* (2008) found a warming of 4.5-5°C by the end of the century, considering a similar radiative forcing relative to the pre-industrial as RCP8.5 (*IPCC* (2013), using the SRES A2 scenario). Assuming a lapse rate of 0.0065°C/m, this temperature increase would thus correspond to a rise in the FLH of about 690 to 770 m, slightly below the increase presented here for the most pessimistic RCP8.5 scenario. Also for other regions in the world, the rise in SLH will be remarkable under RCP8.5. For example, *Viste and Sorteberg* (2015) found that the SLH will move upward by 700-900 m in the Indus, Ganges and Brahmaputra basins, similar to our findings.

The FLH is closely related to ENSO in the Tropics (*Bradley et al.*, 2009), including in the Andes of Ecuador (e.g. *Vuille et al.*, 2000, *Francou et al.*, 2004). This relation might also be valid for the

Peruvian Andes (e.g.*Vuille et al.*, 2008, *Maussion et al.*, 2015). CMIP5 GCMs exhibit a range of behaviors for ENSO variability in the future, some showing an increase in ENSO variability, others a decrease and some no change (*Guilyardi et al.*, 2012). If ENSO events become more frequent in the future, the FLH rise could be even stronger than projected by the mean of all CMIP5 models. Moreover, as suggested by *Tan et al.* (2016), CMIP5 models may strongly underestimate mixed-phase cloud effects (Wegener-Bergeron-Findeisen process) under climate change. Also this may lead to an even higher FLH than projected by RCP2.6 and RCP8.5. Increases in the FLH as a result of rising temperatures has led and will lead to a decline of the surface area above this critical level of mountainous regions around the world (*Diaz et al.*, 2003), having important impacts on e.g. glacier recession as discussed in the following section.

4.5.3 Impact of rising freezing and snowfall level height on glaciers

We found that during the wet season (DJF), where most of the annual precipitation falls (e.g. *Kaser et al.*, 1990), the mean FLH from reanalysis data lies at approximately 4950 m asl (5090 m asl) for the CB (CV), see also Figure 9. SLH analysis indicates that during most of the year snow is falling down to 40 – 420 m below this level (see Figure 4-5a). But snow below the FLH is melting or sublimating within few hours due to the positive temperatures and solar radiation (*Poremba et al.*, 2015). Annual accumulation therefore likely only exists predominantly above the FLH. The FLH not only determines accumulation, it also largely influences net shortwave radiation via albedo effects. Where snow does not accumulate during the wet season, the glacier surface is mostly snow free and has thus a relatively low albedo. A large fraction of the incoming shortwave radiation is absorbed and not reflected, leading to large amounts of energy available for ablation. As a consequence, tropical glaciers are characterized by steep mass balance gradients below the FLH and high accumulation area ratios (AAR, compare to e.g. *Kaser*, 2001). The high glacier ablation below the FLH thus exerts an important control on the glacier terminus. This explains why only approximately 15% of the current total glacier area is below the present-day wet season FLH for both regions (Figure 4-9). Dynamic ice flow effects become more important with larger glaciers with more extensive accumulation areas which thus can form glacier tongues reaching down to lower elevations as enough ice is flowing down to substitute the ice loss.

The FLH has been suggested as an approximation of the equilibrium line altitude (ELA) of glaciers, with the ELA dividing the area of mass loss and gain on a glacier averaged over one year (*Condom et al.*, 2007, *Rabatel et al.*, 2012, *Sagredo et al.*, 2014). Here we analyzed the wet season FLH in relation with the glacier extents in reference to their lowermost elevations. Although at a local, single glacier scale there are considerable variations in this relation we found that a higher coherence of this relation at a regional scale. Furthermore, in consideration of the physical mass gain and loss processes effective at tropical glaciers it is reasonable to assume that an increase of the FLH has a proportional effect on glacier areas. Thus, if we assume that the percentage of glacier area below the wet season FLH remains similar in the future, glaciers will lose more than half of their area under the most optimistic scenario RCP2.6 (see Figures 4-10 and 4-11, Table 4-2). If the temperature increases as much as under RCP8.5, there will be only some small glaciers left on the

top of the highest mountain peaks in both regions. Especially small, low-elevation glaciers will first disappear, as well as glaciers with low lying accumulation areas. These findings are in the same range as results from *Juen et al.* (2007), who simulated changes in glacier extent using a model based on a vertical mass balance profile model (*Kaser*, 2001). They showed that under the B1 (low) emission scenario (*IPCC*, 2000), glaciers in the Llanganuco catchment (86.4 km^2) in the CB would lose about 49% of their area in 2080 compared to 1990. The area loss would increase to 75% under the (pessimistic) A2 scenario.

To fully explain future glacier extents, an energy balance model including glacier dynamics would be needed, requiring different parameters which are typically not available at high altitudes and/or related to large uncertainties. Single glaciers may respond differently to changes in the FLH, depending on their aspect, slope, elevation distribution, area, topographical location, etc. These glacier parameters are probably somewhat different for the CB and CV resulting in a regional difference in glacier retreat. Our projection for the future glacier extents therefore do not apply at the local glacier scale but rather represents an overall estimate for the glacier-covered area at a regional scale (for the CB and CV). Moreover, there might also be substantial changes in other meteorological variables like humidity, cloud cover, precipitation, and downwelling longwave radiation. However, all of these variables and their future changes are associated with uncertainties and a more detailed model will not necessarily offer more reliable results. For instance, due to the small-scaled topographic features of the Andes, the ability of GCMs to simulate precipitation is limited (e.g. *Minvielle and Garreaud*, 2011). *Neukom et al.* (2015) suggest that simulations using a relation between precipitation and the mid- and upper tropospheric flow results in more reliable projections and that precipitation may decrease substantially by the end of this century. With decreasing precipitation, glacier retreat would be even stronger than discussed assuming only an increase in the FLH. Moreover, glaciers are already today out of balance with the current climate conditions (e.g. *Schauwecker et al.*, 2014), which was not considered in our experiment. *Rabatel et al.* (2013) stated that since a marked increase in FLH in the late 1970s, the ablation zones of glaciers in the CB are mostly located within the altitudinal range of the annual mean FLH. Even if warming halted for some decades, glaciers would continue shrinking for years or decades, depending on their response time. For example, larger glaciers like Artesonraju have response times of 10-40 years (e.g. *Schauwecker et al.*, 2014), while small and thin glaciers adapt much faster to the climatic conditions. Furthermore, once the FLH rises above the highest glacier extent, the lack of an accumulation area would lead to an even stronger melt down of the remaining ice. Other feedbacks between the glacier and their environment could also lead to much more extreme glacier shrinkage than assumed here. Despite a number of uncertainties described above, we conclude that our estimate is a robust and even rather optimistic scenario.

Our experiment may only be valid for glaciers that are sensitive to air temperature, which is not the case for all tropical glaciers. Where air temperature is cold enough during the year for solid precipitation across the glacier, mass balance seems most sensitive to precipitation and moisture (e.g. in Bolivia, see *Kaser*, 2001, and *Favier et al.*, 2004a). The dependence and sensitivity of

glaciers to changes in the FLH is thus likely highest where tongues are already today close to 0°C around the year, namely glaciers in Ecuador or Peru.

4.6 Concluding remarks

In this study, we assessed the present-day FLH over the Peruvian Andes as well as the seasonal and regional variability, using multiple data sources. The SLH was estimated from MRR data in Cusco and related to FLH from reanalysis and extrapolated meteorological station data. We used CMIP5 scenario runs to estimate the change in FLH by the end of the 21st century compared to present-day and discussed possible impacts on glacier extents in the CB and CV - the two largest glacierized mountain ranges in Peru. The results enabled us to highlight the following conclusions:

- Reanalysis data are suitable and easily applicable tools to assess the regional and seasonal variability of the FLH and there is a reasonable correlation between reanalysis data and radar derived snow/rain transition. However, for estimating SLH of a single precipitation event, reanalysis FLH data have to be used with caution mainly due to the coarse spatial resolution. The SLH derived from MRR estimates lies about 40 – 420 m below the reanalysis FLH (on average 220 m below ERA-Interim and 240 m below MERRA2). SLH estimates based on extrapolation techniques have to be applied with caution when relatively high air temperatures are measured at the beginning of the precipitation event. The air temperature threshold for the snow/rain transition has to be defined carefully, depending also on temperature measurement techniques. In our analysis, a lapse rate of -0.0065°C/m and a threshold of 0°C seems to be appropriate to estimate the free air snow/rain transition based on a single meteorological station. However, for the phase of near-surface precipitation a typical threshold of about 1.5°C might be more suitable. The methodology to assess the FLH and SLH using multiple data types has a potential to be enhanced and the temporal and spatial resolution of the FLH could be improved by using ground-based meteorological (e.g. UNASAM station data) or additional reanalysis data.
- CMIP5 model data revealed a strong rise in the FLH until the end of this century. Even under the most optimistic scenario RCP2.6, the FLH may continue increasing (approximately 230 m ± 190 m) at a similar rate as in the last three decades. For the most pessimistic scenario RCP8.5, the rise in FLH is very large (approximately 875 m ± 390), being almost three times the observed warming in the last 3 decades. The surface area above the projected FLH under RCP2.6 is about half of the area above the present-day wet season FLH. The area above the RCP8.5 FLH is very small and consists only of the highest peaks in the region. This will certainly have severe impacts on the environment.
- We found a relation of the present-day wet season FLHs from reanalysis data and regional-scale glacier extents, supported by the close relation between FLH, SLH and glacier energy balance. Below the wet season FLH, annual glacier surface ablation is typically very high, thus exerting an important control on the glacier terminus especially for small and mid-sized

glaciers. Based on this relation, even under the most optimistic scenario, at least half of the current glacier area will vanish by the end of this century. Under the most pessimistic scenario, not only small to mid-sized glaciers, but also large glaciers may retreat within this century and only some patches of ice would remain on the summits of the highest peaks. Although we used a very simple experiment, we suggest that this is a robust and rather optimistic estimation for the future glacier extent. Of course, future glacier extents are related to large uncertainties, which are still difficult to quantify (e.g. changes in other climatic variables, glacier response times, glacier geometries, etc.). The large difference between the most optimistic and pessimistic scenarios for the future of our climate and glacier extents, however, is not a result of model uncertainty but is a strong indicator of the differential effects of low-emission and high-emission scenarios on glaciers, and underline the importance of strong greenhouse gas emission reduction policies. In upcoming research our estimates of present-day and future FLHs could be implemented in energy and mass balance models in order to estimate more accurately the future retreat of these glaciers, the timing and the corresponding uncertainties.

4.7 Acknowledgements

This research was developed in the framework of Proyecto Glaciares+, a program financed by the Swiss Agency for Development and Cooperation SDC, in collaboration with CARE Peru. We acknowledge the use of data from the SENAMHI. Stations from the UNASAM were installed in the framework of the project Centro de Información e Investigación Ambiental de Desarrollo Regional Sostenible (CIIADERS). ERA-interim data are obtained from the ECMWF. The MERRA2 data are provided by the Global Modeling and Assimilation Office (GMAO) at NASA Goddard Space Flight Center. TRMM PR 2A23 and 2A25 data are obtained from the Japan Aerospace Exploration Agency (JAXA) and the National Aeronautics and Space Administration (NASA). GLIMS data are provided by the National Snow and Ice Data Center and the ASTER DEM is obtained through the DAAC Global Data Explorer, a product of METI and NASA. Raphael Neukom is supported by the Swiss NSF grant PZ00P2_154802. J.L. Endries and L.B. Perry were supported by the U.S. National Science Foundation through Grant AGS-1347179 (CAREER: Multiscale Investigations of Tropical Andean Precipitation). The data supporting the analysis can be obtained by sending a written request to the corresponding authors (Simone Schauwecker, schauwecker@meteodat.ch).

4.8 References

American Meteorological Society (2016), Glossary of Meteorology. (Available online athttp://glossary.ametsoc.org/wiki/)

Ames, A., and S. Hastenrath (1996), Diagnosing the imbalance of Glaciar Santa Rosa, Cordillera Raura, Peru, Journal of Glaciology, 42, 212-218.

Awaka, J., T. Iguchi, and K. Okamoto (2009), TRMM PR Standard Algorithm 2A23 and its Performance on Bright Band Detection, Journal of the Meteorological Society of Japan, 87A, 31–52.

Baraer, M., B. G. Mark, J. M. McKenzie, T. Condom, J. Bury, K.-I. Huh, C. Portocarrero, J. Gómez, and S. Rathay (2012), Glacier recession and water resources in Peru's Cordillera Blanca, Journal of Glaciology, 58, 134-150.

Battan, L. J. (1973), Radar observation of the atmosphere. - The Univ. of Chicago Press, 324 pp.

Bosilovich, M. G., S. Akella, L. Coy, R. Cullather, C. Draper, R. Gelaro, R. Kovach, Q. Liu, A. Molod, P. Norris, K. Wargan, W. Chao, R. Reichle, L. Takacs, Y. Vikhliaev, S. Bloom, A. Collow, S. Firth, G. Labow, G. Partyka, S. Pawson, O. Reale, S. D. Schubert, and M. Suarez (2015), Merra-2: Initial Evaluation of the Climate. Technical Report Series on Global Modeling and Data Assimilation, Volume 43. Goddard Space Flight Center, Greenbelt, Maryland.

Bradley, R. S, F. T. Keimig, and H. F. Diaz (2004), Projected temperature changes along the American cordillera and the planned GCOS network, Geophysical Research Letters, 31, L16210.

Bradley, R. S., F. T. Keimig, H. F. Diaz, and D. R. Hardy (2009), Recent changes in freezing level heights in the Tropics with implications for the deglacierization of high mountain regions, Geophysical Research Letters, 36, L17701.

Bradley, R. S., M. Vuille, H. F. Diaz, and W. Vergara (2006), Threats to Water Supplies in the Tropical Andes, Science, 312, 1755-1756.

Condom, T., A. Coudrain, J. E. Sicart, and S. Théry (2007), Computation of the space and time evolution of equilibrium-line altitudes on Andean glaciers (10°N-55°S), Global and Planetary Change, 59, 189-202.

Dee, D. P., S. M. Uppala, A. J. Simmons, P. Berrisford, P. Poli, S. Kobayashi, U. Andrae, M. A. Balmaseda, G. Balsamo, P. Bauer, P. Bechtold, A. C. M. Beljaars, L. van de Berg, J. Bidlota, N. Bormann, C. Delsol, R. Dragani, M. Fuentes, A.J.Geer, L. Haimberger, S. B. Healy, H. Hersbacha, E. V. Hólm, L. Isaksen, P. Kållberg, M. Köhler, M. Matricardi, A.P. McNallya, B. M. Monge-Sanz, J.-J. Morcrette, B.-K. Park, C. Peubey, P. de Rosnay, C.Tavolato, J.-N. Thépaut, and F. Vitart (2011), The ERA-Interim reanalysis: Configuration and performance of the data assimilation system, Quarterly Journal of the Royal Meteorological Society, 137, 553–597.

Diaz, H. F., J. K. Eischeid, C. Duncan, and R. S. Bradley (2003), Variability of freezing levels, melting season indicators, and snow cover for selected high-elevation and continental regions in the last 50 years, Climatic Change, 59, 33-52.

Diaz, H. F., R. S. Bradley, and L. Ning (2014), Climatic changes in mountain regions of the American Cordillera and the tropics: historical changes and future outlook, Arctic, Antarctic, and Alpine Research, 46, 1-9.

Drenkhan, F., M. Carey, C. Huggel, J. Seidel, and M. T. Oré (2015), The changing water cycle: climatic and socioeconomic drivers of water-related changes in the Andes of Peru, Wiley Interdisciplinary Reviews: Water, 2, 715-733.

Favier, V., P. Wagnon, and P. Ribstein (2004a), Glaciers of the outer and inner tropics: A different behaviour but a common response to climatic forcing, Geophysical Research Letters, 31, L16403.

Favier, V., P. Wagnon, J.-P. Chazarin, L. Maisincho, and A. Coudrain (2004b), One-year measurements of surface heat budget on the ablation zone of Antizana Glacier 15, Ecuadorian Andes, Journal of Geophysical Research, 109, D18105.

Francou, B., M. Vuille, V. Favier, and B. Cáceres (2004), New evidence for an ENSO impact on low-latitude glaciers: Antizana 15, Andes of Ecuador, 0°28'S, Journal of Geophysical Research, 109, D18106.

Garreaud, R. D., M. Vuille, and A. C. Clement (2003), The climate of the Altiplano: observed current conditions and mechanisms of past changes, Palaeogeography, Palaeoclimatology, Palaeoecology, 194, 5-22.

GLIMS, and National Snow and Ice Data Center (2005), updated 2012. GLIMS Glacier Database, Version 1. Boulder, Colorado USA. NSIDC: National Snow and Ice Data Center.

Guilyardi, E., H. Bellenger, M. Collins, S. Ferrett, W. Cai, and A. Wittenberg (2012), A first look at ENSO in CMIP5, CLIVAR Exchanges, 58, 29-32.

Gurgiser, W., B. Marzeion, L. Nicholson, M. Ortner, M., and G. Kaser (2013a), Modeling energy and mass balance of Shallap Glacier, Peru, The Cryosphere, 7, 1787-1802.

Gurgiser, W., I. Juen, K. Singer, M. Neuburger, S. Schauwecker, M. Hofer, and G. Kaser (2016), Comparing peasants' perceptions of precipiation change with precipiation records in the tropical Callejón de Huaylas, Peru, Earth System Dynamics, 7, 499-515.

Gurgiser, W., T. Mölg, L. Nicholson, and G. Kaser (2013b), Mass-balance model parameter transferability on a tropical glacier, Journal of Glaciology, 59, 845-858.

Harris, G. N., K. P. Bowman, and D.-B. Shin (2000), Comparison of Freezing-Level Altitudes from the NCEP Reanalysis with TRMM Precipitation Radar Brightband Data, Journal of Climate, 13, 4137–4148.

Hellström, R. Å., A. Fernández, B. G. Mark, J. Covert, A.C. Rapre, and A. R. J. Gomez (2017), Examining dynamical processes of tropical mountain hydroclimate, particularly during the wet season, through integration of autonomous sensor observations and climate modeling, Annals of the Association of American Geographers, Special Issue: Mountains (accepted).

Hofer, M., T. Mölg, B. Marzeion, and G. Kaser (2010), Empirical-statistical downscaling of reanalysis data to high-resolution air temperature and specific humidity above a glacier surface (Cordillera Blanca, Peru), Journal of Geophysical Research: Atmospheres, 115, D12120.

IPCC (2000), Special Report on Emission Scenarios. - Cambridge Univesity Press, UK, pp. 570.

IPCC (2013), Climate Change 2013: The Physical Science Basis. Contribution of Working Group I to the Fifth Assessment Report of the Intergovernmental Panel on Climate Change (Stocker, T.F., D. Qin, G.-K. Plattner, M. Tignor, S.K. Allen, J. Boschung, A. Nauels, Y. Xia, V. Bex and P.M. Midgley (eds.)). Cambridge University Press, Cambridge, United Kingdom and New York, NY, USA, 1535 pp.

Juen, I., G. Kaser, G., and C. Georges (2007), Modelling observed and future runoff from a glacierized tropical catchment (Cordillera Blanca, Perú), Global and Planetary Change, 59, 37-48.

Kaser, G. (2001), Glacier-climate interaction at low latitudes, Journal of Geophysical Research: Atmospheres, 47, 195-204.

Kaser, G., A. Ames, and M. Zamora (1990), Glacier fluctuations and climate in the Cordillera Blanca, Peru, Annals of Glaciology, 14, 136–140.

Kaser, G., and C. Georges (1997), Changes of the equilibrium-line altitude in the tropical Cordillera Blanca, Peru, 1930–50, and their spatial variations, Annals of Glaciology, 24, 344–349.

Kaser, G., and H. Osmaston (2002), Tropical Glaciers. Cambridge University Press.

Kaser, G., I. Juen, C. Georges, J. Gómez, and W. Tamayo (2003), The impact of glaciers on the runoff and the reconstruction of mass balance history from hydrological data in the tropical Cordillera Blanca, Peru, Journal of Hydrology, 282, 130-144.

Kaser, G., M. Grosshauser, and B. Marzeion (2010), Contribution potential of glaciers to water availability in different climate regimes, Proceedings of the National Academy of Sciences of the United States of America, 107, 20223-20227.

Klok, E. J., and J. Oerlemans (2002), Model study of the spatial distribution of the energy and mass balance of Morteratschgletscher, Switzerland, Journal of Geophysical Research: Atmospheres, 48, 505-518.

López-Moreno, J. I., S. Fontaneda, J. Bazo, J. Revuelto, C. Azorin-Molina, B. Valero-Garcés, E. Morán-Tejeda, S. M. Vicente-Serrano, R. Zubieta, and J. Alejo-Cochachín (2014), Recent glacier retreat and climate trends in Cordillera Huaytapallana, Peru, Global and Planetary Change, 112, 1-11.Lynch, B. (2012), Vulnerabilities, competition and rights in a context of climate change toward equitable water governance in Peru's Rio Santa Valley, Global Environmental Change, 22, 364-373.

Mark, B. G., and G. O. Seltzer (2003), Tropical glacier meltwater contribution to stream discharge: a case study in the Cordillera Blanca, Peru, Journal of Glaciology, 49, 271-281.

Mark, B. G., and G. O. Seltzer (2005), Evaluation of recent glacier recession in the Cordillera Blanca, Peru (AD 1962-1999): spatial distribution of mass loss and climatic forcing, Quaternary Science Reviews, 24, 2265-2280.

Mark, B. G., J. M. McKenzie, and J. Gómez (2005), Hydrochemical evaluation of changing glacier meltwater contribution to stream discharge: Callejon de Huaylas, Peru, Hydrological Sciences Journal, 50, 975-987.

Maussion, F., W. Gurgiser, M. Grosshauser, G. Kaser, and B. Marzeion (2015), ENSO influence on surface energy and mass balance at Shallap Glacier, Cordillera Blanca, Peru, The Cryosphere, 9, 1663-1683.

Minveille, M., R. D. Garreaud (2011), Projecting Rainfall Changes over the South American Altiplano, Journal of Climate, 24, 4577-4583.

Moss, R. H., J. A. Edmonds, K. A. Hibbard, M. R. Manning, S. K. Rose, D. P. van Vuuren, T. R. Carter, S. Emori, M. Kainuma, T. Kram, G. A. Meehl, J. F. B. Mitchell, N. Nakicenovic, K. Riahi, S. J. Smith, R. J. Stouffer, A. M. Thomson, J. P. Weyant, and T. J. Wilbanks (2010), The next generation of scenarios for climate change research and assessment, Nature, 463, 747-756.

NASA JPL (2009), ASTER Global Digital Elevation Model. NASA JPL. https://doi.org/10.5067/ASTER/ASTGTM.002.

Neukom, R., M. Rohrer, P. Calanca, N. Salzmann, C. Huggel, D. Acuña, D. A. Christie, and M. S. Morales (2015), Facing unprecedented drying of the Central Andes? Precipitation variability over the period AD 1000–2100, Environmental Research Letters, 10, 84017.

NOAA, ftp://tgftp.nws.noaa.gov/data/observations/metar, last access: 1 May 2016.

Perry, L. B., A. Seimon, M. F. Andrade-Flores, J. L. Endries, S. E. Yuter, F. Verlarde, S. Arias, M. Bonshoms, E. J. Burton, I. R. Winkelmann, C. M. Cooper, G. Mamani, M. Rado, N. Montoya, and N. Quispe (2017), Characteristics

of precipitation storms in glacierized tropical Andean Cordilleras of Peru and Bolivia, Annals of the Association of American Geographers, 107, 309-22.
Poremba, R. J., L. B. Perry, A. Semon, D. T. Martin, and A. Tupayachi (2015), Meteorological Characteristics of Heavy Snowfall in the Cordillera Vilcanota, Peru. 72nd Eastern Snow Conference, Sherbrooke, Québec, Canada.
Prinz, R., L. I. Nicholson, T. Mölg, W. Gurgiser, and G. Kaser (2016), Climatic controls and climate proxy potential of Lewis Glacier, Mt. Kenya, The Cryosphere, 10, 133-148.
Rabatel, A., A. Bermejo, E. Loarte, A. Soruco, J. Gomez, G. Leonardini, C. Vincent, and J. E. Sicart (2012), Can the snowline be used as an indicator of the equilibrium line and mass balance for glaciers in the outer tropics?, Journal of Glaciology, 58, 1027–1036.
Rabatel, A., B. Francou, A. Soruco, J. Gomez, B. Cáceres, J. L. Ceballos, R. Basantes, M. Vuille, J. E. Sicart, C. Huggel, M. Scheel, Y. Lejeune, Y. Arnaud, M. Collet, T. Condom, G. Consoli, V. Favier, V. Jomelli, R. Galarraga, P. Ginot, L. Maisincho, J. Mendoza, M. Ménégoz, E. Ramirez, P. Ribstein, W. Suarez, M. Villacis, and P. Wagnon (2013), Current state of glaciers in the tropical Andes: a multicentury perspective on glacier evolution and climate change, The Cryosphere, 7, 81–102.
Racoviteanu, A. E., Y. Arnaud, M. W. Williams, and J. Ordonez (2008), Decadal changes in glacier parameters in the Cordillera Blanca, Peru, derived from remote sensing, Journal of Glaciology, 54, 499–510.
Rienecker, M. M., M. J. Suarez, R. Gelaro, R. Todling, J. Bacmeister, E. Liu, M. G. Bosilovich, S. D. Schubert, L. Takacs, G.-K. Kim, S. Bloom, J. Chen, D. Collins, A. Conaty, A. da Silva, W. Gu, J. Joiner, R. D. Koster, R. Lucchesi, A. Molod, T. Owens, S. Pawson, P. Pegion, C. R. Redder, R. Reichle, F. R. Robertson, A. G. Ruddick, M. Sienkiewicz, and J. Woollen (2011), MERRA2: NASA's modern-era retrospective analysis for research and applications, Journal of Climate, 24, 3624-3648.
Sagredo, E. A., S. Rupper, and T. V. Lowell (2014), Sensitivities of the equilibrium line altitude to temperature and precipitation changes along the Andes, Quaternary Reserach, 81, 355-366.
Salzmann, N., C. Huggel, M. Rohrer, W. Silverio, B. G. Mark, P. Burns, and C. Portocarrero (2013), Glacier changes and climate trends derived from multiple sources in the data scarce Cordillera Vilcanota region, southern Peruvian Andes, The Cryosphere, 7, 103–118.
Schauwecker, S., M. Rohrer, D. Acuña, A. Cochachin, L. Dávila, H. Frey, C. Giráldez, J. Gómez, C. Huggel, M. Jacques-Coper, E. Loarte, N. Salzmann, and E. Loarte (2014), Climate trends and glacier retreat in the Cordillera Blanca, Peru, revisited, Global and Planetary Change, 119, 85-97.
Schauwecker, S., M. Rohrer, M. Schwarb, C. Huggel, A. P. Dimri, and N. Salzmann (2016), Estimation of snowfall limit for the Kashmir Valley, Indian Himalayas, with TRMM PR Bright Band information, Meteorologische Zeitschrift, 25, 501-509.
Tan, I., T. Storelvmo, and M. D. Zelinka (2016), Observational constraints on mixed-phase clouds imply higher climate sensitivity, Science, 352, 224-227.
Taylor, K. E., R. J. Stouffer, and G. A. Meehl (2011), An overview of CMIP5 and the experiment design, Bulletin of the American Meteorological Society, 93, 485-498.
Thurai, M., E. Deguchi, T. Iguchi, and K. Okamoto (2003), Freezing height distribution in the tropics, International Journal of Satellite Communications and Networking, 21, 533–545.
Urrutia, R., and M. Vuille (2009), Climate change projections for the tropical Andes using a regional climate model: Temperature and precipitation simulations for the end of the 21st century, Journal of Geophysical Research, 114, D02108.
Viste, E., and A. Sorteberg (2015), Snowfall in the Himalayas: an uncertain future from a little-known past, The Cryosphere, 9, 1147-1167.
Vuille, M., and R. S. Bradley (2000), Mean annual trends and their vertical structure in the tropical Andes, Geophysical Research Letters, 27, 3885–3888.
Vuille, M., B. Francou, P. Wagnon, I. Juen, G. Kaser, B. G. Mark, and R. S. Bradley (2008), Climate change and tropical Andean glaciers: Past, present and future, Earth Science Reviews, 89, 79-96.
Wang, S., M. Zhang, N. C. Pepin, Z. Li, M. Sun, X. Huang, and Q. Wang (2014), Recent changes in freezing level heights in High asia and their impacts on glacier changes, Journal of Geophysical Research: Atmospheres, 119, 1753-1765.
Zemp, M., H. Frey, I. Gärtner-Roer, S. U. Nussbaumer, M. Hoelzle, F. Paul, W. Haeberli, F. Denzinger, A. P. Ahlstrøm, B. Anderson, S. Bajracharya, C. Baroni, L. N. Braun, B. E. Cáceres, G. Casassa, M. N. Demuth, L. Espizua, A. Fischer, K. Fujita, B. Gadek, A. Ghazanfar, J. O. Hagen, P. Holmlund, N. Karimi, Z. Li, M. Pelto, P. Pitte, V. V. Popovnin, C. A. Portocarrero, R. Prinz, C. V. Sangewar, I. Severskiy, O. Sigurdsson, A. Soruco, R. Usubaliev, and C. Vincent (2015), Historically unprecedented global glacier decline in the early 21st century, Journal of Glaciology, 61, 745-761.

4.9 Supporting information

The following CMIP5 model simulations were used for the analysis:
bcc-csm1-1-m, bcc-csm-1, BNU-ESM, CanESM2, CCSM4, CESM1-CAM5, CNRM-CM5, CSIRO-Mk3-6-0, FGOALS-g2, FIO-ESM, GFDL-CM3, GFDL-ESM2G, GFDL-ESM2M, HadGEM2-AO, IPSL-CM5A-LR, IPSL-CM5A-MR, MIROC-ESM-CHEM, MIROC-ESM, MIROC5, MPI-ESM-LR, MPI-ESM-MR, MRI-CGCM3, NorESM1-M, NorESM1-ME.

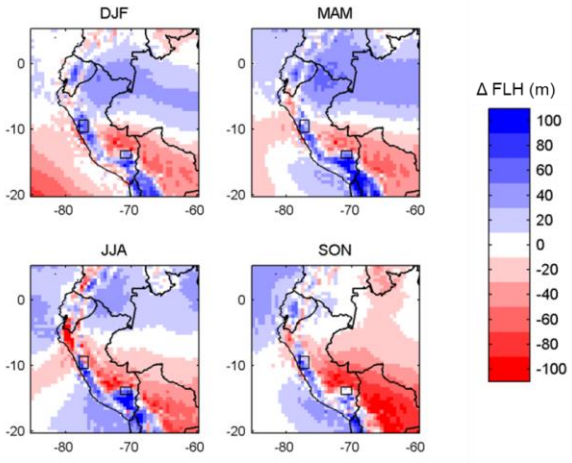

Figure 4-12 Seasonal plots of the difference between MERRA2 and ERA-Interim FLH. Blue means that the MERRA2 FLH lies above the ERA-Interim FLH, red means that the MERRA2 FLH lies below ERA-Interim FLH. The areas of the CB and CV are marked with black boxes.

Table 4-3 Details of meteorological stations

Institution	Region	Station name	Latitude	Longitude	Elevation (m asl.)
UNASAM	CB	Chacas	-10.405	-77.449	3560
UNASAM	CB	Purhuay	-9.315	-77.206	3357
UNASAM	CB	Pasto Ruri	-9.889	-77.304	4125
UNASAM	CB	Quillcayhuanca	-9.498	-77.417	3688
SENAMHI	CB	Cabana	-8.3836	-78.0046	3354
SENAMHI	CB	Cajatambo	-10.4667	-76.9833	3350
SENAMHI	CB	Cerro de Pasco	-10.6936	-76.2503	4260
SENAMHI	CB	Chiquian	-10.15	-77.15	3350
SENAMHI	CB	Dos de Mayo	-9.7169	-76.7736	3442
SENAMHI	CB	Huaraz	-9.5342	-77.5316	3052
SENAMHI	CB	Mayorarca	-10.1578	-77.4322	3351
SENAMHI	CB	Pira	-9.5853	-77.7072	3625
SENAMHI	CB	Santiago Antunez de Mayolo	-9.5165	-77.5249	3079
SENAMHI	CV	Ccatcca	-13.61	-71.5603	3729
SENAMHI	CV	Colquepata	-13.3631	-71.6731	3729
SENAMHI	CV	Crucero	-14.3642	-70.0259	4183
SENAMHI	CV	Macusani	-14.07	-70.4391	4345
SENAMHI	CV	Progreso	-14.6901	-70.0235	3980
SENAMHI	CV	Sicuani	-14.2536	-71.2372	3574

Part III Appendix

S. Schauwecker

1 Personal bibliography

Schauwecker, S., M. Rohrer, D. Acuña, A. Cochachin, L. Dávila, H. Frey, C. Giráldez, J. Gómez, C. Huggel, M. Jacques-Coper, E. Loarte, N. Salzmann, and M. Vuille (2014), Climate trends and glacier retreat in the Cordillera Blanca, Peru, revisited, Global and Planetary Change, 119, 85-97.

Schauwecker, S., M. Rohrer, C. Huggel, A. Kulkarni, AL. Ramanathan, N. Salzmann, M. Stoffel, and B. Brock (2015), Remotely sensed debris thickness mapping of Bara Shigri Glacier, Indian Himalaya, Journal of Glaciology, 61, 675-688.

Molina, E., **S. Schauwecker**, C. Huggel, W. Haeberli, A. Cochachin, T. Condom, F. Drenkhan, C. Giráldez, N. Salzmann, L. Jiménez, N. Montoya, M. Rado, N. Chaparro, J. Samata, W. Suarez, S. Arias, and F. Sikos (2015), Iniciación de un monitoreo del balance de masa en el glaciar Suyuparina, Cordillera Vilcanota, Perú, Climate Change in the Tropical Andes, 2, 1-14.

Gurgiser, W., I. Juen, K. Singer, M. Neuburger, **S. Schauwecker**, M. Hofer, and G. Kaser (2016), Comparing peasants' perceptions of precipitation change with precipitation records in the tropical Callejón de Huaylas, Peru, Earth System Dynamics, 7, 499-515.

Kronenberg, M., **S. Schauwecker,** C. Huggel, N. Salzmann, F. Drenkhan, H. Frey, C. Giráldez, W. Gurgiser, G. Kaser, I. Juen, W. Suarez, J. G. Hernández, J. Fluixá Sanmartín, E. Ayros, B. Perry, and M. Rohrer (2016), The projected precipitation reduction over the Central Andes may severely affect Peruvian glaciers and hydropower production, Energy Procedia, 97, 270-277.

Schauwecker, S., M. Rohrer, M. Schwarb, C. Huggel, A. P. Dimri, and N. Salzmann (2016), Estimation of snowfall limit for the Kashmir Valley, Indian Himalayas, with TRMM PR Bright Band information, Meteorologische Zeitschrift, 25, 501-509.

Colonia, D., J. Torres, W. Haeberli, **S. Schauwecker**, E. Braendle, C. Giráldez, and A. Cochachin, Glacier-bed overdeepenings and possible new lakes in de-glaciating areas of the Peruvian Andes, Global Warming Impacts on Mountain Glaciers and Communities, under review.

Schauwecker, S., M. Rohrer, C. Huggel, J. Endries, N. Montoya, R. Neukom, B. Perry, N. Salzmann, M. Schwarb, and W. Suarez. The freezing level in the tropical Andes, Peru: an indicator for present and future glacier extents. Journal of Geophysical Research – Atmospheres, under review.

2 Curriculum Vitae

First names	Simone Marianna
Last name	Schauwecker
Place of birth	Solothurn, Switzerland
Date of birth	6 May 1985
Place of origin	Schaffhausen (SH) and Feuerthalen (ZH)
Citizenship	Swiss

Education

05/2013 to present	PhD Programme at the Department of Geography, Glaciology and Geomorphodynamics Group, University of Zürich
09/2009 - 02/2012	Master Programme in Environmental Engineering, ETH Zürich Major Courses: Hydrology and Water Resources Management, Hydraulic Engineering Masterthesis: Mapping supraglacial debris thickness on mountain glaciers using satellite data: validation of a new, physically-based method
10/2006 - 08/2009	Bachelor Programme in Environmental Engineering, ETH Zürich Bachelorthesis: Modelling the routing of snow and ice melt in glaciated catchments: improving the linear reservoir approach
05/2005	Matura in the mathematics and natural science profile, Kantonsschule Solothurn Core subjects: Physics and applied mathematics

3 Acknowledgements

Firstly, I would like to thank Christian Huggel for providing me the great opportunity to do this PhD and for the continuous support. I learned a lot – not only about glaciers and climate, but also about international collaboration, teaching, politics and much more. My sincere thanks also go to Mario Rohrer for his enthusiasm, patience, motivation, the numerous discussions and answers to many questions. Special thanks also go to Nadine Salzmann for her support and her great ideas at the right moments and to Holger Frey, Andreas Vieli and Jan Seibert for their time and motivation.

Besides my advisors, I would like to thank the entire team of *Proyecto Glaciares*. Special thanks to Wilfried Haeberli, for the two extremely interesting stays in Peru, for his advices, inputs and countless conversations during these weeks. Special thanks also to Fabian Drenkhan and Jan Baiker for all kind of adventures in Peru. Thanks to Luis Vicuña and Christine Jurt for showing me new ways of thinking beyond the numbers and physics: How do glaciers communicate, sound and smell?

Moreover, my gratitude goes to all the co-authors of my publications for their great help and sharing data as well as experiences: Mathias Vuille, Ben Brock, Raphael Neukom, Baker Perry, Jason Endries, Markus Stoffel, Martín Jacques-Coper and all the others. Thanks go to all the anonymous reviewers of my work – I always got very positive and constructive feedbacks. Thanks also to Wolfgang Gurgiser, Georg Kaser and their team for collaborating and inviting me to an interdisciplinary workshop that finally led to a very interesting paper. Furthermore, I would like to thank Inge Juszak for reading and correcting the thesis.

Thanks also to my colleagues Daniela Lorenzi, Urs Steinegger and Manfred Schwarb from Meteodat GmbH for your great support and motivation. Many thanks go to the glaciology and geomorphodynamics group (3G) and officemates for all the conversations and discussions, new ideas and ways of thinking. Thanks also to Ross Purves, Isabelle Gärtner-Roer and the graduate school of Geography for teaching me what a PhD is.

Sincere thanks go to all my friends around the world and my family. Special thanks go to my parents Barbara and Martin Schauwecker for supporting me in every decision I take.

Last but not least, I thank Matilda and Álvaro Ayala – *por todo*!